PROGRAMA DE PÓS-GRADUAÇÃO EM OCEANOGRAFIA AMBIENTAL
UNIVERSIDADE FEDERAL DO ESPÍRITO SANTO

UNIVERSIDADE FEDERAL DO ESPÍRITO SANTO
CENTRO DE CIÊNCIAS HUMANAS E NATURAIS
PROGRAMA DE PÓS-GRADUAÇÃO EM OCEANOGRAFIA AMBIENTAL

CYBELLE MENOLLI LONGHINI

CONTAMINAÇÃO COSTEIRA COM REJEITOS DE MINÉRIO: ESPECIAÇÃO DO FERRO E IMPACTOS SOBRE A COMUNIDADE FITOPLANCTÔNICA

ARACRUZ – ES
FEVEREIRO, 2020

CYBELLE MENOLLI LONGHINI

CONTAMINAÇÃO COSTEIRA COM REJEITOS DE MINÉRIO: ESPECIAÇÃO DO FERRO E IMPACTOS SOBRE A COMUNIDADE FITOPLANCTÔNICA

Tese de Doutorado apresentada ao Programa de Pós-Graduação em Oceanografia Ambiental da Universidade Federal do Espírito Santo, como requisito parcial para obtenção do título de Doutora em Oceanografia Ambiental.

Orientador: Prof. Dr. Renato Rodrigues Neto

Co-orientadores: Prof. Dr. Fabian Sá;

Prof. Dr. Camilo Dias Júnior

ARACRUZ – ES
FEVEREIRO, 2020

UNIVERSIDADE FEDERAL DO ESPÍRITO SANTO
Centro de Ciências Humanas e Naturais
Programa de Pós-Graduação em Oceanografia Ambiental

TESE DE DOUTORADO

"CONTAMINAÇÃO COSTEIRA COM REJEITOS DE MINÉRIO: ESPECIAÇÃO DO FERRO E IMPACTOS SOBRE A COMUNIDADE FITOPLANCTÔNICA"

por

Cybelle Menolli Longhini

Prof. Dr. Renato Rodrigues Neto
Universidade Federal do Espírito Santo

Prof. Dr. Gilberto Fonseca Barroso
Universidade Federal do Espírito Santo

Profa. Dra. Ana Teresa Macas Lima
Technical University of Denmark (via webconferência)

Profa. Dra. Maristela de Araújo Vicente
Universidade Federal do Espírito Santo (via webconferência)

Prof. Dr. Marco Tadeu Grassi
Universidade Federal do Paraná (via webconferência)

Vitória, 03 de fevereiro de 2020

AGRADECIMENTOS

“Gratidão”... Essa palavra que anda tão em alta pelo seu potencial de transformar a nossa visão do mundo e dos acontecimentos... Acredito no poder da palavra, mas acredito, sobretudo, que a transformação só é possível quando a teoria vem carregada de verdade e de ação. Aqui, apresento os meus sinceros agradecimentos àqueles que não só me deram suporte emocional, mas que me impulsionaram com ações e tomadas de decisões para a conclusão dessa etapa.

A Deus, essa força superior que sempre acalentou meu coração nos momentos de medo e incertezas, me direcionando sempre para os melhores caminhos, os quais eu nem sequer fui capaz de sonhar;

Ao meu painho, àquele que sempre foi meu espelho de luta e integridade. Ver sua realização com as minhas conquistas é a minha maior recompensa!

À minha mainha, mulher de garra que abriu mão dos próprios sonhos para que pudéssemos vivenciar os nossos;

Às minhas raridades, Dani e Tati, por estarem presentes em cada momento e escolha da minha vida e por serem mulheres que me inspiram!

Aos meus “galhegos”, Davi e Dante por encherem as nossas vidas de tanto amor e sentido!

À Su por ser sempre tão solícita, cuidadosa e amorosa conosco e à minha sempre “Tchutchuquinha” Mimim por permitir novos aprendizados com o seu crescimento e evolução;

Aos meus orientadores, Renato Neto e Fabian Sá. Minha profunda gratidão por confiarem no meu trabalho, por permitirem a execução de cada etapa e sempre apresentarem uma visão positiva de tudo! Sinto-me honrada por ter sido acompanhada por pessoas que me inspiram na vida, além do âmbito profissional!

À minha “mãe capixaba” Celinha, pelas intermináveis conversas, conselhos e pelo cuidado de uma verdadeira mãe coruja. Obrigada pelo bolo e café quentinhos servidos nas madrugadas de estudo!

Às amizades verdadeiras, aqui representadas como: “Café com Leite”, “Quarteto Fantástico”, “Meninas”, “Xuxures” e “Best’s”. Mulheres que me inspiram e me apoiam em todos os momentos.

À minha Jelzita, encontro lindo permitido pelo doutorado e amizade para toda uma vida. Obrigada por tanto, especialmente por sempre acreditar e estimular o meu melhor!

Aos meus colegas e amigos do LabGam, não só pelo apoio na parte técnica e discussões científicas, mas também por tornarem os meus dias mais leves e felizes.

À minha querida Clari, pela disponibilidade em ajudar em qualquer aspecto, seja na área pessoal ou técnico-científica. Obrigada, minha amiga!

Aos queridos Fábio Bom, Fernando Lemos e Elisa Milán por sempre me socorrerem na confecção dos mapas;

À minha professora de inglês que se tornou grande amiga, Raissa Arruda, não só pelos ensinamentos linguísticos, mas, principalmente, pelas trocas enriquecedoras e inspiradoras para a vida!

À querida Camila Sukekava por compartilhar o seu valioso conhecimento teórico e prático acerca do método de determinação do Ferro por voltametria. Seu apoio foi imprescindível para a operação do método.

To my deareast friend Jon Higgins for believing in my potential more than myself and for encouraging me to always do my best. Thank you also to his lovely family that many times received me with love in their sweet home;

To my dear friend Anne Maloney for opening the doors of her lovely house for me and for sharing such amazing life experiences;

To my foreign supervisors Pascal Salaün and Stan van den Berg for supporting, supervising and receiving me at the Eletrochemistry Lab. I am so glad and

grateful to have had the opportunity to learn such valuable knowledge during my stay in the University of Liverpool;

To my coleagues from the University of Liverpool, specially Gema Portlock, Léo Mahieu and Arthur Gourain for sharing knowledge and pleasable moments at the lab;

Aos amigos Raquel e Marcelo, que me acolheram como família em seu lar em Liverpool e por me ampararem nos momentos de angústia e medo do “país desconhecido”;

Ao meu co-orientador Camilo Dias por todas as orientações e apoio na discussão dos dados biológicos e à equipe do Laboratório de Fitoplâncton, pela obtenção das amostras e análises de laboratório;

Aos professores Gilberto Barroso e Ana Lima pelas inúmeras contribuições e sugestões para o trabalho desde a etapa da qualificação;

À equipe do Laboratório Poseidon e Oceanografia Geológica, em especial aos professores Renato Ghisolfi e Valéria Quaresma, pela disponibilização dos dados físico-químicos e de Material Particulado em Suspensão;

À Universidade Federal do Espírito Santo e ao Programa de Pós-Graduação em Oceanografia Ambiental pela infraestrutura e apoio logístico-financeiro para a execução dessa pesquisa;

À CAPES pela concessão da bolsa de estudos e pelo financiamento da pesquisa na University of Liverpool a partir do Programa de Doutorado Sanduíche no Exterior;

À FAPES pelo financiamento do projeto “Influência das fontes da matéria orgânica na especiação, biodisponibilidade e biogeoquímica de Ferro na foz do Rio Doce após o desastre de Mariana - MG” que permitiu a consolidação do segundo capítulo da tese;

Enfim, a todos que contribuíram de forma direta ou indiretamente para a conclusão deste trabalho, os meus siceros agradecimentos!

“Veja só a vida como é
Ela é feito o mar é de maré
Tudo vai se acertar
Uma hora vai
(...)
Lembre que existe no céu uma estrela que brilha pra te orientar
Mesmo se o céu escurece ela é como uma prece, não vai se apagar
E se o mar se enfurece, não se desespere, ele vai se acalmar
É só o mundo mostrando que a vida precisa e já sabe nadar
Ao mar.”

Ao Mar - Pedro Pondé

RESUMO

O ciclo biogeoquímico do Fe e de outros metais-traço tem sido amplamente discutido em função do seu papel ecológico como micronutriente para o crescimento da comunidade fitoplanctônica nos oceanos. Estudos experimentais mostram que a fertilização de áreas marinhas com Fe promove o favorecimento de grupos específicos, como diatomáceas e fitoflagelados, embora condições de contaminação por rejeitos de minério não tenham sido avaliadas até o momento. Nesse sentido, o presente estudo teve como objetivo descrever os processos que controlam a estabilidade do Fe dissolvido (dFe) e os efeitos desse metal e de outros nutrientes sobre a comunidade fitoplanctônica na plataforma continental impactada pelo desastre de Fundão. O estudo de revisão bibliográfica indicou que os aportes de dFe provenientes da mineração podem ser mais representativos do que os fluxos por fontes naturais em regiões costeiras vulneráveis a esse tipo de contaminação. Com relação aos impactos dessas atividades, podem ocorrer mudanças na especiação química e biodisponibilidade do Fe, alterações nas estratégias bioquímicas de assimilação pelo fitoplâncton, bem como mudanças na composição desta comunidade, incluindo a proliferação de microalgas tóxicas. A análise da distribuição espaço-temporal do Fe em diferentes frações de tamanho e sua relação com as substâncias húmicas (HS) mostrou que as concentrações desse elemento continuam altas mesmo após três anos do desastre, alcançando máximas de 2,8 µM (dFe, < 0,45 µm), 700 nM (dFe, < 0,22 µm) e 40 nM (Fe solúvel - sFe, < 0,02 µm). HS controla somente 2% e 10% das concentrações de dFe (< 0,22 µm) e sFe, respectivamente, o que estabelece uma condição atípica, uma vez que HS é o principal agente complexante de dFe em áreas costeiras não impactadas. Os resultados sugerem a presença de outra substância complexante (possivelmente compostos de aminas utilizados no beneficiamento do minério de ferro) e/ou a ocorrência de nanopartículas coloidais de óxidos-hidróxidos de Fe (III) que garantem a estabilidade desse elemento em solução. Através da análise das inter-relações entre os metais micronutrientes (Fe, Mn, Zn, Cu, Co e V), nutrientes maiores (Nitrogênio Inorgânico Dissolvido - NID, fosfato e silicato) e a composição fitoplanctônica, constatou-se a influência principalmente de Zn, Cu e V na fração particulada (pZn, pCu e pV) e um menor efeito de Fe particulado (pFe) e dFe sobre a densidade dos grupos algais. Cyanophyceae foi o grupo mais frequente e sua densidade foi determinada pelas concentrações de pFe, que permaneceram elevadas ao longo das campanhas de amostragem. Além disso, a floração de diatomáceas foi definida principalmente pelos níveis de pZn e restrita às condições de aumento da vazão do Rio Doce e níveis específicos de enriquecimento por metais (7pFe, 5pV, 4pCu, 8pZn), sugerindo um controle desse grupo associado aos mecanismos fisiológicos de assimilação de silício. Esses resultados demonstram uma resposta atípica da comunidade em relação ao enriquecimento de Fe, possivelmente associada às formas de metais que estão sendo disponibilizadas através do rejeito. Assim, espécies do grupo das cianobactérias obtém vantagem competitiva em função da sua plasticidade em assimilar diferentes formas de metais. Considerando a continuidade da contaminação por metais na área ao longo de tempo, recomenda-se a análise da inter-relação entre os metais destacados nesse estudo e a possível proliferação de microalgas tóxicas.

Palavras-chave: Contaminação por metais, fitoplâncton, biogeoquímica do Ferro, micronutrientes, rejeito de minério, impactos costeiros.

ABSTRACT

Iron and other trace metal biogeochemistry have been largely discussed because of their ecological role as micronutrients and consequent control on phytoplankton growth in the ocean. Experimental studies have shown that Fe fertilization in marine areas favours specific algae groups, mainly diatoms and flagellates, even though the effects of metal contamination from mining tailings have not been addressed until the moment. The present study describes the processes controlling dissolved Fe (dFe) stability in the water column and the effects of this metal and other nutrients on phytoplankton community in the continental shelf impacted by the Fundão dam mining tailings. The review study indicated that the inputs of dFe from mining activities can be more representative than the fluxes from natural sources in coastal areas vulnerable to this kind of contamination. Regarding to the impacts of those activities, can be predicted changes on Fe chemical speciation and bioavailability, changes on biochemical uptake mechanisms by phytoplankton and also shifts on its community structure, including harmful algae growth. The distribution of Fe in different size-fractions and their relation to humic substances (HS) showed that Fe concentrations remain very high even three years after the disaster, reaching up to 2.8 µM (dFe, < 0.45 µm), 700 nM (dFe, < 0.22 µm) e 40 nM (Soluble Fe - sFe, < 0.02 µm). HS levels control only the binding of 2% and 10% (median values) of dFe (0.22 µm) and sFe concentrations, respectively. This is an unexpected result as HS is the main Fe binding agent in unaffected coastal areas. These results suggest the presence of other organic compounds to bind Fe (possibly amine compounds widely used in the ore extraction process) and/or the occurrence of sFe as colloidal nanoparticulate Fe(III) oxy-hydroxides, both acting to maintain the stability of dFe in solution. The interrelations analyses among metals/micronutrients (Fe, Mn, Zn, Cu, Co e V), major nutrients (Dissolved Inorganic Nirogen - DIN, phosphate and silicate) and phytoplankton composition revealed the influence of Zn, Cu and V in particulate fraction (pZn, pCu e pV) and a lesser contribution of particulate Fe (pFe) and dFe controlling the algae densities. Cyanophyceae was the most frequent group and their density was determined by pFe concentrations that remained high during all sampling surveys. Furthermore, diatoms growth was modulated by pZn levels and restricted to high Doce River discharge and specific metals enrichment conditions (7pFe, 5pV, 4pCu, 8pZn), suggesting a control related to physiological mechanisms of silic acid uptake. These results demonstrated an unexpected behaviour of phytoplankton community in response to metals enrichment and these differences are probably driven by the form of metals from the tailings. Therefore, it has been hypothesized that cyanobacteria species obtained competitive advantages compared to other groups due to their versatile strategies to assimilate metals from a wide range of forms. Considering the continuing metals contamination in the study area during time, it is recommended the integrated analyses between the metals pointed by this study and the possibility of toxic microalgae growth.

Keywords: Metals contamination, phytoplankton, Iron biogeochemisty, micronutrients, mining tailings, coastal impacts.

LISTA DE FIGURAS

LISTA DE TABELAS

SUMÁRIO

1 INTRODUÇÃO GERAL

O Ferro (Fe) é um elemento traço essencial para os organismos marinhos e sua disponibilidade controla a produtividade do fitoplâncton, a estrutura da comunidade e o funcionamento do ecossistema marinho (GLEDHILL; BUCK, 2012). Esse elemento é requerido em processos metabólicos vitais, como a fotossíntese, respiração e captação/assimilação de nitrogênio (MOREL, HUDSON; PRICE, 1991; FALKOWSKI; BARBER; SMETACEK, 1998; MOREL; PRICE, 2003; MOREL; MILLIGAN; SAITO, 2006).

Estudos ecofisiológicos relacionados à influência do Fe sobre a produção fitoplanctônica tiveram incialmente enfoque no Pacífico Subártico, nas regiões com alto teor de nitrato e baixas concentrações de clorofila-*a* (high nitrate, low chlorophyll – HNLC). Essas regiões possuem elevadas concentrações de N e P, mas a baixa disponibilidade de Fe restringe o crescimento e a produtividade do fitoplâncton (KOLBER *et al*., 1994; WELLS; PRICE; BRULAND, 1995). Em regiões oligotróficas, o Fe também é considerado um fator co-limitante para a captação de elementos maiores (nitrogênio, fósforo e silicato). Suas concentrações interferem na cinética das reações e nas propriedades dos sistemas biológicos envolvidos na assimilação dos nutrientes pelos produtores primários (MOREL; HUDSON; PRICE, 1991).

Experimentos de mesoescala têm mostrado que a fertilização com Fe nessas regiões provoca um significativo aumento na produção primária, além de estimular mudanças nos tipos e abundância relativa das espécies planctônicas e afetar níveis tróficos superiores (YOON *et al*., 2016). Com relação à estrutura da comunidade, Bizsel, Öztürk e Metin (1997) constataram que a maior disponibilidade de Fe exerce um controle seletivo sobre o domínio das espécies na assembleia algal, que passa a ser constituída predominantemente por diatomáceas e dinoflagelados.

A influência do Fe sobre a assembleia fitoplanctônica é determinada pela biodispobilidade deste elemento na coluna d'água (WELLS; PRICE; BRULAND, 1995). Para fins de facilitar a avaliação acerca da sua disponibilidade, o Fe é classificado em função da fração de tamanho e especiação química com outros

compostos. Nesse sentido, o Fe pode ser definido operacionalmente pela filtração em fase particulada (pFe; > 0,45 µm) e dissolvida (dFe; < 0,45 µm). A fração dissolvida pode ainda ser subdividida em porção solúvel (sFe; < 1nm) e coloidal (1 nm – 0,45 µm). Apesar de existirem definições das formas coloidais em função do seu peso molecular (< 10 kDa; FITZSIMMONS *et al*., 2015), no presente estudo essa fração está representada pelo material que compreende o intervalo de tamanho inferior a 0,45 µm e maior que 0,02 µm, enquanto que a fração solúvel é inferior a 0,02 µm (WU *et al*., 2001).

Em geral, as formas mais facilmente assimiláveis pelos grupos biológicos incluem-se na fração dissolvida, a qual é altamente influenciada pela complexação com compostos orgânicos naturais, que constituem cerca de 99% das concentrações de dFe (GLEDHILL; van den BERG, 1994; RUE; BRULAND, 1995, 1997). Dentre esses compostos, destacam-se as substâncias húmicas, que constituem a principal classe de ligante orgânico em águas estuarinas e costeiras (LAGLERA; van den BERG, 2009; BATCHELLI *et al*., 2010; LAGLERA; BATTAGLIA; van den BERG, 2011; BUNDY *et al*., 2015), sideróforos produzidos por bactérias heterotróficas e cianobactérias (BARBEAU *et al*., 2001; BARBEAU *et al*., 2003; GLEDHILL *et al*., 2004; MAWJI *et al*., 2008) e as substâncias exopoliméricas (HASSLER *et al*., 2015; NORMAN *et al*., 2015).

Öztürk, Bizsel e Steinnes (2003) mostraram que o *bloom* de fitoplâncton e consequente herbivoria por protozoários foram determinantes para a especiação de Fe na porção interna e média da Baía de Izmir (nordeste do Mediterrâneo, Mar Aegean). Esses autores identificaram uma modificação das espécies de Fe, que estavam predominantemente na forma lábil e, após eventos de floração ocorreram como complexos hidrofóbicos/lipofílicos. Esse resultado foi relacionado à provável complexação com exsudatos celulares, tais como aminoácidos livres ou combinados (ÖZTÜRK; BIZSEL; STEINNES, 2003). A contribuição do fitoplâncton para a especiação de Fe também pode variar em função da estrutura da comunidade. Bizsel, Öztürk e Metin (1997) mostraram que maiores concentrações de Fe reativo ocorrem em função do aumento de populações de Euglenophyceae. Assim, a inter-relação Fe/comunidade fitoplanctônica ocorre na forma de *feedback* positivo e

bidirecional, uma vez que o Fe é um micronutriente essencial para o crescimento algal, enquanto esses organismos determinam a sua especiação e biodisponibilidade em função da produção e liberação de agentes quelantes (WELLS; PRICE; BRULAND, 1995).

Uma das questões chave para a compreensão do ciclo do Fe em ambientes aquáticos envolve a elucidação da influência deste elemento sobre os processos que estimulam a comunidade fitoplanctônica e, contrariamente, de que forma esse grupo interfere na especiação e biodisponibilidade do Fe (WELLS; PRICE; BRULAND, 1995). Desta forma, estudos acerca da biogeoquímica e especiação deste metal e suas implicações sobre a base da teia trófica podem trazer resultados de grande relevância científica, além de fornecer subsídios para a elaboração de estratégias de manejo e conservação em áreas sujeitas ao processo de contaminação com Fe e outros metais.

1.1 Justificativa

O rompimento da barragem de rejeito de minério de ferro de Fundão, em Mariana – MG foi considerado um dos maiores desastres ambientais da indústria da mineração a nível global (CARMO *et al*. 2017). Após o colapso, em 5 de novembro de 2015, mais de 55 milhões de m^3 de água e rejeitos foram carreados para o Rio Doce e se deslocaram por mais de 600 km, alcançando o estado do Espírito Santo e o Oceano Atlântico (ESCOBAR, 2015).

Análises realizadas antes e após a chegada dos rejeitos na foz do Rio Doce e plataforma continental adjacente mostram que o aumento das concentrações de Fe alcançou até duas ordens de grandeza. Para o Fe total, a concentração mais elevada (52.360 mg/L) foi registrada nas amostras de água de fundo coletadas na estação próxima à costa. Para a fração dissolvida, a concentração máxima foi de 226 mg/L em uma estação localizada perto da desembocadura (NETO *et al*., 2016). Em ambiente marinho, o Fe apresenta baixa solubilidade e tende a ser removido da coluna d'água por precipitação na forma de óxidos-hidróxidos de Fe(III) (LIU; MILLERO, 2002). No entanto, estudos de monitoramento na área mostram que as concentrações desse elemento na forma dissolvida permanecem elevadas ao longo do tempo

(BASTOS *et al*., 2017) indicando alta estabilidade na coluna d'água possivelmente relacionada à complexação com compostos orgânicos.

Com relação à assembleia fitoplanctônica, foi constatado o aumento da biomassa em termos de clorofila-*a* nas estações localizadas próximo à foz do Rio Doce, bem como mudanças na composição da comunidade, que anteriormente apresentava predominância do grupo Coccolitophyceae e, após o desastre, passou a ser dominada por espécies do grupo Cyanophyceae (BASTOS *et al*., 2017).

Vários projetos de pesquisa têm sido desenvolvidos na área a fim de avaliar o grau do impacto relacionado ao desastre (e.g. HATJE *et al*., 2017; GOMES *et al*., 2017; QUEIROZ *et al*., 2018). No entanto, ainda não foram elucidados os aspectos relacionados à especiação e estabilidade das concentrações de Fe na área de estudo e os efeitos do enriquecimento com metais sobre a comunidade fitoplanctônica. Assim, o presente trabalho realiza uma análise integrada dos processos geoquímicos e biológicos a fim de compreender os impactos efetivos desse desastre sobre a base da teia trófica na região costeira adjacente à foz do Rio Doce.

2 HIPÓTESES DE PESQUISA

O presente trabalho assume as seguintes hipóteses:

1) A complexação orgânica do Fe dissolvido (dFe) com substâncias húmicas (HS) mantem a estabilidade e disponibilidade desse elemento na coluna d'água após o desastre de Fundão;

2) O aporte de metais para a área costeira decorrente do desastre de Fundão modificou a estrutura da comunidade fitoplanctônica, permitindo o favorecimento de grupos com potencial tóxico para o ecossistema.

3 OBJETIVOS

3.1 Objetivo geral

Descrever os processos que definem a estabilidade do Fe na fração dissolvida e avaliar os efeitos desse metal e de outros elementos traço/micronutrientes (i.e. Mn, Zn, Cu, Co, V) sobre a estrutura da comunidade fitoplanctônica.

3.2 Objetivos específicos

- Determinar os padrões espacial e temporal de distribuição do Fe em diferentes frações de tamanho (particulada, dissolvida e solúvel);
- Avaliar os fatores que definem a disponibilidade/estabilidade do Fe dissolvido (dFe) e solúvel (sFe) na coluna d'água;
- Determinar a influência do Fe particulado e dissolvido sobre os parâmetros quantitativos (clorofila-a, feopigmentos e densidade numérica) e qualitativos (frequência de ocorrência dos grupos predominantes) da comunidade fitoplanctônica;
- Analisar a ocorrência de sinergia com outros elementos limitantes (nutrientes inorgânicos dissolvidos e metais micronutrientes – Cu, Zn, Mn, V, Co) sobre a comunidade fitoplanctônica.

4 ESTRUTURA DA TESE

A tese encontra-se estruturada em quatro capítulos, conforme descrição apresentada nos itens a seguir.

4.1 Capítulo 1: Review and synthesis: iron input, biogeochemistry, and ecological approaches in seawater

No Capítulo 1, foi elaborado um artigo de revisão que descreve as diferentes etapas do ciclo do Fe na água do mar, desde a contribuição das fontes externas, processos de reciclagem interna, especiação química, biodisponibilidade e alterações na estrutura da comunidade fitoplanctônica. Além disso, foi realizada uma contextualização do problema diante do enriquecimento antrópico exemplificado pelo desastre ambiental do rompimento da barragem de Fundão. Esse capítulo forneceu o embasamento teórico para a elaboração das hipóteses de pesquisa do presente trabalho, além de direcionar as discussões dos demais capítulos/etapas de pesquisa. O artigo produzido foi publicado na Revista **Environmental Reviews**, conforme referência abaixo:

• Longhini, C.M.; Sá, F.; Neto, R.R. 2019. Review and synthesis: iron input, biogeochemistry, and ecological approaches in seawater. Environmental Reviews, 27: 2, pp. 125-137. https://doi.org/10.1139/er-2018-0020.

4.2 Capítulo 2: Coastal waters contamination by mining tailings: what triggers the stability of iron in the dissolved fractions?

O artigo que compõe este capítulo apresenta os dados produzidos durante o doutorado sanduíche na University of Liverpool em que foram realizadas as análises de Ferro nas frações coloidal (< 0,22 µm) e solúvel (< 0,02 µm) e a determinação de substâncias húmicas (HS) em amostras de água coletadas na plataforma continental adjacente à foz do Rio Doce após o desastre de Fundão. Este capítulo teve como objetivo descrever os processos que determinam a estabilidade do dFe na área costeira afetada pelos rejeitos de minério de Fundão, a fim de responder à **Hipótese 1** de pesquisa. O artigo intitulado "Coastal waters contamination by mining tailings: what triggers the stability of iron in the dissolved fractions?" foi submetido para a revista **Limnology and Oceanography**.

- Longhini, C.M.; Mahieu, L.; Sá, F.; van den Berg, C.M.G.; Salaün, P.; Neto, R.R. Coastal waters contamination by mining tailings: what triggers the stability of iron in the dissolved fractions?

4.3 Capítulo 3: Phytoplankton response to metal enrichment in coastal area affected by mining tailing catastrophe

Esse capítulo teve como objetivo avaliar a distribuição de metais/micronutrientes e os efeitos desses elementos combinados com outros fatores (i.e., nutrientes maiores e variáveis físico-químicas) sobre a comunidade fitoplanctônica. O trabalho discute, de forma integrada, os impactos do enriquecimento por metais na área costeira afetada pelo rejeito de minério de Fundão, de forma a responder à **Hipótese 2** de pesquisa. O artigo intitulado "Phytoplankton response to metal enrichment in a coastal area affected by a mining tailing disaster" será revisado pelos demais autores e submetido à revista **Science of the Total Environment**.

4.4 Capítulo 4: Conclusões

O Capítulo 4 teve como objetivo realizar uma análise integrada das conclusões dos capítulos 1, 2 e 3, a fim de estabelecer uma inter-relação dos aspectos biogeoquímicos associados à contaminação costeira pelo rejeito de

Fundão e as consequentes respostas ecológicas da comunidade fitoplanctônica na área impactada.

5 REFERÊNCIAS

BARBEAU, K.; RUE, E.L.; BRULAND, K.W.; BUTLER, A. Photochemical cycling of iron in the surface ocean mediated by microbial iron(III)-binding ligands. **Nature**, v. 413, n. 6854, p. 409–413, 2001.

BARBEAU, K.; RUE, E.L.; TRICK, C.G.; BRULAND, K.W.; BUTLER, A. Photochemical reactivity of siderophores produced by marine heterotrophic bacteria and cyanobacteria based on characteristic Fe(III) binding groups. **Limnology and Oceanography**, v. 48, n. 3, p. 1069–1078, 2003.

BASTOS, A.C.; OLIVERIA, K.S.S.; FERNANDES, L.F.; PEREIRA, J.B.; DEMONER, L.E.; NETO, R.R.; COSTA, E.S.; SÁ, F.; SILVA, C.A.; LERHBACK, B.D.; DIAS JR., C.; QUARESMA, V.S.; ORLANDO, M.T.D.; TURBAY, C.V.G.; LOPES, B.A.; LEITE, M.D.; GHISOLFI, R.D.; LEMOS, A.T.; PIVA, T.R.M.; LÁZARO, G.C.S.; CONCEIÇÃO, J.R.; LEMOS, K.N.; ZEN, C.M.; BONECKER, A.C.T.; CASTRO, M.S.; QUINTAS, M.C.; CAVAGGIONI, L.; OLIVEIRA, E.M.C. **Monitoramento da Influência da Pluma do Rio Doce após o rompimento da Barragem de Rejeitos em Mariana/MG – Novembro de 2015**: Processamento, Interpretação e Consolidação de Dados. Vitória: Universidade Federal do Espírito Santo, 2017, 254p. Disponível em: http://www.icmbio.gov.br/portal/images/stories/Rio_Doce/relatorio_consolidado_ufes_rio_doce.pdf [acesso em 07 Agosto de 2017].

BATCHELLI, S.; MULLER, F. L. L.; CHANG, K. C.; LEE, C.L. Evidence for strong but dynamic iron-humic colloidal associations in humic-rich coastal waters**. Environmental Science & Technology**, v. 44, p. 8485–8490, 2010.

BIZSEL, N.; ÖZTÜRK, M.; METIN, G. The role of iron on the phytoplankton growth in heavily polluted Izmir Bay, Aegean sea. **WIT Transactions on Ecology and the Environment**, v. 14, p. 659 – 669, 1997.

BUNDY, R.M.; ABDULLA, H.A.N.; HATCHER, P.G.; BILLER, D.V.; BUCK, K.N.; BARBEAU, K.A. Iron-binding ligands and humic substances in the San Francisco Bay estuary and estuarine-influenced shelf regions of coastal California. **Marine Chemistry**, v. 173, p. 183–194. 2015.

CARMO, F. F. do; KAMINO, L. H. Y.; TOBIAS JUNIOR, R.; CAMPOSA, I.C. de; CARMO, F.F. do; SILVINO, G.; CASTRO, K.J.S.X. de; MAURO, M.L.; RODRIGUES, N.U.A.; MIRANDA, M.P.S.; PINTO, C.E.F. Fundão tailings dam failures: the environment tragedy of the largest technological disaster of Brazilian mining in global context. **Perspectives in Ecology and Conservation**, v. 15, p. 145–151, 2017.

ESCOBAR, H. Mud tsunami wreaks ecological havoc in Brazil. **Science**, v. 350, n. 6265, p. 1138-1139, 2015.

FALKOWSKI, P.G.; BARBER, R.T.; SMETACEK, V.V. Biogeochemical Controls and Feedbacks on Ocean Primary Production. **Science**, v. 281, n. 5374, p. 200-206, 1998.

FITZSIMMONS, J. N.; BUNDY, R. M.; AL-SUBIAI, S. N.; BARBEAU, K. A.; BOYLE, E. A. The composition of dissolved iron in the dusty surface ocean: An exploration using size-fractionated iron-binding ligands. **Marine Chemistry**, v. 173, p. 125-135, 2015.

GLEDHILL, M.; BUCK, K.N. The organic complexation of iron in the marine environment: a review. **Frontiers in Microbiology**, v. 29, p. 1-17, 2012.

GLEDHILL, M.; van den BERG, C.M.G. Determination of complexation of iron(III) with natural organic complexing ligands in seawater using cathodic stripping voltammetry. **Marine Chemistry**, v. 47, p. 41–54, 1994.

GLEDHILL, M.; McCORMACK, P.; USSHER, S.; ACHTERBERG, E.P.; MANTOURA, R.F.C.; WORSFORD, P.J. Production of siderophore type chelates by mixed bacterioplankton populations in nutrient enriched seawater incubations. **Marine Chemistry**, v. 88, p. 75–83, 2004.

GOMES, L.E.O.; CORREA, L.B.; SÁ, F.; NETO, R.R.; BERNARDINO, A.F. The impacts of the Samarco mine tailing spill on the Rio Doce estuary, Eastern Brazil. **Marine Pollution Bulletin***,* v. 120, p. 28–36, 2017.

HASSLER, C.S.; NORMAN, L.; NICHOLS, C.A.M.; CLEMENTSON, L.A.; ROBINSON, C.; SCHOEMANN, V.; .WATSON, R.J., DOBLIN, M.A. Iron associated with exopolymeric substances is highly bioavailable to oceanic phytoplankton. **Marine Chemistry***, v.* 173, p. 136–147, 2015.

HATJE, V.; PEDREIRA, R.M.A.; REZENDE, C.E. de; SCHETTINI, C.A.F.; SOUZA, G.C. de; MARIN, D.C.; HACKSPACHER, P.C. The environmental impacts of one of the largest tailing dam failures worldwide. **Scientific Reports – Nature***,* v. 7, n. 10706, p. 1–16, 2017.

KOLBER, Z.S.; BARBER, R.T.; COALE, K.H.; FITZWATERI, S.E.; GREENE, R.M.; JOHNSON, K.S.; LINDLEY, S.; FALKOWSKI, P.G. 1994. Iron limitation of phytoplankton photosynthesis in the equatorial Pacific Ocean. **Nature**, 371(6493): 145-149.

LAGLERA, L.M.; van den BERG, C.M. Evidence for geochemical control of iron by humic substances in seawater. **Limnology and Oceanogaohy***,* v. 54, n. 2, p. 610–619, 2009.

LAGLERA, L.M.; BATTAGLIA, G.; van den BERG, C.M. Effect of humic substances on the iron speciation in natural waters by CLE/CSV. **Marine Chemistry***,* v. 127, n. 1–4, p. 134–143, 2011.

LIU, X.; F.J. MILLERO. The solubility of iron in seawater. **Marine Chemistry**, v. 77, p. 43–54, 2002. doi:10.1016/S0304-4203(01)00074-3.

MAWJI, E.; GLEDHILL, M.; MILTON, J.A.; TARRAN, G.A.; USSHER, S.; THOMPSON, A.; WOLFF, G.A.; WORSFOLD, P.J.; ACHTERBERG, E.

Hydroxamate siderophores: occurrence and importance in the Atlantic Ocean. **Environmental Science & Technology**, v. 42, p. 8675–8680, 2008.

MOREL, F. M. M.; PRICE, N. M. The biogeochemical cycles of trace metals in the oceans. **Science**, v. 300, n. 5621, p. 944-947, 2003.

MOREL, F. M.; HUDSON, R. J.; PRICE, N. M. Limitation of productivity by trace metals in the sea. **Limnology and Oceanography**, v. 36, n. 8, p. 1742-1755, 1991.

MOREL, F.M.M.; MILLIGAN, A.J.; SAITO, M.A. Marine Bioinorganic Chemistry: The Role of Trace Metals in the Oceanic Cycles of Major Nutrients. In: Elderfield, H., Holland, H. D.; Turekian, K. K. (Org.). **The oceans and marine geochemistry**, v. 26, Elsevier, 2006, 664 p.

NETO, R.R.; SÁ, F.; CARNEIRO, M.T.W.D.; COSTA, E.S.; RODRIGUES, D.R.P. **The worst Brazilian environmental disaster altered the distribution of metals in water ate the Doce River Estuary and marine region**. In: International conference on heavy metals in the environment (ICHMET 2016), 2016.

NORMAN, L.; WORMS, I.A.M.; ANGLES, E.; BOWIE, A.R.; NICHOLS, C.M.; PHAM, A.N.; SLAVEYKOVA, V.I.; TOWNSEND, A.T.; WAITE, T.D.; HASSLER, C.S. The role of bacterial and algal exopolymeric substances in iron chemistry. **Marine Chemistry**, v. 173, p. 148–161, 2015.

ÖZTÜRK, M.; BIZSEL, N.; STEINNES, E. Iron speciation in eutrophic and oligotrophic Mediterranean coastal waters; impact of phytoplankton and protozoan blooms on iron distribution. **Marine Chemistry**, v. 81, n. 1, p. 19-36, 2003.

QUEIROZ, H.M.; NÓBREGA, G.N.; FERREIRA, T.O.; ALMEIDA, L.S.; ROMERO, T.B.; SANTAELLA, S.T.; BERNARDINO, A.F.; OTERO, X.L. The Samarco mine tailing disaster: A possible time-bomb for heavy metals contamination? **Science of the Total Environment**, v. 637–638, p. 498–506, 2018.

RUE, E.L.; BRULAND, K.W. Complexation of iron(III) by natural organic ligands in the Central North Pacific as determined by a new competitive ligand equilibration/adsorptive cathodic stripping voltammetric method. **Marine Chemistry**, v. 50, n. 1–4, p. 117–138, 1995.

RUE, E.L.; BRULAND, K.W. The role of organic complexation on ambient iron chemistry in the equatorial Pacific Ocean and the response of a mesoscale iron addition experiment. **Limnology and Oceanography**, v. 42, n. 5, p. 901–910, 1997.

WELLS, M. L.; PRICE, N. M.; BRULAND, K. W. Iron chemistry in seawater and its relationship to phytoplankton: a workshop report. **Marine Chemistry**, v. 48, n. 2, p. 157-182, 1995.

WU, J.; BOYLE, E.; SUNDA, W.; WEN, L. S. Soluble and colloidal iron in the oligotrophic North Atlantic and North Pacific. **Science**, v. 293, p. 847-849, 2001.

YOON, J.-E.; YOO, K.-C.; MACDONALD, A.M.; YOON, H.I.; PARK, K.-T.; YANG, E.-J.; KIM, H.-C.; LEE, J.I.; LEE, M.K.; JUNG, J.; PARK, J.; SONG, J.-M.; CHOI, T.-J.; KIM, K.; KIM, I.-N. Ocean Iron Fertilization Experiments: Past-Present-Future with Introduction to Korean Iron Fertilization Experiment in the Southern Ocean (KIFES) Project. **Biogeosciences Discussions**, p. 1-41, 2016.

CAPÍTULO 1

REVIEW AND SYNTHESIS: IRON INPUT, BIOGEOCHEMISTRY, AND ECOLOGICAL APPROACHES IN SEAWATER

Longhini, C. M., F. Sá, and R. R. Neto. Review and synthesis: iron input, biogeochemistry, and ecological approaches in seawater. **Environmental Reviews**, v. 27, p. 125–137, 2019. doi:10.1139/er-2018-0020

ABSTRACT

The processes involved in the biogeochemical cycle of Fe in the oceans have been intensely discussed in recent decades because this element is limiting to primary productivity in most oceanic regions. From biogeochemical and ecological perspectives, inputs from anthropogenic sources, especially mining activities, may be more representative than natural inputs in coastal areas affected by metal loads from tailings. Here we provide a review of all the stages related to Fe behaviour in marine ecosystems, including Fe input sources, which may be of natural and (or) anthropogenic origin; input rates; chemical speciation; bioavailability; and changes in the phytoplankton community structure. To allow conceptualization of the anthropogenic processes, the collapse of the Fundão tailings dam (southeast Brazil) was used as a case study of one of the worst environmental disasters of the mining industry. From this perspective, the interrelations among the chemical, biological, and ecological components were discussed. Regarding the chemical component, Fe speciation must be determined by the input of several other materials, mainly organic compounds that can be complexed to this element and increase its solubility. From a biological perspective, the biochemical and physiological processes used for the assimilation of this element, such as the reduction in cell membranes and the production of chelating substances (such as siderophores), will also determine the forms of this element present in the water column. On the other hand, the groups that obtain a competitive advantage due to these assimilation strategies must be dominant in the system. Synergistic effects are also expected with other materials such as the inorganic nutrients, organic compounds, and metals that are carried to the coastal region together with Fe. In the specific case of mine tailings, the accumulation of this material in the river banks and bed should cause an increase in Fe input from other sources, such as atmospheric transport and submarine groundwater discharge, as well as river discharge by erosion and transport under increased river flow conditions. The iron fluxes from mining areas to coastal oceans and the effects of these loads to phytoplankton ecological aspects should be investigated.

Key words: iron cycle, seawater, mine tailings, dissolved iron, iron bioavailability.

6 INTRODUCTION

Although iron (Fe) is one of the most abundant elements in the crust (SILVER, 1993), it occurs in trace concentrations in most of the oceans and limits primary production (WATSON, 2001; BRISTOW *et al*. 2017) because it is required for vital metabolic processes, such as photosynthesis, respiration, and nitrogen assimilation (MOREL; HUDSON; PRICE, 1991; MOREL; MILLIGAN; SAITO, 2003; FALKOWSKI; BARBER; SMETACEK, 1998; MOREL; PRICE, 2003).

The Fe cycle in seawater is determined by the interaction of processes that occur in the chemical–biogeochemical, biological, and ecological components of the ecosystem (WELLS; PRICE; BRULAND, 1995). In the chemical component, concentrations are limited mainly by oxidation reactions that promote precipitation of Fe as insoluble oxides–hydroxides ($Fe(OH)_X^Y$) (BYRNE; KESTER, 1976; KUMA; SUZUKI; MATSUNAGA, 1993; MILLERO; PIERROT, 2002). The complexation of Fe with organic substances, which accounts for approximately 99% of the dissolved fraction of Fe and increases its solubility in the water column, can compensate for this removal (GLEDHILL; van den BERG, 1994; RUE; BRULAND, 1995, 1997). In coastal waters, humic substances from continental inputs are the main forms of organic ligands (LAGLERA; van den BERG, 2009). However, in oceanic regions, the exopolymeric substances (EPS) have a relevant participation in this process (NORMAN *et al*. 2015; HASSLER *et al*. 2015).

From a biological perspective, Fe bioavailability depends on aspects related to the biochemistry and physiology of the phytoplanktonic organisms, which use different assimilation strategies, such as the production of strong siderophore ligands that enable the solubilization of colloidal Fe (KUMA; NISHIOKA; MATSUNAGA, 1996) or absorption of the particulate fraction (GOLDBERG, 1952; RUBIN; BERMAN-FRANK; SHAKED, 2011; SUGIE *et al*. 2013). In the ecological context, artificial and natural fertilization with Fe in areas where this element is limiting modifies the relative abundance of the species (KOLBER *et al*. 1994; WELLS; PRICE; BRULAND, 1995), resulting in increased dominance of specific groups such as toxic microalgae (ZHUO-PING *et al*. 2009; TRICK *et al*. 2010).

Fe input in the oceans from anthropogenic sources, resulting from the exploitation, processing, and storage of Fe ore, has gained global attention in the last 2 years due to the collapse of the Fundão dam in the region known as Quadrilátero Ferrífero (Minas Gerais, Brazil). At that time, more than 50 million m^3 of water and tailings were carried to the Doce River, where they travelled for more than 600 km, reaching the Atlantic Ocean (ESCOBAR, 2015). This event was classified as the worst global disaster in the mining industry in terms of tailings volume, geographic extent, and the magnitude of the damage caused (CARMO *et al*. 2017).

The review articles published in the last 10 years on Fe in the oceans have focused on its biogeochemical cycle and solubility (BAKER; CROOT, 2010; BOYD; ELLWOOD, 2010; NORMAN *et al*. 2014; TAGLIABUE *et al*. 2017), evolution of the oxidation process (WILLIAMS, 2012; ILBERT; BONNEFOY, 2013), organic speciation–chelating compounds, dissolved Fe distribution and bioavailability (BUTLER; THEISEN, 2010; GLEDHILL; BUCK, 2012; TAGLIABUE *et al*., 2012; BOYD; TAGLIABUE, 2015; von der HEYDEN; ROYCHOUDHURY, 2015; KHAN; SINGH; SRIVASTAVA, 2018; BRISTOW *et al*., 2017), analytical techniques (WORSFOLD *et al*., 2014; LAGLERA; FILELLA, 2015; LAGLERA; MONTICELLI, 2017), experimental research (BOYD *et al*., 2007; YOON *et al*., 2018), and the effects of natural and artificial fertilization on the structure of planktonic communities (QUÉGUINER, 2013). However, the interrelation of these different factors under anthropogenic enrichment conditions has not been discussed.

This review provides an integrated evaluation of the processes that regulate the cycle of dissolved Fe in seawater, focusing on the external input of Fe. In addition, a schematic is developed to discuss the importance of the interrelations in the chemical, biological, and ecological components in situations of anthropogenic Fe enrichment, as in the case of the Fundão environmental disaster.

7 BIOGEOCHEMICAL CYCLE OF FE IN THE OCEANS

In seawater, Fe can be found in different types of associations and is operationally divided into particulate (> 0.45 μm) and dissolved (<0.45 μm)

fractions based on filtration. The dissolved fraction is subdivided into colloidal (1 nm–0.45 µm) and soluble (<1 nm) fractions. Considering that the biologically available forms of Fe are mainly in the dissolved state (RAISWELL; CANFIELD, 2012), this fraction is most frequently used in studies on biogeochemistry. The Fe cycle in the oceans involves complex interactions between the external inputs, transformations, and chemical speciation of this element and the processes of removal and internal recycling (BOYD; ELLWOOD, 2010).

The external sources addressed in this work include atmospheric dust, rivers–estuaries, hydrothermal vents, and submarine groundwater discharge (SGD). The anthropogenic input will also be discussed, especially contamination with tailings from Fe ore exploitation and processing activities.

7.1 External sources of Fe

7.1.1 Atmospheric dust

The atmosphere is the main source of Fe for the oceanic region (JOHNSON; GORDON; COALE, 1997) and is probably the dominant entry route of this element in the photic zone (DUCE; TINDALE, 1991). This source is represented by the transport and deposition of dust from the arid and semi-arid regions, most of them located at the midlatitudes of the Northern Hemisphere (SCHUTZ *et al*., 1990), with the African deserts accounting for 50%–70% of the global emissions (GINOUX *et al*., 2012).

This export occurs mainly in a region called the Saharan Air Layer, an area between 1.5 and 3.7 km of altitude, characterized by dry, hot, dust-laden air that expands northwest of Africa in the North Atlantic (PROSPERO; CARLSON, 1972). In this region, the influence of atmospheric dust can be seen up to a distance of 5000 km from the source (PROSPERO, 1999), mainly because of the long distance transportation of particles smaller than 10 µm in diameter (PYE, 1987). On a global ocean scale, the Fe input from dust is restricted to the tropical Atlantic (TAGLIABUE; AUMONT; BOPP, 2014). Studies conducted in the northeastern part of the Tropical Atlantic Ocean showed a significant increase in the concentrations of dissolved Fe from 0.20 nmol to 0.25 nmol after a dust event in the Sahara Desert (RIJKENBERG *et al*., 2008). In

Namibia, alluvial deposits in ephemeral river valleys are sources of bioavailable Fe that is transported by wind erosion and contributes to the fertilization of adjacent marine systems (DANSIE; WIGGS; THOMAS, 2017).

The atmospheric input of Fe in the oceans occurs either through dry or wet deposition. According to de Baar, de Jong (2001), dry deposition corresponds to 70% of this source, contributing 175–440 × 10^9 mol yr^{-1} of total Fe. The wet deposition, on the other hand, is more relevant for the input of dissolved Fe (10–26 × 10^9 mol yr^{-1} of dissolved Fe) (JICKELLS; SPOKES, 2001; de BAAR; de JONG, 2001), which is the most bioavailable form of this element. The results from 13 different global ocean biogeochemistry models shows high variability of the Fe fluxes from dust, ranged from 1.4 to 32.7 × 10^9 mol dFe yr^{-1} (TAGLIABUE *et al*., 2016) (Table 1).

The solubility and contribution of the atmospheric minerals to the dissolved Fe pool increases because of the presence of acid pollutants (RAVELO-PÉREZ *et al*., 2016), complexation with organic compounds present in the marine aerosol solution (MESKHIDZE *et al*., 2017), and the presence of combustion products (WOZNIAK *et al*., 2015).

Table 1 - Dissolved iron inputs from natural sources to ocean and regional iron fluxes in areas affected by mining activities.

External sources of dissolved iron	Fluxes	Scale	Reference
Natural inputs to ocean (× 10^9 mol dFe yr^{-1})			
Atmospheric dust	10.0–26.0	Global	de Baar, de Jong (2001)
	1.4–32.7	Global	Tagliabue *et al*. (2016)
Gross river fluxes[b]	26.0	Global	de Baar, de Jong (2001)
Rivers–estuaries	1.5[c]	Global	de Baar, de Jong (2001)
	0.06–2.5	Global	Tagliabue *et al*. (2016)[a]
SGD	2.0 × 10^6 mol dFe d^{-1}	South Atlantic Ocean, south of Brazil	Windom *et al*. (2006)
Hydrothermal vents	20 × 10^9 g dFe yr^{-1} (0.4 × 10^9 mol dFe yr^{-1})	Southern Ocean	Tagliabue *et al*. (2010)
	11.3–17.7	Global	Tagliabue *et al*. (2016)

Table 1 - Dissolved iron inputs from natural sources to ocean and regional iron fluxes in areas affected by mining activities.

External sources of dissolved iron	Fluxes	Scale	Reference
Benthic fluxes–sediment	47.0–89.0	Global (continental shelf)	Elrod *et al*. (2004)[d]
	0.6–84.6	Global	Tagliabue *et al*. (2016)
Upwelling	2.2	Global (continental shelf)	Elrod *et al*. (2004)
Iron fluxes in areas affected by mining activities			
Submarine groundwater discharge	4.0–32.0 mol dFe d^{-1} km^{-1}	Regional, El Gorguel Bay (Cartagena–La Unión Pb–Zn mining district, Murcia, Spain)	Trezzi *et al*. (2016)
Gross river fluxes[b]	1800 tons dFe yr^{-1} (3.2×10^7 mol dFe yr^{-1})	Regional, Tinto and Odiel Rivers (South West Spain)	Braungardt *et al*. (2003)
	7922 tons dFe yr^{-1} (1.4×10^8 mol dFe yr^{-1})	Regional, Tinto and Odiel Rivers (South West Spain)	Olías *et al*. (2006)
	770.0 tons dFe (1.4×10^7 mol dFe)[e]	Regional, Tinto River (South West Spain)	Cánovas *et al*. (2008)
Rivers–estuaries	58.8 mg dFe s^{-1} (1.1×10^{-5} mol dFe s^{-1})	Regional, Doce River Mouth (Southeast Brazil)	Hatje *et al*. (2017)
Water discharges from abandoned mines[f]	550 tons yr^{-1} (9.8×10^6 mol Fe yr^{-1})	Regional, England and Wales	Mayes, Potter and Jarvis (2010)

a - Range of data from 13 global ocean biogeochemistry models compiled by Tagliabue et al. (2016).
b - Without discount the estuarine trapping.
c - Truly dissolved iron (discounting the estuarine trapping and considering the relative molar mass for dissolved iron).
d - Measured with flux chambers along the California coast and extrapolated to global shelf.
e - Fluxes measured only in a month during a flood event (value not converted by time period).
f - Total iron mass flux released to surface waters from abandoned mine sites.

7.1.2 Rivers and estuaries

The fluvial input of Fe to the oceans occurs mainly in particulate form (RICKARD, 2012), and input is limited by the deposition of the metal matrices associated with the particulate matter as well as by the flocculation of dissolved Fe in the estuarine portion (BOYLE; EDMOND; SHOLKOVITZ, 1977; SHOLKOVITZ; BOYLE; PRICE, 1978; JOHNSON; GORDON; COALE, 1997).

In fluvial waters, dissolved Fe is present in the form of colloids that are stabilized by the association of Fe oxides–hydroxides with organic matter. In estuarine areas, these negatively charged colloids are neutralized by seawater

cations, thereby allowing flocculation and formation of the precipitates that remove dissolved Fe (BOYLE; EDMOND; SHOLKOVITZ, 1977). *In situ* observations and laboratory experiments show that the removal rate by estuarine mixing ranges from 90% to 95% due to flocculation with organic matter (SHOLKOVITZ; BOYLE; PRICE, 1978; BOYLE; EDMOND; SHOLKOVITZ, 1977), mainly high molecular-weight humic acids (SHOLKOVITZ; BOYLE; PRICE, 1978) (Fig. 1).

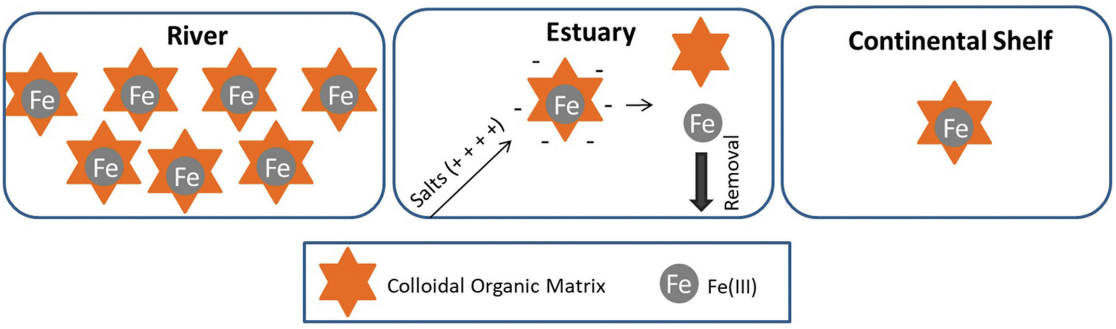

Figure 1. Dissolved Fe, present in the form of colloids in the rivers, is released in the estuaries due to the neutralization of the colloids by seawater cations and precipitates in the form of oxides and hydroxides. Only 5%–10% is transported to the continental shelf, reaching up to 20% when complexed with low molecular-weight fulvic acids.

However, the contribution of this source to the Fe input increases by 20% because of its complexation with low molecular weight fulvic acids (KRACHLER; JIRSA; AYROMLOU, 2005) reaching 3300 nmol L^{-1} (KRACHLER *et al*., 2010) and a release rate in seawater from 6.25 to 8.4 mol L^{-1} of Fe in tributaries of bog environments rich in these organic substances (KRACHLER *et al*., 2016). It is possible that the electrostatic stability conditioned by these complexes limits flocculation in the estuarine mixing zone, causing bog ecosystems to act as important sources of dissolved Fe to the coastal waters and continental shelves (KRACHLER *et al*., 2010, 2015, 2016).

In addition, a significant fraction of the particulate matter of river origin dissolves in seawater because of ligand exchange reactions with marine Fe binding ligands and plays a large role in the bioavailability of Fe and other trace elements in coastal regions (JEANDEL; OELKERS, 2015).

Among the large rivers of the world, the Amazon River Basin accounts for 5%–30% of the total fluvial Fe transport to the oceans (POITRASSON *et al*., 2014). According to estimates by de Baar, de Jong (2001), the dissolved Fe

input to the oceans from continental discharge, already discounting the estuarine removal rate, is 1.5 × 10^9 mol yr^{-1}. According to data from models compiled by Tagliabue *et al*. (2016), the fluxes of dissolved Fe from rivers to ocean ranged from 0.06 to 2.5 × 10^9 mol dFe yr^{-1} (Table 1).

The sediment transported from the continental margin and the resuspension on the continental shelf are also important sources of Fe to the coastal area (JOHNSON; CHAVEZ; FRIEDERICH, 1999; ELROD *et al*., 2004; TAGLIABUE; BOPP; AUMONT, 2009; ELLWOOD *et al*., 2014; GRAHAM *et al*., 2015; de JONG *et al*. 2015). The influence of these factors, especially resuspension and contribution of the benthic component, will be discussed in section 2.2, which addresses the internal recycling processes.

7.1.3 Hydrothermal vents

Hydrothermal vents are enriched in many trace elements, and their fumaroles on the ocean floor allow hot and acid fluid to mix rapidly with the cool, alkaline, and oxygenated bottom waters. In these conditions, Fe is predominantly found as insoluble oxide-hydroxide particles (FEELY *et al*., 1990; MOTTL; McCONACHY, 1990). The precipitation rate of these particles is approximately the same as the release rate, reaching up to 95% (GERMAN; CAMPBELL; EDMOND, 1991). As a result, the net input of Fe dissolved from this route is considered negligible by some authors (GERMAN; CAMPBELL; EDMOND, 1991; de BAAR; de JONG, 2001). However, based on ^{3}He flux measurements and modelling, Tagliabue *et al*. (2010) showed that dissolved Fe concentrations in deep waters are strongly affected by hydrothermalism, particularly in the Southern Hemisphere. According to these authors, the dissolved Fe flux from hydrothermal vents is constant on a millennial timescale and must buffer the changes originating from sources with short-term variability such as atmospheric deposition (TAGLIABUE *et al*., 2010). The strong complexation of Fe with organic matter, whose concentration is generally high in these areas, prevents its oxidation and precipitation thus allowing this element to remain in suspension and available in the water column (TAGLIABUE *et al*., 2010; KLEINT; PICHLER; KOSCHINSKY, 2017).

Kleint, Pichler and Koschinsky (2017) showed that hydrothermal vents located in shallow waters (5 m depth) of the Dominica Coast (Lesser Antilles Island Arc, Caribbean) release high concentrations of stabilized, bioavailable Fe(II) into the photic zone, which may determine the biogeochemical cycle of the dissolved Fe in surface waters in other regions influenced by these systems.

Hydrothermal input is driven by ridge spreading rate and is most important in the Southern Ocean (Tagliabue *et al*., 2010), mainly the eastern Pacific and the Pacific and Indian sectors (TAGLIABUE; AUMONT; BOPP, 2014). Quantitatively, hydrothermalism contributes 20 × 10^9 g yr^{-1} of dissolved Fe (approximately 0.4 × 10^9 mol yr^{-1} of dissolved Fe) of "new" dissolved Fe to the Southern Ocean, which corresponds to 37%-79% of nonsedimentary inputs (TAGLIABUE *et al*., 2010). On a global scale, the gross hydrothermal fluxes to Fe input varied from 11.3 to 17.7 × 10^9 mol yr^{-1} (TAGLIABUE *et al*., 2016) (Table 1).

7.1.4 Submarine groundwater discharge (SGD)

SGD is the process where seawater infiltrates the lower portion of the coastal aquifers due to differences in density, mixes with a small fraction of meteoric water, and then flows back into the ocean (MULLIGAN; CHARETTE, 2009). Owing to the chemical and biological reactions in aquifers, SGD is enriched with the nutrients, organic matter, metals, and pathogens that are transported to the marine environment.

Using radium (Ra) isotope tracers, Windom *et al*. (2006) and Niencheski, Windom and Moore (2014) showed that SGD constitutes the main source of dissolved Fe for the southern continental shelf of Brazil. The dissolved Fe flux through SGD was estimated to be 2 × 10^6 mol d^{-1} of dissolved Fe and the transport to be 3.2 × 10^5 mol d^{-1} of dissolved Fe along the shelf. Comparatively, the latter corresponds to approximately 10% of the soluble Fe input via atmosphere in the entire South Atlantic Ocean (WINDOM *et al*., 2006). In El Gorguel Bay (Pb–Zn mining district, Murcia, Spain), Fe inputs to the coastal marine area derived from SGD range from 4 to 32 mol d^{-1} km^{-1} of dissolved Fe (TREZZI *et al*., 2016).

According to Kwon *et al*. (2014) the SGD fluxes in the Indo-Pacific and Atlantic Oceans (between 60°S and 70°N) are (12 ± 3) × 10^{13} m^3 yr^{-1}, which is threefold to fourfold larger than freshwater fluxes from river discharges. These authors note that in the areas influenced by SGD input, this input should be the main source of Fe to coastal waters (KWON *et al*., 2014).

7.1.5 Anthropogenic input – mine tailings

Tailings from the extraction and processing of Fe ore act as an important source of metals, mainly Fe and Mn, to the environments surrounding the extraction areas and tailings dams (RATHA; VENKATARAMAN, 1995; WONG, 1981; ZABOWSKI *et al*., 2001; PEREIRA *et al*., 2008).

In the region of the Quadrilátero Ferrífero (Minas Gerais, Brazil), the Fe content in mine tailings varies from 33.9% to 67.0% (PIRES *et al*. 2003; PEREIRA *et al*., 2008; WOLLF, 2009; GOMES, 2009; ANDRADE, 2014), affecting the levels of this element from the area near the tailings dam to the Mãe-Bá coastal lagoon (Espírito Santo, Brazil) where dissolved Fe concentrations reached 0.50 mg L^{-1} and 0.55 mg L^{-1}, respectively, before the disaster (PEREIRA *et al*., 2008). In the sediment, metal enrichment was found north of the dam where Fe levels reached up to 443 mg kg^{-1}, with the highest concentrations associated with the finest grain size (silt + clay) (PEREIRA *et al*., 2008). The Mãe-Bá Lagoon is located south of the state of Espírito Santo next to a port terminal for Fe ore export.

In November 2015, the Doce River and the Espírito Santo coast suffered disastrous impacts due to the collapse of the Fundão tailings dam, located in the city of Mariana (Minas Gerais, Brazil) (ESCOBAR, 2015). Analyses performed before and after the arrival of these tailings in the coastal area showed that the concentrations of Fe increased by up to two orders of magnitude. For the dissolved fraction, maximum values ranging from 102 µg L^{-1} to 226 µg L^{-1} were observed (NETO *et al*., 2016; HATJE *et al*., 2017).

The dissolved Fe transport rate in the Doce River Basin after the collapse of this dam was estimated to be 58.8 µg s^{-1}. A substantial increase was also observed in the transport of suspended sediments, whose concentration was

higher than 33,000 mg L^{-1} in the middle course of the river, with a maximum of 48,143 µg g^{-1} of Fe associated with the particulate matter (HATJE *et al*., 2017).

Additionally, in the context of this disaster, a large amount of sediment carried by the tailings mud accumulated in the river banks and dam reservoirs along the riverbed. In periods of intense rainfall and increased flow, this material may be eroded and transported by river discharge, promoting a high input of suspended particulate matter and metals (HATJE *et al*., 2017) including Fe. In addition, alternation of meteo-oceanographic forces, such as wind and wave regimes, causes the resuspension and transport of the sediment deposited in the marine substrate, with consequent remobilization of the associated metals (BASTOS *et al*., 2017).

Studies in El Gorguel Bay (Spain) showed that an accumulation of Pb–Zn tailings resulted in the enrichment of SGD with metals, mainly Zn, with a significant increase of its concentrations in the coastal environment (TREZZI *et al*., 2016). The contaminants from tailings can still be transported over long distances by wind erosion (CSAVINA *et al*., 2012). Thus, in addition to river transport, material concentrated in exposed areas is likely to be carried to marine areas by atmospheric transport or to infiltrate the ground and contaminate groundwater, which would lead to an increase in input by SGD.

The global Fe ore production increased by 280 million tons from 2012 through 2016, reaching 2,350 million tons (USGS, 2018). Thirty six coastal environments around the world have been impacted because of the mining and processing of ores in areas both nearby or hundreds of kilometres from the shoreline (KOSKI, 2012). Dold (2014) identified 38 coastal areas impacted by tailings deposition (including shore deposition, shallow, and deep-sea disposal). This scenario is probably underestimated since the Fe ore mine areas in Australia, Brazil, China, and India (the most important for global Fe ore production, according to USGS, 2018) are not included in these analyses.

The metal sources by mining activities include Fe sulphide (mainly pyrite and pyrrhotite) and their chemical reactions in oxygenated surface waters results on low-pH fluids. These conditions support the production of ferric iron (Fe^{3+}), which is an oxidant for sulfides and produces divalent metals, such as

Fe^{2+}, Cu^{2+}, Zn^{2+}, Pb^{2+}, promoting large dissolved metal fluxes to the coastal ocean (KOSKI, 2012).

The annual loads for dissolved Fe from mining activities were estimated from extrapolation of the instantaneous flux data from four seasonal surveys (from November 1996 to October 1998) along the Tinto and Odiel Rivers System (southwest Spain) and reached 1,800 tons yr^{-1} (BRAUNGARDT *et al*., 2003). Estimates using the relationship between river flow and concentration of dissolved metals between the periods from 1995–1996 to 2002–2003 showed the annual fluxes of dissolved Fe along the Tinto and Odiel Rivers System are even higher, reaching 7,900 tons yr^{-1} (OLÍAS *et al*., 2006). During a month of flood conditions, 770 tons of Fe were carried by the Tinto River toward the estuary (CÁNOVAS *et al*., 2008) (Table 1). Previous studies in this region confirm the influence of mining activities on metal contamination in the Gulf of Cadiz and the Mediterranean Sea (ELBAZ-POULICHET *et al*., 2001), although the Fe fluxes had not been measured. The rates of metal loads from mining activities should increase substantially in case of extreme events such as the collapse of tailings dams (KOSKI, 2012). According to Bowker and Chambers (2015), 63% of all accidents and dam failures during 1960–2010 were classified as serious and very serious and is a warning to the increased risk of catastrophic dam failures during the last 10 years. In Brazil alone, approximately 126 tailing dams are estimated to be vulnerable to malfunctions and could collapse (GARCIA *et al*., 2017).

Table 1 shows the regional Fe fluxes due to SGD, riverine-estuarine, and water discharge. These rates are restricted to areas affected by mining activities since there is a lack of information on Fe fluxes on a global scale. The load transported by the Tinto and the Odiel rivers represents 0.6% of the global gross river flux of Fe to oceans (OLÍAS *et al*., 2006). Considering that this is only area among the 38 coastal environments vulnerable to mining impacts, these nonquantified fluxes could represent considerable sources of dissolved Fe to the global ocean budget.

7.2 Sinks and internal recycling of Fe

Fe has strong interactions with organic and inorganic particles and can be removed from the water column through a process called scavenging, defined as the scavenging of elements by surface adsorption of particles (BRULAND; LOHAN, 2003). For dissolved Fe, the importance of this process will be determined by the physical-chemical balance between the concentration of inorganic particles (HONEYMAN; BALISTRIERI; MURRAY, 1988) and organic particles (such as senescent organisms and faecal pellets) (DEUSER, 1986; DEUSER *et al*., 1995) and the concentration of Fe in water (de BAAR; de JONG, 2001). This relation may be better understood as dissolved Fe speciation, whereby the size classes and the settling velocity of the particles are determined. The fine (<10 μm) and colloidal (<0.4 μm) particles generally have a high residence time, which makes the settling velocity negligible. For the larger biogenic particles, the settling rate varies from 50 to 100 m per day (de BAAR; de JONG, 2001).

In the open ocean, sedimentation is directly related to higher primary productivity (DEUSER, 1986; WEFER; FISCHER, 1991) and to changes in the assemblage of pelagic species that produce external shells (DEUSER *et al*., 1995). During events of higher production in the Southern Ocean, krill feed on phytoplankton *bloom* and incorporate small particles into faecal pellets, which constitute the dominant sedimentation route in these periods (WEFER; FISCHER, 1991). This material is still able to aggregate high-density mineralogical particles, which accelerates the deposition process and Fe removal to the ocean floor (de BAAR; de JONG, 2001).

Biological assimilation, regeneration, and recycling processes also control the distribution of dissolved Fe in the marine environment (HUTCHINS; DiTULLIO; BRULAND, 1993; HUTCHINS; BRULAND, 1994; ELLWOOD *et al*., 2014; BOWN *et al*., 2017). Ellwood *et al*. (2014) showed a shift in the Fe partition from the dissolved phase to the particulate phase in just days throughout the initial and final phase of a phytoplankton bloom, which was associated with the efficiency in the recycling and retention of Fe by the biota. The contributions of the diatoms at this stage are relevant, considering their role

in the assimilation and export of nutrients and carbon (BRULAND; LOHAN, 2003; REMBAUVILLE *et al*., 2016). The remineralization of Fe in the water column is also significantly enhanced as a result of zooplankton grazing activities, which make the trace metals present in the predated phytoplankton cells available again (HUTCHINS; BRULAND, 1994).

The Fe export rate via a biological route is quantified through association with global carbon productivity at the ocean surface. de Baar and de Jong (2001) estimated that the Fe flux from organic production should be 61×10^9 mol yr^{-1} of Fe in coastal areas and 5×10^9 mol yr^{-1} of Fe in the open ocean, a total of 66×10^9 mol yr^{-1}. This element can also be regenerated by microbial reduction in the bottom waters and diagenetic processes in the marine sediment (BRULAND; ORIANS; COWEN, 1994; FERNANDES *et al*., 2015; KUSTKA *et al*., 2015). Flux measurements using sediment chambers on the coast of California (USA) (ELROD *et al*., 2004) determined high dissolved Fe release rates from the sediment to the water column on the continental shelf. This flux was related to the oxidation of organic matter and allows Fe(II) to escape from the sediment. All the Fe released by this process would be in the dissolved fraction, with an estimated global input of 89×10^9 mol yr^{-1} of dissolved Fe, where 2.2×10^9 mol yr^{-1} of dissolved Fe should reach the euphotic zone because of upwelling processes (ELROD *et al*., 2004). Recent studies of benthic fluxes using two-dimensional mapping shows that macrofaunal bio-irrigation accounts for more than 80% of these fluxes in estuarine mudflats, controlling the dissolved Fe export from the sediment to the coastal ocean (de CHANVALON *et al*., 2017).

In equatorial Pacific Ocean ecosystems influenced by the California Current system, high concentrations of dissolved Fe (up to 20 nmol) have been associated with the resuspension of benthic particles in response to the upwelling phenomenon (JOHNSON; CHAVEZ; FRIEDERICH, 1999). A model developed to evaluate dissolved Fe cycling and primary productivity in the Southern Ocean showed that the sediment has a greater contribution to Fe input and consequent production compared with other sources such as

icebergs, sea ice, or atmospheric dust (WADLEY; JICKELLS; HEYWOOD, 2014).

Fe nanoparticles deposited on the continental shelf can be transported to oceanic areas through successive reworking processes, including reduction, resuspension, and re-oxidation steps. The continuous action of these mechanisms drives the particles into the oceanic region through the mineralogical ageing-rejuvenation cycle (RAISWELL, 2011; RICKARD, 2012), undergoing, on average, 7.4 cycles of dissolution–precipitation before becoming available to the water column (de CHANVALON *et al*., 2017).

Figure 2 shows the fluxes of external inputs, internal recycling, and removal of dissolved Fe in the oceans, including the rates, according to the authors specified in the legend.

The sediment sources are most important for approximately 74% of the ocean area, followed by hydrothermal sources (23%) and dust (2%) (TAGLIABUE; AUMONT; BOPP, 2014). Our review supports this pattern, with the exception of atmospheric dust, which was higher than hydrothermalism, and sedimentary rates were lower than atmospheric dust and hydrothermalism in some estimates (Table 1; Fig. 2). This divergence is explained by the substantial degree of intermodel disagreement in the strength of different sources (dust, sediment, hydrothermal, and rivers) because there are data uncertainties with respect to scavenging rates of Fe in these models (TAGLIABUE *et al*., 2016). Moreover, we emphasize the need to measure or estimate the fluxes from mining input to evaluate the magnitude and contribution of these anthropogenic sources to the global ocean.

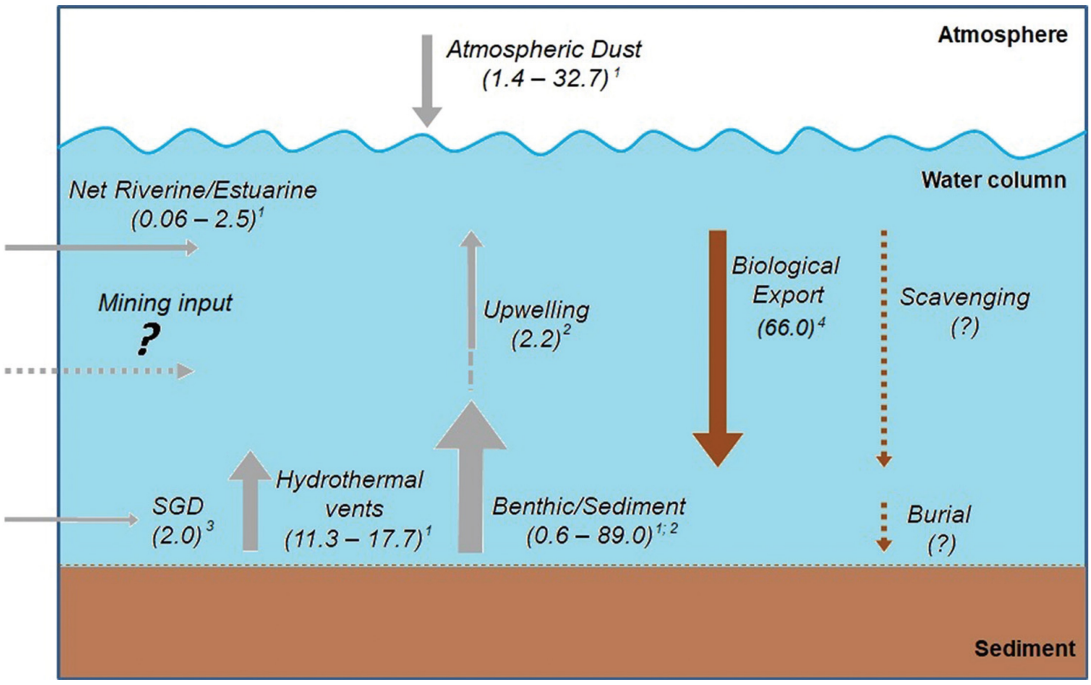

Figure 2. Fluxes of the external sources, input processes and internal removal of dissolved Fe in seawater (values in $\times 10^9$ mol yr^{-1} of dissolved Fe, except by submarine groundwater discharge (SGD), whose fluxes are in $\times 10^6$ mol dFe d^{-1}). The light grey arrows represent the input processes, either by external input or internal recycling; the brown arrows comprise the removal processes from the water column. The thickness of the arrows indicates the importance of these processes for Fe cycling, according to the cited references. Dotted arrows are uncertainties or lack of data. [1]Range of data from 13 global ocean biogeochemistry models compiled by Tagliabue *et al*. (2016); [2]Elrod *et al*. (2004); [3]Windom *et al*. (2006); [4]de Baar and de Jong (2001). See Table 1 for more details about the specific rates and references.

8 SPECIATION AND SOLUBILITY OF DISSOLVED FE IN SEAWATER

Speciation comprises the different chemical forms and associations in which Fe can be found in the environment. The particulate form of Fe (> 0.45 µm) includes organisms (phytoplankton and zooplankton); crystalline structures such as haematite (Fe_2O_3), magnetite (Fe_3O_4), limonite ($2Fe_2O_3 \cdot 3H_2O$), and pyrite (FeS_2) (GREENWOOD; EARNSHAW, 1984); aluminosilicates; cell debris; or Fe coprecipitates with other authigenic minerals (MILLERO; PIERROT, 2002; NORMAN *et al*., 2014). In the dissolved fraction (< 0.45 µm), the colloidal material (1 nm - 0.45 µm) is represented by large organic ligands, Fe oxides, and Fe hydroxides, and the soluble material (< 1 nm) is composed of free ions, complex inorganic complexes, and small organic ligands (exopolymeric substances) (NORMAN *et al*., 2014) (Fig. 3).

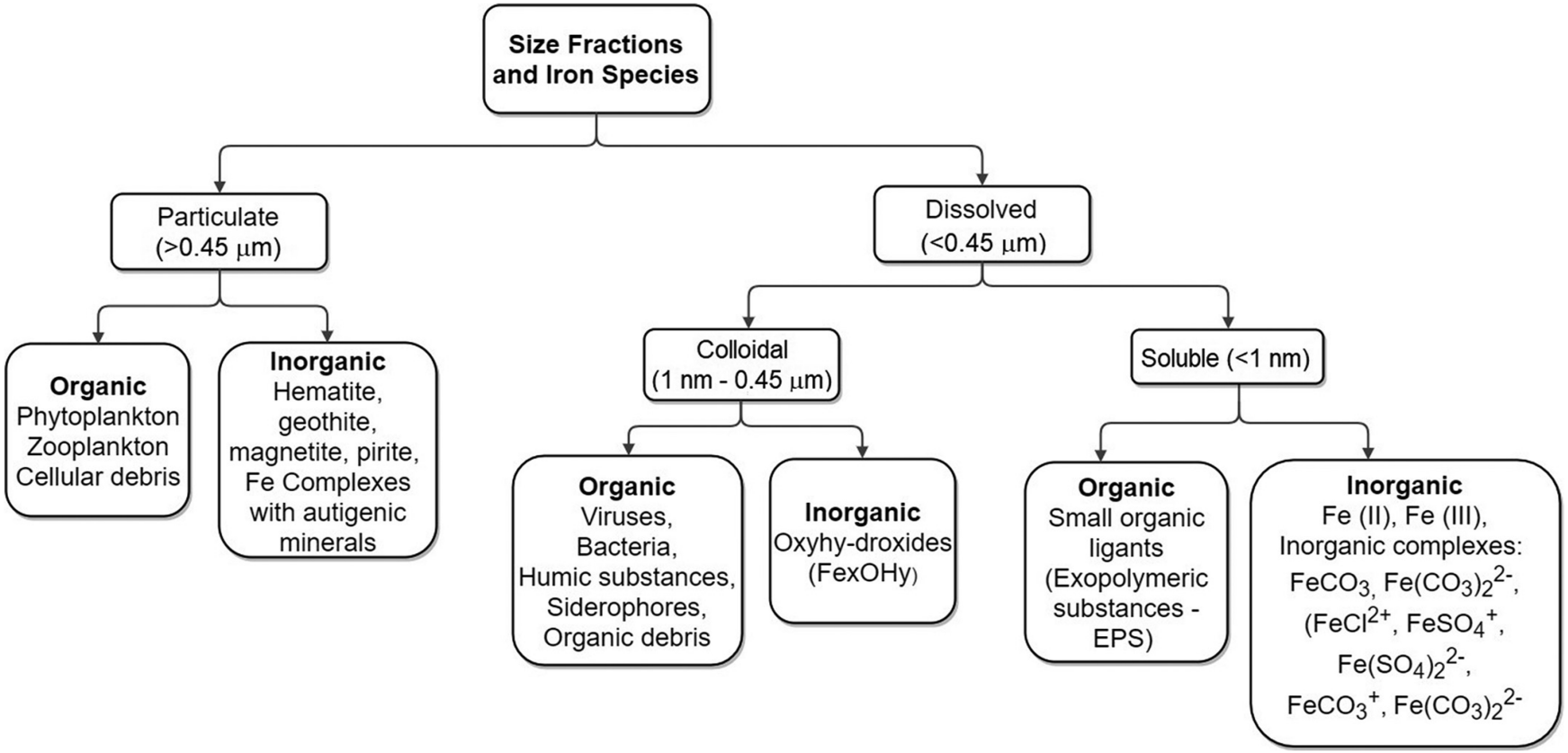

Figure 3. Size fractions according to the operational concept and types of Fe associations in the marine environment.

The speciation of dissolved Fe in natural waters is mainly controlled by the reduction potential (Eh), the potential of hydrogen (pH) and the ionic interactions of this metal with inorganic (such as Cl^{-}, OH^{-}, and CO_3^{2-}) and organic ligands (MILLERO; PIERROT, 2002). Under natural seawater conditions (high Eh and pH close to 8.0), the thermodynamically stable chemical form is Fe(III), and the inorganic speciation of this metal is predominantly determined by hydrolysis reactions with four different products being generated: $FeOH^{2+}$, $Fe(OH)_2^{+}$, $Fe(OH)_3^{0}$, and $Fe(OH)_4^{-}$ (MILLERO; PIERROT, 2002).

In the pH range of seawater, the main hydrolysis products are $Fe(OH)^{2+}$ and $Fe(OH)_3^{0}$ (BYRNE; KESTER, 1976; KUMA; SUZUKI; MATSUNAGA, 1993), with $Fe(OH_4)^{-}$ constituting only 1% of the dissolved Fe (Byrne and Kester 1976). However, Kuma, Nishioka and Matsunaga (1996) determined that in the pH ranges of 5.7–7.2 for coastal waters and 5.7-7.6 for ocean waters (pH controlled in laboratory), only the $Fe(OH)_2^{+}$ species is significant.

Fe hydroxides produced from Fe(III) hydrolysis present low solubility, being rapidly precipitated and removed from the water column (BYRNE; KESTER, 1976; KUMA; SUZUKI; MATSUNAGA, 1993). As a result, the dissolved Fe concentrations in the oceans are extremely low, reaching 0.4 nmol L^{-1} when measured as 0.05 µm membrane filtrates and up to 20 nmol L^{-1} when considering fractions up to 0.45 µm (BYRNE; KESTER, 1976). In addition, the Fe solubility can be reduced up to 0.2 nmol L^{-1} due to the reworking of Fe hydroxides and the formation of stable crystalline structures such as goethite and haematite (KUMA; NISHIOKA; MATSUNAGA, 1996). In contrast, Fe complexation with natural organic compounds increases the solubility of this metal (JOHNSON; GORDON; COALE, 1997; MILLERO, 1998; MILLERO; PIERROT, 2002; BOYD; ELLWOOD, 2010; GLEDHILL; BUCK, 2012; KRACHLER *et al.*, 2015), with the complex acting as a buffer for the hydrolysis, thereby reducing the kinetics of the oxidation reactions and promoting the permanence of the complex in the dissolved fraction (ROSE; WAITE, 2002; BOYD; ELLWOOD, 2010).

The quantity and the properties of the organic matter are the main controlling factors of dissolved Fe species (GUAN; YAN; YUAN, 2016) whose complexed forms comprise more than 99% of its concentrations in seawater (GLEDHILL; van den BERG, 1994; RUE; BRULAND, 1995, 1997). The levels of these compounds are reflected in spatial variations of dissolved Fe concentrations and solubility, which are higher in estuarine and coastal waters than in ocean regions (KUMA; NISHIOKA; MATSUNAGA, 1996; SU *et al*., 2015).

The organic substances that complex with Fe are classified operationally based on the conditional stability constant $K_{FeLi,Fe}^{cond}$, corresponding to the equilibrium of the complexation reactions, which can be evaluated from electrochemical techniques (e.g., competitive ligand exchange adsorptive cathodic stripping voltammetry (van den BERG, 1995; LAGLERA; BATTAGLIA; van den BERG, 2007; ABUALHAIJA; van den BERG, 2014). The classes are defined as Li, where i = 1 corresponds to the strongest ligands, and i = 2, 3, etc. correspond to progressively weaker classes (GLEDHILL; BUCK, 2012).

To standardize this categorization, Gledhill and Buck (2012) suggested that L1 should be used when $logK_{FeLi,Fe}^{cond}$ > 12; L2 for $logK_{FeLi,Fe}^{cond}$, = 11 to 12; and L3 when $logK_{FeLi,Fe}^{cond}$ < 11. In general, the concentrations of total ligands and the strongest classes are distributed in the mixture layer, corresponding to the highest chlorophyll-a concentrations, the maximum fluorescence, and (or) high primary production (RUE; BRULAND, 1995; van den BERG, 1995; KUMA; NISHIOKA; MATSUNAGA, 1996; BUCK; SOHST; SEDWICK, 2015). Biological productivity is possibly one of the factors that determines the seasonal variations in the complexation strength of organic ligands in the East China Sea, being higher in the spring than in the autumn (SU *et al*., 2015).

The natural organic compounds that complex with Fe in seawater range from low molecular-weight substances produced by heterotrophic bacteria and cyanobacteria, such as siderophores (GLEDHILL *et al*., 2004; MAWJI *et al*., 2008), to macromolecular complexes represented by humic substances (HS) (LAGLERA; van den BERG, 2009; LAGLERA; BATTAGLIA; van den BERG,

2011; BUNDY *et al*., 2015; MAHMOOD *et al*., 2015) and EPS (NORMAN *et al*., 2015; HASSLER *et al*., 2015).

The HS are important dissolved Fe chelators in estuarine and coastal environments (LAGLERA; van den BERG, 2009; LAGLERA; BATTAGLIA; van den BERG, 2011; BUNDY *et al*., 2015; MAHMOOD *et al*., 2015), which can be attributed to the multifunctional nature of its molecular groups (predominantly polyphenols and benzoic acids or carboxylic acids) as well as its high refractivity (LAGLERA; van den BERG, 2009; LAGLERA; BATTAGLIA; van den BERG, 2011). Laglera and van den Berg (2009) have shown that HS from continental sources maintain Fe in solution in coastal regions of the Irish Sea. The dissolved Fe-complexing capacity in these samples was the same as the total binding capacity evaluated for HS (7.5-11.5 nmol L^{-1} and 6.5–11.9 nmol L^{-1}, respectively), indicating that HS is the main or only complexing agent in those waters. In San Francisco Bay (California, USA), approximately 23% of dissolved Fe is complexed with humic substances, which contribute to the input of this element and strong ligands in the shelf waters of the California Current (BUNDY *et al*., 2015).

Other authors have described the importance of the production of chelators by biological communities for the complexation of dissolved Fe (KUMA; NISHIOKA; MATSUNAGA, 1996; ÖZTÜRK; BIZSEL; STEINNES, 2003). Buck *et al*. (2007) found a strong direct correlation between the concentrations of dissolved Fe and L1 organic ligands in the colloidal fraction. According to these authors, these ligands likely are products of the association of siderophores with colloidal particles. Rue and Bruland (1995) associated strong organic ligands (L1) in surface water with the presence of siderophores or other biomolecules, such as porphyrins, that are produced by phytoplankton and (or) heterotrophic bacteria.

The EPS produced by bacteria and by the phytoplankton community have functional groups with high affinity for Fe, whose conditional stability constant is similar to that of siderophores $K^{cond}_{FeLi,Fe'}$ = 10^{12}. This material significantly increases Fe solubility, possibly avoiding the aggregation of Fe oxides–

hydroxides in seawater and contributing to the biogeochemical cycle of this element in remote ocean regions (NORMAN *et al*., 2015).

9 FE BIOAVAILABILITY AND THE PHYTOPLANKTON COMMUNITY

The bioavailability of Fe in the oceans varies according to (i) the chemical speciation of Fe in the seawater, (ii) the metabolic uptake preference of the species that compose the algal assemblage, and (iii) the equilibrium between the kinetics of chemical reactions in the environment and of the assimilation and demand by the primary producers (WELLS; PRICE; BRULAND, 1995).

In general, marine phytoplankton species use soluble and free Fe forms, which must be dissociated from Fe oxide-hydroxide particles (WELLS; ZORKIN; LEWIS, 1983) and (or) decomplexed from organic compounds (ANDERSON; MOREL, 1982). The reduction reactions play an important role in this stage (FINDEN *et al*., 1984; WELLS; MAYER, 1991) since the reduced form Fe(II) is kinetically more labile, forms weaker bonds with the organic complexing agents, and increases the solubility of the Fe oxide-hydroxide particles (SUNDA, 2001).

The reduction may occur either photochemically in the environment or be biologically mediated on the surface of the cell membranes. In the photochemical cycle, solar energy is absorbed by the Fe(III) complex with organic ligand promoting a charge transfer in which Fe becomes reduced and the ligand is oxidized. The Fe(II) then dissociates from the ligand molecule and can be re-oxidized, forming Fe(III) which will again bind to the organic complexing agents, restarting the cycle. The free forms of Fe(III) and Fe(II), however, must bind to Fe-carrying proteins present in cell membranes (SUNDA, 2001). Thus, the photochemical reduction mechanism allows the biological assimilation, since it guarantees the stability of the Fe(III) and Fe(II) free forms in the environment (MILLER; KESTER, 1994; FINDEN *et al*., 1984).

In addition to the use of free Fe, the organisms have developed mechanisms to assimilate this element into other fractions. The siderophores, for example, are able to effectively compete with hydroxyl ion for the ferric state of Fe to solubilize the Fe of the oxide-hydroxide particles (NEILANDS, 1995).

The photochemical reactions mediated by specific groups of the Fe(III)-siderophore complex lead to an increase in the production of the reactive and easily assimilated forms of Fe(II) and Fe(III), increasing their availability for the phytoplankton (BARBEAU *et al*., 2001, 2003). In heterotrophic bacteria such as *Escherichia coli*, the Fe–siderophore complex is transported by specific membrane receptors (NEILANDS, 1995). In marine organisms, this uptake must involve a previous reduction step by reductase proteins on the cell surface to release Fe bound to the siderophore, followed by diffusion of Fe(II) to the intracellular medium (HOPKINSON; MOREL, 2009).

For some species of marine phytoplankton, Fe is also bioavailable in particulate form (SUGIE *et al*., 2013). Cyanobacteria of the genus *Trichodesmium* are able to dissolve the Fe on the cell surface that is associated with mineral dust and oxides, thus increasing the uptake rates of this element. These organisms possibly promote the suction of particles into the colony, with subsequent active shuttling and packaging (RUBIN; BERMAN-FRANK; SHAKED, 2011). The diatom *Asterionella japonica* uses Fe in particulate and (or) colloidal forms (GOLDBERG, 1952). Amorphous forms such as Fe hydroxides can adsorb to the cell surface of the diatoms where they undergo bio-reductive dissolution by transmembrane proteins or by the production of organic substances that reduce the pH to create a favourable microenvironment for this process (SUNDA, 2001). Figure 4 shows the processes that determine the bioavailability of Fe in the water column in marine environments.

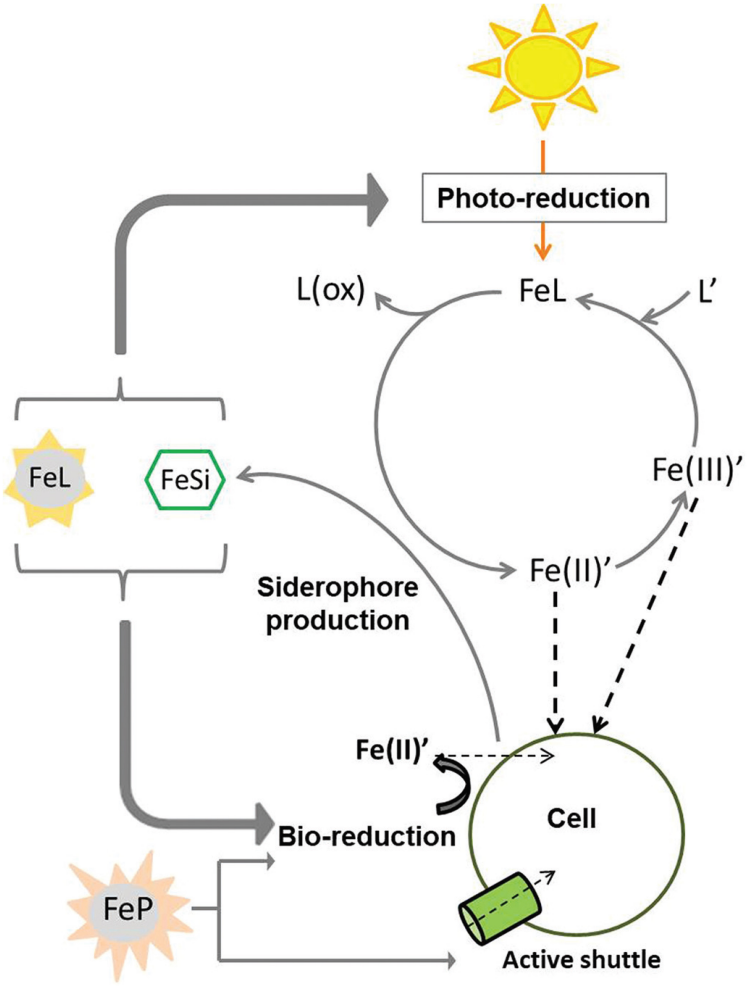

Figure 4. Processes that determine Fe bioavailability in the marine environment, considering the photochemical cycle, biological cycle, and the assimilation strategies by different species. FeL, Fe + Natural organic ligand; FeSi, Fe + Siderophore; FeP, Particulate Fe; L (ox), Oxidized ligand; L=, Free natural organic ligand; Fe(III)= and Fe(II)=, free Fe(III) and Fe(II) ions, respectively. The dashed arrows indicate the assimilation phases. The size of the illustration is not proportional to the operational fractions.

Öztürk, Bizsel and Steinnes (2003) showed that phytoplankton *bloom* and consequent herbivory by protozoa were determinant for Fe speciation in the inner and middle portions of Izmir Bay (Aegean Sea, northeastern Mediterranean). These authors observed a change in the Fe species, which were predominantly in the labile form, and after bloom events the Fe occurred as hydrophobic-lipophilic complexes. This result was likely due to complexation with cellular exudates such as free or combined amino acids (ÖZTÜRK; BIZSEL; STEINNES, 2003).

The contribution of phytoplankton to Fe speciation may also vary depending on the community structure where higher concentrations of reactive Fe occur with an increase in Euglenophyceae populations (BIZSEL; ÖZTÜRK; METIN, 1997). Thus, the bioavailability of this element is controlled directly or indirectly by biologically mediated chemical reactions, which determine the productivity, composition, and trophic structure of the marine planktonic communities (SUNDA, 2001).

Bioavailability is also determined by the demand for this element by different taxa. Phytoplankton species that bloom in coastal areas require a much higher amount of Fe for their growth compared with groups adapted to pelagic conditions (SUNDA; HUNTSMAN, 1995). This demand is even higher for prokaryotic organisms (*Synechococcus bacillaris* cyanobacteria), whose cell Fe:C ratio required to sustain their growth rate in coastal environments is five to eight times higher than for eukaryotic algae (SUNDA; HUNTSMAN, 2015). Thus, the biological composition of the ecosystem also has profound effects on the chemical speciation of Fe (WELLS; PRICE; BRULAND, 1995).

Regarding phytoplankton community structure, the increased bioavailability of Fe in the oceans exerts a selective control over the dominance of species and functional groups in the community (QUÉGUINER, 2013), which becomes predominantly composed of diatoms (MARTIN; GORDON; FITZWATER, 1991; PRICE; ANDERSEN; MOREL, 1991; FITZWATER *et al*., 1996; COALE *et al*., 1996; BIZSEL; ÖZTÜRK; METIN, 1997) and dinoflagellates (BIZSEL; ÖZTÜRK; METIN, 1997). Variations in size classes were also observed, where larger cell fractions are favoured (> 10 µm) compared with control conditions (TAKEDA; OBATA, 1995). These changes may be associated with enrichment with specific forms of Fe complexation, such as the EPS (HASSLER *et al*., 2015).

Although there is little evidence for Fe effects to the growth and toxin production in harmful algal species (SUNDA, 2008), Lampitt *et al*. (2008) drew attention to the consequences of the process of artificial enrichment of ocean areas with Fe on the reduction of biological diversity as well as the possible development of toxic algae. With respect to the latter, Zhuo-Ping *et al*. (2009)

found that the combination of high light intensity and high Fe concentration accelerates cell growth and pigment biosynthesis in the toxic microalgae *Scrippsiella trochoidea*, leading to the *bloom* of these harmful algae in the environment.

In situ observation and experimental analyses show that Fe enrichment promotes an increase in the abundance of the toxic diatom *Pseudo-nitzschia* spp. and the production of the neurotoxin domoic acid (DA) associated with it (SILVER *et al*., 2010), mainly when in synergy with other trace metals such as copper (Cu) (WELLS *et al*., 2005; TRICK *et al*., 2010). The combined effect of Fe and Cu increased by up to three times the DA content in the cell and by 160% its concentration in particulate form in water samples (TRICK *et al*., 2010). The authors emphasized that chronic exposure to this neurotoxin is known to have substantial neurological impacts on mammals and may thus affect other trophic levels (TRICK *et al*., 2010).

Thus, the effects of Fe input by mining tailings loads on the phytoplankton composition and growth should be further studied. Research including laboratory toxicity tests and field methodologies of species richness and biodiversity is crucial for a broader understanding of ecological impacts by metal contamination in coastal areas affected by mining (KOSKI, 2012).

10 INTERRELATIONS BETWEEN THE CHEMICAL, BIOLOGICAL, AND ECOLOGICAL COMPONENTS OF THE FE CYCLE IN THE MARINE ENVIRONMENT

Figure 5 facilitates an integrated discussion of the aspects related to Fe behaviour in the marine environment, considering the input of new Fe, chemical speciation, biological assimilation, and community structure. This schematic summarizes the interrelations among the chemical, biological, and ecological components that promote changes in the system from the cellular to the ecosystem level.

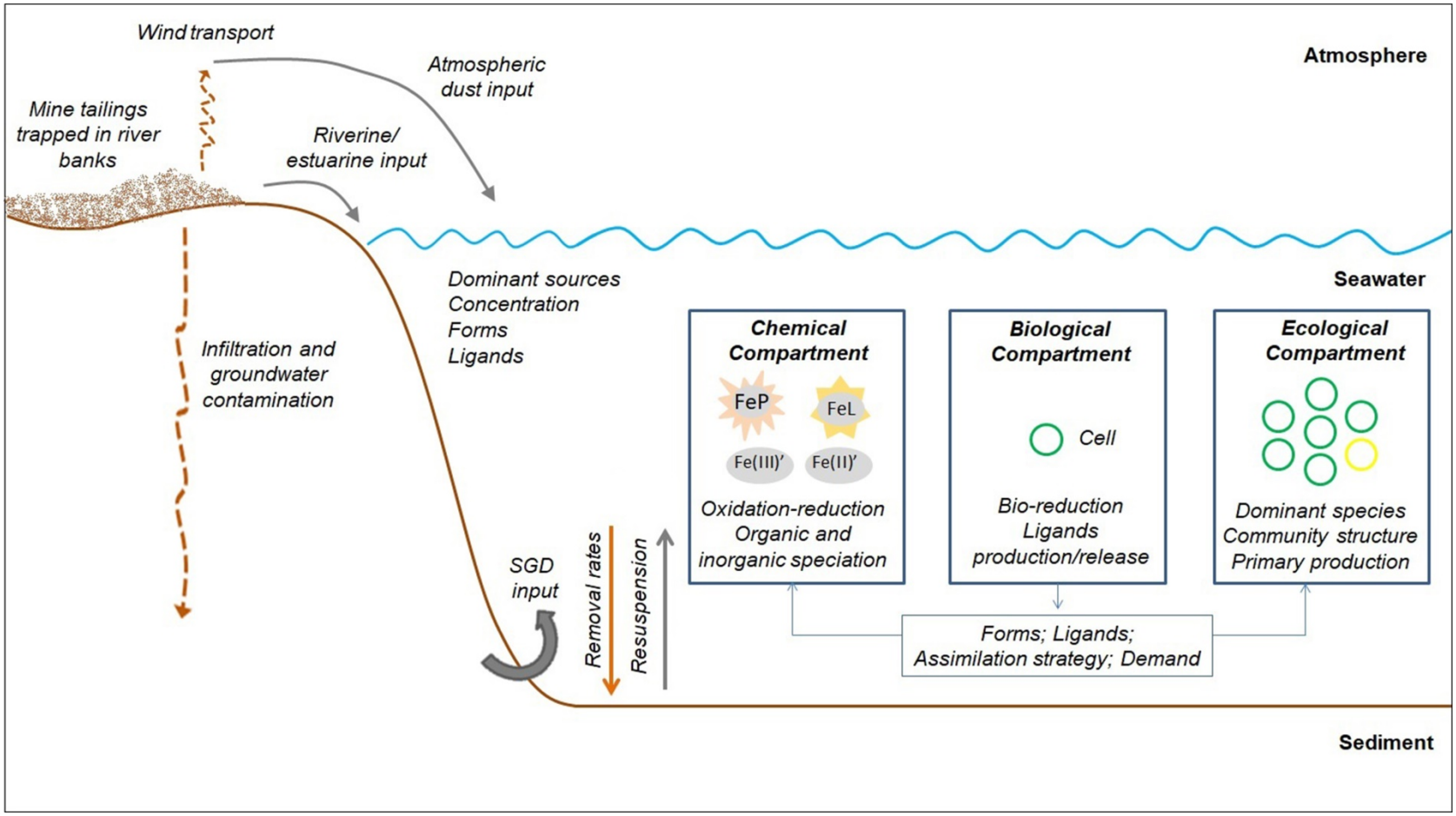

Figure 5. Schematic of Fe behaviour in the marine environment conditioned by the interrelationship of the chemical, biological, and ecological processes of the system. In the chemical component: FeP, Fe in the particulate fraction (considering both mineral and biogenic forms); FeL, Fe in the dissolved fraction + organic ligand; Fe(III)= and Fe(II)=, free Fe(III) and Fe(II) ions, respectively. The size of the illustration is not proportional to the operational fractions. The distance scale is not represented in the image.

Considering the input of new Fe as a starting point, the biogeochemical behaviour of this element in the marine environment will depend on (i) the types of sources that contribute to the entry into the system, (ii) the concentrations/input rates, (iii) the partition of Fe in different forms–fractions (dissolved–particulate), (iv) the concentration and nature of the organic ligands, (v) the complexed forms, and (vi) the removal rates.

In the case of anthropogenic sources, specifically the tailing inputs, other metals and elements in addition to Fe, such as the various organic compounds (mainly, humic substances by river sources) and inorganic nutrients, can be transported to coastal marine areas. These compounds should contribute to the processes of complexation, adsorption removal, and other factors that will define the chemical speciation of this metal.

This effect is even more pronounced in the case of environmental disasters such as the collapse of the Fundão dam because the input of different chemical and mineralogical components can have synergistic effects in the system. In addition, because much of the material was retained in the river channel and its tributaries, it can be remobilized with an increase in the river flow. In the marine region, to where much of the material was transported, this fine particulate will remain in the system for a long period (still undetermined), and the effects of the particulate on the chemical, biological, and ecological components can be repeated at each resuspension and remobilization event. Furthermore, the accumulation of this material should cause an increase in the Fe input to the marine system by different sources (fluvial, atmospheric dust, and SGD) also for a still unknown period.

In the chemical component, the different forms of Fe will participate in complexation and reduction reactions that will define the speciation of this element in the organic and inorganic fractions as well as the availability of Fe(III) and Fe(II) as free ions. The concentrations and types of Fe associations may be altered by the cell use of this element in the biological component through bioreduction reactions and the production-release of the chelating compounds that may be complexed with this element (such as siderophores and exopolymeric substances). The forms available in the system, in turn, may increase the frequency of phytoplankton species that obtain competitive

advantage over others due to adaptations and biochemical-physiological specificities in the assimilation strategies. Thus, the bioavailability of this element will affect the ecological component due to changes in community structure, with a possible decrease in the diversity and richness indices and an increase in the dominance of opportunistic groups, with possible toxic microalgal blooms. The latter has an interrelation with the chemical component, since the chemical forms of Fe present in the water column will also be the result of the demand and the assimilation mechanisms determined by the community composition. The increase in primary production is another important change in the ecological component, considering the greater availability of this element from external input and (or) internal recycling. Thus, the processes that define the biogeochemistry of Fe, including the rates of input sources, chemical interactions, bioavailability, and changes in the phytoplankton community structure are key issues for understanding the Fe cycle in marine environments. Studies on this topic will enable predictive decision-making regarding the anthropogenic impacts of environmental disasters that lead to the enrichment of marine environments with Fe.

11 CONCLUSION

The biogeochemistry and bioavailability of Fe for marine organisms depends on the new Fe input rates, the forms available in the environment, the speciation reactions, and the selective control of the algal assemblage, whose ecological structure can be defined by this availability. One of the determining factors for this issue is the identification of the predominant sources in the area, which reflects variations in the input rates by natural and (or) anthropogenic processes.

From a biogeochemical and ecological perspective, anthropogenic sources must cause more pronounced changes in the functioning of the ecosystem. The input of new Fe due to environmental disasters, such as the collapse of the Fundão tailings dam, promotes both acute and chronic impacts. Anthropogenic Fe enrichment events will lead to changes in the chemical speciation, Fe bioavailability, and structure of biological communities, with possible proliferation of toxic microalgae.

The schematic of Fe behaviour in the marine environment presented in this work shows the interrelations of the chemical, biological and ecological components to explain the biogeochemical behaviour of Fe in the marine environment and describes the effects on the primary link in the food chain. However, changes at this level can determine species composition and community structure in the higher levels of the food chain, especially considering the synergistic effects of Fe with other elements such as nutrients, organic compounds, suspended particulate matter and other metals.

Thus, in addition to monitoring the taxa and the physicochemical conditions of the environment, usually carried out independently in cases of environmental disasters, integrated studies that consider the different chemical, biological, and ecological variables should provide strong support for the development of management and conservation strategies in areas vulnerable to anthropogenic enrichment.

Because of the disaster with the Fundão dam, we emphasize the need to better determine the areas of influence of mining activities during the environmental licensing process, as the input of Fe tailings occurred hundreds of kilometres away from the site of collapse of the dam. Therefore, coastal regions, even if distant from anthropogenic sources of Fe, are not safe from possible environmental impacts.

Moreover, the quantification of the fluxes of Fe from mining areas and its impact to phytoplankton have not been addressed and constitute a knowledge gap that needs to be considered in future studies involving the Fe cycle. Addressing these concerns will improve our understanding of: (i) the potential implications in the biogeochemical behaviour, speciation and bioavailability of the Fe, (ii) the magnitude and importance of these sources of dissolved Fe to the global ocean budget, and (iii) the ecological issues for coastal areas affected by this anthropogenic source.

12 REFERENCES

ABUALHAIJA, M.M.; VAN DEN BERG, C.M.G. Chemical speciation of iron in seawater using catalytic cathodic stripping voltammetry with ligand competition against salicylaldoxime. **Marine Chemistry,** v. 164, p. 60-74, 2014.

ANDERSON, M.A.; MOREL, F.M. The influence of aqueous iron chemistry on the uptake of iron by the coastal diatom *Thalassiosira weissflogii*. **Limnology Oceanography**, v. 27, n. 5, p. 789-813, 1982.

ANDRADE, L.C.R. **Caracterização de rejeitos de mineração de ferro, in natura e segregados, para aplicação como material de construção civil.** 2014. 96p. Tese (Doutorado em Engenharia Civil) – Departamento de Engenharia Civil, Universidade Federal de Viçosa, Viçosa, 2014.

BAKER, A.R.; CROOT, P.L. Atmospheric and marine controls on aerosol iron solubility in seawater. **Marine Chemistry**, v. 120, n. 1-4, p. 4-13, 2010.

BARBEAU, K.; RUE, E.L.; BRULAND, K.W.; BUTLER, A. 2001. Photochemical cycling of iron in the surface ocean mediated by microbial iron(III)-binding ligands. **Nature**, v. 413, n. 6854, p.409-413, 2001.

BARBEAU, K.; RUE, E.L.; TRICK, C.G.; BRULAND, K.W.; BUTLER, A. Photochemical reactivity of siderophores produced by marine heterotrophic bacteria and cyanobacteria based on characteristic Fe(III) binding groups. **Limnology Oceanography,** v. 48, n. 3, p. 1069–1078, 2003.

BASTOS, A.C.; OLIVEIRA, K.S.S.; FERNANDES, L.F.; PEREIRA, J.B.; DEMONER, L.E.; NETO, R.R.; et al.. **Monitoramento da Influência da Pluma do Rio Doce após o rompimento da Barragem de Rejeitos em Mariana/MG – Novembro de 2015: Processamento, Interpretação e Consolidação de Dados**. Universidade Federal do Espírito Santo, Vitória, 2017. 254p. Disponível em: http://www.icmbio.gov.br/portal/images/stories/Rio_Doce/relatorio_ consolidado_ufes_rio_doce.pdf. Acesso em: 07 ago. 2017.

BIZSEL, N.; ÖZTÜRK, M.; METIN, G. The role of iron on the phytoplankton growth in heavily polluted Izmir Bay, Aegean Sea. **Transactions on Ecology and Environment,** v. 14, p.659–669, 1997.

BOWKER, L.N.; CHAMBERS, D.M. **The risk, public liability; economics of tailings storage facility failures**. 2015. Disponível em: https://earthworks.org/cms/assets/uploads/archive/files/pubs-others/BowkerChambers-RiskPublicLiability_EconomicsOfTailingsStorageFacility%20Failures-23Jul15.pdf. Acesso em: 27 jul. 2018.

BOWN, J.; LAAN, P.; OSSEBAAR, S.; BAKKER, K.; ROZEMA, P.; DE BAAR, H.J.W. Bioactive trace metal time series during Austral summer in Ryder Bay, Western Antarctic Peninsula. **Deep Sea Research Part II: Topical Studies in Oceanography**, v. 139, p. 103-119, 2017.

BOYD, P.W.; ELLWOOD, M.J. The biogeochemical cycle of iron in the ocean. **Nature Geoscience**, v. 3, p. 675-682, 2010.

BOYD, P.W.; TAGLIABUE, A. Using the L* concept to explore controls on the relationship between paired ligand and dissolved iron concentrations in the ocean. **Marine Chemistry**, v. 173, p. 52-66, 2014.

BOYD, P.W.; JICKELLS, T.; LAW, C.S.; BLAIN, S.; BOYLE, E.A.; BUESSELER, K.O., et al. Mesoscale iron enrichment experiments 1993–2005: synthesis and future directions. **Science**, v. 315, n. 5812, p. 612-617, 2007.

BOYLE, E.A.; EDMOND, J.M.; SHOLKOVITZ, E.R. The mechanism of iron removal in estuaries. **Geochimica et Cosmochimica Acta**, v. 41, n. 9, p. 1313-1324, 1977.

BRAUNGARDT, C.B.; ACHTERBERG, E.P.; ELBAZ-POULICHET, F.; MORLEY, N.H. Metal geochemistry in a mine-polluted estuarine system in Spain. **Applied Geochemistry**, v. 18, n. 11, p. 1757-1771, Nov. 2003. DOI 10.1016/S0883-2927(03)00079-9. Disponível em: https://doi.org/10.1016/S0883-2927(03)00079-9. Acesso em: 13 dez. 2017.

BRISTOW, L.A.; MOHR, W.; AHMERKAMP, S.; KUYPERS, M.M.M. Nutrients that limit growth in the ocean. **Current Biology**, v. 27, n. 11, p. R474–R478, 2017.

BRULAND, K.W.; LOHAN, M.C. Controls of trace metals in seawater. **Treatise on Geochemistry**. 1. ed. Pergamon: Elsevier, v.6, p. 23-47, 2003.

BRULAND, K.W.; ORIANS, K.J.; COWEN, J.P. 1994. Reactive trace metals in the stratified central North Pacific. **Geochimica et Cosmochimica Acta**, v. 58, n. 15, p. 3171-3182, 1994.

BUCK, K.N.; LOHAN, M.C.; BERGER, C.J.; BRULAND, K.W. Dissolved iron speciation in two distinct river plumes and an estuary: Implications for riverine iron supply. **Limnology Oceanography**, v. 52, n. 2, p. 843-855, 2007.

BUCK, K.N.; SOHST, B.; SEDWICK, P.N. The organic complexation of dissolved iron along the U.S. GEOTRACES (GA03). **Deep Sea Research Part II: Topical Studies in Oceanography**, v. 116, p. 152-165, 2015.

BUNDY, R.M.; ABDULLA, H.A.N.; HATCHER, P.G.; BILLER, D.V.; BUCK, K.N.; BARBEAU, K.A. Iron-binding ligands and humic substances in the San Francisco Bay estuary and estuarine-influenced shelf regions of coastal California. **Marine Chemistry**, v. 173, p. 183-194, 2015.

BUTLER, A.; THEISEN, R.M.. Iron(III)–siderophore coordination chemistry: reactivity of marine siderophores. **Coordination Chemistry Reviews**, v. 254, p. 288-296, 2010.

BYRNE, R.H.; KESTER, D.R. Solubility of hydrous ferric oxide and iron speciation in seawater. **Marine Chemistry**, v. 4, n. 3, p. 255-274, 1976.

CÁNOVAS, C.R.; HUBBARD, C.G.; OLÍAS, M.; NIETO, J.M.; BLACK, S.; COLEMAN, M.L. Hydrochemical variations and contaminant load in the Río Tinto (Spain) during flood events. **Journal of Hydrology**, v. 350, n. 1-2, p. 25-40, 2008.

COALE, K.H.; JOHNSON, K.S.; FITZWATER, S.E.; GORDON, R.M.; TANNER, S.; CHAVEZ, F.P.; et al. 1996. A massive phytoplankton bloom induced by an ecosystem-scale iron fertilization experiment in the equatorial Pacific Ocean. **Nature**, v. 383, n. 6600, p. 495-501, 1996.

CSAVINA, J.; FIELD, J.; TAYLOR, M.P.; GAO, S.; LANDÁZURI, A.; BETTERTON, E.A.; SÁEZ, A.E. A review on the importance of metals and metalloids in atmospheric dust and aerosol from mining operations. **Science of The Total Environment**, v. 433, p. 58-73, 2012.

DANSIE, A.P.; WIGGS, G.F.S.; THOMAS, D.S.G. Iron and nutrient content of wind-erodible sediment in the ephemeral river valleys of Namibia. **Geomorphology**, v. 290, p. 335-346, 2017.

DE BAAR, H.J.W.; DE JONG, J.T.M. **Distributions, sources and sinks of iron in seawater. In Biogeochemistry of iron in seawater**. Editores: TURNER, D.R.; HUNTER, K. A. Nova Iorque: Wiley, v. 7, 2001. p. 123-253.

DE CHANVALON, A.T., METZGER, E., MOURET, A., KNOERY, J., GESLIN, E., MEYSMAN, F.J.R. Two dimensional mapping of iron release in marine sediments at submillimeter scale. **Marine Chemistry**, v. 191, p. 34-49, 2017.

DE JONG, J.T.M.; STAMMERJOHN, S.E.; ACKLEY, S.F.; TISON, J.L.; MATTIELLI, N.; SCHOEMANN, V. Sources and fluxes of dissolved iron in the Bellingshausen Sea (West Antarctica): the importance of sea ice, icebergs and the continental margin. **Marine Chemistry**, v. 177, p. 518-535, 2015.

DEUSER, W.G. Seasonal and interannual variations in deep-water particle fluxes in the Sargasso Sea and their relation to surface hydrography. **Deep Sea Research Part A. Oceanographic Research Papers**, v. 33, n. 2, p. 225-246, 1986.

DEUSER, W.G.; JICKELLS, T.D.; KING, P.; COMMEAU, J.A. Decadal and annual changes in biogenic opal and carbonate fluxes to the deep Sargasso Sea. **Deep Sea Research Part A, Oceanographic Research Papers**, v. 42, n. 11-12, p. 1923-1932, 1995.

DO CARMO, F.F.; KAMINO, L.H.Y.; TOBIAS, R. JR.; DE CAMPOS, I.C.; DO CARMO, F.F.; SILVINO, G.; et al. 2017. Fundão tailings dam failures: the environment tragedy of the largest technological disaster of Brazilian mining in global context. **Perspectives in Ecology and Conservation**, v. 15, n. 3, p. 145-151, 2017.

DOLD, B. Submarine tailings disposal (STD) - a review. **Minerals**, v. 4, n. 3, p. 642-666, 2014.

DUCE, R.A.; TINDALE, N.W. Atmospheric transport of iron and its deposition in the ocean. **Limnology Oceanography**, v. 36, n. 8, p. 1715-1726, 1991.

ELBAZ-POULICHET, F., BRAUNGARDT, C., ACHTERBERG, E., MORLEY, N., COSSA, D., BECKERS, J.-M., et al. Metal biogeochemistry in the Tinto-Odiel rivers (southern Spain) and in the Gulf of Cadiz: a synthesis of the results of TOROS project. **Continental Shelf Research**, v. 21, n. 18-19, p. 1961-1973, 2001.

ELLWOOD, M.J.; NODDER, S.D.; KING, A.L.; HUTCHINS, D.A.; WILHELM, S.W.; BOYD, P.W. Pelagic iron cycling during the subtropical spring bloom, east of New Zealand. **Marine Chemistry,** v. 160, p. 18-33, 2014.

ELROD, V.A., BERELSON, W.M., COALE, K.H.; JOHNSON, K.S. The flux of iron from continental shelf sediments: a missing source for global budgets. **Geophysical Research Letters**, v. 31, n. 12, p. L12307, 2004.

ESCOBAR, H. Mud tsunami wreaks ecological havoc in Brazil. **Science**, v. 350, n. 6265, p. 1138-1139, 2015.

FALKOWSKI, P.G., BARBER, R.T., SMETACEK, V.V. Biogeochemical controls and feedbacks on ocean primary production. **Science**, v. 281, n. 5374, p. 200-206, 1998.

FEELY, R.A.; GEISELMAN, T.L.; BAKER, E.T.; MASSOTH, G.J.; HAMMOND, S.R. Distribution and composition of hydrothermal plume particles from the ASHES Vent Field at Axial Volcano, Juan de Fuca Ridge. **Journal Geophysical Research, Solid Earth**, v. 95, n. B8, p. 12855-12873, 1990.

FERNANDES, C.E.G., GONSALVES, M.J.B.D., NAZARETH, D.R., NAGARCHI, L.; KAMALESO, S.A. 2015. Microbial iron reduction and methane oxidation in subsurface sediments of the Arabian Sea. **Marine and Petroleum Geology**, v. 67, p. 327-335, 2015.

FINDEN, D.A.S.; TIPPING, E.; JAWORSKI, G.H.M.; REYNOLDS, C.S. Light induced reduction of natural iron(III) oxide and its relevance to phytoplankton. **Nature**, v. 309, n. 5971, p. 783-784, 1984.

FITZWATER, S.E.; COALE, K.H.; GORDON, R.M.; JOHNSON, K.S.; ONDRUSEK, M.E. Iron deficiency and phytoplankton growth in the equatorial Pacific. **Deep Sea Research Part II: Topical Studies in Oceanography**, v. 43, n. 4-6, p. 995-1015, 1996.

GARCIA, L.C.; RIBEIRO, D.B.; ROQUE, F.D.O.; OCHOA-QUINTERO, J.M.; LAURANCE, W.F. Brazil's worst mining disaster: corporations must be compelled to pay the actual environmental costs. **Ecological Applications**, v. 27, n. 1, p. 5-9, 2017.

GERMAN, C.R.; CAMPBELL, A.C.; EDMOND, J.M. 1991. Hydrothermal scavenging at the Mid-Atlantic Ridge: modification of trace element dissolved fluxes. **Earth and Planetary Science Letters**, v. 107, n. 1, p. 101-114, 1991.

GINOUX, P.; PROSPERO, J.M.; GILL, T.E.; HSU, N.C.; ZHAO, M. Global-scale attribution of anthropogenic and natural dust sources and their emission rates based on MODIS Deep Blue aerosol products. **Reviews of Geophysics**, v. 50, n. 3, p. RG3005, 2012.

GLEDHILL, M.; BUCK, K.N. The organic complexation of iron in the marine environment: a review. **Frontiers in Microbiology**, v. 3, n. 69, 2012.

GLEDHILL, M.; VAN DEN BERG, C.M.G. Determination of complexation of iron(III) with natural organic complexing ligands in seawater using cathodic stripping voltammetry. **Marine Chemistry,** v. 47, n. 1, p. 41-54, 1994.

GLEDHILL, M.; MCCORMACK, P.; USSHER, S.; ACHTERBERG, E.P.; MANTOURA, R.F.C.; WORSFORD, P.J. Production of siderophore type chelates by mixed bacterioplankton populations in nutrient enriched seawater incubations. **Marine Chemistry**, v. 88, n. 1-2, p. 75-83, 2004.

GOLDBERG, E.D. Iron assimilation by marine diatoms. **Biological Bulletin**, v. 102, n. 3, p. 243-248, 1952.

GOMES, M.A. **Caracterização do rejeito de minério de ferro da mina de córrego do feijão**. 2009. 84p. Dissertação (Mestrado em Engenharia Mineral) – Departamento de Engenharia de Minas, Universidade Federal de Ouro Preto, Ouro Preto, 2009.

GRAHAM, R.M.; DE BOER, A.M.; VAN SEBILLE, E.; KOHFELD, K.E.; SCHLOSSER, C. 2015. Inferring source regions and supply mechanisms of iron in the southern ocean from satellite chlorophyll data. **Deep Sea Research Part I: Oceanographic Research Papers**, v. 104, p. 9-25, 2015.

GREENWOOD, N.N.; EARNSHAW, A. Iron, ruthenium and osmium. *In:* **Chemistry of the elements**. 2. ed. Nova Iorque: Pergamon Press, 1984, cap. 25, p. 1070-1112.

GUAN, J.; YAN, B.; YUAN, X. Variations of total dissolved iron and its impacts during an extreme spring flooding event in the Songhua River. **Journal of Geochemical Exploration**, v. 166, p. 27-32, 2016.

HASSLER, C.S., NORMAN, L., NICHOLS, C.A.M., CLEMENTSON, L.A., ROBINSON, C., SCHOEMANN, V., et al. 2015. Iron associated with exopolymeric substances is highly bioavailable to oceanic phytoplankton. **Marine Chemistry**, v. 173, p. 136-147, 2015.

HATJE, V., PEDREIRA, R.M.A., DE REZENDE, C.E., SCHETTINI, C.A.F., DE SOUZA, G.C., MARIN, D.C., HACKSPACHER, P.C. The environmental impacts of one of the largest tailing dam failures worldwide. **Scientific Reports**, v. 7, p. 10706, 2017.

HONEYMAN, B.D.; BALISTRIERI, L.S.; MURRAY, J.W. Oceanic trace metal scavenging: the importance of particle concentration. **Deep Sea Research Part A. Oceanographic Research Papers**, v. 35, n.2, p. 227-246, 1988.

HOPKINSON, B.M.; MOREL, F.M.M. The role of siderophores in iron acquisition by photosynthetic marine microorganisms. **Biometals**, v. 22, p. 659-669, 2009.

HUTCHINS, D.A.; BRULAND, K.W. Grazer-mediated regeneration and assimilation of Fe, Zn and Mn from planktonic prey. **Marine Ecology Progress Series**, v. 110, n. 2-3, p. 259-269, 1994.

HUTCHINS, D.A.; DITULLIO, G.R.; BRULAND, K.W. Iron and regenerated production: evidence for biological iron recycling in two marine environments. **Limnology Oceanography**, v. 38, n. 6, p. 1242-1255, 1993.

ILBERT, M.; BONNEFOY, V. Insight into the evolution of the iron oxidation pathways. **Biochimica et Biophysica Acta - Bioenergetics**, v. 1827, p. 161-175, 2013.

JEANDEL, C.; OELKERS, E.H. The influence of terrigenous particulate material dissolution on ocean chemistry and global element cycles. **Chemical Geology**, v. 395, p. 50-66, 2015.

JICKELLS, T.D.; SPOKES, L.J. Atmospheric iron inputs to the ocean. *In:* D.R. TURNER; K.A. HUNTER. (eds.). **The biogeochemistry of iron in seawater**. Chichester: Wiley, v. 7, p. 85-121, 2001.

JOHNSON, K.S.; GORDON, R.M.; COALE, K.H. What controls dissolved iron concentrations in the world ocean? Authors' closing comments. **Marine Chemistry**, v. 57, n. 3-4, p. 181-186, 1997.

JOHNSON, K.S.; CHAVEZ, F.P.; FRIEDERICH, G.E. Continental-shelf sediment as a primary source of iron for coastal phytoplankton. **Nature**, v. 398, n. 6729, p. 697-700, 1999.

KHAN, A.; SINGH, P.; SRIVASTAVA, A. Synthesis, nature and utility of universal iron chelator – siderophore: a review. **Microbiological Research**, p. 212-213, p. 103-111, 2018.

KLEINT, C.; PICHLER, T.; KOSCHINSKY, A. Geochemical characteristics, speciation and size-fractionation of iron (Fe) in two marine shallow-water hydrothermal systems, Dominica, Lesser Antilles. **Chemical Geology**. v. 454, p. 44-53, 2017.

KOLBER, Z.S.; BARBER, R.T.; COALE, K.H.; FITZWATERI, S.E.; GREENE, R.M.; JOHNSON, K.S.; et al. Iron limitation of phytoplankton photosynthesis in the equatorial Pacific Ocean. **Nature**, v. 371, n. 6493, p. 145-149, 1994.

KOSKI, R.A. Metal dispersion resulting from mining activities in coastal environments: a pathways approach. **Oceanography**, v. 25, n. 2, p. 170-183, 2012.

KRACHLER, R.; JIRSA, F.; AYROMLOU, S. Factors influencing the dissolved iron input by river water to the open ocean. **Biogeosciences**, v. 2, p. 311-315, 2005.

KRACHLER, R.; KRACHLER, R.F.; VON DER KAMMER, F.; SÜPHANDAG, A.; JIRSA, F.; AYROMLOU, S.; et al. Relevance of peat-draining rivers for the riverine input of dissolved iron into the ocean. **Science of the Total Environment**, v. 408, n. 11, p. 2402-2408, 2010.

KRACHLER, R.; KRACHLER, R.F.; WALLNER, G.; HANN, S.; LAUX, M.; RECALDE, M.F.C.; et al. River-derived humic substances as iron chelators in seawater. **Marine Chemistry,** v. 174, p. 85-93, 2015.
KRACHLER, R.; KRACHLER, R.F.; WALLNER, G.; STEIER, P.; EL ABIEAD, Y.; WIESINGER, H.; et al. 2016. Sphagnum-dominated bog systems are highly effective yet variable sources of bio-available iron to marine waters. **Science of the Total Environment**, v. 556, p. 53-62, 2016.

KUMA, K.; SUZUKI, Y.; MATSUNAGA, K. Solubility and dissolution rate of colloidal y-FeOOH in seawater. **Water Research**, v. 27, n. 4, p. 651-657, 1993.

KUMA, K.; NISHIOKA; J.; MATSUNAGA, K. Controls on iron(III) hydroxide solubility in seawater: the influence of pH and natural organic chelators. **Limnology Oceanography**, v. 41, n. 3, p. 396-407, 1996.

KUSTKA, A.B.; KOHUT, J.T.; WHITE, A.E.; LAM, P.J.; MILLIGAN, A.J.; DINNIMAN, M.S.; et al. The roles of MCDW and deep water iron supply in sustaining a recurrent phytoplankton bloom on central Pennell Bank (Ross Sea). **Deep Sea Research Part I: Oceanographic Research Papers**, v. 105, p. 171-185, 2015.

KWON, E.Y.; KIM, G.; PRIMEAU, F.; MOORE, W.S.; CHO, H.M.; DEVRIES, T.; et al. Global estimate of submarine groundwater discharge based on an observationally constrained radium isotope model. **Geophysical Research Letters**, v. 41, n. 23, p. 8438-8444, 2014.

LAGLERA, L.M.; FILELLA, M. The relevance of ligand exchange kinetics in the measurement of iron speciation by CLE–AdCSV in seawater. **Marine Chemistry**, v. 173, p. 100-113, 2015.

LAGLERA, L.M.; MONTICELLI, D. Iron detection and speciation in natural waters by electrochemical techniques: a critical review. **Current Opinion in Electrochemistry,** v. 3, p. 123-129, 2017.

LAGLERA, L.M.; VAN DEN BERG, C.M. Evidence for geochemical control of iron by humic substances in seawater. **Limnology Oceanography**, v. 54, n. 2, p. 610-619, 2009.
LAGLERA, L.M.; BATTAGLIA, G.; VAN DEN BERG, C.M. Determination of humic substances in natural waters by cathodic stripping voltammetry of their complexes with iron. **Analytica Chimica Acta**, v. 599, p. 58-66, 2007.

LAGLERA, L.M.; BATTAGLIA, G.; VAN DEN BERG, C.M. Effect of humic substances on the iron speciation in natural waters by CLE/CSV. **Marine Chemistry**, v. 127, n. 1-4, p. 134-143, 2011.

LAMPITT, R.S.; ACHTERBERG, E.P.; ANDERSON, T.R.; HUGHES, J.A.; IGLESIAS-RODRIGUEZ, M.D.; KELLY-GERREYN, B.A.; et al. Ocean fertilization: a potential means of geoengineering? **Philosophical Transactions of the Royal Society**, v. 366, p. 3919-3945, 2008.

MAHMOOD, A.; ABUALHAIJA, M.M.; VAN DEN BERG, C.M.G.; SANDER, S.G. Organic speciation of dissolved iron in estuarine and coastal waters at multiple analytical windows. **Marine Chemistry**, v. 177, p. 706-719, 2015.

MARTIN, J.H.; GORDON, M.; FITZWATER, S.E. The case for iron. **Limnology Oceanography**, v. 36, n. 8, p. 1793-1802, 1991.

MAWJI, E.; GLEDHILL, M.; MILTON, J.A.; TARRAN, G.A.; USSHER, S.; THOMPSON, A.; et al. Hydroxamate siderophores: occurrence and importance in the Atlantic Ocean. **Environmental Science & Technology**, v. 42, p. 8675-8680, 2008.

MAYES, W.M.; POTTER, H.A.B.; JARVIS, A.P. Inventory of aquatic contaminant flux arising from historical metal mining in England and Wales. **Science of the Total Environment**, v. 408, p. 3576-3583, 2010.

MESKHIDZE, N.; HURLEY, D.; ROYALTY, T.M.; JOHNSON, M.S. Potential effect of atmospheric dissolved organic carbon on the iron solubility in seawater. **Marine Chemistry**, v. 194, p. 124-132, 2017.

MILLER, W.L.; KESTER, D. Photochemical iron reduction and iron bioavailability in seawater. **Journal of Marine Research**, v. 52, n. 2, p. 325-343, 1994.

MILLERO, F.J. Solubility of Fe(III) in seawater. **Earth and Planetary Science Letters**, v. 154, n. 104, p. 323-329, 1998.

MILLERO, F.; PIERROT, D. Speciation of metals in natural waters. *In:* MILLERO, F.; PIERROT, D. **Chemistry of marine water and sediments**. 1. ed. Berlim: Springer, p. 193-220, 2004.

MOREL, F.M.M.; PRICE, N.M. The biogeochemical cycles of trace metals in the oceans. **Science**, v. 300, n. 5621, p. 944-947, 2003.

MOREL, F.M.M., HUDSON, R.J.; PRICE, N.M. Limitation of productivity by trace metals in the sea. **Limnology Oceanography**, v. 36, n. 8, p. 1742-1755, 1991.

MOREL, F.M.M., MILLIGAN, A.J.; SAITO, M.A. Marine bioinorganic chemistry: the role of trace metals in the oceanic cycles of major nutrients. *In:* **Treatise on geochemistry**. 1. ed. Elsevier, Pergamon, v. 6, 2003, p. 113-143.

MOTTL, M.J.; MCCONACHY, T.F. Chemical processes in buoyant hydrothermal plumes on the East Pacific Rise near 21°N. **Geochimica et Cosmochimica Acta**, v. 54, n. 7, p. 1911-1927, 1990.

MULLIGAN, A.E.; CHARETTE, M.A. Groundwater flow to the coastal ocean. **Encyclopedia of ocean sciences**, p. 88-97, 2009.

NEILANDS, J.B. Siderophores: structure and function of microbial iron transport compounds. **Journal of Biological Chemistry**, v. 270, n. 45, p. 26723-26726, 1995.

NETO, R.R.; SÁ, F.; CARNEIRO, M.T.W.D.; COSTA, E.S.; RODRIGUES, D.R.P. 2016. The worst Brazilian environmental disaster altered the distribution of metals in water ate the Doce River Estuary and marine region. *In:* Proceedings of ICHMET 2016: International Conference on Heavy Metals in the Environment, 18, Ghent, 2016. Disponível em: https://ojs.ugent.be/ichmet/article/view/3991/3975. Acesso em: 05 fev. 2018.

NIENCHESKI, L.F., WINDOM, H.L.; MOORE, W.S. Controls on water column chemistry of the southern Brazilian continental shelf. **Continental Shelf Research**, v. 88, p. 126-139, 2014.

NORMAN, L.; CABANESA, D.J.; BLANCO-AMEIJEIRAS, S.; MOISSET, S.A.; HASSLER, C.S. Iron biogeochemistry in aquatic systems: from source to bioavailability. **CHIMIA International Journal for Chemistry**, v. 68, n. 11, p. 764-771, 2014.

NORMAN, L.; WORMS, I.A.M.; ANGLES, E.; BOWIE, A.R.; NICHOLS, C.M.; PHAM, A.N.; et al. 2015. The role of bacterial and algal exopolymeric substances in iron chemistry. **Marine Chemistry**, v. 173, p. 148-161, 2015.

OLÍAS, M.; CÁNOVAS, C.R.; NIETO, J.M.; SARMIENTO, A.M. Evaluation of the dissolved contaminant load transported by the Tinto and Odiel rivers (south west Spain). **Applied Geochemistry**, v. 21, p. 1733-1749, 2006.

ÖZTÜRK, M.; BIZSEL, N.; STEINNES, E. Iron speciation in eutrophic and oligotrophic Mediterranean coastal waters; impact of phytoplankton and protozoan blooms on iron distribution. **Marine Chemistry**, v. 81, n. 1-2, p. 19-36, 2003.

PEREIRA, A.A.; VAN HATTUM, B.; BROUWER, A.; VAN BODEGOM, P.M.; REZENDE, C.E.; SALOMONS, W. Effects of iron-ore mining and processing on metal bioavailability in a tropical coastal lagoon. **Journal of Soils and Sediments**, v. 8, p. 239-252, 2008.

PIRES, J.M.M.; DE LENA, J.C.; MACHADO, C.C.; PEREIRA, R.S. Potencial poluidor de resíduo sólido da Samarco Mineração: estudo de caso da barragem de germano [online]. **Revista Árvore**, v. 27, n. 3, p.393-397, 2003.

POITRASSON, F.; VIEIRA, L.C.; SEYLER, P.; PINHEIRO, G.M.D.S.; MULHOLLAND, D.S.; BONNET, M.P.; et al. Iron isotope composition of the bulk waters and sediments from the Amazon River Basin. **Chemical Geology**, v. 377, p. 1-11, 2014.

PRICE, N.M.; ANDERSEN, L.F.; MOREL, F.M. Iron and nitrogen nutrition of equatorial Pacific plankton. **Deep Sea Research Part A. Oceanographic Research Papers**, v. 38, n. 11, p. 1361-1378, 1991.

PROSPERO, J.M. Long-range transport of mineral dust in the global atmosphere: impact of African dust on the environment of the southeastern United States. **Proceedings of the National Academy of Sciences**, v. 96, p. 3396-3403, 1999.

PROSPERO, J.M.; CARLSON, T.N. Vertical and areal distribution of Saharan dust over the western Equatorial North Atlantic Ocean. **Journal of Geophysical Research**, v. 77, n. 27, p. 5255-5265, 1972.

PYE, K. Dust sources, sinks and rates of deposition. *In:* **Aeolian dust and dust deposits**. 1. ed. Londres: Academic press, p. 63-91, 1987.

QUÉGUINER, B. Iron fertilization and the structure of planktonic communities in high nutrient regions of the southern ocean. **Deep Sea Research Part II: Topical Studies in Oceanography**, v. 90, p. 43-54, 2013.

RAISWELL, R. Iron transport from the continents to the open ocean: the aging–rejuvenation cycle. **Elements**, v. 7, n. 2, p. 101-106, 2011.

RAISWELL, R.; CANFIELD, D.E. The iron cycle: biogeochemistry and mineralogy. In The iron biogeochemical cycle past and present. Geochemical perspectives. European Association of Geochemistry, Houten, Netherlands. v. 1, n. 1, p. 12-18, 2012. Disponível em: http://www.geochemicalperspectives.org/wp-content/uploads/2011/12/GPv1n1_online.pdf. Acesso em 07 jan. 2018

RATHA, D.S.; VENKATARAMAN, G. Environmental impact of iron ore mines in Goa, India. **International Journal of Environmental Studies**, v. 47, n. 1, p. 43-53, 1995.

RAVELO-PÉREZ, L.M.; RODRÍGUEZ, S.; GALINDO, L.; GARCÍA, M.I.; ALASTUEY, A.; LÓPEZ-SOLANO, J. Soluble iron dust export in the high altitude Saharan Air Layer. **Atmospheric Environment**, v. 133, p. 49-59, 2016.

REMBAUVILLE, M.; MANNO, C.; TARLING, G.A.; BLAIN, S.; SALTER, I. Strong contribution of diatom resting spores to deep-sea carbon transfer in naturally iron-fertilized waters downstream of South Georgia. **Deep Sea Research Part I: Oceanographic Research Papers**, v. 115, p. 22-35, 2016.

RICKARD, D. Sedimentary iron biogeochemistry. *In:* **Developments in sedimentology**. v. 65, p. 85-119, 2012.

RIJKENBERG, M.J.A.; POWELL, C.F.; DALL'OSTO, M.; NIELSDOTTIR, M.C.; PATEY, M.D.; HILL, P.G.; et al. Changes in iron speciation following a Saharan dust event in the tropical North Atlantic Ocean. **Marine Chemistry**, v. 110, p. 56-67, 2008.

ROSE, A.L.; WAITE, T.D. Kinetic model for Fe(II) oxidation in seawater in the absence and presence of natural organic matter. **Environmental Science & Technology,** v. 36, n. 3, p. 433-444, 2002.

RUBIN, M.; BERMAN-FRANK, I.; SHAKED, Y. Dust- and mineral-iron utilization by the marine dinitrogen-fixer Trichodesmium. **Nature Geoscience**, v. 4, n. 8, p. 529-534, 2011.

RUE, E.L.; BRULAND, K.W. Complexation of iron(III) by natural organic ligands in the Central North Pacific as determined by a new competitive ligand equilibration/adsorptive cathodic stripping voltammetric method. **Marine Chemistry**, v. 50, n. 1-4, p. 117-138, 1995.

RUE, E.L.; BRULAND, K.W. The role of organic complexation on ambient iron chemistry in the equatorial Pacific Ocean and the response of a mesoscale iron addition experiment. **Limnology Oceanography**, v. 42, n. 5, p. 901-910, 1997.

SCHUTZ, L.W.; PROSPERO, J.M.; BUAT-MÉNARD, P.; HARRISS, R.; CARVALHO, R.A.; HEIDAM, N.Z.; et al. The long-range transport of mineral aerosols: group report. *In:* **The long-range atmospheric transport of natural and contaminant substances**. Dordrecht: Springer, p. 197-229, 1990.

SHOLKOVITZ, E.R.; BOYLE, E.A.; PRICE, N.B. The removal of dissolved humic acids and iron during estuarine mixing. **Earth and Planetary Science Letters**, v. 40, n. 1, p. 130-136, 1978.

SILVER, J. Introduction to iron chemistry. *In:* **Chemistry of iron**. 1. ed. Dordrecht: Springer, p. 1-29, 1993.

SILVER, M.W.; BARGU, S.; COALE, S.L.; BENITEZ-NELSON, C.R.; GARCIA, A.C.; ROBERTS, K.J.; et al. Toxic diatoms and domoic acid in natural and iron enriched waters of the oceanic Pacific. **Proceedings of the National Academy of Sciences**, v. 107, n. 48, p. 20762–20767, 2010.

SU, H., YANG, R., ZHANG, A.; LI, Y. Dissolved iron distribution and organic complexation in the coastal waters of the East China Sea. **Marine Chemistry**, **v.** 173, p. 208-221, 2015.

SUGIE, K.; NISHIOKA, J.; KUMA, K.; VOLKOV, Y.N.; NAKATSUKA, T. Vailability of particulate Fe to phytoplankton in the Sea of Okhotsk. **Marine Chemistry**, v. 152, p. 20-31, 2013.

SUNDA, W.G. Bioavailability and bioaccumulation of iron in the sea. *In:* TURNER, D.R.; HUNTER, K. A. (eds.). **The biogeochemistry of iron in seawater**. Chichester: John Wiley & Sons, v. 7, p. 41-84, 2001.

SUNDA, W.G. Trace metals and harmful algal blooms. *In:* GRANÉLI, E.; TURNER, J.T. **Ecology of harmful algae**. Berlim: Springer, Berlin, v. 189, p. 203-214, 2006.

SUNDA, W.G.; HUNTSMAN, S.A. Iron uptake and growth limitation in oceanic and coastal phytoplankton. **Marine Chemistry**, v. 50, n. 1-4, p. 189-206, 1995.

SUNDA, W.G.; HUNTSMAN, S.A. High iron requirement for growth, photosynthesis; low-light acclimation in the coastal cyanobacterium *Synechococcus bacillaris*. **Frontiers in Microbiology,** v. 6, p. 561, 2015.

TAGLIABUE, A.; BOPP, L.; AUMONT, O. Evaluating the importance of atmospheric and sedimentary iron sources to Southern Ocean biogeochemistry. **Geophysical Research Letters**, v. 36, n. 13, p. L13601, 2009.

TAGLIABUE, A.; BOPP, L.; DUTAY, J.C.; BOWIE, A.R.; CHEVER, F.; JEAN-BAPTISTE, P.; et al. Hydrothermal contribution to the oceanic dissolved iron inventory. **Nature Geoscience**, v. 3, n. 4, p. 252-256, 2010.

TAGLIABUE, A.; MTSHALI, T.; AUMONT, O.; BOWIE, A.R.; KLUNDER, M.B.; ROYCHOUDHURY, A.N.; SWART, S. A global compilation of dissolved iron measurements: focus on distributions and processes in the Southern Ocean. **Biogeosciences**, v. 9, p. 2333-2349, 2012.

TAGLIABUE, A.; AUMONT, O.; BOPP, L. The impact of different external sources of iron on the global carbon cycle. **Geophysical Research Letters**, v. 41, p. 920-926, 2014.

TAGLIABUE, A.; AUMONT, O.; DEATH, R.; DUNNE, J.P.; DUTKIEWICZ, S.; GALBRAITH, E.; et al. How well do global ocean biogeochemistry models simulate dissolved iron distributions? **Global Biogeochemical Cycles**, v. 30, p. 149-174, 2016

TAGLIABUE, A.; BOWIE, A.R.; BOYD, P.W.; BUCK, K.N.; JOHNSON, K.S.; SAITO, M.A. The integral role of iron in ocean biogeochemistry. **Nature**, v. 543, p. 51-59, 2017.

TAKEDA, S.; OBATA, H. Response of equatorial Pacific phytoplankton to subnanomolar Fe enrichment. **Marine Chemistry**, v. 50, n. 1-4, p. 219-227, 1995.

TREZZI, G.; GARCIA-ORELLANA, J.; SANTOS-ECHEANDIA, J.; RODELLAS, V.; GARCIA-SOLSONA, E.; GARCIA-FERNANDEZ, G.; MASQUÉ, P. The influence of a metal-enriched mining waste deposit on submarine groundwater discharge to the coastal sea. **Marine Chemistry**, v. 178, p. 35-45, 2016.

TRICK, C.G.; BILL, B.D.; COCHLAN, W.P.; WELLS, M.L.; TRAINER, V.L.; PICKELL, L.D. Iron enrichment stimulates toxic diatom production in high-nitrate, low-chlorophyll areas. **Proceedings of the National Academy of Sciences**, v. 107, n. 13, p. 5887-5892, 2010.

U.S. Geological Survey (USGS). **Mineral commodity summaries 2018**. Reston: U.S. Geological Survey, 2018. 200 p. DOI 10.3133/70194932.

VAN DEN BERG, C.M. Evidence for organic complexation of iron in seawater. **Marine Chemistry**, v. 50, n. 1-4, p. 139-157, 1995.

VON DER HEYDEN, B.P.; ROYCHOUDHURY, A.N. A review of colloidal iron partitioning and distribution in the open ocean. **Marine Chemistry**, v. 177, n. 9-19, 2015.

WADLEY, M.R.; JICKELLS, T.D.; HEYWOOD, K.J. The role of iron sources and transport for Southern Ocean productivity. **Deep Sea Research Part I: Oceanographic Research Papers**, v. 87, p. 82-94, 2014.

WATSON, A.J. Iron limitation in the oceans. *In:* TURNER, D.R.; HUNTER, K.A. (eds.). **The biogeochemistry of iron in seawater**. Chichester: Wiley. v. 7, 2001, p. 9-39.

WEFER, G.; FISCHER, G. Annual primary production and export flux in the southern ocean from sediment trap data. **Marine Chemistry**, v. 35, n. 1-4, p. 597-613, 1991. DOI 10.1016/S0304-4203(09)90045-7.
WELLS, M.L.; MAYER, L.M. The photoconversion of colloidal iron oxyhydroxides in seawater. **Deep Sea Research Part A. Oceanographic Research Papers**, v. 38, n. 11, p. 1379-1395, 1991.

WELLS, M.L.; ZORKIN, N.G.; LEWIS, A.G. The role of colloid chemistry in providing a source of iron to phytoplankton. **Journal of Marine Research**, v. 41, n. 4, p. 731-746, 1983.

WELLS, M.L.; PRICE, N.M.; BRULAND, K.W. Iron chemistry in seawater and its relationship to phytoplankton: a workshop report. **Marine Chemistry**, v. 48, n. 2, p. 157-182, 1995.

WELLS, M.L.; TRICK, C.G.; COCHLAN, W.P.; HUGHES, M.P.; TRAINER, V.L. Domoic acid: the synergy of iron, copper; the toxicity of diatoms **Limnology Oceanography**, v. 50, n. 6, p. 1908-1917, 2005.

WILLIAMS, R.J.P. Iron in evolution. **FEBS Letters**, v. 586, p. 479-484, 2012.

WINDOM, H.L.; MOORE, W.S.; NIENCHESKI, L.F.H.; JAHNKE, R.A. Submarine groundwater discharge: a large, previously unrecognized source of dissolved iron to the South Atlantic Ocean. **Marine Chemistry**, v. 102, n. 3–4, p. 252-266, 2006.

WOLLF, A.P. **Caracterização de Rejeitos de Minério de Ferro de Minas da Vale**. 2009. 107p. Dissertação (Doutorado em Engenharia Mineral) – Departamento de Engenharia de Minas, Universidade Federal de Ouro Preto, Ouro Preto, 2009.

WONG, M.H. Environmental impacts of iron ore tailings-the case of Tolo Harbor, Hong-Kong. **Environment Management**, v. 5, n. 2, p. 135-145, 1981.

WORSFOLD, P.J.; LOHAN, M.C.; USSHER, S.J.; BOWIE, A.R. Determination of dissolved iron in seawater: a historical review. **Marine Chemistry**, v. 166, p. 25-35, 2014.

WOZNIAK, A.S.; SHELLEY, R.U.; MCELHENIE, S.D.; LANDING, W.M.; HATCHER, P.G. Aerosol water soluble organic matter characteristics over the North Atlantic Ocean: Implications for iron-binding ligands and iron solubility. **Marine Chemistry**, v. 173, p. 162-172, 2015.

YOON, J.E.; YOO, K.C.; MACDONALD, A.M.; YOON, H.I.; PARK, K.T.; YANG, E.J.; et al. Ocean iron fertilization experiments: past-present-future with introduction to Korean Iron fertilization experiment in the southern ocean (KIFES) project. **Biogeosciences**, v. 15, p. 5847-5889, 2018.

ZABOWSKI, D.; HENRY, C.L.; ZHENG, Z.; ZHANG, X. Mining impacts on trace metal content of water, soil; stream sediments in the Hei River basin, China. **Water, Air, & Soil Pollution**, v. 131, n. 1-4, p. 261-273, 2001.

ZHUO-PING, C.; WEI-WEI, H.; MIN, A.; SHUN-SHAN, D. Coupled effects of irradiance and iron on the growth of a harmful algal bloom-causing microalga Scrippsiella trochoidea. **Acta Ecologica Sinica**, v. 29, p. 297-301, 2009.

CAPÍTULO 2

COASTAL WATERS CONTAMINATION BY MINING TAILINGS: WHAT TRIGGERS THE STABILITY OF IRON IN THE DISSOLVED FRACTIONS?

Longhini, C.M.; Mahieu, L.; Sá, F.; van den Berg, C.M.G.; Salaün, P.; Neto, R.R.

Submitted to Limnology and Oceanography journal

ABSTRACT

The solubility of dissolved iron (dFe) in seawater is greatly enhanced by complexation with organic ligands, predominantly occurring as humic substances (HS) in coastal areas. Aside from the natural processes, mining exploitation is believed to change Fe biogeochemistry in coastal waters impacted by those activities. However, the impacts of iron ore tailings on the physical and chemical speciation of dFe and soluble (sFe) are not known. Here we show that dFe and sFe concentrations in coastal waters affected by a mining catastrophe (Fundão dam collapse, Southeast Brazil) remain very high, even almost 3 years after the event, with concentrations of dFe up to 2.8 μM (0.45 μm), 700 nM (0.22 μm) and sFe up to 40 nM. These are unusually high concentrations of Fe, more representative of rivers, not waters of salinity 35 and above. However, HS levels in these coastal waters are comparable to unaffected areas and can only explain the binding of 2% and 10% (median values) of dFe (0.22 μm) and sFe concentrations, respectively. Our results show that processes other than complexation with HS are at play to maintain such high dFe and sFe concentrations. We hypothesize that Fe is present under nanoparticulate Fe(III) oxy-hydroxides in the soluble fraction and/or is complexed by amine compounds that are widely used in the ore extraction process. In view of the apparent high stability of Fe sustained over several years, this mining tailing catastrophe, and all other mining effluents worldwide might provide a non-negligible amount dFe to the open ocean.

Key words: Dissolved iron, humic substances, mine tailings disaster, CLE-ACSV, iron ligands, nanoparticulate colloids.

13 INTRODUCTION

Iron is a bio-essential element that is limiting primary productivity in 40% of the world oceans. It is entering the marine system through multiple external sources and the atmospheric dust is dominant to the Fe supply at the low latitudes whereas continental margin and hydrothermal inputs are more important for Fe inventory at the high latitudes (TAGLIABUE; AUMONT; BOPP, 2014). Nevertheless these natural inputs, dFe residence time in the water column is much shorter than other nutrients due to its low solubility (LIU; MILLERO, 2002) and its propensity to adsorb on any reactive surface, thus removing it from the water column (BRULAND; LOHAN, 2003). Understanding the distribution of Fe between different size fractions is a key factor to describe the chemical reactivity and bioavailability of Fe in seawater and its biogeochemical behaviour (TAGLIABUE *et al*., 2017). Speciation is usually done in one of the three operationally-defined size fractions: particulate (pFe; > 0.45 µm), dissolved (dFe; < 0.45 µm) and to a much lesser extent, soluble iron (sFe; < 0.02 µm).

Much of the exploration of Fe speciation in the dissolved fraction has been focused on the complexation with organic compounds as Fe bound to natural organic ligands represents more than 99% of the dFe concentrations in marine ecosystems (GLEDHILL; van den BERG, 1994; RUE; BRULAND, 1995, 1997). Organic complexes increase the dFe solubility by reducing its removal by precipitation from the water column (LIU; MILLERO, 2002; BOYD; ELLWOOD, 2010; GLEDHILL; BUCK, 2012; KRACHLER *et al*., 2015). In the absence of organic ligands, Fe concentrations in natural seawater with high Eh levels and pH around 8.0 would not be more than 0.01 nM (BYRNE; KESTER, 1976; LIU; MILLERO, 2002), due to extensive precipitation. The presence of organic ligands, their reactivity and own biogeochemical cycling, thus defines the distribution patterns of dFe concentrations in the ocean (KUMA; NISHIOKA; MATSUNAGA, 1996; SU *et al*., 2015; HASSLER; van den BERG; BOYD, 2017).

Natural iron-binding ligands in seawater are thought to be mostly siderophores, strong chelators released by heterotrophic bacteria and cyanobacteria as a biochemical strategy to assimilate dFe (BARBEAU *et al*., 2001; BARBEAU *et al*., 2003; GLEDHILL *et al*., 2004; MAWJI *et al*., 2008), exopolymeric substances (EPS)

from cellular exudates (HASSLER *et al*., 2015; NORMAN *et al*., 2015) and refractory organic matter like humic substances (HS) (LAGLERA; van den BERG, 2009; BATCHELLI *et al*., 2010; LAGLERA; BATTAGLIA; van den BERG, 2011; BUNDY *et al*., 2015; MAHMOOD *et al*., 2015; GERRINGA *et al*., 2017; MULLER; CUSCOV, 2017; SLAGTER *et al*., 2017). These compounds are different in their origin, conditional stability and dispersal patterns from coastal to offshore oceanic regions (HASSLER; van den BERG; BOYD, 2017). In estuarine and coastal waters, there is mounting evidence that HS dominate the bulk of organic ligands (LAGLERA; van den BERG, 2009; BATCHELLI *et al*., 2010; LAGLERA; BATTAGLIA; van den BERG, 2011; BUNDY *et al*., 2015; MAHMOOD *et al*., 2015; GERRINGA *et al*., 2017; MULLER; CUSCOV, 2017; SLAGTER *et al*., 2017). These HS compounds are believed to be mostly of terrestrial origin (LAGLERA; BATTAGLIA; van den BERG, 2007; LAGLERA; van den BERG, 2009; BATCHELLI *et al*., 2010; SU *et al*., 2018) and although they undergo extensive removal within estuaries through coagulation and flocculation processes (e.g. SHOLKOVITZ; BOYLE; PRICE, 1978; SU *et al*., 2018), a significant proportion make it through the estuarine trapping (MULLER, 2018).

Speciation of sFe fraction in terms of organic ligands has not been largely addressed but the presence of soluble chelates from microbial degradation of settling biogenic particles (e.g. faecal pellets) has been suggested to explain the sFe levels in the North Atlantic and North Pacific waters (WU *et al*., 2001). Recent studies using both the size partitioning method and ligands determination by cathodic stripping voltammetry showed the presence of two organic ligand classes (stronger L1 and weaker L2) occurring in excess in soluble fraction of surface waters in the Atlantic Ocean (CULLEN; BERGQUIST; MOFFETT, 2006; FITZSIMMONS *et al*., 2015). Although the type of ligands has not been specified by these authors, the range of ligand conditional stability constants observed by Fitzsimmons *et al*. (2015) for L1 (log K1 from 12.11 to 13.08) fall into siderophores log K1 values (higher than 12) while L2 values (log K2 from 10.81 to 11.86) can represent a wide class of ligands with high similarity in complex stability (e.g. HS, HS-like and EPS) (HASSLER; van den BERG; BOYD, 2017). In addition to the stabilization of sFe by organic complexation, recent studies in hydrothermal vents have suggested that sFe stability is mostly related to the presence of colloids as inorganic nanoparticles of pyrite FeS2

(YÜCEL *et al*., 2011), FexSiy (GARTMAN; FINDLAY; LUTHER, 2014) and $FeO_x(OH)_y$ (FITZSIMMONS *et al*., 2017). As colloidal substances (SAÑUDO-WILHELMY; RIVERA-DUARTE; FLEGAL, 1996; MUNKSGAARD; PARRY, 2001) whose size is assumed to range from 1 nm to 1 µm (BUFFLE; LEPPARD, 1995) can be present in all the operational Fe size-fractions, the soluble Fe compounds (SAÑUDO-WILHELMY; RIVERA-DUARTE; FLEGAL, 1996; MUNKSGAARD; PARRY, 2001; NORMAN *et al*., 2014) can be assumed to be mostly consisted of various small organic complexes (TAGLIABUE *et al*., 2017), a smaller colloidal inorganic fraction (essentially Fe oxy-hydroxide) and a minute amount of free metal ion (MILLERO; PIERROT, 2002; NORMAN *et al*., 2014).

In addition to the natural sources, anthropogenic inputs have strongly modified metal distributions and associated biogeochemical processes in coastal seas. In this context, extraction and processing of ores have impacted several coastal environments, modifying the dispersal of metals by various physical and chemical processes that are fundamentally different than those that disperse natural inputs (KOSKI, 2012). In November 2015, the collapse of the Fundão dam in South-eastern Brazil spilled more than 55 million m^3 of iron ore tailings along the Doce River which reached the coastal area in the Espírito Santo state, more than 600 km downstream. This event was considered one of the largest dam tailings failure worldwide (CARMO *et al*., 2017). This same region up to the Northeast of Brazil is even more intriguing for researchers as since late of August 2019 it has been impacted by crude oil residue from an unknown source from open sea which is affecting hundreds of sensitive environments, such as estuaries, reefs and mangroves along a 2,500 km of the shoreline (ESCOBAR, 2019).

Major changes in the marine iron biogeochemistry can be expected due to environmental disasters such as this Fundão dam collapse; these include changes in the main source of Fe (in regards to its physical and chemical nature), its input rate, the physical and chemical transformations of this Fe in seawater, its organic speciation by binding to different organic ligands as well as synergistic effects with other metals and nutrients (LONGHINI; SÁ; NETO, 2019). Studies focusing on the identification of the various metal forms and their distribution are required to evaluate the potential bioavailability and toxicity of such species, leading to a range of

ecological aspects, such as assimilation by biological groups and associated changes in community structures (LONGHINI; SÁ, NETO, 2019).

The aim of this study is to evaluate the impact of chemical speciation on the distribution of iron in the coastal waters affected by the dam failure, and changes therein as a result of the greatly increased Fe concentrations. We determined the distribution of three size-fractionated species of dFe (< 0.45, < 0.2 and < 0.02 μm) and their relation with HS in the coastal area affected by the Fundão iron ore tailings. This study brings insights into the biogeochemical factors related to the Fe fluxes and tailings deposition in coastal areas impacted by mining activities. This study also presents the first direct measurements of HS in marine area directly affected by mining tailings.

14 MATERIALS AND METHODS

14.1 Study area

The Doce River watershed (Southeast Brazil) comprises two states (Minas Gerais and Espírito Santo). In Minas Gerais, this watershed is located in the Quadrilátero Ferrífero mineral province, the largest iron ore complex in Latin America (DORR; LICINIO; BARBOSA, 1963). One of the most important ore deposits exploited in this region is the Itabirite, a low-grade iron ore that requires several treatment steps to a higher mass recovery (JOSÉ; BROD; PEREIRA, 2018). The flotation method is mostly used to reduce the presence of quartz and other impurities in iron ore concentrates (ARAUJO; VIANA; PERES, 2005; PEARSE, 2005; MA, 2012; FILIPPOV; SEVEROV; FILIPPOVA, 2014). Tailings sludge with high iron content (PIRES *et al*., 2003) is generated as a waste product of the iron ore processing and stored in dams, structures built of earthfill to contain the tailings (https://www.samarco.com/en/barragens/ accessed 23 September 2019). The activities of exploitation and processing of iron ore in this region were known to affect the metal levels in water bodies near the tailings dam including a coastal lagoon located in Espírito Santo state, even prior to the Fundão dam rupture (PEREIRA *et al*., 2008).

The object of this study is the continental shelf adjacent to the Doce River mouth (Espírito Santo state) (Fig. 6) which has been impacted by the tailings sludge

deposition after the Fundão mining disaster. The hydrological and oceanographic conditions (winds/waves regimes) are known to affect the Doce River discharge conditions, defining the flow of the turbidity plume (RUDORFF *et al*., 2018), the sedimentary processes (QUARESMA *et al*., 2015) and consequently the dispersion pattern of the tailings along the Doce River continental shelf. The average Doce River flow is 900 $m^3.s^{-1}$, ranging from 250 to 300 $m^3.s^{-1}$ during the dry winter (from April to September) to 1,800 $m^3.s^{-1}$ in January. Flooding events occurring for one or two days usually exceed 5,000 $m^3.s^{-1}$ with a maximum flood record of approximately 9,000 m3.s-1 (HATJE *et al*., 2017).

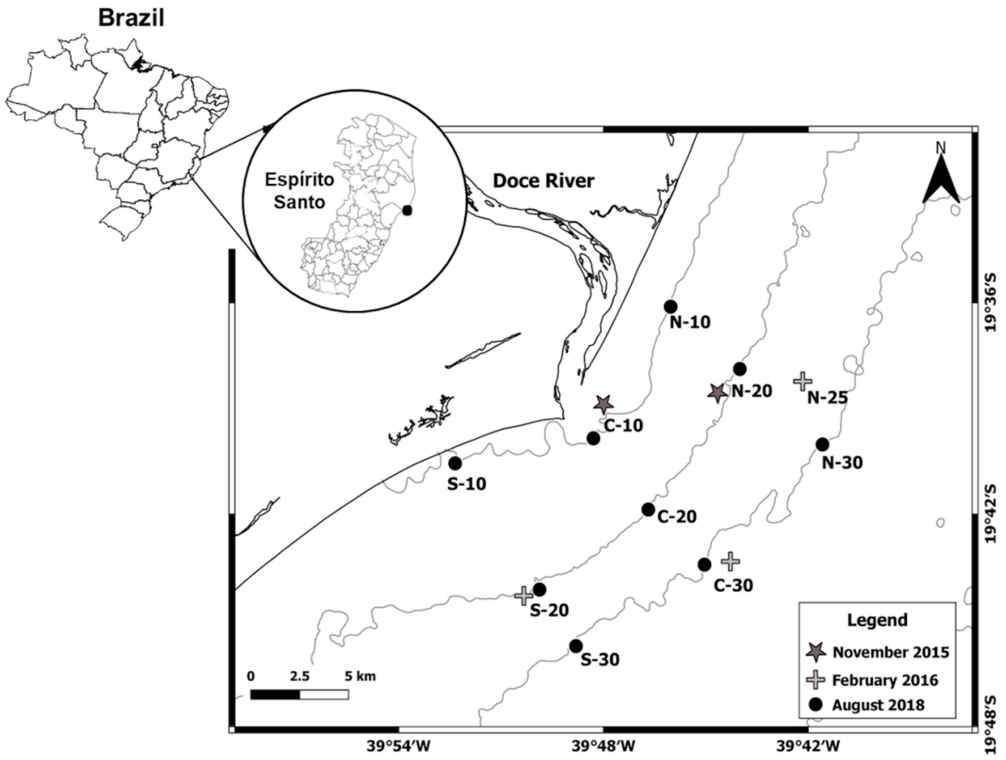

Figure 6. Distribution of sampling stations on the continental shelf adjacent to the Doce River mouth (Southeast, Brazil) after the Fundão dam rupture. N, C and S correspond to the sectors North, Central and South, respectively; 10, 20 and 30 indicate the isobaths 10, 20 and 30 meters.

14.2 Sampling design

Sampling was carried out in August 2018, approximately two years and nine months after the iron tailings reached the coastal area. Three transects were established perpendicular to the shoreline: North (N), Central (C) and South (S), each composed of three stations from 10 to 30 m isobaths. Seawater samples were also collected 6 days (on 27 November 2015) and 3 months (February 2016) after

the Fundão dam failure to evaluate the geochemical conditions during the acute phase of the impact. Two and three stations were sampled in November 2015 and February 2016, respectively (Fig. 6).

Coastal water samples from surface (~50 cm below the water surface) and bottom (~2 m above the bottom) waters were collected using a 5 litre Niskin horizontal bottle sampler (General Oceanics) (n = 4 in November 2015; n = 6 in February 2016; n = 18 in August 2018) into 500 mL acid-cleaned LDPE bottles. Temperature and seawater pH were measured on-board using a portable pH meter (Metrohm model 826). The pH was calibrated using Metrohm buffer solutions of 4.01, 7.00 and 9.00 pH (NBS scale). Salinity was measured from a CTD instrument (11 plus Sea-Bird in Nov/2015 and 9 plus Sea-Bird in Feb/2016). In Aug/2018 this parameter was measured using a refractometer.

14.3 Hydroclimatic conditions during the samplings

The Fundão dam rupture occurred in the context of an extreme hydrological drought in the region (RUDORFF *et al*., 2018). After the dam failure on 5 November 2015, the iron ore tailings reached the coast on the 21 November 2015 by low streamflow conditions (267.5 $m^3.s^{-1}$) (Fig. 7). The samplings were conducted under low Doce River discharge which ranged from 291.3 $m^3.s^{-1}$ in Nov/2015, 457.8 $m^3.s^{-1}$ in Feb/2016 and 231.8 $m^3.s^{-1}$ in Aug/2018 (Fig. 7; Table 2). A flooding event occurred towards the end of January 2016 reaching a maximum of 3,667.1 $m^3.s^{-1}$ on 22 January (Fig. 7).

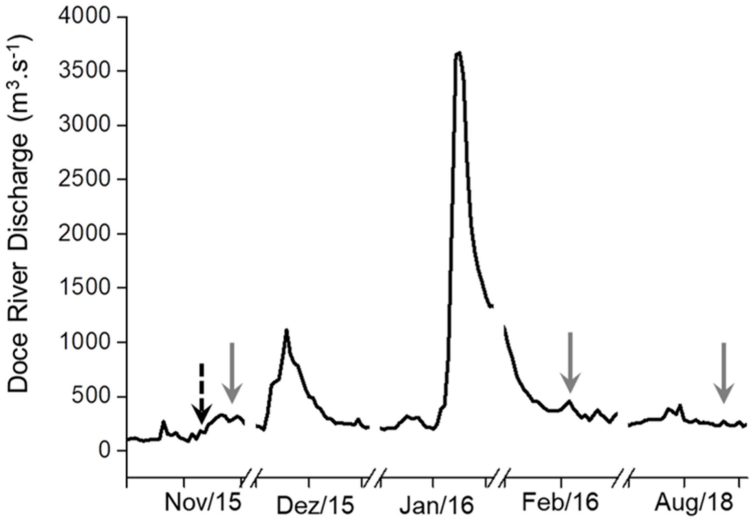

Figure 7. Daily average of the Doce River discharge ($m^3.s^{-1}$) for the months November 2015, December 2015, January 2016, February 2016 and August 2018. Black dashed arrow represents the day that the iron ore tailings reached the coastal waters after the Fundão dam rupture; Light grey arrows indicate the sampling days. Data from Agência Nacional de Água – ANA (Colatina station): https://www.snirh.gov.br/.

The winds predominantly came from N, NE and S in Nov/2015 promoting the Doce River turbidity plume to disperse southward, southwest-ward and northward. In Feb/2016 the plume was dispersed mainly to the southern region while in Aug/2018 it was concentrated parallel to the coast and moved southwest-ward (see Table 2).

Table 2. General hydroclimatic conditions during the sampling on the continental shelf adjacent to the Doce River mouth.

Date	River Discharge ($m^3.s^{-1}$)	Wind	Cold front passage[d]	Doce River plume dispersion
27/11/2015	291.3	N, NE, S[a]	Yes	Northward, Southward and Southwest-ward[a]
17/02/2016	457.8	N, NE[a]	No	Southward and Southeast-ward[a]
24/08/2018	231.8	N, NE[c]	No	Parallel to the coast and Southwest-ward[b]

a - Bastos et al. (2017); b - MODIS-Aqua imagery; c - NCEP Climate Forecast System Version 2 (CFSv2); d – Data from *Grupo de Estudos Climáticos, Universidade de São Paulo – USP*: http://www.grec.iag.usp.br/data/frentes-frias_BRA.php

14.4 Processing and preservation of samples

The samples were filtered once back at the laboratory, immediately after collection. Unfiltered seawater was passed either through 0.45 µm or through 0.22 µm cellulose acetate membrane (Millipore®) using a vacuum pump system to evaluate the iron concentration in two dissolved size fractions: dFe (0.45 µm) and

dFe (0.22 µm), respectively. The aliquots filtered through 0.22 µm membrane were also used to determine humic substances (HS). The filtrates for dFe (0.45 µm) were acidified to reach pH < 2.0 by adding HNO_3 65% (previously distilled using sub-boiling procedure; boiling sub-distill acid mark Berghof BSB-939-IR model) and stored at 4°C until analysis. Samples for dFe (0.22 µm) determination were stored in a frozen state and transported in a thermic box filled with dry ice from Brazil to the University of Liverpool (Liverpool, UK). The soluble fraction (sFe; 0.02 µm) was obtained by filtration of the 0.22 µm filtrate through acid-cleaned 0.02 µm Anotop filter syringes (25 mm diameter). Samples were always analysed within 24h of thawing. Iron was thus determined in three different size fractions: a) dFe (0.45 µm) by ICP-MS which corresponds to the total dissolved iron; b) dFe (0.22 µm) and sFe (0.02 µm) by voltammetry. HS were measured by voltammetry in the 0.22 µm fraction.

Chlorophyll-a pigments were concentrated by filtration on board through Glass Microfibre Filter (Sartorius) of 25 mm diameter. The filters were kept frozen until the extraction procedure. The Suspended Particulate Material (SPM) was determined by gravimetric method after filtration through pre-weighted glass fibre membranes (porosity of 0.45 µm).

14.5 Chemical analyses

14.5.1 Mass spectroscopy

dFe (0.45 µm) in seawater samples was determined by Inductively Coupled Plasma – Mass Spectroscopy (ICP-MS, Agilent, 7500 cx). The pH in the pre-acidified aliquots was adjusted using 1 M NaOH to a final pH around 7.0. The samples were then pre-concentrated by passing through a cationic resin column (Chelex®). The trace metal extracts were eluted from the resin column with HNO_3 2% solution. The compounds were quantified according to the EPA 6020A method for multi-element determination using ICP-MS (U.S. EPA, 1998). The fluctuations in the signals during the measurements were corrected by using a multi-element internal standard (Internal Standard Mix - Bi, Ge, In, Li, Sc, Tb and Y, Agilent Technologies). Multi-element standards (ICP multi-element standard solution XXI for MS, CentiPUR ® MERCK, Darmstadt - Germany) were used to carry the calibration curve (concentration range from 0 to 300 $\mu g.L^{-1}$). The dFe (0.45 µm) concentrations were determined by the linear regression (y = ax+ b) plotted as a result of the calibration

curve. Three analytical modes were used (no gas, Helium and Hydrogen) and the optimum one, as determined by the method of recovery from spiked samples, was used for each metal. All solutions were prepared with ultra-pure water processed using a PURELAB ultra (Model Ultra an MKZ, the brand Elgar).

14.5.2 Adsorptive cathodic stripping voltammetry (AdCSV)

The voltammetric system used for dFe (0.22 µm), soluble iron (sFe) and humic substances (HS) determination was a µAutolab(III) potentiostat connected to a VA663 Stand (Metrohm, Switzerland) and a 663 IME interface and controlled with the GPES software. The working, counter and reference electrodes were a static mercury drop electrode (SMDE), a glassy carbon rod and an Ag/AgCl//KCl (3 M), respectively. The voltammetric cell was an acid cleaned polytetrafluoroethylene (PTFE) cell placed into a home-made acrylic holder to allow analysis of small sample volume (5 mL). The stirrer, a specially made rotating PTFE rod, was set to a fixed stirring speed of 5. All the materials used during the analytical procedure and for storing samples and reagents were cleaned by 1 M HCl (1 week), 0.1 M HCl (1 week), 0.01 M during storage and rinsed using Milli-Q water between steps and prior to usage.

dFe (0.22 µm) and sFe determination: Diluted iron standard solution (1 µM and 10 µM iron) was prepared from a 1,000 $mg.L^{-1}$ standard (SpectrosoL®) diluted with ultra-pure water (Millipore, UK, 18 $M\Omega.cm^{-1}$ resistivity) and acidified to pH 2 using 9 M HCl (10 µL 9 M HCl/10 mL). HCl trace analysis grade (Fisher Scientific), and ammonia trace metal grade (Fisher Scientific) were employed. The Buffer was 0.2 M HEPPS (3-[4-(2-hydroxyethyl)-1-piperazinyl]propanesulfonic acid; Merck, ≥ 99.0%) prepared in ultra-pure water and the pH was adjusted using adequate amount of solid sodium hydroxide (Fisher, 99.2% trace reagent grade) to a final pH_{NBS} of 8.15. The HEPPS buffer was purified by two overnight equilibrations with 100 µM MnO_2, removed by filtration using 0.2 µm cellulose acetate membrane (Whatman) (OBATA; van den BERG, 2001). The added ligand was 2 mM DHN (2,3-dihydroxynaphthalene) which was prepared by dissolving DHN (Fluka, ≥ 98.0%) in Milli-Q water.

The voltammetric procedure used to determine Fe levels in dFe (0.22 µm) and in sFe was the method of Caprara, Laglera and Monticelli (2015), based on the

reduction of the electroactive complex Fe-DHN by Cathodic Stripping Voltammetry (CSV), but slightly modified to suit the high iron concentrations present in our samples. Standard additions were used to determine Fe in each sample, with a minimum of 2 additions and a minimum of 3 voltammetric scans per addition. Prior to the analysis, the samples were acidified to pH < 2.0 by addition of HCl (Fisher, Trace Analysis) (3.6 µL of 30% HCl/3 mL sample) and UV-digested for 2 hours using a home-built system with a 100-W, high-pressure, mercury vapour lamp in 30 mL quartz tubes. Then 1 M NaOH (21 µL of 1 M NaOH/3 mL sample) was added to adjust the pH to around 8.0 before measurements. For dFe (0.22 µm) determination, the samples were diluted using oceanic seawater (dFe concentration was 1 ± 0.1 nM; n = 6) which was UV-irradiated (1 hour) freshly prior to use. This oceanic seawater is referred below as the background seawater.

The deposition time and the dilution factor were defined by a series of calibration curves using 30 seconds, 15 seconds, 10 seconds and 5 seconds deposition time and a range of iron concentrations from 5 nM to 40 nM. The best linear range was achieved using 5 seconds deposition time until 14 nM iron concentration. Subsequently the dilution factor for dFe (0.22 µm) samples was adjusted so that a maximum of 14 nM was present in the cell at the end of the standard addition (minimum of 2 additions). sFe determinations were mostly made in undiluted samples.

Regarding dFe (0.22 µm) analysis, 5 mL of the background seawater was pipetted into the PTFE cell then DHN (final concentration 10 µM) and HEPPS buffer (final concentration 10 mM) were added. The solution was air-purged using cylinder air (1 Bar pressure) for 90 seconds and five voltammetric scans were made to determine the background peak height. Then the sample was added to the background seawater with a dilution factor of at least 30 to ensure an increase of the signal of between 2 and 3 times the background seawater signal. The solution was air-purged again for 90 seconds and six more voltammetric scans were made. The first iron standard addition was made sufficient to approximately double the original peak and a minimum of three voltammetric scans were carried out. A second iron standard addition was made to confirm the sensitivity. The sensitivity (nA/nM) was calculated from the slope of the increase in peak height by the iron standard additions and used to calculate the Fe concentration in the sample. The iron

concentration in the background seawater was calculated in the same way and subtracted from those of the samples. A number of samples were analysed from repeated measurements to determine the precision (standard deviation) of the method. For sFe samples no dilution was required because the Fe concentrations were sufficiently low. The sample (5 mL) was pipetted directly into the PTFE cell and the same procedure as that described for dFe (0.22 µm) analyses was performed. The sFe method was validated by using the sample C-10 Bottom (Aug/2018) as control which was previously analysed in triplicate to confirm its concentration. This control sample was measured several times along the days of analysis. Only the certified results for sFe are given here (n = 14, from a total of n = 28) because of a contamination issue resulting on higher sFe values and non-validation from the control sample. Measurement errors ranged around 5.1% when dilution was required (dFe (0.22 µm) analyses) and around 4.4% for non-diluted samples (sFe determination).

The PTFE cell was rinsed five times using Milli-Q water and then with Milli-Q water plus 10 µM DHN between the analyses to avoid adsorption on the cell wall. Measurements were made using square wave cathodic stripping voltammetry with a deposition time of 5 s at -0.1 V, a 5 s equilibration time (no stirrer) and stripping from -0.35 to −0.75 V (5 mV step, 50 mV amplitude and 10 Hz frequency).

Humic substances (HS) determination: The borate buffer (boric acid, BDH, UK; 99.8%) and the oxidant (potassium bromate, Fisher) were prepared in a mixed solution of 0.2 M borate and 0.4 M potassium bromate. The pH of this mixture was adjusted with ~0.08 M ammonia to a final pH_{NBS} of 8.30. The boric acid solution was UV-irradiated for 1 h to ensure that the solution was free of organic contamination. The borate/bromate mixture was purified twice by overnight equilibration with 100 µM MnO_2, as previously described (OBATA; van den BERG, 2001). Fulvic acid stock solutions (0.2 g SRFA.L^{-1}) were prepared in ultra-pure water from standard reagents (Suwannee River, IHSS reference material, 2S101F) and stored on dark and refrigerated conditions. The SRFA standard solution was previously saturated with iron standard solution in order to avoid underestimation related to possible binding groups under-saturated with iron (SUKEKAVA *et al*., 2018). The binding capacity of 16.7 nM Fe (mg FA)$^{-1}$ for SRFA (LAGLERA; van den BERG, 2009) was used as reference to saturate the SRFA standard.

HS concentrations were determined on dissolved samples (< 0.22 µm) using the method described by Laglera, Battaglia and van den Berg (2007) which includes a step of saturation of the sample with iron in high concentration, equilibration time for 2 to 16 h followed by catalytic CSV analysis and internal calibration with Suwannee River Fulvic Acid (SRFA) standard. To confirm that the concentration of added iron was sufficient to saturate all the HS binding groups, experiments were performed to evaluate the reaction kinetic in two samples (higher and lower iron concentration) after two iron spikes of 100 nM (SUKEKAVA *et al*., 2018). Immediately after the first iron standard addition, a rapid increase followed by a slower decrease of the Fe signal was observed (Fig 8). This decrease might correspond to a competition between weak HS functional groups and hydroxide ions for the complexation of Fe while the signal at equilibrium is due to Fe-SRFA complexes. After the second iron addition of 100 nM, the catalytic CSV signal decreased back to its original value after 2 h 30 min confirming that the first addition of 100 nM was enough to saturate all HS binding groups (see Fig. 8).

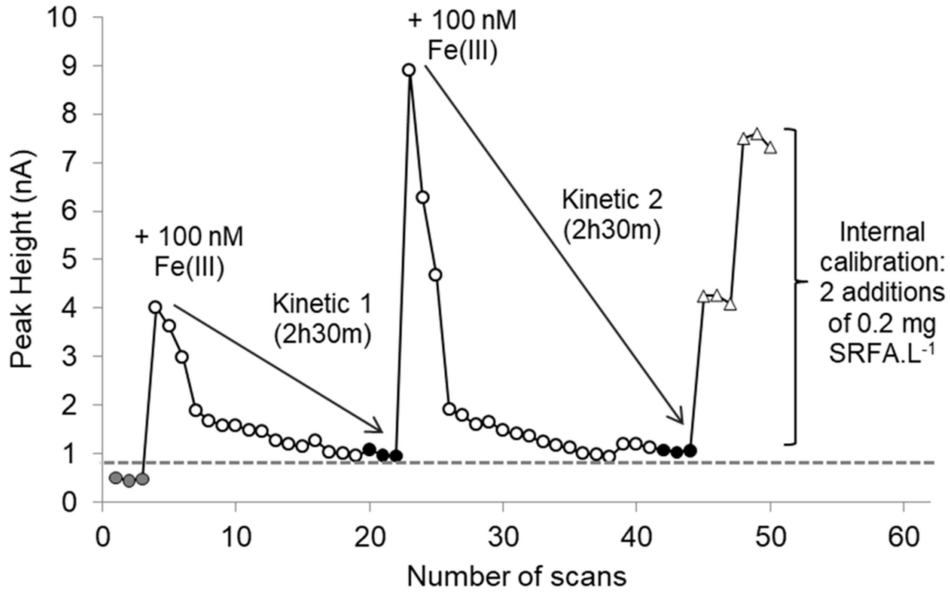

Figure 8. Catalytic CSV peak heights obtained from the sample N-20 bottom (Aug/2018) before and after two iron additions of 100 nM and kinetic stabilization for 2 h 30 min. Light grey markers define the original Fe-HS complexes in the sample; black markers are Fe-HS complexes after saturation of all HS binding with iron; triangle markers: internal calibration with iron-saturated SRFA standard to determine the HS concentration. dFe (0.22 µm) concentration in the sample was 698 ± 44 nM. Procedure as described by Sukekava *et al.* (2018).

An aliquot of 10 mL of each sample was pipetted into sterilin tubes (Sterilin, polyethylene, Fisher Scientific), saturated with 100 nM iron and 500 µL of 0.2 M borate/0.4 M bromate mixed solution were added (final concentration of 10 mM borate buffer/20 mM bromate). The solution was left to equilibrate for 2 h 30 min to allow iron in excess to compete with other cations and then saturate all the HS binding groups. The sample was transferred to the PTFE cell for measurements and the oxygen was removed by purging the solution with nitrogen for 300 s. The catalytic CSV analysis consisted in five voltammetric scans followed by internal calibration with two additions of iron-spiked SRFA standard solution (with a minimum of 3 voltammetric scans per addition) to determine the original HS concentration. The analytical parameters were: sampled direct current mode at 50 mV s^{-1}, deposition potential −0.1 V, 60 sec deposition time, 10 sec equilibration time (no stirrer), scan from 0 to −1.0 V.

14.6 Biological parameters - chlorophyll-a and phaeophytin

Filters were left overnight into centrifuge tubes filled with 10 mL of 90% acetone (HPLC grade acetone) on dark and refrigerated conditions to allow the extraction of the pigments (APHA, 2012). Extracts were centrifuged at 5,000 rpm for 10 minutes. The absorbance in the extract were determined spectrophotometrically (BEL Photonics UV-M51-Vis spectrophotometer) at 665 nm, 647 nm, 630 nm and 750 nm wavelength before and after acidification with 0.1 mL of 1 N HCl. Chlorophyll-a and phaeophytin (phytoplanktonic detrital material) concentrations were calculated by the equations from the monochromatic method (LORENZEN, 1967). The detection limit (DL) was 0.01 µg.L^{-1} for both analytes.

14.7 Statistical analyses

Shapiro-Wilk normality test (SHAPIRO; WILK, 1965) was used to test the normality of the data distribution, which attested a non-normal distribution ($p < 0.05$). The non-parametric Kruskal-Wallis test (KRUSKAL; WALLIS, 1952) was used to identify significant differences between the samplings (Nov/2015; Feb/2016; Aug/2018), the distance from the Doce River mouth (isobaths 10, 20 and 30 m) and the spatial compartment (North, Central and South). When a significant difference was evident, the Mann-Whitney U test (WILCOXON, 1945; MANN; WHITNEY, 1947) was used as a-posteriori test to reveal how the samplings/isobaths/compartments

differed from each other. The Mann-Whitney U test was also applied to reveal the depth stratification for the physico-chemical, biological parameters, dFe and sFe forms and HS concentrations. Spearman rank order correlation test (SPEARMAN, 1904) was used to test the correlation of size-fractionated Fe forms with HS, SPM and biological parameters. All statistical analyses were based on $\alpha = 0.05$. Statistics were performed using the software PAST 3.26 (HAMMER; HARPER; RYAN, 2001).

15 RESULTS

15.1 Physico-chemical and biological parameters

Over the course of the 3 sampling campaigns, there were no significant differences with depth, neither for the physico-chemical nor the biological parameters (Mann-Whitney, $p > 0.05$). Significant differences in the temporal distribution were only observed for SPM (Kruskal-Wallis, $p < 0.05$), which reached the highest values in Nov/2015 (from 30 to 300 $mg.L^{-1}$) (Table 3). In Aug/2018, the SPM levels decreased with distance from the Doce River mouth (Kruskal-Wallis, $p < 0.05$), ranging from 16.5 to 25.3 $mg.L^{-1}$ at the 10 m isobaths and from 14.1 to 17.3 $mg.L^{-1}$ at the 30 m isobaths (Table 3).

The temperature varied between 20.9 to 26.7°C with generally, lower values in the bottom waters when compared to surface (Table 3). There was no trend of depth stratification for the salinity (Mann-Whitney, $p > 0.05$) which ranged from 36.0 to 36.6 at bottom and from 34.5 to 36.8 at surface (Table 3). The pH was measured between 8.00 and 8.15 in the last sampling campaign; it was not recorded in November 2015, nor in February 2016.

The biological results indicate that there was low Chlorophyll-a compared to the higher concentrations of phaeophytin, mainly in Aug/2018 (Table 3). Most of the Chlorophyll-a concentration in the surface waters occurred below the detection limit (BDL). In the bottom, the concentrations averaged 1.5 ± 1.6 $\mu g.L^{-1}$ for Chlorophyll-a ($n = 9$) and 1.3 ± 1.1 $\mu g.L^{-1}$ for phaeophytin ($n = 12$) (Table 3).

Table 3. Physico-chemical (temperature, salinity, pH and SPM) and biological parameters (chlorophyll-*a* and phaeophytin) recorded in the continental shelf adjacent to the Doce River mouth at two depths (surface and bottom) and at three different times after the environmental disaster (November/2015, February/2016; August/2018). ND = not determined; BDL = Below detection limit.

SAMPLE	T (°C)		Salinity		pH		SPM ($mg.L^{-1}$)		Chl-*a* ($\mu g.L^{-1}$)		Phaeophytin ($\mu g.L^{-1}$)	
	Surface	Bottom	Surface	Bottom	Surface	Bottom	Surface	Bottom	Surface	Bottom	Surface	Bottom
Nov/2015												
N-20	26.5	21.8	36.5	36.6	ND	ND	30.0	42.0	0.62	5.35	0.68	BDL
C-10	24.8	24.4	36.4	36.5	ND	ND	85.0	300.0	BDL	BDL	1.87	3.03
Feb/2016												
N-25	26.7	20.9	36.7	36.5	ND	ND	2.93	1.20	1.23	BDL	BDL	0.50
C-30	26.1	21.1	36.8	36.5	ND	ND	1.60	0.27	0.45	BDL	0.18	0.67
S-20	24.0	21.9	34.5	36.5	ND	ND	1.07	62.0	1.78	1.78	0.30	3.21
Aug/2018												
N-10	24.8	25.1	36.0	36.5	8.07	8.09	16.5	25.3	BDL	1.91	2.51	BDL
C-10	24.5	25.3	36.0	36.5	8.11	8.11	23.3	24.7	BDL	1.49	2.86	0.59
S-10	25.0	24.6	36.0	36.5	8.09	8.07	18.3	21.4	BDL	BDL	2.27	3.70
N-20	23.6	26.5	35.0	36.0	8.13	8.07	16.6	16.9	BDL	0.41	1.70	1.01
C-20	25.4	25.0	36.5	36.5	8.09	8.07	14.1	15.8	BDL	0.41	2.96	0.73
S-20	25.7	24.5	36.0	36.0	8.14	8.12	16.9	16.2	2.03	0.89	BDL	0.98
N-30	24.0	23.6	36.0	36.5	8.15	8.12	17.3	14.1	BDL	BDL	1.42	0.85
C-30	25.0	25.3	36.5	36.5	8.06	8.04	14.3	15.7	BDL	0.45	2.67	0.49
S-30	25.1	24.7	36.5	36.5	8.00	8.02	14.4	15.5	BDL	0.42	1.42	1.06
Min	23.6	20.9	34.5	36.0	8.00	8.02	1.07	0.27	0.45	0.41	0.18	0.49
Max	26.7	26.5	36.8	36.6	8.15	8.12	85.00	62.00	2.03	5.35	2.96	3.70
Average	25.1	23.9	36.1	36.4	8.09	8.08	19.44	20.86	1.22	1.45	1.74	1.25
SD	0.9	1.8	0.6	0.2	0.05	0.03	20.50	16.20	0.69	1.58	0.97	1.11

15.2 Distribution of dFe (0.45 µm), dFe (0.22 µm), sFe and HS

Over the course of the 3 sampling campaigns, the parameters dFe (0.45 µm), dFe (0.22 µm), sFe and HS presented homogeneous distributions along the water column depth (Mann-Whitney, $p > 0.05$) and distance from the Doce River mouth (Kruskal-Wallis, $p > 0.05$).

The dFe (0.45 µm) concentrations in surface and bottom waters were similar, ranging from 784 to 2,784 nM at the surface, and between 739 and 2,570 nM for the bottom waters (Table 4). During the acute phase of the impact (Nov/2015), the highest dFe (0.45 µm) values in both the surface and bottom waters were found at station C-10, located in front of the Doce River mouth (Fig. 9). For the central and north sections, dFe (0.45 µm) concentrations decreased with time at similar rates, while the south section shows a different behaviour, with concentrations increasing from Feb/2016 to Aug/2018 (Fig. 9a). In Aug/2018, it is remarkable that the central and north measurements are within a close range of concentration (863 ± 90 nM on north stations; 1,166 ± 166 nM on central stations) while much higher concentrations were observed for the south stations (2,010 ± 248 nM) (Kruskal-Wallis, $p < 0.05$) (Fig. 9a and Table 4). The same pattern was observed for sedimentary Fe distribution (Supplemental, Table S1; Fig. S1) indicating a trend of material accumulation on the south sector over time.

The concentrations of dFe (0.22 µm) were higher during the acute phase of the disaster (Nov/2015; Kruskal-Wallis, $p < 0.05$) and increased again in Aug/2018 (Kruskal-Wallis, $p < 0.05$) (Fig. 9b). The levels ranged from 30 to 245 nM in surface waters, whereas the values in bottom waters were found to vary between 30 and 698 nM. In Aug/2018 the highest values occurred at station N-10 for the surface waters and N-20 at bottom. The sediment collected at station N-20 in Aug/2018 presented a marked reddish colour characteristic of the presence of iron oxide. This factor can explain the local high value of dFe (0.22 µm) concentration in the water column just above the sediment by processes such as resuspension, remobilisation and diffusion. The lowest dFe (0.22 µm) concentrations were observed in Feb/2016 at the isobaths of 30 meters (station C-30 for the surface samples and N-30 for those at bottom) (Fig. 9b; Table 4).

Table 4. Iron concentrations for dFe (0.45 *μ*m), dFe (0.22 *μ*m) and soluble (sFe) fractions in the continental shelf adjacent to the Doce River mouth. The dFe (0.45 *μ*m) concentrations were determined by ICP-MS; dFe (0.22 *μ*m) and sFe were analysed by cathodic stripping voltammetry (CSV). The standard deviation of the dFe (0.22 *μ*m) indicated for some samples was obtained from repeated determinations. ND: not determined. Percentage between brackets indicates the proportion of total dFe (0.45 *μ*m) recovered under 0.2 *μ*m and 0.02 *μ*m fractions.

Sample	dFe (0.45 *μ*m) nM		dFe (0.22 *μ*m) nM		sFe (0.02 *μ*m) nM	
	Surface	Bottom	Surface	Bottom	Surface	Bottom
Nov/2015						
N-20	1,136	1,177	204 ± 11 (n = 3) (17%)	109 (10%)	10 (1%)	ND
C-10	2,607	2,570	182 (6%)	ND	15 ± 1 (1%)	ND
Feb/2016						
N-25	1,756	2,184	35 ± 2 (n = 2) (2%)	30 (2%)	ND	ND
C-30	1,666	1,550	30 (3%)	61 (5%)	ND	38 ± 2 (3%)
S-20	1,032	1,337	97 (6%)	71 (5%)	11 ± 0.4 (1%)	ND
Aug/2018						
N-10	964	739	245 (26%)	75 (10%)	ND	11 ± 0.4 (1%)
C-10	990	964	137 (14%)	91 (9%)	16 ± 1 (2%)	29 ± 1 (3%)
S-10	1,641	1,776	148 (9%)	206 (12%)	9 ± 1 (1%)	ND
N-20	784	925	117 (15%)	698 ± 44 (n = 2) (76%)	25 ± 1 (3%)	ND
C-20	1,238	1,281	64 (5%)	51 (4%)	ND	17 ± 1 (1%)
S-20	2,170	1,975	102 (5%)	194 ± 13 (n = 2) (10%)	ND	ND
N-30	837	927	125 (15%)	176 ± 5 (n = 2) (19%)	18 ± 1 (2%)	28 ± 1 (3%)
C-30	1,140	1,383	155 (14%)	185 (13%)	ND	10 ± 1 (1%)
S-30	2,784	1,716	186 ± 7 (n = 3) (7%)	95 (6%)	10 ± 0.4 (0.4%)	ND
Min	784	739	30	30	9	10
Max	2,784	2,570	245	698	25	38

Similar distribution patterns were observed for HS and dFe (0.22 μm) in surface waters. In general, the concentrations of dFe (0.22 μm) and HS showed a trend of decrease with the distance from the Doce River mouth in the surface samples and increased again in the 30 m isobaths (Fig. 9d; Table 5). The highest value of HS was found at station N-10 in Aug/2018 (350 μg SRFA.L^{-1}) and the lowest occurred at station C-30 in Feb/2016 (15 μg SRFA.L^{-1}) (Fig. 9d; Table 5). In bottom waters, the highest HS concentration occurred at station C-30 in Feb/2016 (241 μg SRFA.L^{-1}) while the lowest value occurred at station N-

20 in Nov/2015 (44 µg SRFA.L^{-1}). The dFe (0.22 µm) concentrations increased from North to the South sectors whereas the HS decreased until the station C-20 and increased again from the station S-20 (Fig. 9d; Table 5).

The sFe concentrations ranged from 10 to 25 nM (stations S-30 and N-20, respectively) in the surface waters and varied between 10 and 37 nM at bottom, with the lowest concentrations at station C-30 in Aug/2018 and the highest occurring at station C-30 in Feb/2016 (Fig. 9c; Table 5).

Table 5. HS concentrations on dissolved (< 0.22 *µ*m) samples, and maximum iron bound by HS according to the binding capacity of HS determined by Laglera and van den Berg (2009). %dFe (0.22 *µ*m)-HS and %sFe-HS indicates the % of dFe (0.22 *µ*m) and sFe concentrations can be explained by the binding capacity of HS. ND: not determined.

Sample	HS (*µ*g SRFA.L^{-1}) (< 0.22 *µ*m)		[(a)]Fe bound by HS (nmol)		%dFe (0.22 *µ*m)-HS		%sFe-HS**	
	Surface	**Bottom**	**Surface**	**Bottom**	**Surface**	**Bottom**	**Surface**	**Bottom**
Nov/2015								
C-10	219	ND	4	ND	2	ND	24	ND
N-20	247	44	4	1	2	1	43	2
Feb/2016								
S-20	ND	129	ND	2		3	ND	ND
C-30	15	241	0.2	4	1	7	0.2	11
N-25	ND	229	ND	4		13	ND	8
Aug/2018								
N-10	350	196	6	3	2	4	15	31
C-10	328	91	6	2	4	2	34	5
S-10	ND	79	ND	1	ND	1	ND	2
N-20	127	65	2	1	2	0.2	8	3
C-20	56	68	1	1	2	2	1	7
S-20	257	181	4	3	4	2	6	13
N-30	103	141	2	2	1	1	10	8
C-30	189	99	3	2	2	1	4	16
S-30	47	ND	1	ND	0.4	ND	8	ND
Min	15	44	0.2	1	0.4	0.2	0.2	2
Max	350	241	6	4	4	13	43	31

[(a)]Normalized with 16.7 nmol Fe (mg FA)$^{-1}$ according Laglera and van den Berg (2009). **: Assuming HS levels measured in dFe (< 0.22 □m).

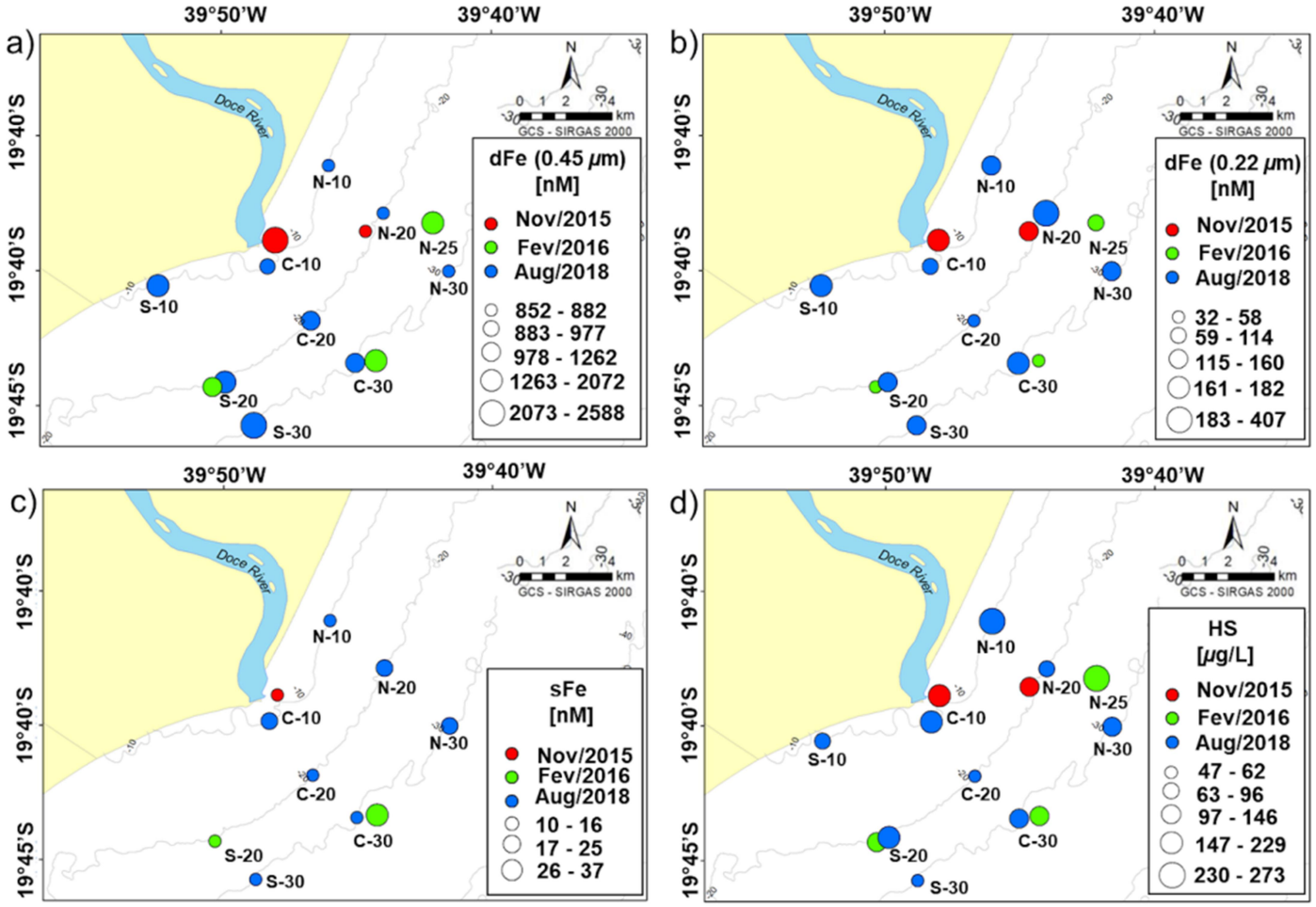

Figure 9. Spatial and temporal distribution of dFe (0.45 µm), dFe (0.22 µm), sFe and HS concentrations (average between the surface and bottom data) of the continental shelf adjacent to the Doce River mouth.

15.3 Size-fractionated iron proportion and iron-binding HS

The concentrations of dFe (0.22 µm) were up to 98 % smaller than those of dFe (0.45 µm) (Table 4; Fig. 10) suggesting that most Fe is present in a large (> 0.22 µm) colloidal form. Similarly, ultrafiltration (0.02 µm) of some pre-filtered samples (0.22 µm) caused significant removal, from 39 to 95% of the iron from dFe (0.22 µm) to the soluble fraction (Table 4; Fig. 10), suggesting that a significant proportion of dFe (0.22 µm) fraction was present in a smaller colloidal form (> 0.02 µm).

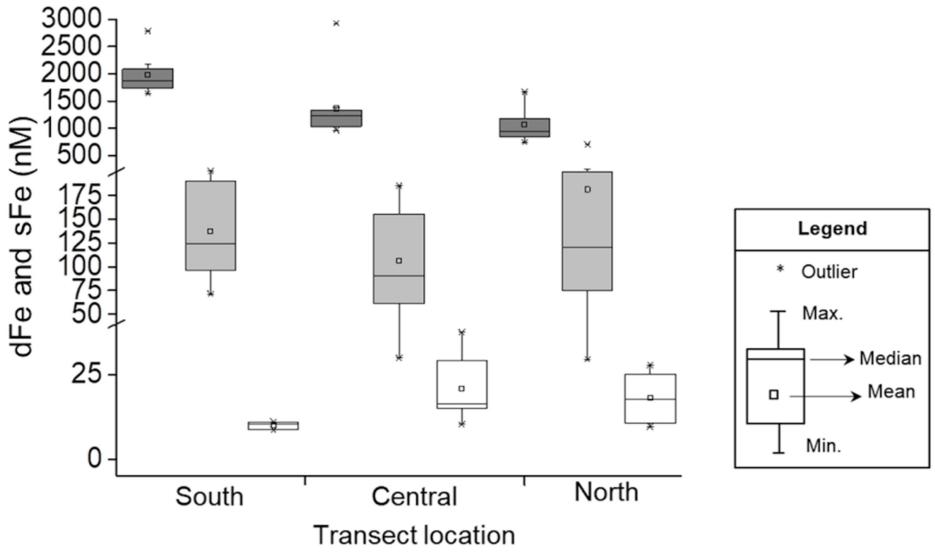

Figure 10. Spatial distribution of dFe (0.45 µm) (dark grey boxplots), dFe (0.22 µm) (light grey boxplots) and sFe (white boxplots) to highlight the difference in concentrations between the size-factions (see scale breaks) in each transect over the course of the three samplings (Nov/2015, Feb/2016 and Aug/2018).

Assuming a ratio of 16.7 nmol Fe (mg FA)$^{-1}$ for the binding capacity of HS (Laglera and van den Berg, 2009), the marine HS in these seawater bound from 0.2 to 5.8 nmol of Fe (Table 5). It was expected that most of dFe was occurring as organic complexes, mainly with HS (LAGLERA; van den BERG, 2009). However, the binding capacity of HS can only explain a maximum of between 0.2 and 13% (median is 2%) of the dFe (0.22 µm) (Table 5). Assuming that HS levels in the soluble fraction are the same as in the < 0.22 µm fraction, they would only explain from 0.2 to 43% (median is 10%) of the sFe levels (Table 5). Although low, these percentages corresponds to the maximum binding that would occur if there was no competition from other metals. Indeed, when

carrying out our HS measurements (Fig. 8), it was clear that HS present in the sample were not saturated with Fe since a significant increase (52% for the sample shown in Fig. 8) of the Fe-HS signal was observed upon additions of Fe (light grey and black markers in Fig. 8). This increase can be explained by the presence of competing metals for complexation with HS (SUKEKAVA *et al.*, 2018). It is thus clear that HS levels measured in this study cannot explain the Fe dissolved and soluble concentrations, indicating that there are other processes and/or other compounds that maintain the iron in the dissolved/soluble fraction.

15.4 Correlation analyses

No significant correlation was observed between dFe (0.45 µm) and SPM, neither with Chl-a nor Phaeophytin (Table 6). For the dFe (0.22 µm) a positive correlation with HS was found in surface waters (Table 5; Fig. 6a; R = 0.62; p = 0.02; n = 12) suggesting that these variables originate from the same source. The coeficient of correlation in these samples was relatively low due to three outliers (open circles in Fig. 11a). Exclusion of these points resulted in a strong linear fit (R = 0.98; r2 = 0.97; p = 0.00001; n = 9), as shown in the inserted diagram (Fig. 11a). On the contrary, no significant correlation was found between HS and dFe (0.22 µm) concentrations in the bottom waters (R = -0.44; p = 0.15; n = 11). The dFe (0.22 µm) concentrations increased with the SPM levels in surface waters (Table 6; R = 0.60; p = 0.02; n = 14). A weak positive correlation was also found between phaeophytin and dFe (0.22 µm) (Table 6; Fig. 11b; R = 0.40, p = 0.04; n = 25) which can be related to a possible influence of the riverine input delivering phytoplanktonic debris material beyond the marine sources.

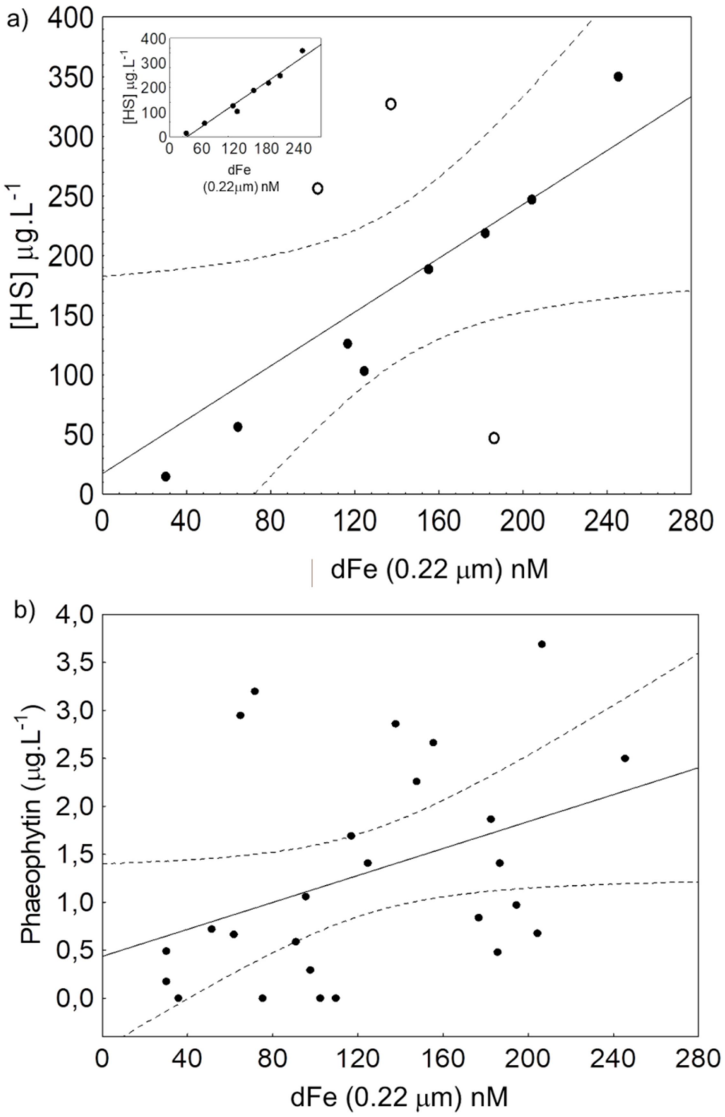

Figure 11. Scatterplot diagrams between a) HS and dFe (0.22 µm) concentrations in surface seawater, R = 0.62, p = 0.04, n = 12 (excluding the points out of the linear fit as showed in the inserted diagram: R = 0.98, p = 0.00001, n = 9); b) Phaeophytin and dFe (0.22 µm) concentrations including surface and bottom results, R = 0.40, p = 0.04, n = 25. Dashed lines represent the upper and lower 95% confidence limit (α = 0.05).

Table 6. Spearman rank order correlation of Fe size-fractionated forms with HS, SPM and biological parameters. *R* Spearman correlation and *p*-value (between brackets). Significant correlations ($p < 0.05$) are highlighted as bold and italic letters. [a]Results after excluding outliers.

	PARAMATERS	HS	SPM	Clh-*a*	Phaeophytin
Surface and Bottom	**dFe (0.45 *µ*m)**	0.05 (0.84)	-0.07 (0.71)	0.12 (0.56)	0.08 (0.70)
	dFe (0.22 *µ*m)	0.12 (0.58)	0.37 (0.06)	-0.25 (0.20)	***0.40 (0.04)***
	sFe (0.02 *µ*m)	-0.03 (0.91)	-0.30 (0.30)	-0.24 (0.41)	-0.02 (0.93)
Surface Data	**dFe (0.45 *µ*m)**	-0.10 (0.77)	-0.02 (0.93)	0.36 (0.20)	-0.31 (0.28)
	dFe (0.22 *µ*m)	***0.62 (0.04)***	***0.60 (0.02)***	-0.45 (0.10)	0.39 (0.17)
	dFe (0.22 *µ*m)[a]	***0.98 (0.00001)***	–	–	–
	sFe (0.02 *µ*m)	-0.14 (0.80)	-0.12 (0.79)	-0.34 (0.46)	0.14 (0.73)
Bottom Data	**dFe (0.45 *µ*m)**	0.20 (0.54)	-0.04 (0.89)	-0.09 (0.77)	0.53 (0.06)
	dFe (0.22 *µ*m)	-0.44 (0.15)	0.20 (0.50)	0.02 (0.94)	0.33 (0.27)
	sFe (0.02 *µ*m)	0.26 (0.66)	-0.43 (0.42)	-0.49 (0.33)	0.49 (0.36)

16 DISCUSSION

16.1 dFe concentrations and sources

The results of this study demonstrate that the concentrations of dFe are very high across all size fractions even almost three years after the disaster. The dFe (0.45 µm) levels found here are consistent with previous work in the same area 75 days (HATJE *et al*., 2017) and one year after the Fundão dam rupture (BASTOS *et al.*, 2017) (Table 7). In general, the results indicate higher concentrations of dFe (0.45 µm) and dFe (0.22 µm) than other marine environments affected by mining tailings, such as the Pórtman Bay (ALORDA-KLEINGLASS *et al*., 2019) and Bing Bong Coast (northern Australia) (MUNKSGAARD; PARRY, 2001). The minimum value observed in this study is compatible only to the mean concentration of dFe (0.22 µm) found in coastal system from Mediterranean Sea impacted by abandoned lead mining (TOVAR-SÁNCHEZ *et al.*, 2016) (Table 7).

Table 7. Comparison of dFe (0.45 *μ*m) and dFe (0.22 *μ*m) concentrations found in this study (interval range) with other coastal areas affected by mining tailings inputs.

System	dFe (nM)[a]	Fraction (*μ*m)	Local	Reference
Coastal Waters	30 to 245 (Surface) 30 to 194 (Bottom)	0.22	Doce River Mouth (southeast Brazil)	This study
	784 to 2,784 (Surface) 739 to 2,570 (Bottom)	0.45		
Coastal Waters	4 to 8	0.22	Portmán Bay (southwest Spain)	Alorda-Kleinglass et al. (2019)
Estarine/ Coastal Waters	21 to 1,821	0.45	Doce River Mouth (southeast Brazil)	Hatje et al. (2017)[b]
Coastal Waters	110 to 2,490 (Surface) 160 to 2,640 (Bottom)	0.45	Doce River Mouth (southeast Brazil)	Bastos et al. (2017)[c]
Coastal Waters	30 ± 12 (June 2012) 24 ± 3 (April 2013)	0.22	Mediterranean Sea (northern Africa)	Tovar-Sánchez et al. (2016)
Coastal Waters	4 to 10	0.45	Bing Bong Coast (northern Australia)	Munksgaard and Parry (2001)

[a]Outliers are not included; [b]75 days after the Fundão dam rupture; [c]One year after the Fundão dam rupture.

The spatial distribution pattern of dFe (0.45 μm) and dFe (0.22 μm) concentrations indicates that there are two main sources of dFe to consider: the fluvial input from the Doce river and sediment resuspension; both of them are likely to play a significant role. The positive correlation between dFe (0.22 μm) and SPM in surface waters indicates that the Doce River plume plays a significant role in regulating the concentrations of dFe at the continental shelf. The Doce River turbidity plume extended more than 75 km into the continental shelf during the acute phase of the impact and could extend further in extreme flooding events (RUDORFF *et al*., 2018). A substantial increase in the transport of suspended sediments was also observed by Hatje *et al*. (2017). In that study, the concentration of SPM was up to 33 g L^{-1} with a maximum of particulate Fe reaching 48 mg $Fe.g^{-1}$ of SPM (HATJE *et al*. 2017). Even in non-affected systems, fluvial input of Fe is mostly in particulate form (RICKARD, 2012) releasing bioavailable dFe in coastal areas by ligand association with marine binding compounds (JEANDEL; OELKERS, 2015). The riverine iron fluxes are limited by the estuarine trapping of metals associated with particulate matter and by the flocculation of colloidal organic matter (BOYLE; EDMOND; SHOLKOVITZ, 1977; SHOLKOVITZ; BOYLE; PRICE, 1978; JOHNSON; GORDON; COALE, 1997, SU *et al*., 2018). However, the estuarine removal rates are lowered by the input of stable crystalline lattice structures that reach

the coastal waters as suspended particles (TREFRY, 1977) and also by the complexation of dFe with low molecular weight fulvic acids and other ligands which effectively increase its solubility in the water column (KRACHLER; JIRSA; AYROMLOU, 2005; KRACHLER *et al*., 2010; KRACHLER *et al*., 2016). It is worthy to mention, however, that the transport of tailings mud to the continental shelf in the acute phase of the disaster occurred as a massive loading of material highly enriched with crystalline oxides (QUEIROZ *et al*., 2018) which clearly reached the coastal area as an orange coloured plume. So, we have assumed that although the estuarine trapping had removed a part of the material along the transport downstream it was not enough to avoid the large input of particulate material from the tailings. Monitoring program has been developed monthly in the area since the disaster and the results have shown that this material remains in the continental shelf and affects the suspended particles and metal distribution in the water column after resuspension events (F. Sá pers. comm.).

The increase of sedimentary Fe and dFe (0.45 µm) concentrations on south stations over time and the higher values of bottom dFe (0.22 µm) at those stations are matching with the pattern of the sediment (QUARESMA *et al*., 2015) and Doce River plume transport in the study area (MARTA-ALMEIDA *et al*., 2016), which occurs from North to South when trade winds are prevalent. This is an evidence of iron inputs from the sediment and the accumulation of sedimentary material on south sector, which remain fluid in mud and easily remobilised, even in the continental shelf (RUDORFF *et al*., 2018). Granulometric and mineralogical analyses from the tailings deposited in urban sites (ALMEIDA *et al*., 2018) and in the Doce River estuary (QUEIROZ *et al*., 2018) after the disaster showed a predominance of fine particles (e.g. mud plus fine sand: 74%) mainly composed of hematite, goethite, kaolinite and quartz which are related to mined iron ore composition (ALMEIDA *et al*., 2018; QUEIROZ *et al*., 2018). The Fe concentrations in that material reached 5.2 ± 2.9 g kg^{-1} whereas the iron content was predominantly associated with crystalline oxides (89 ± 2.3%) (QUEIROZ *et al*., 2018). Mobility tests using the Fundão dam tailings suggested that Fe (and other metals like Ba, Sr, Mn and Al) can enter the dissolved phase from mud particles, especially in

environments with high calcium content, like marine ecosystems (SEGURA *et al*., 2016). This is also supported by the findings of Hatje *et al*. (2017) who showed an increase of 16% in the proportion of bioavailable dFe from the sediment during the transport from the riverine portion to the estuary mouth, suggesting the mobilisation of Fe during its transport. So, the dFe supply in the continental shelf adjacent to the Doce River appears to come from the direct sedimentary inputs of this metal associated to the mineral composition of the tailings (HATJE *et al*., 2017).

Sedimentary inputs have been described as important sources of dFe to the coastal sea as by resuspension of particles and upwelling of Fe-rich bottom waters in equatorial Pacific (JOHNSON; CHAVEZ; FRIEDERICH, 1999) as well as by supply from the continental margin sediments in eastern New Zealand (ELLWOOD *et al*., 2014), in the Bellingshausen Sea (West Antarctica) (de JONG *et al*., 2015) and in the Southern Ocean (TAGLIABUE; BOPP; AUMONT, 2009; TAGLIABUE; AUMONT; BOPP, 2014). The factors sustaining these sediment-derived dFe inputs are mainly related to sedimentary diagenetic processes which favour reductive conditions and allow the release of Fe(II) to the overlying water column (ELROD *et al.*, 2004). Pore-water fluxes of trace metals after resuspension events by bottom currents (HATTA *et al*., 2013) and benthic diffusion and bioirrigation (SEVERMANN *et al*., 2010; SCHROLLER-LOMNITZ *et al.*, 2019; SHI *et al*., 2019) are also process that allow the dFe being released from the sediment to the water column.

Aside from the natural sources, a recent critical review study suggested that the fluxes of dFe to the coastal areas vulnerable to mining impacts are highly intensified by the Fe inputs from mining tailings (LONGHINI; SÁ, NETO, 2019). These loads can reach the coastal zone by riverine inputs (BRAUNGARDT *et al*., 2003; OLÍAS *et al.*, 2006; CÁNOVAS *et al*., 2008), pore-water exchange (ALORDA-KLEINGLASS *et al*., 2019) and submarine groundwater discharge (SGD) (TREZZI *et al*., 2016; ALORDA-KLEINGLASS *et al*., 2019). In Portmán Bay (Cartagena - La Unión mining district) the SGD represents the main conveyor of dFe from mine tailings deposit in coastal waters resulting in maximum fluxes of 3,200 ± 1,800 mol d^{-1} km^{-1} even more than 25 years after the cessation of dumping mine waste in that region (ALORDA-KLEINGLASS *et*

al., 2019). In our study, dFe (0.45 µm) and dFe (0.22 µm) concentration levels remain high almost 3 years post dam failure. These results indicate that the changes on the ecosystem remain still significant due to the continuous remobilisation of the tailings sludge stored along the river channel as well as by the resuspension of the sediment deposited on the marine substrate (HATJE *et al*., 2017). It is also important to note that the samplings achieved here were conducted during low river discharge and no cold fronts passage (excepted in November 2015), i.e. during conditions where loads and remobilisation processes are probably at their lowest.

16.2 HS concentrations and sources

In surface waters, HS showed the same distribution pattern as dFe (0.22 µm). This result reveals the continental input from the Doce River is the main source to HS in surface waters, which is also verified by the higher HS concentrations near to the coast. The role of terrestrial sources for the HS inputs in coastal environments has been assessed in some studies (LAGLERA; BATTAGLIA; van den BERG, 2007; LAGLERA; van den BERG, 2009; BATCHELLI *et al*., 2010; SU *et al*., 2018). These substances accounted for more than 90% of the iron-binding capacity in the Irish Sea where the highest HS concentration was found at the lowest salinity conditions, strongly supporting the finding that HS are terrestrially derived substances (LAGLERA; van den BERG, 2009). The main role of terrestrial inputs as source of HS in continental sea was also described to the Thurso Bay (BATCHELLI *et al*., 2010), Artic Ocean (SLAGTER *et al*., 2017), in marine areas influenced by peatland (MULLER; CUSCOV, 2017), and in the East China Sea (SU *et al*., 2018). The lack of significant correlation between HS and dFe (0.22 µm) concentrations in the bottom waters might be because different processes are decoupling their concentrations as HS are sourced mainly from riverine inputs, while dFe (0.22 µm) can be delivered to the continental shelf from two main sources (riverine and sedimentary).

Additionally to the terrestrial inputs, our results suggest some influence of marine sourced HS as their concentrations increased again at the 30 m isobaths. Laglera *et al*. (2007) showed not only a freshwater origin for the HS in Liverpool Bay, but also a non-described marine source which increased the HS

concentrations off-shore. In coastal waters of Western Antarctic Peninsula and Drake Passage, HS-like compounds (determined by the AdCSV method) was attributed to the mucus production (as EPS) by phytoplanktonic assemblages (TRIMBORN *et al*., 2015) confirming the marine origin of these compounds. The high concentrations of phaeophytin against the very low clh-*a* levels are proxies of the presence of phytoplanktonic debris/senescence which can be transformed by microorganisms to marine HS-like compounds and possibly contribute to the HS bulk in our system. Senescence of biological material is also a source of EPS released to the water column as cellular exudates (HASSLER *et al*., 2015; NORMAN *et al*., 2015), which is believed to be included in the pool of HS-like compounds (NORMAN *et al*., 2015). Moreover, HS-like can be released either as biological excretion (HASSLER; van den BERG; BOYD, 2017) or during the microbial degradation of phytoplanktonic debris material (STOLPE *et al*., 2014).

The kinetic experiments revealed the presence of under-saturated HS by iron as the HS signal of the sample N-20 bottom (Aug/2018) shown in Fig. 3 was increased by 52% after the saturation with 100 nM Fe(III). Similarly, Sukekava *et al.* (2018) observed an increase of about 67% on HS signal after the saturation with 60 nM Fe(III) in seawater samples from Arctic Ocean. This result could indicate that the behaviour of HS to outcompete iron and other metals may be similar, irrespective of the origin of the seawater, as our samples are fundamentally different than those analysed by Sukekava *et al*. (2018) in terms of metal concentrations, physico-chemical conditions and possibly organic ligands contents. In our case, it was expected that the HS binding groups were already saturated considering the high dFe concentrations in the samples. So, the increase of HS initial signal after Fe saturation can be explained by two hypotheses: 1) the dFe is already complexed by other compounds or stabilized as colloidal forms (see next item); and/or 2) HS are bound by other metals. The co-existence of multiple metals should change the iron organic speciation due to the differences on binding capacity of specific organic compounds with different metals (HASSLER; van den BERG; BOYD, 2017). HS may be also an important ligand for copper, zinc, cobalt and aluminium in seawater (YANG; van den BERG, 2009). Experiments conducted

by Abualhaija *et al*. (2015) demonstrated the competition between Cu and Fe for HS-like ligands which affects both metals to HS complexation in the marine environment. Considering the levels of dCu (0.45 µm) were lower than dFe (0.45 µm) (Supplemental, Table S2), competition with copper does not seem to be a plausible explanation. However, compared to other dissolved metals, dAl (0.45 µm) reached as high levels as 9,926 to 12,519 nM in Nov/2015, from 387 to 9,205 nM in Feb/2016 and from 3,394 to 14,805 in Aug/2018 (Supplemental, Table S2) suggesting that Al can be a potential metal to outcompete against Fe to complex by HS in the area. Similarly, dZn (0.45 µm) was a possible candidate for HS competition in the acute phase of the impact as its concentrations occurred between 719 and 1,055 nM in Nov/2015 (Supplemental, Table S2).

The range of HS concentrations found in the current work was consistent with the values measured in Liverpool Bay (LAGLERA; van den BERG, 2009), in the East China Sea (YANG *et al*., 2017; SU *et al*., 2018) and Artic Ocean (SLAGTER *et al*., 2017) (Table 8). Although these levels coincide with other natural values, higher HS concentrations were expected as a massive loading of a mixing of tailings and terrigenous material has reached the area affected by the Fundão mud (GOMES *et al*., 2017). HS and iron are known to be subject to co-precipitation in the estuarine mixing zone reaching a removal rate ranges from 90% to 95% (BOYLE; EDMOND; SHOLKOVITZ, 1977; SHOLKOVITZ; BOYLE; PRICE, 1978). dFe (0.22 µm) concentrations reached 21.8 ± 46.1 µM in continental water bodies affected by the tailings (SEGURA *et al*., 2016) and part of this material was deposited during the transport, probably carrying downward HS and other compounds. The imbalance between dFe (0.22 µm) and HS concentrations is likely related to the origin of the material, which is predominantly unnatural (iron ore tailings source) for dFe and natural (terrigenous and marine sources) for HS.

Table 8. Comparison of dFe (0.22 *μ*m) and HS concentrations evaluated in this study (interval range) with other studies developed in coastal areas.

dFe (0.22 *μ*m) nM	HS (*μ*g SRFA.L^{-1})	Local	Reference
30 to 245*	15 to 350	Doce River Mouth (Brazil)	This study
0.3 to 14	81 to 364	East China Sea	Su et al. (2018)
3 to 95	121 to 339	East China Sea	Yang et al. (2017)
0.12 to 4.42	10 to 320	Arctic Ocean	Slagter et al. (2017)
15 ± 11	_	East China Sea	Su et al. (2015)
7 to 132	23 to 560	San Francisco Bay	Bundy et al. (2015)
1 to 9	50 to 370	Liverpool Bay, Irish Sea (UK)	Laglera and van den Berg (2009)
_	60 to 583	Liverpool Bay, Irish Sea (UK)	Laglera et al. (2007)

* Outlier is not included.

16.3 Forms of dFe and sFe

The significant removal rate of Fe among the size-fractions is probably related to the high content of Fe in colloidal forms whose encompass a wide range of size. Colloidal model used to explain the particle concentration effect (PCE) in dissolved samples showed that within 0.45 μm filtrate fraction, the metals (Fe >> Al >> Mn) tended to occur preferentially as colloids (BENOIT; ROZAN, 1999). Similarly, Fe was shown to be dominant in colloidal size fraction in seawater, considering the size range from 0.02 to 0.4 μm (WU *et al*., 2001; CULLEN; BERGQUIST; MOFFETT, 2006) and from 10 kDa to 0.2 μm (FITZSIMMONS *et al*., 2015). Iron, aluminium, manganese and several dissolved trace metals in our study area are also suggested to be mostly present under the colloidal phase (HATJE *et al*., 2017). These colloids, highly modified by unnatural chemical and physical processes (mineral treatment for iron ore pre-concentration), may be the main reason for the high dFe levels in the < 0.45 μm and < 0.22 μm size fractions.

This is also in agreement with changes to flocculation processes that were demonstrated by settling experiments performed with mud sediment fraction (< 63 μm) from the continental shelf before and after the disaster. The increase of fine flocs residence time on water column was suggested to be as a result of changes of the sediment composition, like the presence of porous iron oxide goethite (GRILO *et al*., 2018). In addition, adsorptive characterisation of tailings from the Fundão dam is consistent to a monolayer model with low adsorption

capacity and low interaction among adjacent molecules (ALMEIDA *et al*., 2018) which means that this material is probably less prone to processes of flocculation.

HS played a minor role on sFe stabilization. sFe is a minor sub-fraction of the dFe which is nearer to truly dissolved Fe and tends to be complexed with ligands (CULLEN; BERGQUIST; MOFFETT, 2006; FITZSIMMONS *et al*., 2015). Considering that HS (from terrestrial and HS-like marine sources) are normally expected to be the most important organic ligands in coastal waters affected by riverine inputs (LAGLERA; van den BERG, 2009; BATCHELLI *et al*. 2010; LAGLERA; BATTAGLIA; van den BERG, 2011; BUNDY *et al*., 2015; MAHMOOD *et al*., 2015; GERRINGA *et al*. 2017; MULLER; CUSCOV, 2017; SLAGTER *et al*., 2017), it is therefore likely that in our case, different processes are at play to stabilise sFe in the water column.

Complexation to other natural organic substances is one hypothesis. Biological production of siderophores is shown to be enhanced under iron enrichment conditions in the northeast subarctic Pacific Ocean (ADLY *et al*., 2015). However, siderophores are unlikely to be the predominant ligand due to the low levels of chl-*a* that were consistently measured in our study.

Another hypothesis is the complexation of dFe with unnatural organic ligands. Organic compounds are frequently used during the flotation stage employed to concentrate the mineral product as a richer iron ore pulp (ARAUJO; VIANA; PERES, 2005). Reverse cationic flotation route using amine-based as collectors is largely the most common process performed by the iron ore processing industry (ARAUJO; VIANA; PERES, 2005; PEARSE, 2005; MA, 2012). Amine adsorb on silicates (mainly quartz) surface and also on metal oxides causing the flotation of quartz and other associated mineral (FILIPPOV; SEVEROV; FILIPPOVA, 2014), such as goethite. The waste material composed by flotation reagents and impurities is deposited as tailings. Infrared spectroscopy analyses confirmed the presence of primary and secondary amines and amides in the Fundão tailing composition (ALMEIDA *et al*., 2018). This material appears to be highly stable as aromatic amine have been frequently identified in seawater samples collected on the continental shelf adjacent to the Doce River mouth since the disaster (R.R. NETO unpubl.).

Aromatic amine was widespread registered either in atmospheric particulate matter (QUEROL *et al.*, 1999) or in water bodies affected by Aznalcóllar pyrite mine disaster (SW Spain) (ALZAGA *et al*., 1999). These compounds were related to the pyrite spillage as by resuspension of the sludge particles from the material accumulated after the disaster (QUEROL *et al*., 1999) as well as from the degradation of flocculants used during the ore processing which is wasted in the pyrite dam and act as an important source of these specific compounds (ALZAGA *et al*., 1999). Stability of the complex dFe-amine and concentrations of that amine ligand could be high enough to compete with the binding from other natural ligands, such as HS, but this is presently unknown.

Moreover, the presence of colloidal Fe species smaller than 0.02 µm is a likely hypothesis for the sFe levels in the study area. Inorganic Fe as nanoparticles have been suggested to encompass the pool of dFe, mainly in the colloidal phase (10 kDa < cFe < 0.2 µm range) (FITZSIMMONS *et al*., 2015). Inorganic colloids as nanoparticulate pyrite (FeS_2) (YÜCEL *et al*., 2011; GARTMAN; FINDLAY; LUTHER, 2014), iron-containing silicate particles (GARTMAN; FINDLAY; LUTHER, 2014) and nanoparticulate Fe(III) oxy-hydroxides (FITZSIMMONS *et al*., 2017) have been identified to encompass the bulk of dFe of fluids emissions from hydrothermal vents. These compounds must be also included in colloidal and soluble iron fractions (LOUGH *et al*., 2019) as their aggregates reach from 3 nm to 200 nm in size (YÜCEL *et al*., 2011; GARTMAN; FINDLAY; LUTHER, 2014; FITZSIMMONS *et al*., 2017). The stability of inorganic nanoparticles is defined by the relatively high half-life (estimated as 1-12 months at 25°C for pyrite) (YÜCEL *et al*., 2011), slower settling rates than larger particles and then higher chances to be transported over long distances (YÜCEL *et al*., 2011; GARTMAN; FINDLAY; LUTHER, 2014). Analyses of sedimentary metal partitioning in areas affected by the Fundão dam tailing show that pyrite represent only 1% of all metals whereas crystalline Fe oxy-hydroxides are the most important fraction for Fe and other metals (QUEIROZ *et al*., 2018), which could support the occurrence of sFe as nanoparticulate Fe(III) oxy-hydroxides.

Another process controlling the stability of nanoparticles in fluid vents emissions is the reversible scavenging mediated by desorption: sorption ligand

exchanges from particulate iron (pFe) to the colloidal phase which protect it from precipitation and settling (FITZSIMMONS *et al*., 2017). These proccesses are also expected to occur in other ocean regions with high pFe inputs, including continental margins (FITZSIMMONS *et al*., 2017). Considering the different size fractions as a continuum of inorganic and organic components regulating the dFe speciation (TAGLIABUE *et al*., 2017), we predict that both complexation with organic ligands (inferred to be amine compounds) and stable forms as nanoparticulate Fe(III) oxy-hydroxides are controlling the stability of small colloids in the sFe fraction, the former possibly also preventing the aggregation of the small colloids.

16.4 Can this Fe be transported to the open ocean?

As the continuing input and high stability of dFe and sFe in those waters, it is worth considering the possibility of Fe transport from the continental shelf to the open ocean. The riverine water residence time on the shelf is a key factor to determine the transport of inorganic N and P to the oceans and similar behaviour is expected for trace metals (SHARPLES *et al*., 2017). Shelves with short residence time of riverine plume (essentially located at low latitudes) present higher loads of nutrients to the open ocean (SHARPLES *et al*., 2017). In this context, the mean residence time at Abrolhos continental shelf (17.5° S, 37.5° W; located 250 km far from Doce river mouth) was estimated as 7 days and the supplies of riverine DIN and DIP reaching the oceans were 84% and 97%, respectively (SHARPLES *et al*., 2017). Considering that Abrolhos is a wider shelf (250 km in mean of extension against 50 km in our study area) (ALBINO; CONTTI NETO; OLIVEIRA, 2016) the residence time in the continental shelf adjacent to the Doce river mouth is expected to be even lower. Additionally, modelling study evaluating the dispersion of contaminated Doce River plume two months after the disaster shows a net flow mainly southward along the outer shelf, shelf break and reaching the open ocean about 200 km from the coast (MARTA-ALMEIDA *et al*., 2016). These findings support the hypothesis that those coastal waters enriched with stable dFe and sFe are being exported to the open ocean. Furthermore, there is evidence of dFe transport from hydrothermal vents on a scale of several thousand kilometres showing a nearly conservative behaviour of dFe probably related to

complexation by organic ligands or by stabilization as colloids (RESING *et al*., 2015). Although our study evaluates a specific event, it has been estimated that mining effluents affect other 38 coastal areas worldwide (KOSKI, 2012). Therefore, these continental shelves might be non-negligible sources of stable forms of dFe and sFe to the oceans and may affect the global iron ocean budget (LONGHINI; SÁ, NETO, 2019).

16.5 Processes changing the iron size-fractioned speciation

This section describes the main processes that control the stability and distribution of dFe and sFe in seawater adjacent to the Doce River, according to the findings outlined above, which are summarized in Fig. 12. The most important changes are related to the source of iron, transport and remobilisation of tailings and iron forms reaching the continental shelf and present in the water column. After the disaster, a huge volume of material highly modified by anthropogenic process (chemical and physical treatments for iron ore processing) changed the quantity (input rates) and quality (composition) of the sediment deposited on the continental shelf. The Fundão dam rupture provoked a massive loading of tailings as a sludge pulse downstream with high accumulation on the river banks and deposition on marine substrate (Fig. 12a). dFe in the water column comes from the sedimentary inputs by the river discharge, remobilisation of accumulated materials along the riverine flow and resuspension of fine muddy materials on the continental shelf, characterised by a high content in goethite (iron oxide). High dFe and sFe suggests high solubility due to processes that prevent Fe precipitation, such as complexation or stabilised colloidal particles. While HS have been previously proposed in numerous occasions as the main Fe ligands in coastal waters, their concentration in our study are relatively low, suggesting that there might be other organic substances (here supposed to be amine compounds) that are able to stabilise dFe in the water column. Another hypothesis, possibly complementary to the first one, would be the presence of small colloidal Fe, able to pass through the 0.22 and 0.02 µm filters, mostly nanoparticulate Fe(III) oxy-hydroxides (Fig. 12b).

Therefore, the massive loading of tailings to the coastal waters during the acute phase of the disaster, the continuing inputs by remobilisation from the

material accumulated along the Doce river flow and the resuspension in the continental shelf have changed the forms of dFe and complexation with HS in the area. The low binding capacity of HS found in this study is an unusual result compared to the major influence of Fe-HS complexes in other coastal areas. Further studies should evaluate the relation between dFe and unnatural organic ligands used during iron ore processing (specifically aromatic amine groups). Microscopy studies to identify the presence of nanoparticulate colloidal species in the sFe fraction could also shed lights on the processes at play that maintain Fe in the soluble fraction. The residence time of this iron in the water column, its transport to open oceans, its bioavailability and biogeochemical cycling are still open questions. The role of mining tailings as sources of stable forms of dFe and sFe is currently unknown but this study suggest that it should be investigated further.

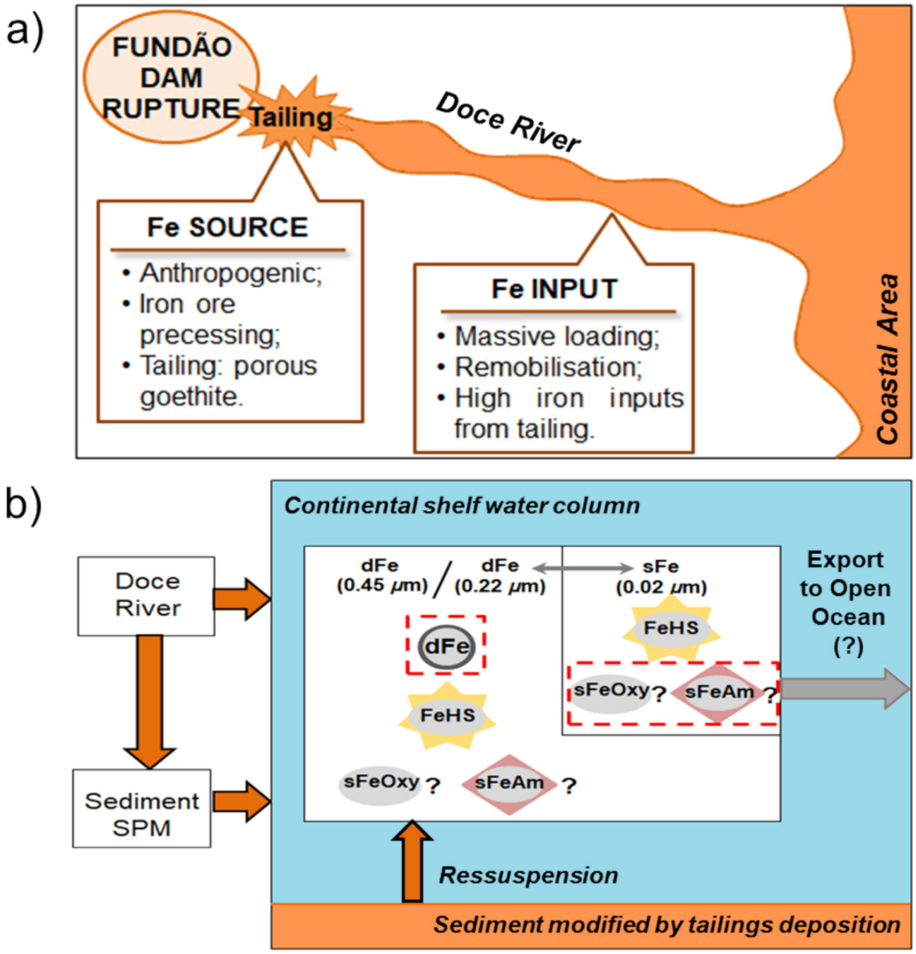

Figure 12. Processes changing dFe and sFe distribution in the continental shelf affected by Fundão mining tailings. a) shows the Fe sources and transport/inputs after the Fundão dam rupture (not to scale); and b) represents the input processes in the continental shelf and the Fe forms as a result of the disaster. dFe = dissolved Fe (0.45 µm and/or 0.22 µm); FeHS = Fe complexed by HS; sFeAm = soluble iron complexed by amine; sFeOxy = small colloidal Fe (lower than 0.02 µm) as nanoparticulate Fe(III) oxy-hydroxides. Red squares with dotted lines indicate the predominant forms in each fraction. Question marks refer to sFe forms and Fe transport to the open ocean inferred from our study but still uncertainties that should be further investigated. The size of the symbols is not proportional to the operational fractions.

17 REFERENCES

ABUALHAIJA, M.M.; WHITBY, H.; VAN DEN BERG, C.M.G.. Competition between copper and iron for humic ligands in estuarine waters. **Marine Chemistry,** v. 172, p. 46-56, 2015.

ADLY, C. L.; TREMBLAY, J.E.; POWELL, R.T.; ARMSTRONG, E.; PEERS, G.; PRICE, N.M.. Response of heterotrophic bacteria in a mesoscale iron enrichment in the northeast subarctic Pacific Ocean. **Limnology and Oceanography**, v. 60, p. 136-148, 2015.

ALBINO, J.; CONTTI NETO, N.; OLIVEIRA, T.C.A. The Beaches of Espírito Santo. *In:* SHORT, A.D.; KLEIN, A.H.F. (eds.). **Brazilian Beach Systems**. Vitória: Springer, 2016, p. 333-361.

ALMEIDA, C. A.; OLIVEIRA, A.F.; PACHECO, A.A.; LOPES, R.P.; NEVES, A.A.; QUEIROZ, M.E.L.R. Characterization and evaluation of sorption potential of the iron mine waste after Samarco dam disaster in Doce River basin – Brazil. **Chemosphere**, v. 209, p. 411-420, 2018.

ALORDA-KLEINGLASS, A.; GARCIA-ORELLANA, J.; RODELLAS, V. et al. Remobilization of dissolved metals from a coastal mine tailing deposit driven by groundwater discharge and porewater exchange. **Science of the Total Environment** v. 688, p. 1359-1372, 2019.

ALZAGA, R.; MESAS, A.; ORTIZ, L.; BAYONA. J.M. Characterization of organic compounds in soil and water affected by pyrite tailing spillage. **Science of the Total Environment**, v. 242, p. 167-178, 1999.

American Public Health Association (APHA). **Standard method for examination of water and wastewater**. 22. ed. Nova Iorque: American Public Health Association, 2012.

ARAUJO, A. C.; VIANA, P.R.M; PERES, A.E.C. Reagents in iron ores flotation. **Minerals Engineering**, v. 18, p. 219-224, 2005.

BARBEAU, K., RUE, E.L.; BRULAND, K.W.; BUTLER, A. Photochemical cycling of iron in the surface ocean mediated by microbial iron(III)-binding ligands. **Nature**, v. 413, p. 409–413, 2001.

BARBEAU, K..; RUE, E.L.; TRICK, C.G.; BRULAND, K.W.; BUTLER, A. Photochemical reactivity of siderophores produced by marine heterotrophic bacteria and cyanobacteria based on characteristic Fe(III) binding groups. **Limnology and Oceanography**, v. 48, n. 3, p. 1069-1078, 2003.

BASTOS, A.C.; OLIVERIA, K.S.S.; FERNANDES, L.F.; PEREIRA, J.B.; DEMONER, L.E.; NETO, R.R.; COSTA, E.S.; SÁ, F.; SILVA, C.A.; LERHBACK, B.D.; DIAS JR., C.; QUARESMA, V.S.; ORLANDO, M.T.D.; TURBAY, C.V.G.; LOPES, B.A.; LEITE, M.D.; GHISOLFI, R.D.; LEMOS, A.T.; PIVA, T.R.M.; LÁZARO, G.C.S.; CONCEIÇÃO, J.R.; LEMOS, K.N.; ZEN, C.M.; BONECKER, A.C.T.; CASTRO, M.S.; QUINTAS, M.C.; CAVAGGIONI, L.; OLIVEIRA, E.M.C. 2017. **Monitoramento da Influência da Pluma do Rio Doce após o rompimento da Barragem de Rejeitos em Mariana/MG – Novembro de 2015**: Processamento, Interpretação e Consolidação de Dados [online]. Universidade Federal do Espírito Santo, Vitória, Espírito Santo, Brazil. 2017. 254p. Disponível em:http://www.icmbio.gov.br/portal/images/stories/Rio_Doce/relatorio_consolidado_ufes_rio_doce.pdf. Acesso em: 07 ago. 2017.

BATCHELLI, S.; MULLER, F.L.L.; CHANG, K.C.; LEE, C.L. Evidence for strong but dynamic iron-humic colloidal associations in humic-rich coastal waters. **Environmental Science & Technology**, v. 44, p. 8485-8490, 2010.

BENOIT, G., ROZAN, T.F. The influence of size distribution on the particle concentration effect and trace metal partitioning in rivers. **Geochimica et Cosmochimica Acta**, v. 63, p.113-127, 1999.

BOYD, P. W., ELLWOOD, M. J. The biogeochemical cycle of iron in the ocean. **Nature Geoscience**, v.3, p. 675-682, 2010.

BOYLE, E. A.; EDMOND, J. M.; SHOLKOVITZ, E. R. 1977. The mechanism of iron removal in estuaries. **Geochimica et Cosmochimica Acta**, v. 41, p. 1313-1324, 1977.

BRAUNGARDT, C. B.; ACHTERBERG, E. P.; ELBAZ-POULICHET, F.; MORLEY, N. H. 2003. Metal geochemistry in a mine-polluted estuarine system in Spain. **Applied Geochemistry**, v. 18, p. 1757-1771, 2003.

BRULAND, K.W.; LOHAN, M.C. Controls of trace metals in seawater. *In:* TUREKIAN, K.K.; HOLLAND, H.D. (eds.). **Treatise on Geochemistry**. 1. ed. Elsevier, Pergamon. v. 6, 2003, p. 23-47.

BUFFLE, I.; LEPPARD, G.G. Characterization of Aquatic Colloids and Macromolecules. 1. Structure and Behavior of Colloidal Material. **Environmental Science & Technology**, v. 29, p. 2169-2175, 1995.

BUNDY, R. M.; ABDULLA, H.A.N.; HATCHER, P.G.; BILLER, D. V.; BUCK, K.N.; BARBEAU, K.A. Iron-binding ligands and humic substances in the San Francisco Bay estuary and estuarine-influenced shelf regions of coastal California. **Marine Chemistry**, v. 173, p. 183-194, 2015.

BYRNE, R. H.; KESTER, D. R. Solubility of hydrous ferric oxide and iron speciation in seawater. **Marine Chemistry**, v. 4, p. 255-274, 1976.

CÁNOVAS, C. R.; HUBBARD, C. G.; OLÍAS, M.; NIETO, J. M.; BLACK, S.; COLEMAN, M. L. 2008. Hydrochemical variations and contaminant load in the Río Tinto (Spain) during flood events. **Journal of Hydrology**, v. 350, p. 25-40, 2008.

CAPRARA, S.; LAGLERA, L. M.; MONTICELLI, D. Ultrasensitive and Fast Voltammetric Determination of Iron in Seawater by Atmospheric Oxygen Catalysis in 500 µl Samples. **Analytical Chemistry**, v. 87, p. 6357-6363, 2015.

CARMO, F.F.; KAMINO, L.H.Y.; JUNIOR, R.T.; et al. Fundão tailings dam failures: the environment tragedy of the largest technological disaster of Brazilian mining in global context. **Perspectives in Ecology and Conservation**, v. 15, p. 145-151, 2017.

CULLEN, J. T.; BERGQUIST, B.A.; MOFFETT, J.W. Thermodynamic characterization of the partitioning of iron between soluble and colloidal species in the Atlantic Ocean. **Marine Chemistry**, v. 98, p. 295-303, 2006.

DE JONG, J.T.M.; STAMMERJOHN, S.E.; ACKLEY, S.F.; TISON, J.L.; MATTIELLI, N.; SCHOEMANN, V. Sources and fluxes of dissolved iron in the Bellingshausen Sea (West Antarctica): The importance of sea ice, icebergs and the continental margin. **Marine Chemistry**, v. 177, p. 518-535, 2015.

DORR, J.V.N.; LICINIO, A.; BARBOSA, M. **Geology and Ore Deposits of the Itabira District**. Geological Survey Professional Paper 341-C, United States Department of the Interior, Washington 25, D.C., 1963, 110p.

ELLWOOD, M. J., S.; NODDER, D.; KING, A. L.; HUTCHINS, D. A.; WILHELM, S. W.; BOYD, P. W. Pelagic iron cycling during the subtropical spring bloom, east of New Zealand. **Marine Chemistry**, v. 160, p. 18-33, 2014.

ELROD, V.A.; BERELSON, W. M.; COALE, K. H.; JOHNSON, K. S. The flux of iron from continental shelf sediments: A missing source for global budgets. **Geophysical Research Letters**, v. 31, p. 2-5, 2004.

ESCOBAR, H. Mystery oil spill threatens marine sanctuary in Brazil. **Science**, v. 366, n. 6466, p. 672, 2019.

FILIPPOV, L. O., SEVEROV, V. V.; FILIPPOVA, I. V. An overview of the beneficiation of iron ores via reverse cationic flotation. **International Journal of Mineral Processing**, v.127, p. 62-69, 2014.

FITZSIMMONS, J. N.; BUNDY, R. M.; AL-SUBIAI, S. N.; BARBEAU, K. A.; BOYLE, E. A. The composition of dissolved iron in the dusty surface ocean: An exploration using size-fractionated iron-binding ligands. **Marine Chemistry**, v. 173, p. 125-135, 2015.

FITZSIMMONS, J. N.; JOHN, S. G.; MARSAY, C. M.; HOFFMAN, C. L.; NICHOLAS, S. L.; TONER, B. M.; GERMAN, C. R.; SHERRELL, R. M. Iron persistence in a distal hydrothermal plume supported by dissolved-particulate exchange. **Nature Geoscience**, v. 10, p. 195-201, 2017.

Gartman, A.; Findlay, A. J.; Luther, G. W. Nanoparticulate pyrite and other nanoparticles are a widespread component of hydrothermal vent black smoker emissions. **Chemical Geology**, v. 366, p. 32-41, 2014.

GERRINGA, L.J.A.; SLAGTER, H.A.; BOWN, J.; VAN HAREN, H.; LAAN, P.; DE BAAR, H.J.W.; RIJKENBERG, M.J.A. Dissolved Fe and Fe-binding organic ligands in the Mediterranean Sea – GEOTRACES G04. **Marine Chemistry**, v. 194, p. 100-113, 2017.

GLEDHILL, M.; VAN DEN BERG, C.M.G. Determination of complexation of iron(III) with natural organic complexing ligands in seawater using cathodic stripping voltammetry. **Marine Chemistry**, v. 47, p. 41-54, 1994.

GLEDHILL, M., BUCK, K.N. The organic complexation of iron in the marine environment: A review. **Frontiers in Microbiology**, v. 3, p. 1-17, 2012.

GLEDHILL, M.; MCCORMACK, P.; USSHER, S.; ACHTERBERG, E.P.; MANTOURA, R.F.C.; WORSFOLD, P. J. Production of siderophore type chelates by mixed bacterioplankton populations in nutrient enriched seawater incubations. **Marine Chemistry**, v. 88, p. 75-83, 2004.

GOMES, L.E.O.; CORREA, L.B.; SÁ, F.; NETO, R.R.; BERNARDINO, A.F. The impacts of the Samarco mine tailing spill on the Rio Doce estuary, Eastern Brazil. **Marine Pollution Bulletin,** v. 120, p. 28-36, 2017.

GRILO, C.F.; QUARESMA, V.S.; AMORIM, G.F.L.; BASTOS, A.C. Changes in flocculation patterns of cohesive sediments after an iron ore mining dam failure. **Marine Geology**, v. 400, p. 1-11, 2018.

HAMMER, D.; HARPER, D.A.T.; RYAN, P.D. PAST: Paleontological statistics software package for education and data analysis. **Palaeontologia Electronica**, v. 4, n. 1, 9p., 2001.

HASSLER, C. S.; VAN DEN BERG, C.M.G.; BOYD, P.W. Toward a Regional Classification to Provide a More Inclusive Examination of the Ocean Biogeochemistry of Iron-Binding Ligands. **Frontiers in Marine Science,** v. 4, 2017.

HASSLER, C. S.; NORMAN, L.; MANCUSO NICHOLS, C. A.; CLEMENTSON, L.A.; ROBINSON, C.; SCHOEMANN, V.; WATSON, R.J.; DOBLIN, M.A. Iron associated with exopolymeric substances is highly bioavailable to oceanic phytoplankton. **Marine Chemistry**, v. 173, p. 136-147, 2015.

HATJE, V.; PEDREIRA, R.M.A.; DE REZENDE, C.E.; SCHETTINI, C.A.F.; DE SOUZA, G.C.; MARIN, D.C.; HACKSPACHER, P.C. The environmental impacts of one of the largest tailing dam failures worldwide. **Scientific Reports**, v. 7, p. 1-13, 2017.

HATTA, M.; MEASURES, C. I.; SELPH, K. E.; ZHOU, M.; HISCOCK, W. T. Iron fluxes from the shelf regions near the South Shetland Islands in the Drake Passage during the austral-winter 2006. **Deep Sea Research Part II: Topical Studies in Oceanography**, v. 90, p. 89-101, 2013.

JEANDEL, C.; OELKERS, E. H. The influence of terrigenous particulate material dissolution on ocean chemistry and global element cycles. **Chemical Geology,** v. 395, p. 50-66, 2015.

JOHNSON, K.S.; CHAVEZ, F.P.; FRIEDERICH, G.E. Continental-shelf sediment as a primary source of iron for coastal phytoplankton. **Nature**, v. 398, n. 6729, p. 697–700, 1999.

JOHNSON, K.S.; GORDON, R.M.; COALE, K.H. What controls dissolved iron concentrations in the world ocean? Authors' closing comments. **Marine Chemistry**, v. 57, n. 3-4, p. 181-186, 1997.

JOSÉ, F.S., BROD, E.R.; PEREIRA, C.A. Simultaneous use of direct and reverse flotation in the production of iron ore concentrate plant. **International Engineering Journal**, v. 71, n. 2, p. 299-304, 2018.
KOSKI, R.A. Metal dispersion resulting from mining activities in coastal environments: a pathways approach. **Oceanography**, v. 25, n. 2, p. 170-183, 2012.

KRACHLER, R.; JIRSA, F.; AYROMLOU, S. Factors influencing the dissolved iron input by river water to the open ocean. **Biogeosciences**, v. 2, p. 311-315, 2005.

KRACHLER, R.; KRACHLER, R.F.; VON DER KAMMER, F.; SÜPHANDAG, A.; JIRSA, F.; AYROMLOU, S.; HOFMAN, T.; KEPPLER, B.K. Relevance of peat-draining rivers for the riverine input of dissolved iron into the ocean. **Science of the Total Environment**, v. 408, n. 11, p. 2402-2408, 2010.

KRACHLER, R.; KRACHLER, R.F.; WALLNER, G.; et al. River-derived humic substances as iron chelators in seawater. **Marine Chemistry**, v. 174, p. 85-93, 2015.

KRACHLER, R., KRACHLER, R.F.; WALLNER, G.; STEIER, P.; EL ABIEAD,Y.; WIESINGER, H.; JIRSA, F.; KEPPLER, B.K. Sphagnum-dominated bog systems are highly effective yet variable sources of bio-available iron to marine waters. **Science of the Total Environment**, v. 556, p. 53-62, 2016.

KRUSKAL, W.H.; WALLIS, W.A. Use of ranks in one-criterion variance analysis. **Journal of the American Statistical Association**, v. 47, p. 583-621, 1952.

KUMA, K.; NISHIOKA, J.; MATSUNAGA, K. Controls on iron(III) hydroxide solubility in seawater: The influence of pH and natural organic chelators. **Limnology and Oceanography**, v. 41, p. 396-407, 1996.

LAGLERA, L. M.; BATTAGLIA, G.; VAN DEN BERG, C.M.G. Determination of humic substances in natural waters by cathodic stripping voltammetry of their complexes with iron. **Analytica Chimica Acta**, v. 599, p. 58-66, 2007.

LAGLERA, L.M.; BATTAGLIA, G.; VAN DEN BERG, C.M.G. Effect of humic substances on the iron speciation in natural waters by CLE/CSV. **Marine Chemistry**, v. 127, p. 134-143, 2011.

LAGLERA, L. M.; VAN DEN BERG, C.M.G. Evidence for geochemical control of iron by humic substances in seawater. **Limnology and Oceanography**, v. 54, p. 610-619, 2009.

LIU, X.; MILLERO, F.J. The solubility of iron in seawater. **Marine Chemistry**, v. 77: p. 43-54, 2002.

LONGHINI, C. M.; SÁ, F.; NETO, R. R. Review and synthesis: iron input, biogeochemistry, ecological approaches in seawater. **Environmental Reviews**, v. 27, p. 125-137, 2019.

LOUGH, A. J. M.; HOMOKY, W. B.; CONNELLY, D. P.; COMER-WARNER, S. A.; NAKAMURA, K.; ABYANEH, M. K.; KAULICH, B.; MILLS, R. A. Soluble iron conservation and colloidal iron dynamics in a hydrothermal plume. **Chemical Geology**, v. 511, p. 225-237, 2019.
LORENZEN, C.J. Determination of chlorophyll and pheopigments: spectrophotometric equations. **Limnology and Oceanography**, v. 12, p. 343-346, 1967.

MA, M. Froth Flotation of Iron Ores. **International Journal of Mineral Processing**, v. 1, p. 56-61, 2012.

MAHMOOD, A.; ABUALHAIJA, M. M.; VAN DEN BERG, C.M.G.; SANDER, S.G. Organic speciation of dissolved iron in estuarine and coastal waters at multiple analytical windows. **Marine Chemistry**, v. 177, p. 706-719, 2015.

MANN, H.B.; WHITNEY, D.R. On a test whether one of two random variables is stochastically larger than the other. **Annals of Mathematical Statistics,** v. 18, p. 50-60, 1947.

MARTA-ALMEIDA, M.; MENDES, R.; AMORIM, F. N.; CIRANO, M.; DIAS, J. M. Fundão Dam collapse: Oceanic dispersion of River Doce after the greatest Brazilian environmental accident. **Marine Pollution Bulletin**, v. 112, p. 359-364, 2016.

MAWJI, E.; GLEDHILL, M.; MILTON, J.A. et al. Hydroxamate siderophores: Occurrence and importance in the Atlantic Ocean. **Environmental Science & Technology**, v. 42, p. 8675-8680, 2008.

MILLERO, F.; PIERROT, D. Speciation of metals in natural waters. *In:* GIANGUZZA, A.; PELIZZETTI, E.; SAMMARTANO, S. (eds.). **Chemistry of marine water and sediments**. 1. ed. Berlim: Springer, 2002, p. 193-220. doi:10.1007/978-3-662-04935-8_8.

MULLER, F.L.L. Exploring the potential role of terrestrially derived humic substances in the marine biogeochemistry of iron. **Frontiers in Earth Science**, v. 6, p. 1-20, 2018.

MULLER, F.L.L.; CUSCOV, M. Alteration of the Copper-Binding Capacity of Iron-Rich Humic Colloids during Transport from Peatland to Marine Waters. **Environmental Science & Technology**, v. 51, p. 3214-3222, 2017.

MUNKSGAARD, N. C.; PARRY, D. L. Trace metals, arsenic and lead isotopes in dissolved and particulate phases of North Australian coastal and estuarine seawater. **Marine Chemistry**, v. 75, p. 165-184, 2001.

NORMAN, L., CABANESA, D.J.E.; BLANCO-AMEIJEIRAS, S.; MOISSET, A.M.; HASSLER, C.S. Iron Biogeochemistry in Aquatic Systems: From Source to Bioavailability. **Chimica International Journal of Chemistry**, v. 68, p. 764-771, 2014.

NORMAN, L.; WORMS, I.A.M.; ANGLES, E.; et al 2015. The role of bacterial and algal exopolymeric substances in iron chemistry. **Marine Chemistry**, v. 173, p. 148-161, 2015.

OBATA, H.; VAN DEN BERG, C.M.G. Determination of picomolar levels of iron in seawater using catalytic cathodic stripping voltammetry. **Analytical Chemistry**, v. 73, p. 2522-2528, 2001.
OLÍAS, M.; CÁNOVAS, C.R.; NIETO, J.M.; SARMIENTO, A. M. Evaluation of the dissolved contaminant load transported by the Tinto and Odiel rivers (South West Spain). **Applied Geochemistry**, v. 21, p. 1733-1749, 2006.

PEARSE, M. J. An overview of the use of chemical reagents in mineral processing. **Minerals Engineering**, v. 18, p. 139-149, 2005.

PEREIRA, A.A.; VAN HATTUM, B.; BROUWER, A.; VAN BODEGOM, P.M.; REZENDE, C.E.; SALOMONS, W. Effects of iron-ore mining and processing on metal bioavailability in a tropical coastal lagoon. **Journal of Soils and Sediments**, v. 8, p. 239-252, 2008.

PIRES, J.M.M.; DE LENA, J.C.; MACHADO, C.C.; PEREIRA, R.S. Potencial poluidor de resíduo sólido da Samarco Mineração: estudo de caso da barragem de germano. **Revista Árvore**, v. 27, n. 3, p. 393-397, 2003.

QUARESMA, V.S.; CATABRIGA, G.; BOURGUIGNON, S.N.; GODINHO, E.; BASTOS, A.C. Modern sedimentary processes along the Doce river adjacent continental shelf. **Brazilian Journal of Geology**, v. 45, n. 4, p. 635-644, 2015.

QUEIROZ, H.M.; NÓBREGA, G.N.; FERREIRA, T.O.; ALMEIDA, L.S.; ROMERO, T.B.; SANTAELLA, S.T.; BERNARDINO, A.F.; OTERO, X.L. The Samarco mine tailing disaster: A possible time-bomb for heavy metals contamination? **Science of the Total Environment**, v. 637-638, p. 498–506, 2018.

QUEROL, X.; ALASTUEY, A.; LOPEZ-SOLER, A. et al. Physico-chemical characterisation of atmospheric aerosols in a rural area affected by the aznalcollar toxic spill, south-west Spain during the soil reclamation activities. **Science of the Total Environment**, v. 242, p. 89-104, 1999.

RESING, J. A.; SEDWICK, P.N.; GERMAN, C.R.; JENKINS, W.J.; MOFFETT, J.W.; SOHST, B.M.; TAGLIABUE, A. Basin-scale transport of hydrothermal dissolved metals across the South Pacific Ocean. **Nature**, v. 523, p. 200-203, 2015.

RICKARD, D. Sedimentary iron biogeochemistry. In: Rickard, D. (ed.). **Developments in sedimentology**. v. 65, 2012, p. 85-119, 2012. doi:10.1016/B978-0-444-52989-z.00003-9.

RUDORFF, N.; RUDORFF, C. M.; KAMPEL, M.; ORTIZ, G. Remote sensing monitoring of the impact of a major mining wastewater disaster on the turbidity of the Doce River plume off the eastern Brazilian coast. **ISPRS Journal of Photogrammetry and Remote Sensing (P&RS)**, v. 145, p. 349-361, 2018.

RUE, E. L.; BRULAND, K. W. Complexation of iron(III) by natural organic ligands in the Central North Pacific as determined by a new competitive ligand equilibration/adsorptive cathodic stripping voltammetric method. **Marine Chemistry**, v. 50, p.117-138, 1995.

RUE, E.L.; BRULAND, K.W. The role of organic complexation on ambient iron chemistry in the equatorial Pacific Ocean and the response of a mesoscale iron addition experiment. **Limnology and Oceanography**, v.42, p. 901-910, 1997.

SAÑUDO-WILHELMY, S. A.; RIVERA-DUARTE, I.; FLEGAL, A.R. Distribution of colloidal trace metals in the San Francisco Bay estuary. **Geochimica et Cosmochimica Acta**, v. 60, p. 4933-4944, 1996.

SCHROLLER-LOMNITZ, U.; HENSEN, C.; DALE, A. W.; SCHOLZ, F.; CLEMENS, D.; SOMMER, S.; NOFFKE, A.; WALLMANN; K. Dissolved benthic phosphate, iron and carbon fluxes in the Mauritanian upwelling system and implications for ongoing deoxygenation. **Deep Sea Research Part I: Oceanographic Research Papers**, v. 143, p. 70-84, 2019.

SEGURA, F.R.; NUNES, E.A.; PANIZ, F.P.; et al. Potential risks of the residue from Samarco's mine dam burst (Bento Rodrigues, Brazil). **Environmental Pollution,** v. 218, p. 813-825, 2016.

SEVERMANN, S.; MCMANUS, J.; BERELSON, W. M.; HAMMOND, D. E. The continental shelf benthic iron flux and its isotope composition. **Geochimica et Cosmochimica Acta**, v. 74, p. 3984-4004, 2010.

SHAPIRO, S.S.; WILK, M.B. An analysis of variance test for normality (complete samples). **Biometrika**, v. 52, n. 3-4, p. 591-611, 1965.

SHARPLES, J.; MIDDELBURG, J.J.; FENNEL, K.; JICKELLS, T.D. What proportion of riverine nutrients reaches the open ocean? **Global Biogeochemical Cycles**, v. 31, p. 39-58, 2017.

SHI, X.; WEI, L.; HONG, Q.; LIU, L.; WANG, Y.; SHI, X.; YE, Y.; CAI, P. Large benthic fluxes of dissolved iron in China coastal seas revealed by 224Ra/228Th disequilibria. **Geochimica et Cosmochimica Acta**, v. 260, p. 49-61, 2019.

SHOLKOVITZ, E.R.; BOYLE, E.A.; PRICE, N.B. 1978. The removal of dissolved humic acids and iron during estuarine mixing. **Earth and Planetary Science Letters**, v. 40, p. 130-136, 1978.

SLAGTER, H. A.; READER, H. E.; RIJKENBERG, M. J. A.; RUTGERS VAN DER LOEFF, M.; DE BAAR, H.J.W.; GERRINGA, L.J.A. Organic Fe speciation in the Eurasian Basins of the Arctic Ocean and its relation to terrestrial DOM. **Marine Chemistry**, v. 197, p. 11-25, 2017.

SPEARMAN, C. The proof and measurement of association between two things. **Journal of Applied Psychology,** v. 15, n. 1, p. 72-101, 1904.

STOLPE, B.; ZHOU, X.; GUO, L.; SHILLER, A. M. Colloidal size distribution of humic- and protein-like fluorescent organic matter in the northern Gulf of Mexico. **Marine Chemistry**, v. 164, p. 25-37, 2014.

SU, H.; YANG, R.; ZHANG, A.; LI, Y. Dissolved iron distribution and organic complexation in the coastal waters of the East China Sea. **Marine Chemistry**, v. 173, p. 208-221, 2015.

SU, H.; YANG, R.; LI, Y.; WANG, X. Influence of humic substances on iron distribution in the East China Sea. **Chemosphere**, v. 204, p. 450-462, 2018.

SUKEKAVA, C.; DOWNES, J.; SLAGTER, H.A.; GERRINGA, L.J.A.; LAGLERA, L.M. Determination of the contribution of humic substances to iron complexation in seawater by catalytic cathodic stripping voltammetry. **Talanta**, v. 189, p. 359-364, 2018.

TAGLIABUE, A.; BOPP, L.; AUMONT, O. Evaluating the importance of atmospheric and sedimentary iron sources to Southern Ocean biogeochemistry. **Geophysical Research Letters**, v. 36, p. 1-5, 2009.

TAGLIABUE, A.; AUMONT, O.; BOPP, L. The impact of different external sources of iron on the global carbon cycle. **Geophysical Research Letters**, v. 41, p. 920-926, 2014.

TAGLIABUE, A.; BOWIE, A. R.; BOYD, P. W.; BUCK, K. N.; JOHNSON, K. S.; SAITO, M. A. The integral role of iron in ocean biogeochemistry. **Nature**, v. 543, p. 51-59, 2017.

TOVAR-SÁNCHEZ, A.; BASTERRETXEA, G.; BEN OMAR, M.; et al. Nutrients, trace metals and B-vitamin composition of the Moulouya River: A major North African river discharging into the Mediterranean Sea. **Estuarine, Coastal and Shelf Science**, v. 176, p. 47-57, 2016.

TREFRY, J.H. **The transport of heavy metals by the Mississippi River and their fate in the Gulf of Mexico**. 1977. 238p. Tese (Doutorado em Geoquímica) – Departamento de Oceanografia, Texas A&M University, College Station, 1977.

TREZZI, G.; GARCIA-ORELLANA, J.; SANTOS-ECHEANDIA, J.; RODELLAS, V.; GARCIA-SOLSONA, E.; GARCIA-FERNANDEZ, G.; MASQUÉ, P. The influence of a metal-enriched mining waste deposit on submarine groundwater discharge to the coastal sea. **Marine Chemistry**, v. 178, p. 35-45, 2016.

TRIMBORN, S.; HOPPE, C.J.M.; TAYLOR, B.B.; BRACHER, A.; HASSLER, C. Physiological characteristics of open ocean and coastal phytoplankton communities of Western Antarctic Peninsula and Drake Passage waters. **Deep Sea Research Part I: Oceanographic Research Papers**, v. 98, p. 115-124, 2015.

U.S. EPA. **Method 6020A**: Inductively Coupled Plasma-Mass Spectrometry, Revision 1. Washington, DC, 1998.

WILCOXON, F. Individual Comparisons by Ranking Methods. **Biometrics Bulletin**, v. 1, n. 6, p. 80-83, 1945.

WU, J.; BOYLE, E.; SUNDA, W.; WEN, L. S. Soluble and colloidal iron in the oligotrophic North Atlantic and North Pacific. **Science**, v. 293, p. 847-849, 2001.

YANG, R.; VAN DEN BERG, C.M.G. Metal complexation by humic substances in seawater. **Environmental Science & Technology**, v. 43, p. 7192-7197, 2009.

YANG, R.; SU, H.; QU, S.; WANG, X. Capacity of humic substances to complex with iron at different salinities in the Yangtze River estuary and East China Sea. **Scientific Reports**, v. 7, p. 1-9, 2017.

YÜCEL, M.; GARTMAN, A.; CHAN, C. S.; LUTHER, G. W. Hydrothermal vents as a kinetically stable source of iron-sulphide-bearing nanoparticles to the ocean. **Nature Geoscience**, v. 4, p. 367-371, 2011.

CAPÍTULO 3

PHYTOPLANKTON RESPONSE TO METAL ENRICHMENT IN A COASTAL AREA AFFECTED BY A MINING TAILING DISASTER

Longhini, C.M.; Sá, F.; Lázaro, G.C.S.; Lemos, K.N.L.; Costa, E.S.; Gomes, L. E. de O.; Oliveira. K.S.S.; Grilo C.F.; Costa Júnior, A.A.; Leite, M.D.A.; Quaresma, V. da S.; Bastos, A.C.; Ghisolfi, R.D.; Dias Júnior, C.; Neto, R.R.

To be submitted to Science of the Total Environment journal

Abstract

Phytoplankton community is highly controlled by trace metals/micronutrients acting as enzymatic co-factors to many biochemical processes. Fe, Mn, Zn, Cu, Co and V are some metals required in physiological mechanisms, so their distribution and bioavailability will drive biological responses from cellular to ecological levels. Metals enrichment in seawater is known to affect phytoplankton assemblage as by toxicity factor as well as by favouring some harmful algae growth. However, the impact of metal contamination by mining tailings on phytoplankton community has not been addressed. Here we evidence that coastal phytoplankton community impacted by a mining disaster (Fundão dam collapse, Southeast Brazil) is controlled by metals in particulate fraction (mainly pZn, pCu, pV and pFe with lower contribution). Cyanophyceae was the most frequent group during the samplings and their densities were related to pFe concentration that remained high during time scale. Furthermore, we found that diatoms growth was mainly controlled by pZn levels, as well as, during higher Doce River freshwater discharge. Specific conditions of metals enrichment (7pFe, 5pV, 4pCu, 8pZn) suggest physiological control associated to silicon uptake. Our results demonstrate that phytoplankton community in coastal waters impacted by the Fundão mining disaster changes their community organization as a response to metal enrichment, as previous studies have consistently shown that diatoms and flagellates are the dominant groups in Fe-fertilized conditions. Our results evidence that these differences are driven by the form of metals from the tailings and cyanobacteria obtained competitive advantages compared to other groups due to their versatile strategies to assimilate metal from a wide range of substrates. The integrated analyses among metals and their relation with toxic algae proliferation can shed light to mining impacts on ecosystems ecological functioning and human health.

Keywords: Trace metals; mining contamination; harmful algae; phytoplankton ecophysiology; particulate iron

18 INTRODUCTION

Phytoplankton community plays a main ecological role in marine ecosystems for comprising the first level of trophic chain and for controlling the biogeochemical cycle of several elements such as Carbon (C), Nitrogen (N), Phosphorus (P) and Silicate (Si) (TILMAN; KILHAM; KILHAM, 1982; SUNDA, 1989; WANG, 2002; MOREL; MILLIGAN; SAITO, 2003; BEHRENFELD *et al*., 2005). Phytoplankton growth and community structure is greatly controlled by numerous major nutrients (N, P and Si) and trace metals acting as micronutrients and cofactors for enzymatic metabolism (e.g. Fe, Mn, Zn, Cu, Co, Mo, Ni) (SUNDA, 1989; MASMOUDI *et al*., 2013). The interrelations among metals/micronutrients and algae behaviour involve the understanding of different levels of complexity, such as: 1) geochemistry distribution and speciation of metals in the seawater; 2) biomolecular interaction such as physiological mechanisms to elemental uptake; 3) metabolism response and growth rate at cellular level; and 4) algae densities and community composition (SUNDA, 1989).

Particles play a main role in controlling metal inputs, distribution and recycling in coastal areas (OLSEN; CUTSHALL; LARSEN, 1982; YUAN-HUI, 1991). The interaction between metals and suspended particulate material is driven by processes of ionic adsorption-desorption, organic and/or inorganic flocculation, aggregation with oxy-hydroxy Fe and Mn particles and also by biological assimilation and cycling of these elements as biogenic particles (OLSEN; CUTSHALL; LARSEN, 1982). Considering the continental sources, trace metal concentrations and fluxes to coastal regions are highly limited by the process of estuarine trapping (BOYLE; EDMOND; SHOLKOVITZ, 1977; SHOLKOVITZ; BOYLE; PRICE, 1978; JOHNSON; GORDON; COALE, 1997; BRULAND; LOHAN, 2006). In fluvial waters, these elements are stabilized on water column by association with colloidal organic matter as the repulsion forces of ionic charges allows the material to remain in solution. During estuarine transport, charges are neutralized by positive ions with the increasing salinity. As a response, colloidal organic particles become bound by cohesive association resulting on precipitation from the water column and consequently

removal of associated metals (BOYLE; EDMOND; SHOLKOVITZ, 1977; SHOLKOVITZ; BOYLE; PRICE, 1978; JOHNSON; GORDON; COALE, 1997).

Fe and Zn are two of the most important metals/micronutrients for marine plankton cellular requirements (HO *et al*., 2003; HO *et al*., 2007; TWINING; BAINES; FISHER, 2004). Fe is largely required on photosynthetic apparatus by composing the structural frame of important proteins involved in transfer of electrons and redox reactions. This metal is also demanded for biochemical steps in respiration and nitrogen assimilation (MOREL; HUDSON; PRICE, 1991; MOREL; MILLIGAN; SAITO, 2003; FALKOWSKI; BARBER; SMETACEK, 1998; MOREL; PRICE, 2003). Zn is involved in carbon concentrating mechanisms in marine diatom (as *Thalassiosira weissflogi*; MOREL *et al*., 2002) and also in silic acid acquisition which occurs by a Zn-dependent enzymatic system (RUETER; MOREL, 1981). However, some metals/micronutrients, especially Cu and Zn, are toxic at high levels or under conditions of imbalance of the optimum concentrations ratio resulting on physiological disequilibrium and growth limitation (SUNDA, 1989; MASMOUDI *et al*., 2013).

Although there are no direct evidences of Fe toxic effects on phytoplankton growth, Fe fertilization experiments have shown significant shifts in the community structure (BIZSEL; ÖZTÜRK; METIN, 1997; YOON *et al*., 2016), impacts on ecological diversity indices (LAMPITT *et al*., 2008) and proliferation of toxic microalgae (WELLS *et al*., 2005; LAMPITT *et al*., 2008; ZHUO-PING *et al*., 2009; TRICK *et al*., 2010). Therefore, understanding the responses of metals/micronutrients on the phytoplankton community is a lack knowledge and key factor to describe the impacts of metal-enriched marine systems on biological and ecological structure (GOMES *et al*., 2017; LONGHINI; SÁ; NETO, 2019).

In November 2015, the collapse of the Fundão dam in South-eastern Brazil spilled more than 55 million m^3 of iron ore tailings along the Doce River which reached the coastal area in the Espírito Santo state, more than 600 km downstream. This event was considered one of the largest dam tailings failure worldwide (CARMO *et al*., 2017). Monitoring program in the continental shelf adjacent to the Doce River mouth affected by those mining tailings have shown high inputs of metals, mostly Fe, Al and Mn, whereas increases on

phytoplankton biomass and shifts on species composition compared to pre disaster conditions were also observed (BASTOS *et al*., 2017). Even though the interrelations between metals and phytoplankton assemblage have not been addressed in this area until the moment, major changes in that and other biological group are predicted due to environmental disasters such as this Fundão dam collapse (see GOMES *et al*., 2017; LONGHINI; SÁ; NETO, 2019). On biochemical and physiological level, uptake strategies used by each algae group will be associated to the forms of metals available in the system while on ecological levels, shifts on species composition will occur in response of favouring the groups that obtain a competitive advantage due to these assimilation strategies (LONGHINI; SÁ; NETO, 2019).

The aim of this study is to evaluate the metal/micronutrients distribution in the water column and their effects on the phytoplankton community structure and also synergistic effects with major nutrients and physico-chemical variables in order to understand the impacts of tailings and metal enrichment therein to the phytoplankton composition in the coastal area affected by the Fundão disaster. We hypothesize that the input of metals to the marine ecosystems changed the phytoplankton community improving taxa within hazard potential to environmental and human health. This study presents the first integrated analyses of metal/micronutrients and phytoplankton interrelations in marine area directly affected by mining tailings.

19 MATERIAL AND METHODS

19.1 Study area and sampling design

The study area comprises the continental shelf adjacent to the Doce River mouth (Espírito Santo state, Brazil) (Fig. 13) which has been affected by tailing deposition after the Fundão dam mining disaster. The climate is tropical humid with average annual temperature about 23.8 °C and annual rainfall greater than 1,200 mm.year^{-1}. The dry season occurs from April to September (rainfall pattern of 53.0 to 97.0 mm.mo^{-1}) whereas the wet season falls within October and March (rainfall pattern of 101.1 to 211.5 mm.mo^{-1}; ALVARES *et al*., 2014; NÓBREGA *et al*., 2008; SERVINO; GOMES; BERNARDINO, 2018). The hydrological and oceanographic conditions (winds/waves regimes) are known to

define the flow of the Doce River turbidity plume (RUDORFF *et al*., 2018), the sedimentary processes (QUARESMA *et al*., 2015) and consequently the dispersion pattern of the tailings on the continental shelf. Winds regime in the region is modulated by seasonal climatology and also by the incidence of cold fronts and the establishment of the South Atlantic Convergence Zone (SACZ) system, occurring mostly during the summer. These factors result on more frequent and intense winds blowing from NE, N and E along the year and south quadrant wind (predominantly coming from SE) occurring during the passage of cold fronts (DERECZYNSKI *et al.*, 2019). The pattern of waves follows the bimodal winds regime and *Swell* waves from northeast and easterly of 0.5 and 1.5 m of height are associated to the winds from NE-ENE and occur more frequently offshore, whereas larger waves of 2.0 m from southeast are less common and related to storm events. In the onshore region waves from northeast averaging between 1.0 and 1.5 m are frequent. The tidal regime in the narrower continental shelf is microtidal, with the maximum amplitude varying from 0.8 to 1.9 m (ALBINO; CONTTI NETO; OLIVEIRA, 2016).

In order to evaluate the impacts of metals and nutrients on phytoplankton assemblage after the Fundão dam mining disaster, five samplings were carried out in the continental shelf adjacent to the Doce River mouth in November 2015 (Nov/2015; n = 14), January 2016 (Jan/2016; n = 14), two surveys in February 2016 (Feb/2016a, n = 27; Feb/2016b, n = 14) and April 2016 (Apr/2016; n = 14). Sampling stations were established perpendicularly to the shoreline from 10 to 50 m isobaths and composed by three main spatial compartments/sectors: Central (C) – in front of the river mouth; North (N) – northern from the river mouth; and South (S) – southern from the river mouth (Figure 13).

Coastal water samples from sub-surface (~50 cm below the water surface) and bottom (~2 m above the bottom) were collected using a 5 litre Niskin horizontal bottle sampler (General Oceanics) into 500 mL acid-cleaned LDPE bottles. Temperature and salinity were measured on board from a CTD instrument (*11* plus Sea-Bird Electronics). Samples for qualitative phytoplankton analysis were collected by vertical tow in low velocity using plankton net with 60 µm mesh while the aliquots for quantitative determination were obtained from

the Niskin bottle. Both qualitative and quantitative samples of phytoplankton were fixed in 2% formalin solution.

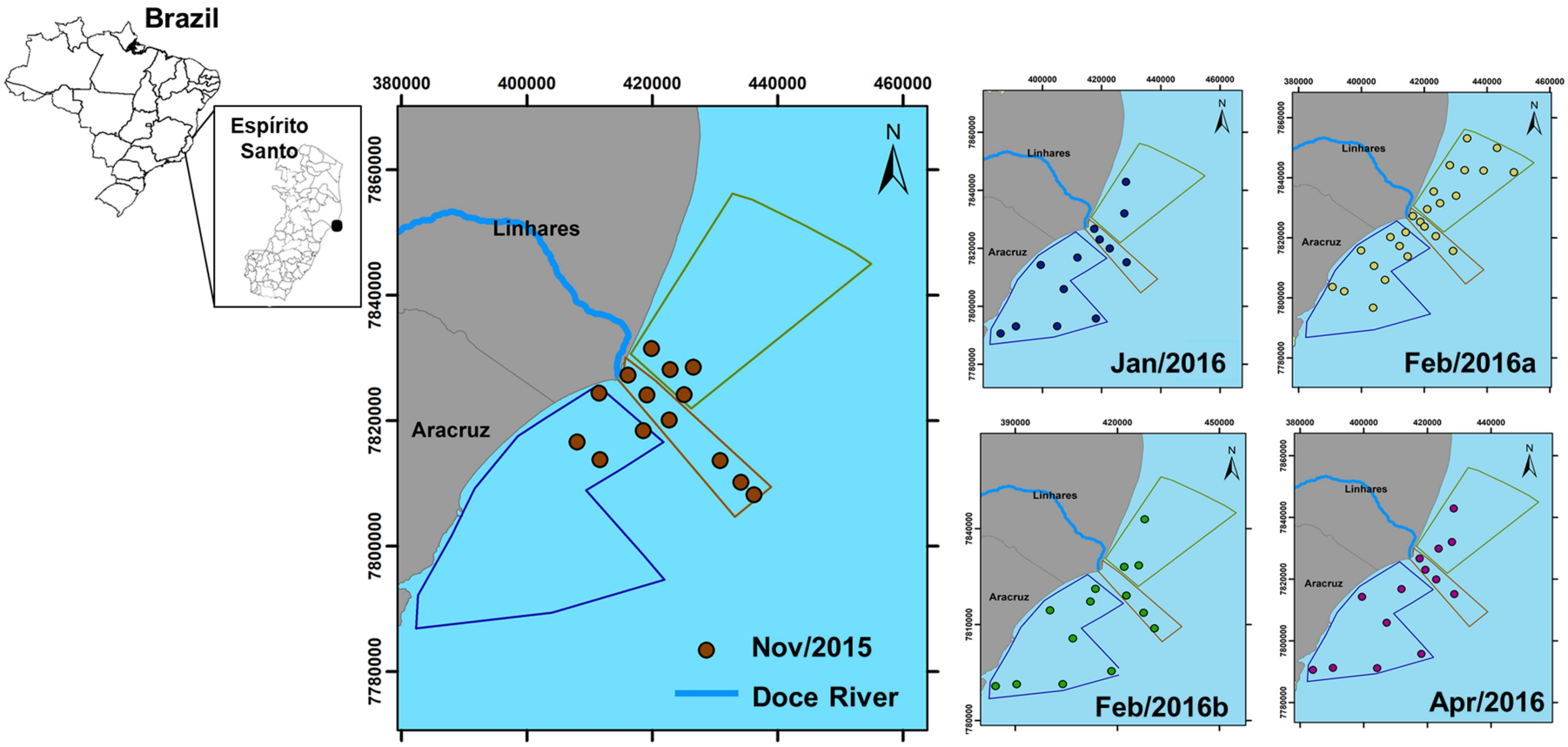

Figure 13. Distribution of sampling stations on the continental shelf adjacent to the Doce River mouth (Southeast, Brazil) after the Fundão dam rupture from Nov/2015 to Apr/2016. Polygons indicate the sectors North, Central and South; 10, 20 and 30 indicate the isobaths 10, 20 and 30 meters.

19.2 Hydroclimatic conditions during the samplings

The mining tailings reached the coast on the 21 November 2015 by low streamflow conditions (267.5 $m^3.s^{-1}$), where the first sampling was conducted 6 days after the contamination of the continental shelf by tailings plume also under low Doce River discharge (291.3 $m^3.s^{-1}$) (Table 9). Similar conditions of low river flow occurred in Feb/2016b (490.1 $m^3.s^{-1}$) and Apr/2016 (248.5 $m^3.s^{-1}$) (Table 9). A flooding event was registered towards the end of Jan/2016 reaching 1,333.1 $m^3.s^{-1}$ in Jan/2016 and 729.0 $m^3.s^{-1}$ in Feb/2016a samplings (Table 9).

In Nov/2015 the winds pattern was changed by the cold front passage, resulting winds from S quadrant, beyond the most common winds coming from N and NE (Table 9). In the following samplings the winds blew predominantly from N, NE and promoted the Doce River turbidity plume to disperse southward and concentrated parallel to the coast in some occasions (e.g. Jan/2016 and Apr/2016) (Table 9).

Table 9. General hydroclimatic conditions in the day when the mining tailings reached the coastal area (first line) and during the samplings on the continental shelf adjacent to the Doce River mouth.

Date	Sampling identification	River Discharge ($m^3.s^{-1}$)[a]	Wind[b]	Cold front[c]	Doce River plume dispersion[b]
21/11/2015: mining tailings reached the coastal area	–	267.5	N, ENE, SSE	Yes	–
27/11/2015	Nov/2015	291.3	N, NE, S	Yes	Northward, Southward and Southwest-ward
28/01/2016	Jan/2016	1,333.1	N, NE	No	Southward, parallel to the coast and Southwest-ward
03/02/2016 – 05/02/2016	Fev/2016a	729.0	N, NE	No	Southward and Southwest-ward
16/02/2016 – 18/02/2016	Fev/2016b	490.1	N, NE	No	Southward and Southeast-ward
19/04/2016 – 27/04/2016	Apr/2016	248.5	N, NE	No	Southwest-ward, Southward and parallel to the coast

a - Agência Nacional de Água – ANA (Colatina station): https://www.snirh.gov.br/ ; b - Bastos et al. (2017); c - NCEP Climate Forecast System Version 2 (CFSv2); d – Data from *Grupo de Estudos Climáticos, Universidade de São Paulo – USP*: http://www.grec.iag.usp.br/data/frentes-frias_BRA.php

19.3 Processing and preservation of samples

Chlorophyll-*a* pigments were concentrated by filtration on board through glass microfiber filter (Millipore AP400) of 25 mm diameter. The filters were kept frozen until the extraction procedure. Samples used to inorganic nutrients and metals determination in dissolved fraction were filtered through 0.45 *μ*m cellulose acetate membrane (Millipore®) using a vacuum pump system once back at the laboratory, immediately after collection. The filtrates for dissolved inorganic nutrients were frozen until analyses while the aliquots for dissolved metals (dMe) were acidified to reach pH < 2.0 by adding HNO_3 65% (previously distilled using sub-boiling procedure; boiling sub-distill acid mark Berghof BSB-939-IR model) and stored at 4°C until determination procedures. The 0.45 *μ*m membranes containing the particulate material retained by filtration procedure were frozen and followed by freeze drying/lyophilisation prior to particulate metals (pMe) analyses. Suspended Particulate Material (SPM) was determined by gravimetric method after filtration through dried and pre-weighted glass fibre membranes (porosity of 0.45 *μ*m).

19.4 Laboratory analysis

19.4.1 Chlorophyll-a and phaeophytin

Filters saturated with pigments were left overnight into centrifuge tubes filled with 10 mL of 90% acetone (HPLC grade acetone) on dark and refrigerated conditions to allow the extraction of the pigments (APHA, 2012). Extracts were centrifuged at 5,000 rpm for 10 minutes. The absorbance in the extract were determined spectrophotometrically (BEL Photonics UV-M51-Vis spectrophotometer) at 665 nm and 750 nm wavelength before and after acidification with 0.1 mL of 1 N HCl. Chlorophyll-a and phaeophytin (chlorophyll-*a* in senescence stage) concentrations were calculated by the equations from the monochromatic method (LORENZEN,1967). The detection limit (DL) was 0.01 $\mu g.L^{-1}$ for both analytes.

19.4.2 Quantitative and qualitative phytoplankton analyses

Quantitative phytoplankton analysis (phytoplankton density) was performed using Uthermöhl sedimentation chamber (UTHERMÖHL, 1958) and observation under inversed biological microscopy (Bell, NIB-100) with magnification of 400x or 600x after 24 hours of sedimentation. It was applied the random field counting procedure (UEHLINGER, 1964) and the fields were indicated from computerised program in order to analyse at least 100 organisms of the most abundant specie (LUND; KIPLING; LE CREN, 1958). The organisms were also classified in two groups according the size class as nano-phytoplankton (from 2 to 19 µm) and micro-phytoplankton (from 20 to 200 µm). The samples were analysed in replicate (n = 2) and the average was presented. The phytoplankton density was expressed as organisms per litres (orgs.L^{-1}) and calculated according to the Equation 1:

$$\boldsymbol{N = n \cdot \frac{A}{a} \cdot \frac{1}{V}} \qquad \text{(Equation 1)}$$

Where,

N = number of organisms in 1 mL of sample

n = number of organisms counted

a = area counted (mm^2)

A = chamber's total area (mm^2)

V = total settled volume (mL)

The optical microscopy with calibrated ocular micrometrer and a microscope adapter to capture images of microscope by USB camera was used for qualitative analysis. The organisms were drawn and identified based on morphological features according to specialized bibliography. The Shannon-Weaver diversity index was calculated from the phytoplankton density dada assuming a randomly infinite population from all of the organisms in the samples (SHANNON; WEAVER, 1949).

19.4.3 Metals

Iron (Fe), Vanadium (V), Manganese (Mn), Cobalt (Co), Copper (Cu) and Zinc (Zn) were analysed as in particulate (pMe, > 0.45 µm) as well as in dissolved fractions (dMe, < 0.45 µm). These metals were selected because of their role as micronutrients to the phytoplankton growth (O'KELLEY, 1974).

Particulate metals were extracted from the particulate material retained on the membrane using concentrated HNO_3 (65%, distilled, sub-boiling) followed by a step of heating in microwave (Mars X-press CEM) (EPA 3051A method; U.S. EPA, 2007). After the acid digestion, samples were filtered using quantitative membrane and diluted prior quantification by ICP-MS. For dMe analyses, the pH in the pre-acidified aliquots was adjusted using 1 M NaOH to a final pH around 7.0. The samples were then pre-concentrated by passing through a cationic resin column (Chelex®). The trace metal extracts were eluted from the resin column with HNO_3 2% solution. The compounds were quantified according to the EPA 6020A method for multi-element determination by Inductively Coupled Plasma – Mass Spectroscopy (ICP-MS, Agilent, 7500 cx) (U.S. EPA, 1998).

Fluctuations in the signals during the measurements were corrected by using a multi-element internal standard (Internal Standard Mix - Bi, Ge, In, Li, Sc, Tb and Y, Agilent Technologies). Multi-element standards (ICP multi-element standard solution XXI for MS, CentiPUR ® MERCK, Darmstadt - Germany) were used to carry the calibration curve (concentration range from 0 to 300 $\mu g.L^{-1}$). Particulate and dissolved metals concentrations were determined by the linear regression (y = ax+ b) plotted as a result of the calibration curve. Three analytical modes were used (no gas, Helium and Hydrogen) and the optimum one, as determined by the method of recovery from spiked samples (Supplemental Table S3), was used for each metal. All solutions were prepared with ultra-pure water processed using a PURELAB ultra (Model Ultra an MKZ, the brand Elgar).

The partitioning coefficient (K_d) of each metal was calculated from the ratio between particulate and dissolved metal concentrations, according to the Equation 2:

$K_d = \frac{[pMe]}{[dMe]}$ Equation 2

[pMe] = concentration of metal in particulate fraction (*μ*M)

[dMe] = concentration of metal in dissolved fraction (*μ*M)

19.4.4 Dissolved inorganic nutrients

Dissolved inorganic nutrients (phosphate, nitrite, nitrate, ammoniacal nitrogen and silicate) were analysed by colorimetric method according to Grasshoff *et al*. (1999) and absorbance was measured by UV/VIS spectrophotometer (MICRONAL AJX-6100PC). Certified standard solutions (Quemis high purity) were used to make the calibration curves (concentration range from 0.05 to 50 µM) for each nutrient and the concentrations were determined by the linear regression (y = ax + b). Nitrogen compounds are shown in the results as Dissolved Inorganic Nitrogen (DIN) (sum of nitrite, nitrate and ammoniacal nitrogen). Quantification and detection limit for each nutrient are described on Supplemental Table S4. The nutrients limitation for the phytoplankton growth was evaluated from the ratios of DIN against DSi (dissolved silicate) and DIN against DIP (dissolved inorganic phosphorous) and the scatter distribution was analyzed according to the Redfield ratios (16:1:16; N:P:Si) (REDFIELD, 1934).

19.5 Statistical analyses

In order to determinate the influence of metal enrichment on the phytoplankton composition, there was selected a control sample (FRD-06 Surface, Apr/2016) with the lower median values of pFe (4.0 µM), pV (0.01 µM), pCu (0.01 µM) and pZn (0.02 µM). These concentrations were applied as a background of the enrichment level in the water column (1pFe, 1pV, 1pV and 1pCu) and the values higher than those medians were represented as *n*pMe (*n* times higher than the background concentration for each particulate metal). The median of relative abundance (%) of each phytoplankton group was plotted in pie charts to compare the phytoplankton composition under different levels of enrichment with the control.

Water SPM, temperature (ºC), salinity, dissolved inorganic nutrients (phosphate, DIN and silicate), metals in particulate fraction (pFe, pV, pMn, pCu

and pZn), metals in dissolved fraction (dFe, dV, dMn, dCu and dZn), metals partitioning coefficient - Kd (KdFe, KdV, KdMn, KdCu and KdZn) and biological variables (Chlorophyll-*a*, phaeophytin, density of nano-phytoplankton and micro-phytoplankton as well as phytoplankton composition within their taxa density - diatoms, Haptophyta, Cyanophyceae, Chlorophyceae, Cryptophyceae and phytoflagellates) were examined for the relation to the Fundão dam disaster. The analyses were performed considering the variations from 5 the sampling periods (1 = Nov/2015, 2 = Jan/2016, 3 = Feb/2016a, 4 = Feb/2016b, and 5 = Apr/2016), from the spatial sector of sampling (sectors north, central and south) and from the depth (surface and bottom) using a three-way permutational multivariate analysis of variance (PERMANOVA) with 9999 permutations of residuals under a reduced model (CLARKE; GORLEY, 2006; ANDERSON; GORLEY; CLARKE, 2008). The abiotic parameters were previously normalized applying a Euclidean distance dissimilarity resemblance matrix, while the biotic data were square-root transformed using abundance data with the Bray-Curtis resemblance matrix under a reduced residuals model to give more weight to less abundant taxa in the analyses. The biological parameters of chlorophyll-*a*, phaeophytin, total phytoplankton density, nano-phytoplankton density, micro-phytoplankton density and phytoplankton diversity were also tested during the same sampling periods (except sampling 1 = Nov/2015 due to the lack of data), spatial variations and depth. If significant, a post-hoc pairwise test was performed on biotic and abiotic to assess significant differences in the global PERMANOVA (ANDERSON; GORLEY; CLARKE, 2008). The particulate and dissolved Co were not included in the analyses due the very low concentrations (< limit of quantification = 0.003 µM).

A second stage multidimensional scaling analysis (MDS) was applied through the sampling period using the squar-root abundance of all taxa from the Bray-Curtis similarity matrix. Phytoplankton assemblages were compared by MDS clustering significance using similarity percentage analysis (SIMPER; CLARKE; GORLEY, 2006).

Distance-based Linear Model (DistLM) routines were performed to assess the influence of water SPM, temperature, salinity, dissolved inorganic nutrients (phosphate, DIN and silicate), metals in particulate fraction (pFe, pV, pMn, pCu

and pZn) and metals in dissolved fraction (dFe, dV, dMn, dCu and dZn) to phytoplankton assemblage in the Easter Brazil continental shelf after the Fundão dam disaster. Phytoplankton assemblages were analysed using a step-wise procedure (selection criterion = adjusted AICc on the biological phytoplankton abundance and water related data; McARDLE; ANDERSON, 2001; CLARKE; GORLEY, 2006; ANDERSON; GORLEY; CLARKE, 2008). Because of the lack of biological data in Nov/2015 sampling (e.g. results of chlorophyll-*a*, phaeophytin, total phytoplankton density, nano-phytoplankton density and micro-phytoplankton density) as well as by their redundancy compared to the phytoplankton composition taxa density (diatoms, Haptophyta, Cyanophyceae, Chlorophyceae, Cryptophyceae and phytoflagellates) only the data from the taxa composition were included in the DistLM routines. Similarly, the partitioning coefficient - Kd (KdFe, KdV, KdMn, KdCu and KdZn) data were not used in DistLM analyses to avoid redundancy with particulate and dissolved metals fraction. Phytoplankton composition data was square-root transformed and analyzed using the Bray-Curtis similarity matrix, while water SPM, temperature, salinity, dissolved inorganic nutrients, metals as particulate fraction and metals as dissolved fraction were analysed using Euclidean distance. The BIO-ENV procedure was applied to relate the multivariate patterns of the phytoplankton assemblages with the water related data (Spearman's classification, p between the two matrices of similarity). All analyses were performed using PRIMER v 6.0 software with the PERMANOVA + add-on package (CLARKE; GORLEY, 2006; ANDERSON; GORLEY; CLARKE, 2008).

Pearson correlation test was employed to evaluate the correlation between some geochemical variables selected from the DistLM results (e.g. pFe, pV, pCu, pZn, dFe, DIN, silicate and salinity) and the density of each phytoplankton community group.

20 RESULTS

20.1 Physico-chemical parameters

Physico-chemical parameters (salinity, temperature and SPM) showed heterogeneous pattern of distribution with time and sampling location. Salinity

ranged from 25.4 (Nov/2015) to 37.2 (Apr/2016) (Table 10) and there were no significant differences with sampling period, depth and sectors (PERMANOVA, p > 0.115, Table 11). Temperature changed with sectors (PERMANOVA, df = 2, pseudo-F = 13.479, p = 0.002, Table 11) and these changes were mainly explained by the lower values registered at the south (Table 10; PERMANOVA, $p < 0.003$, Supplemental Table S4). Significant differences in the temporal distribution were only observed for SPM (PERMANOVA, df = 4, pseudo-F = 14.578, p = 0.001, Table 11), which reached the highest values in the acute phase of the disaster - Nov/2015 (from 0.9 to 300.0 $mg.L^{-1}$) (Table 10; PERMANOVA, $p < 0.002$, Supplemental Table S5), six days after the turbidity plume with mining tailings reached the coastal area.

Table 10. Physico-chemical parameters (temperature, salinity, and SPM) recorded in the continental shelf adjacent to the Doce River mouth in the three sampling sectors (South – S, Central – C, North – N).

Sampling	Statistics	PARAMETERS AND SECTORS								
		Salinity			Temperature (°C)			SPM ($mg.L^{-1}$)		
		S	C	N	S	C	N	S	C	N
Nov/2015	Min	36.2	25.4	36.2	21.1	18.7	19.6	0.9	4.0	0.9
	Max	36.6	37.1	37.0	25.0	26.2	28.1	147.0	300.0	215.0
	Average	36.5	35.7	36.6	23.3	23.4	23.0	35.6	73.8	43.6
	± DP	0.1	3.3	0.2	1.4	2.7	2.5	54.7	107.0	71.7
Jan/2016	Min	35.3	35.3	35.4	19.6	21.1	21	0.2	0.0	0.0
	Max	37	36.8	36.5	28.1	28.2	27.5	41.9	8.6	54.4
	Average	36.3	36.4	36.3	23	22.9	24.4	12.4	0.0	27.7
	± DP	0.4	0.5	0.4	2.5	2.5	3.3	15.7	3.3	23.2
Feb/2016a	Min	33.4	27.6	35.7	20.1	20.6	19.7	0.1	0.1	0.4
	Max	36.6	36.5	36.7	27.1	29.7	27.8	84.4	39.7	109.2
	Average	36.1	35.2	36.4	23.1	24.3	24.1	9.4	10.0	12.9
	± DP	0.8	2.9	0.2	2.6	3.4	3.2	18.7	13.7	26.4
Feb/2016b	Min	34.5	36.4	36.4	19.1	20.2	20.9	0.4	0.3	1.2
	Max	37.1	36.8	36.7	27.3	27.1	27.8	62.0	6.3	13.7
	Average	36.3	36.6	36.6	22.4	23.2	23.9	5.8	1.9	5.1
	± DP	0.6	0.2	0.1	2.1	2.8	2.9	15.1	2.3	4.7
Apr/2016	Min	34.9	36.4	36.4	20.5	20.7	20.3	2.2	3.2	2.8
	Max	37.1	37.2	37.1	27.1	27.6	28	14.4	13.4	13.8
	Average	36.5	36.8	36.8	22.6	24.2	24	6.6	6.5	8.2
	± DP	0.5	0.3	0.39	2.3	3.3	3.8	3.6	3.3	5.3

Table 11. PERMANOVA results of physical-chemical parameters across the sampling period (Sa), Sectors of sampling (Se) and Depth (De) at the continental shelf adjacent to the Doce River mouth. **Bold** Pseudo F-values indicate significant p values.

Source	df	SS	MS	Pseudo-F	P	Unique perms
SPM						
Sa	4	37.748	9.437	**14.578**	**0.001**	996
Se	2	1.3105	0.65526	1.012	0.368	999
De	1	6.8044	6.8044	**10.511**	**0.001**	999
SaxSe	8	12.3	1.5375	**2.375**	**0.036**	999
SaxDe	4	17.636	4.4089	**6.811**	**0.001**	998
SexDe	2	2.2656	1.1328	1.750	0.183	998
SaxSexDe	8	9.9471	1.2434	1.921	0.078	998
Res	126	81.565	0.64734			
Total	155	155				
Temperature (ºC)						
Sa	4	0.98889	0.24722	1.204	0.327	999
Se	2	5.5333	2.7667	**13.479**	**0.002**	996
De	1	92.393	92.393	**450.130**	**0.001**	996
SaxSe	8	0.98415	0.12302	0.599	0.793	999
SaxDe	4	5.0251	1.2563	**6.120**	**0.001**	997
SexDe	2	3.8995	1.9497	**9.499**	**0.001**	999
SaxSexDe	8	1.0771	0.13464	0.656	0.725	997
Res	126	25.863				
Total	155	155				
Salinity						
Sa	4	7.2772	1.8193	1.930	0.115	998
Se	2	2.0752	1.0376	1.101	0.320	999
De	1	1.834	1.834	1.946	0.199	998
SaxSe	8	6.0674	0.75842	0.805	0.573	998
SaxDe	4	6.0749	1.5187	1.611	0.195	999
SexDe	2	3.4281	1.7141	1.819	0.190	999
SaxSexDe	8	5.3133	0.66417	0.705	0.671	999
Res	126	118.75	0.94248			
Total	155	155				

20.2 Biological paratemers

Changes on chlorophyll-*a* and phaeophytin concentrations were controlled by the depth (PERMANOVA, $p < 0.003$, Table 12) with higher levels observed in bottom than surface waters (Supplemental Table S6). Phytoplankton community was markedly dominated by nano-phytoplankton group, mainly Cyanophyceae (1,662 ± 128 x 10^3 orgs.L^{-1}) and Chlorophyceae (1,209 ± 51 x 10^3 orgs.L^{-1}), representing respectively up to 84% and 49% of the phytoplankton community during the study (Figure 14). The densities of these groups remained high during all the samplings and they did not show either temporal or spatial (sector and depth) variability in the continental shelf (PERMANOVA, $p > 0.075$, Table 12).

Table 12. PERMANOVA results of pigments (chl-*a* and phaeophytin), phytoplankton density (total, nano-phytoplankton and micro-phytoplankton), phytoplankton diversity indices and pjytoplankton density of each phytoplankton group (diatoms, Haptophyta, Cyanophyceae, Chlorophyceae and phytoflagellates) across the sampling period (Sa), Sectors of sampling (Se) and Depth (De) at the continental shelf adjacent to the Doce River mouth. **Bold** PseudoF-values indicate significant *p* values.

Source	df	SS	MS	Pseudo-F	*p*	Unique perms
Chlorophyll-a						
Sa	3	0.86959	0.28986	1.459	0.239	999
Se	2	0.33158	0.16579	0.835	0.451	998
De	1	0.24826	0.24826	1.250	0.276	998
SaxSe	6	1.1049	0.18415	0.927	0.512	999
SaxDe	3	3.3678	1.1226	**5.651**	**0.003**	999
SexDe	2	0.86753	0.43376	2.184	0.102	998
SaxSexDe	6	1.2133	0.20222	1.018	0.426	999
Res	110	21.852	0.19865			
Total	133	31.461				
Phaeophytin						
Sa	3	0.24567	8.19E-02	0.553	0.659	998
Se	2	9.63E-02	4.81E-02	0.325	0.710	999
De	1	2.4826	2.4826	**16.756**	**0.001**	999
SaxSe	6	0.78214	0.13036	0.880	0.495	997
SaxDe	3	0.61604	0.20535	1.386	0.243	998
SexDe	2	1.90E-02	9.52E-03	0.064	0.940	998
SaxSexDe	6	0.96973	0.16162	1.091	0.360	997
Res	110	16.298	0.14816			
Total	133	22.269				
Total Density						
Sa	3	7.60E+05	2.53E+05	0.818	0.491	999
Se	2	3.88E+05	1.94E+05	0.626	0.546	999
De	1	1.13E+05	1.13E+05	0.365	0.545	999
SaxSe	6	9.57E+05	1.59E+05	0.515	0.775	999
SaxDe	3	5.38E+05	1.79E+05	0.579	0.619	998
SexDe	2	6.23E+05	3.11E+05	1.006	0.374	999
SaxSexDe	6	2.04E+06	3.41E+05	1.100	0.405	998
Res	110	3.41E+07	3.10E+05			
Total	133	4.05E+07				
Nano-phytoplankton						
Sa	3	2.21E+05	73527	0.237	0.888	998

Source	df	SS	MS	Pseudo-F	*p*	Unique perms
Phytoplankton assemblage						
Sa	4	17546	4386.6	**9.198**	**0.001**	996
Se	2	3168.8	1584.4	**3.322**	**0.006**	999
De	1	730.43	730.43	1.532	0.216	999
SaxSe	8	5790.7	723.84	**1.518**	**0.048**	997
SaxDe	4	2564.4	641.09	1.344	0.185	999
SexDe	2	976.91	488.46	1.024	0.426	998
SaxSexDe	8	3354.4	419.3	0.879	0.636	999
Res	126	60094	476.94			
Total	155	97873				
Diatoms density						
Sa	4	1.57E+06	3.92E+05	**17.435**	**0.001**	999
Se	2	80376	40188	1.788	0.163	998
De	1	93291	93291	**4.150**	**0.035**	997
SaxSe	8	3.39E+05	42432	**1.888**	**0.080**	998
SaxDe	4	1.37E+05	34255	1.524	0.194	999
SexDe	2	27285	13642	0.607	0.532	998
SaxSexDe	8	1.15E+05	14334	0.638	0.758	999
Res	126	2.83E+06	22480			
Total	155	5.87E+06				
Haptophyta density						
Sa	4	7828.1	1957	2.478	0.061	997
Se	2	1657	828.51	1.049	0.387	999
De	1	633.43	633.43	0.802	0.377	998
SaxSe	8	8767.1	1095.9	1.387	0.224	998
SaxDe	4	6459.9	1615	2.045	0.078	999
SexDe	2	1289.3	644.63	0.816	0.436	999
SaxSexDe	8	4603	575.38	0.728	0.660	999
Res	126	99529	789.91			
Total	155	1.41E+05				
Cyanophyceae density						
Sa	4	6.39E+05	1.60E+05	0.790	0.521	998

Se	2	4.87E+05	2.44E+05	0.784	0.466	998
De	1	68666	68666	0.221	0.650	998
SaxSe	6	1.34E+06	2.24E+05	0.719	0.639	999
SaxDe	3	6.60E+05	2.20E+05	0.708	0.533	999
SexDe	2	5.90E+05	2.95E+05	0.949	0.411	999
SaxSexDe	6	1.79E+06	2.98E+05	0.958	0.437	999
Res	110	3.42E+07	3.11E+05			
Total	133	4.03E+07				
Micro-phytoplankton						
Sa	3	1.07E+06	3.56E+05	**12.211**	**0.001**	999
Se	2	1.04E+05	52195	1.789	0.193	998
De	1	60541	60541	2.075	0.161	997
SaxSe	6	1.50E+05	24979	0.856	0.503	999
SaxDe	3	2.19E+05	72970	2.501	0.070	998
SexDe	2	18488	9243.9	0.317	0.713	999
SaxSexDe	6	1.50E+05	25034	0.858	0.502	999
Res	110	3.21E+06	29178			
Total	133	5.54E+06				
Diversity						
Sa	3	2.4484	0.81614	**13.169**	**0.001**	999
Se	2	0.63273	0.31636	**5.105**	**0.005**	999
De	1	3.03E-02	3.03E-02	0.489	0.506	996
SaxSe	6	1.0237	0.17061	**2.753**	**0.022**	999
SaxDe	3	0.69299	0.231	**3.727**	**0.016**	999
SexDe	2	5.95E-02	2.97E-02	0.480	0.632	999
SaxSexDe	6	0.23005	3.83E-02	0.619	0.714	996
Res	110	6.8171	6.20E-02			
Total	133	12.072				

Se	2	1.15E+06	5.74E+05	2.839	0.075	998
De	1	6215.9	6215.9	0.031	0.867	995
SaxSe	8	1.21E+06	1.51E+05	0.746	0.638	999
SaxDe	4	1.12E+06	2.80E+05	1.386	0.243	998
SexDe	2	7.51E+05	3.75E+05	1.858	0.161	999
SaxSexDe	8	1.02E+06	1.27E+05	0.628	0.719	996
Res	126	2.55E+07	2.02E+05			
Total	155	3.26E+07				
Chlorophyceae density						
Sa	4	5.05E+05	1.26E+05	1.104	0.342	998
Se	2	17303	8651.3	0.076	0.937	999
De	1	1.17E+05	1.17E+05	1.022	0.332	995
SaxSe	8	6.75E+05	84421	0.738	0.569	999
SaxDe	4	40063	10016	0.087	0.984	999
SexDe	2	55778	27889	0.244	0.790	999
SaxSexDe	8	4.91E+05	61358	0.536	0.748	998
Res	126	1.44E+07	1.14E+05			
Total	155	1.67E+07				
Cryptophyceae density						
Sa	4	1.46E+05	36597	**5.577**	**0.001**	999
Se	2	21408	10704	1.631	0.189	997
De	1	471.15	471.15	0.072	0.766	993
SaxSe	8	1.23E+05	15435	**2.352**	**0.034**	999
SaxDe	4	14530	3632.6	0.554	0.663	999
SexDe	2	12856	6427.8	0.979	0.371	998
SaxSexDe	8	64851	8106.3	1.235	0.294	998
Res	126	8.27E+05	6562.6			
Total	155	1.19E+06				
phytoflagellates density						
Sa	4	1190.2	297.56	0.708	0.526	998
Se	2	809.89	404.95	0.964	0.425	999
De	1	318.55	318.55	0.758	0.478	996
SaxSe	8	2527.2	315.9	0.752	0.504	999
SaxDe	4	1389.8	347.44	0.827	0.445	998
SexDe	2	693.8	346.9	0.826	0.469	999
SaxSexDe	8	2075.5	259.44	0.618	0.634	997
Res	126	52926	420.05			
Total	155	64440				

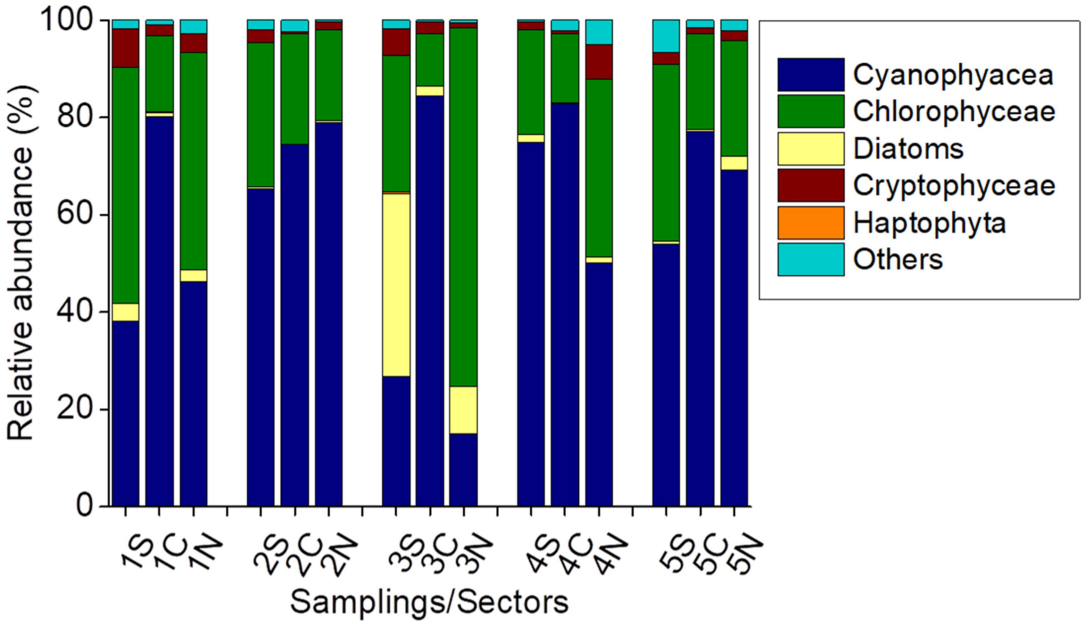

Figure 14. Relative abundance (%) of each phytoplankton group at the continental shelf adjacent to the Doce River mouth. 1: Nov/2015; 2: Jan/2016; 3: Fev/2016a; 4: Fev/2016b; 5: Abr/2016. S, C, N corresponds to the sectors South, Central and North, respectively. Phytoflagellates was grouped in others due to the very low % compared to the other groups.

Phytoplankton assemblage changed across the sampling period that follows the Fundão dam disaster (PERMANOVA, df = 4, Pseudo-F = 9.198, *p* = 0.001, Table 12; Supplemental Table S5). In general, these changes matched with the increase in micro-phytoplankton density (PERMANOVA, df = 3, Pseudo-F = 12.211, p = 0.001, Table 12), represented by the increase of diatoms and Cryptophyceae densities (fifteen and two-fold higher than their densities in the previous samplings, respectively) during the sampling 3 – Feb/2016a (Figure 15b and Figure 15d; PERMANOVA, p = 0.034, Supplemental Table S5; Supplemental Table S6), following the flooding event by the end of January (Table 9). These differences on phytoplankton community were also in agreement to the increase of diversity indices at the same sampling period (PERMANOVA, df = 6, Pseudo-F = 2.753, *p* = 0.022, Table 12; Supplemental Table S5; Supplemental Table S6).

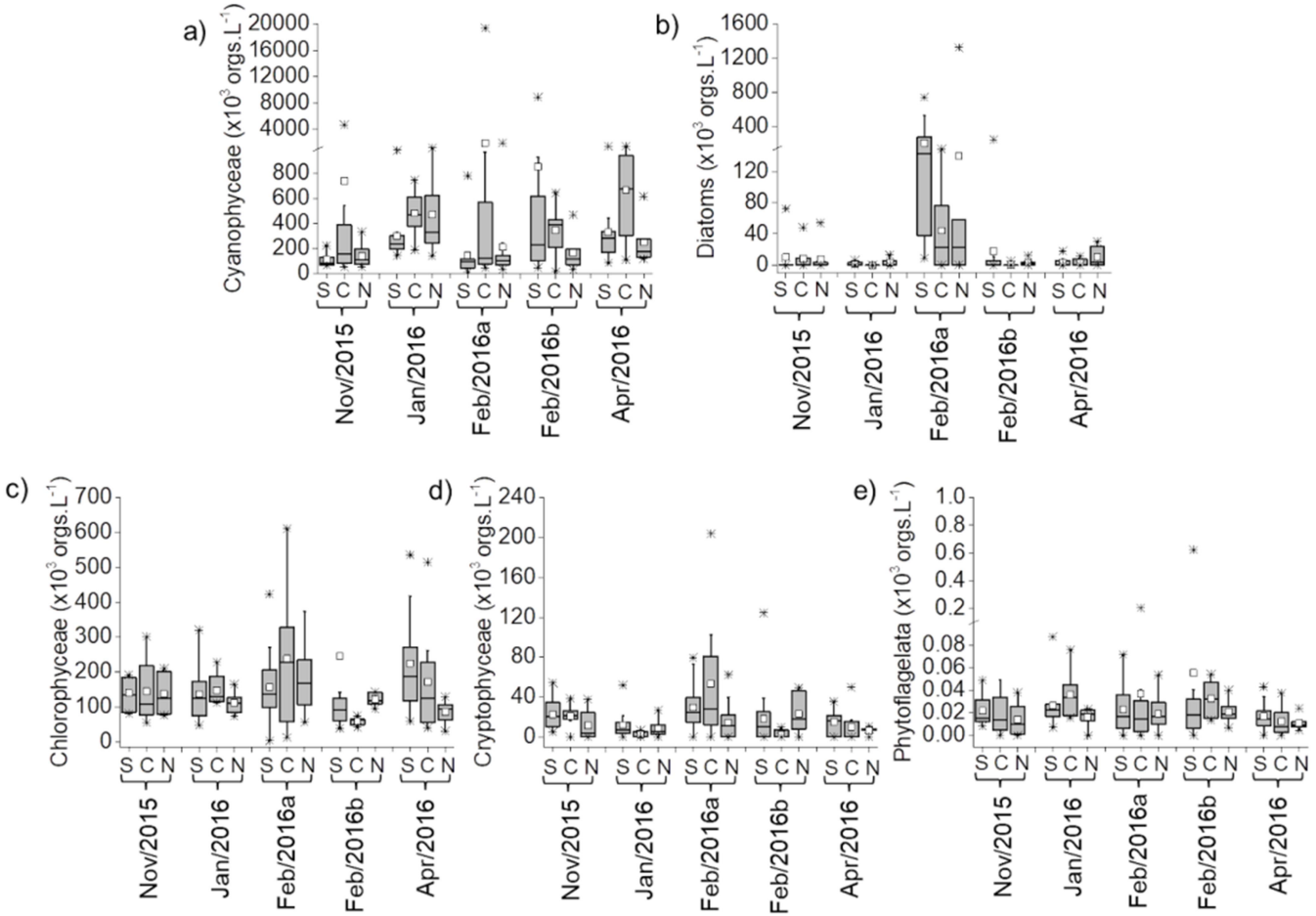

Figure 15. Temporal and spatial distribution of phytoplankton density for each phytoplankton group registered at the continental shelf adjacent to the Doce River mouth. S, C, N corresponds to the South, Central and North sampling sectors, respectively. Haptophyta is not shown due to the very low density and absence of significant changes during samplings.

20.3 Geochemical parameters (metals and dissolved inorganic nutrients)

In general, the geochemical parameters acting as macro (phosphate, DIN and silicate) and micronutrients (Fe, V, Mn, Co, Cu and Zn) to the phytoplankton growth changed during the sampling period after the disaster (PERMANOVA, $p < 0.029$, Table 13).

For metals in particulate fraction, the temporal variation was mainly related to the higher concentrations of pFe (381.3 ± 634.9 μM), pMn (14.7 ± 15.0 μM) and pCu (0.15 ± 0.06 μM) in the acute phase of the impact (Nov/2015) (Fig. 15a, 15c, 15e; Supplemental Table S7; PERMANOVA, $p < 0.014$, Supplemental Table S5). However, concentrations of pV (0.09 ± 0.11 μM) and pZn (0.32 ± 0.28 μM) increased in Fev/2016a (Fig. 15b, 15f; Supplemental Table S7; PERMANOVA, $p < 0.05$, Supplemental Table S5), in agreement with the temporal increase of diatoms and Cryptophyceae densities.

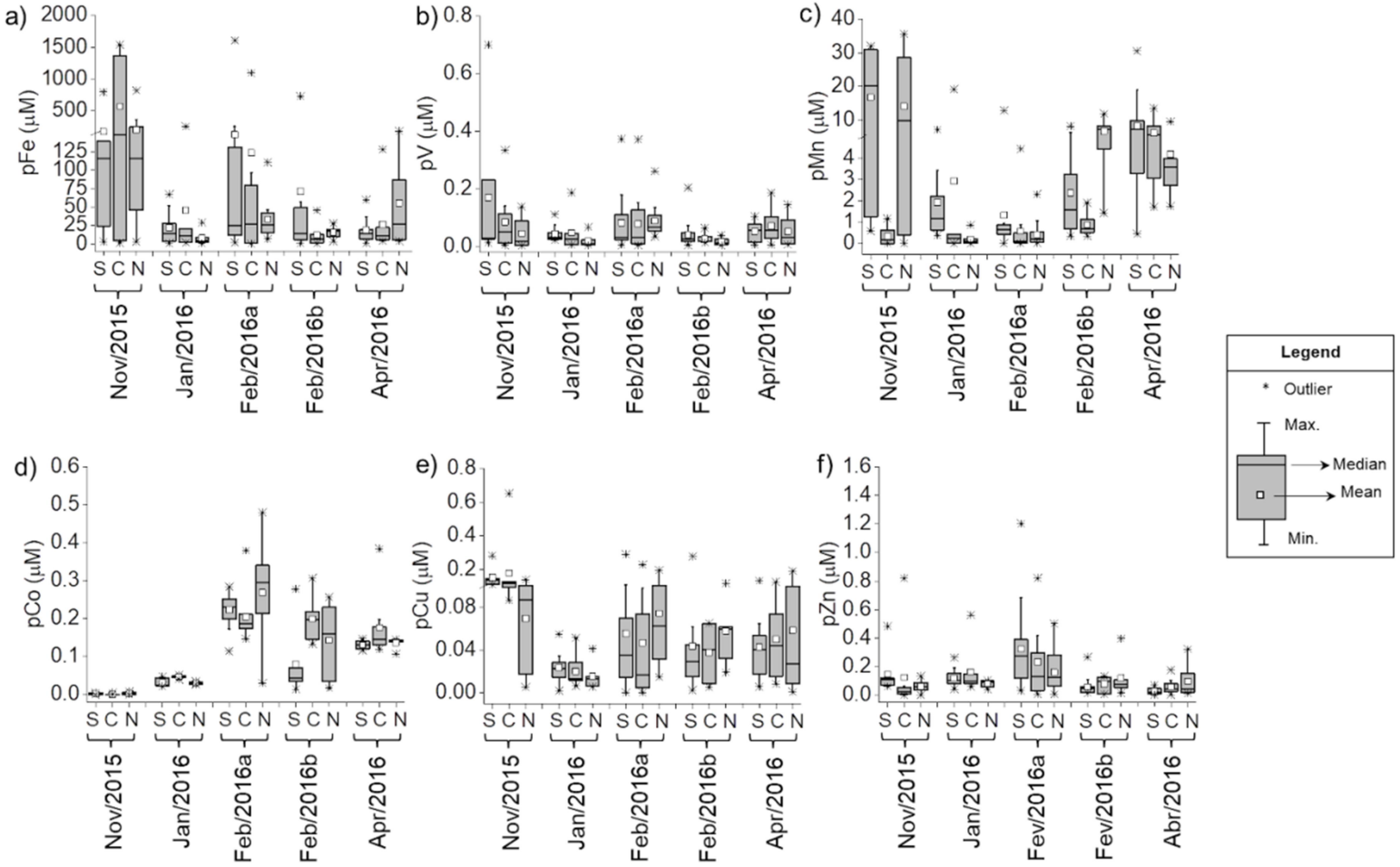

Figure 16. Temporal and spatial distribution of particulate metals (> 0.45 µm) in the continental shelf adjacent to the Doce River mouth. S, C, N corresponds to the South, Central and North sampling sectors, respectively.

Temporal changes of dissolved metals were mostly explained by the higher levels of dFe (1.38 ± 1.08 µM), dV (0.15 ± 0.06 µM) and dCu (0.30 ± 0.22 µM) in Nov/2015 (Fig. 16a, 16b, 16e; Supplemental Table S7; PERMANOVA, $p < 0.029$, Supplemental Table S5). Considering the importance of each element, Fe presented higher concentrations than the other metals evaluated (at least one order of magnitude) for both particulate and dissolved fraction, ranging from 0.28 µM (Feb/2016a) to 1,602.4 µM (Feb/2016a) for pFe (Figure 15a and 16a; Supplemental Table S7) whereas dFe reached a maximum of 4.0 µM in Nov/2015 (Figure 16a; Supplemental Table S7). In terms of metal partitioning, Fe and Mn partition coefficients (K_d) were up to the order of 10^5 and 10^4, respectively, showing high affinity to the particulate phase, while Zn and Cu occurred predominantly as dissolved phase. However, an overall increase of K_d and then a predominance of particulate metals was observed in Feb/2016a which resulted on changes of Cu and Zn partitioning behaviour from dissolved to particulate phase (PERMANOVA, $p < 0.017$, Table 14; Supplemental Table S5 and S8).

Higher levels of Phosphate (0.38 ± 0.35 µM) and DIN (51.2 ± 12.3 µM) occurred during the sampling 5 (Apr/2016) (PERMANOVA, $p < 0.039$, Supplemental Tables S5 and S9), whereas no significant changes on DSi concentrations were observed either with sampling, sectors or depth. In general, the continental shelf adjacent to the Doce River mouth showed limitation of PID and DSi during the samplings. In Feb/2016a, DIN: DSi and DIN: DIP ratio reveals not only limitation for DIP and DSi but also DIN limitation (Figure 17d). In spite of the DSi limitation during the samplings, increase of its concentration was observed in Feb/2016a (high Doce River discharge), especially in the South sector (Supplemental Table S9) in agreement with remarkable diatoms growth in those sampling and sector (see Figure 15).

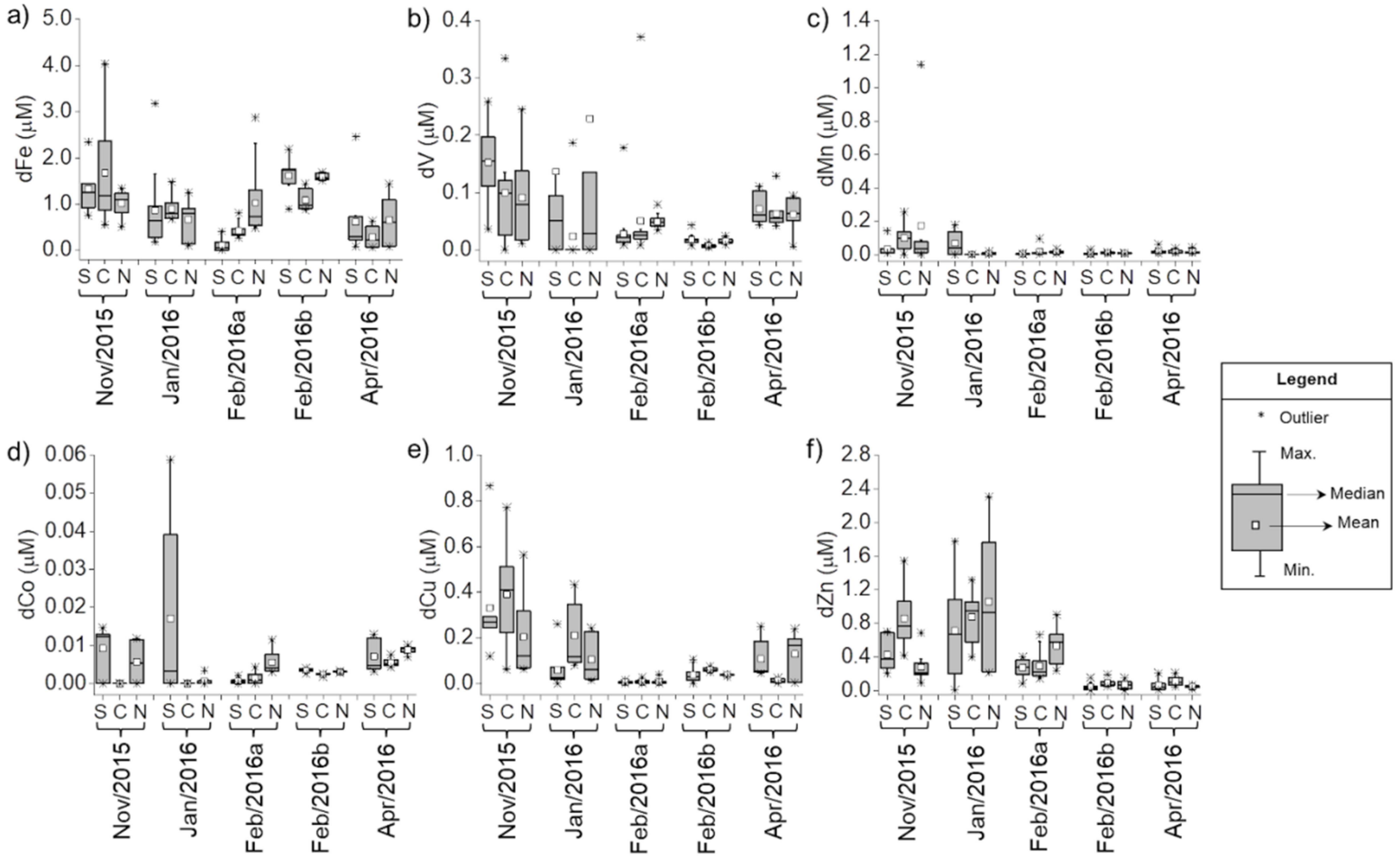

Figure 17. Temporal and spatial distribution of dissolved metals (< 0.45 µm) in the continental shelf adjacent to the Doce River mouth. S, C, N corresponds to the South, Central and North sampling sectors, respectively.

Table 13. PERMANOVA results of metals in particulate (pMe, > 0.45 µm) and dissolved (dMe, < 0.45 µm) fractions and dissolved inorganic nutrients (Phosphate, DIN and Silicate) across the sampling period (Sa), Sectors of sampling (Se) and Depth (De) at the continental shelf adjacent to the Doce River mouth. Bold PseudoF-values indicate significant p values.

Source	df	SS	MS	Pseudo-F	P	Unique perms
pFe						
Sa	4	24.897	6.2242	**7.797**	**0.001**	999
Se	2	3.4921	1.746	2.187	0.111	998
De	1	3.7247	3.7247	4.666	0.038	996
SaxSe	8	12.861	1.6076	2.014	0.051	999
SaxDe	4	10.111	2.5278	**3.167**	**0.018**	999
SexDe	2	5.49E-02	2.75E-02	0.034	0.959	999
SaxSexDe	8	6.9457	0.86821	1.088	0.358	999
Res	126	100.58	0.79828			
Total	155	155				
pV						
Sa	4	13.985	3.4962	**3.839**	**0.008**	999
Se	2	2.5559	1.278	1.403	0.236	998
De	1	4.0456	4.0456	**4.442**	**0.033**	998
SaxSe	8	8.769	1.0961	1.204	0.307	996
SaxDe	4	3.4899	0.87247	0.958	0.465	999
SexDe	2	4.4769	2.2384	2.458	0.115	998
SaxSexDe	8	7.8465	0.98081	1.077	0.401	998
Res	126	114.76	0.91081			
Total	155	155				
pMn						
Sa	4	34.205	8.5511	**12.541**	**0.001**	998
Se	2	8.1388	4.0694	**5.968**	**0.004**	999
De	1	0.15206	0.15206	0.223	0.661	995
SaxSe	8	22.138	2.7673	**4.059**	**0.003**	999
SaxDe	4	1.1997	0.29991	0.440	0.780	998
SexDe	2	1.3256	0.66281	0.972	0.377	999
SaxSexDe	8	4.2577	0.53222	0.781	0.609	997
Res	126	85.912	0.68184			
Total	155	155				
pCu						
Sa	4	26.349	6.5872	**8.253**	**0.001**	999
Se	2	0.82751	0.41375	0.518	0.591	998

Source	df	SS	MS	Pseudo-F	p	Unique perms
dFe						
Sa	4	42.067	10.517	**17.449**	**0.001**	996
Se	2	0.38862	0.19431	0.322	0.710	999
De	1	1.5043	1.5043	2.496	0.118	996
SaxSe	8	21.869	2.7336	**4.536**	**0.002**	999
SaxDe	4	0.64368	0.16092	0.267	0.898	999
SexDe	2	0.24847	0.12423	0.206	0.809	999
SaxSexDe	8	1.9382	0.24227	0.402	0.905	998
Res	126	75.942	0.60272			
Total	155	155				
dV						
Sa	4	12.598	3.1495	**3.461**	**0.029**	999
Se	2	4.1254	2.0627	2.267	0.109	999
De	1	1.2451	1.2451	1.368	0.250	999
SaxSe	8	6.9568	0.8696	0.956	0.476	997
SaxDe	4	9.3853	2.3463	2.579	0.046	999
SexDe	2	1.6968	0.84838	0.932	0.397	998
SaxSexDe	8	5.39	0.67375	0.740	0.637	999
Res	126	114.66	0.90996			
Total	155	155				
dMn						
Sa	4	14.459	3.6147	**4.024**	**0.009**	998
Se	2	0.52107	0.26053	0.290	0.756	999
De	1	0.20115	0.20115	0.224	0.659	996
SaxSe	8	12.038	1.5048	1.675	0.183	998
SaxDe	4	1.3487	0.33719	0.375	0.792	999
SexDe	2	2.1606	1.0803	1.203	0.333	998
SaxSexDe	8	7.5979	0.94973	1.057	0.371	997
Res	126	113.2	0.89838			
Total	155	155				
dCu						
Sa	4	73.82	18.455	**38.114**	**0.001**	996
Se	2	1.9981	0.99906	2.063	0.146	998

De	1	3.9303	3.9303	**4.924**	**0.025**	996
SaxSe	8	12.313	1.5391	1.928	0.073	999
SaxDe	4	2.5433	0.63582	0.797	0.545	998
SexDe	2	2.2113	1.1057	1.385	0.252	999
SaxSexDe	8	11.057	1.3822	1.732	0.115	999
Res	126	100.57	0.79818			
Total	155	155				
pZn						
Sa	4	20.596	5.149	**6.069**	**0.002**	999
Se	2	0.8736	0.4368	0.515	0.618	998
De	1	0.43486	0.43486	0.513	0.500	999
SaxSe	8	7.8661	0.98326	1.159	0.309	999
SaxDe	4	5.7263	1.4316	1.687	0.174	999
SexDe	2	1.7065	0.85324	1.006	0.384	997
SaxSexDe	8	2.8833	0.36041	0.425	0.902	998
Res	126	106.9	0.84841			
Total	155	155				
Phosphate						
Sa	4	48.479	12.12	**19.352**	**0.001**	999
Se	2	7.6288	3.8144	**6.091**	**0.005**	999
De	1	1.171	1.171	1.870	0.154	995
SaxSe	8	14.795	1.8494	**2.953**	**0.017**	999
SaxDe	4	2.3499	0.58747	0.938	0.457	999
SexDe	2	3.1312	1.5656	2.500	0.094	998
SaxSexDe	8	10.151	1.2689	2.026	0.052	999
Res	126	78.91	0.62627			
Total	155	155				
DIN						
Sa	4	48.616	12.154	**23.263**	**0.001**	999
Se	2	12.514	6.2568	**11.976**	**0.001**	999
De	1	0.42969	0.42969	0.822	0.382	996
SaxSe	8	18.082	2.2602	**4.326**	**0.001**	999
SaxDe	4	4.4977	1.1244	2.152	0.098	998
SexDe	2	3.279	1.6395	3.138	0.062	999
SaxSexDe	8	9.1366	1.1421	**2.186**	**0.046**	997
Res	126	65.83	0.52246			
Total	155	155				
Silicate						

De	1	8.49E-03	8.49E-03	0.018	0.902	995
SaxSe	8	12.514	1.5643	**3.231**	**0.006**	998
SaxDe	4	0.17365	4.34E-02	0.090	0.984	999
SexDe	2	1.0485	0.52424	1.083	0.331	998
SaxSexDe	8	2.6166	0.32707	0.675	0.719	999
Res	126	61.01	0.48421			
Total	155	155				
dZn						
Sa	4	65.277	16.319	**31.612**	**0.001**	999
Se	2	3.2453	1.6226	**3.143**	**0.045**	998
De	1	2.1629	2.1629	**4.190**	**0.046**	996
SaxSe	8	11.918	1.4898	**2.886**	**0.010**	998
SaxDe	4	2.1971	0.54927	1.064	0.363	999
SexDe	2	0.65598	0.32799	0.635	0.535	999
SaxSexDe	8	1.6698	0.20872	0.404	0.910	998
Res	126	65.046	0.51624			
Total	155	155				
KdZn						
Sa	4	12.181	3.0451	**3.149**	**0.017**	999
Se	2	3.0564	1.5282	1.580	0.224	998
De	1	1.1455	1.1455	1.185	0.294	999
SaxSe	8	5.3487	0.66859	0.691	0.654	997
SaxDe	4	1.6393	0.40982	0.424	0.789	998
SexDe	2	0.40866	0.20433	0.211	0.794	999
SaxSexDe	8	2.0454	0.25568	0.264	0.968	998
Res	126	121.85	0.96704			
Total	155	155				
KdV						
Sa	4	9.9	2.475	2.492	0.079	998
Se	2	2.2137	1.1069	1.115	0.313	999
De	1	4.13E-02	4.13E-02	0.042	0.836	998
SaxSe	7	4.2918	0.61311	0.617	0.709	998
SaxDe	4	2.1077	0.52691	0.531	0.662	998
SexDe	2	0.4443	0.22215	0.224	0.787	998
SaxSexDe	7	6.5878	0.94112	0.948	0.434	999
Res	114	113.2	0.99302			
Total	141	141				
KdMn						

Sa	4	3.9927	0.99818	1.045	0.377	999
Se	2	2.6819	1.341	1.404	0.246	998
De	1	5.6939	5.6939	**5.960**	**0.015**	996
SaxSe	8	4.138	0.51725	0.541	0.819	999
SaxDe	4	4.3866	1.0966	1.148	0.354	998
SexDe	2	2.1774	1.0887	1.140	0.317	999
SaxSexDe	8	5.6621	0.70776	0.741	0.628	999
Res	126	120.38	0.95543			
Total	155	155				

KdFe

Sa	4	3.1213	0.78032	0.758	0.476	998
Se	2	1.1545	0.57723	0.561	0.548	997
De	1	0.28048	0.28048	0.273	0.707	998
SaxSe	8	7.003	0.87537	0.851	0.403	999
SaxDe	4	1.8852	0.47131	0.458	0.668	999
SexDe	2	0.68822	0.34411	0.334	0.764	999
SaxSexDe	8	4.0216	0.5027	0.488	0.721	999
Res	126	129.67	1.0291			
Total	155	155				

Sa	4	9.3524	2.3381	2.516	0.066	999
Se	2	5.8238	2.9119	3.133	0.070	997
De	1	0.62332	0.62332	0.671	0.357	995
SaxSe	7	5.714	0.81629	0.878	0.442	999
SaxDe	4	1.074	0.2685	0.289	0.816	998
SexDe	2	2.0159	1.0079	1.084	0.304	997
SaxSexDe	7	3.3194	0.47419	0.510	0.688	998
Res	106	98.525	0.92948			
Total	133	133				

KdCu

Sa	4	24.052	6.013	**6.478**	**0.003**	999
Se	2	0.48912	0.24456	0.263	0.775	999
De	1	0.74599	0.74599	0.804	0.371	997
SaxSe	8	4.0541	0.50676	0.546	0.815	999
SaxDe	4	4.4087	1.1022	1.187	0.306	998
SexDe	2	0.17066	8.53E-02	0.092	0.913	998
SaxSexDe	8	0.94736	0.11842	0.128	0.993	999
Res	116	107.68	0.92826			
Total	145	145				

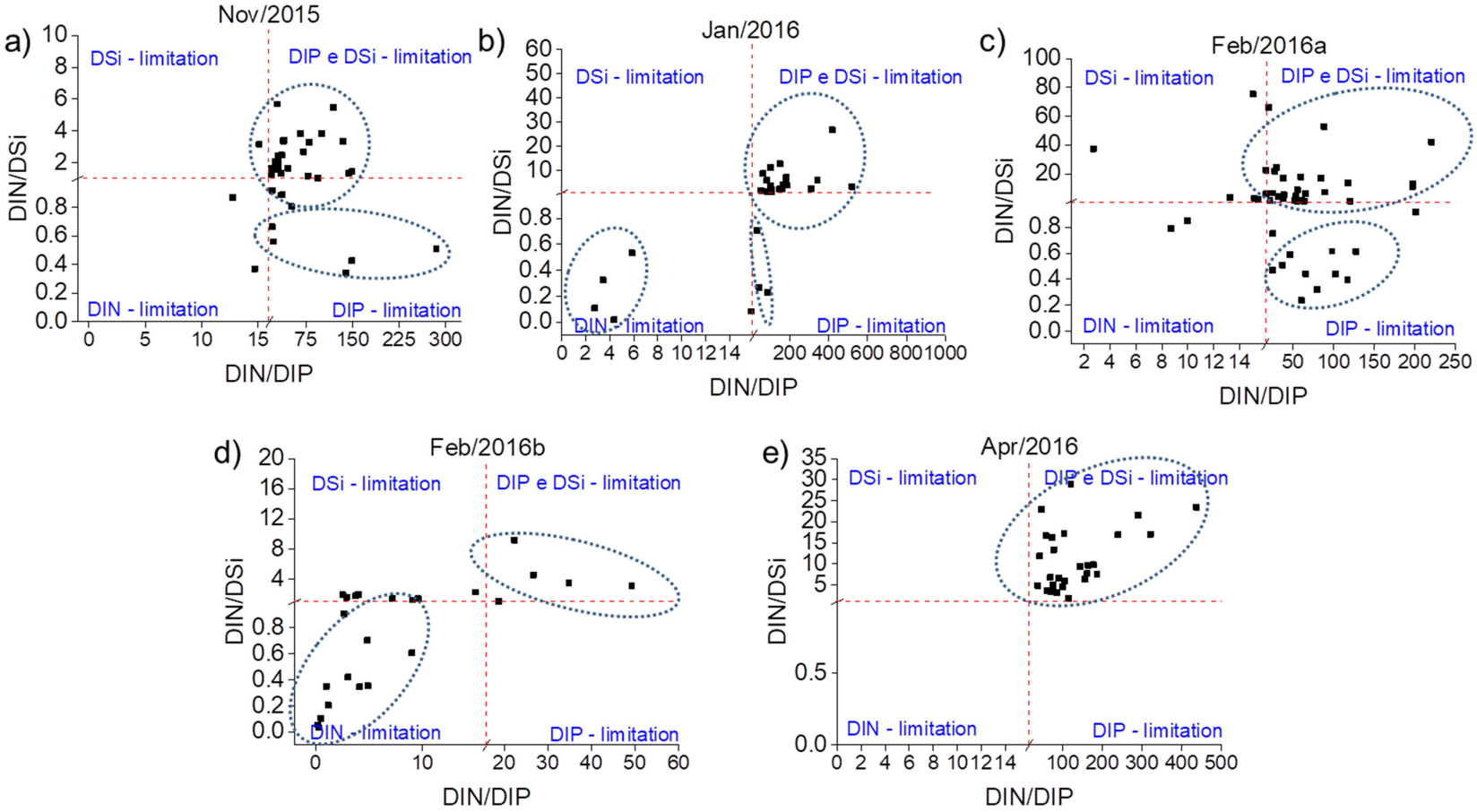

Figure 18. Scatterplot diagrams of DIN: DSi and DIN: DIP ratio at the continental shelf adjacent to the Doce River mouth along the samplings after the Fundão dam disaster. Dotted red lines indicate the reference values from Redfield ratio and dotted blue circles highlight the limitation conditions.

20.4 Factors changing the phytoplankton community

The changes showed by the multivariate analyses in the phytoplankton community during the short to middle-term monitoring of Fundão dam disaster were explained by pV, pCu, pZn and salinity (8.7%), with lesser contribution from other important water variables (e.g. pFe, dFe and Silicate; all water variables explained 18.9% of phytoplankton total variation). The increase of pV, pZn and pCu in Feb/2016a influenced within higher intensity the changes of phytoplankton community through the sampling period (BEST R = 0.226, p = 0.001; Table 15, Table 16; Fig. 18 Supplemental Table. S5).

Table 14. Distance-based linear model (DistLM) of Bray-Curtis similarity in phytoplankton community, physico-chemical parameters (salinity, temperature and SPM), macronutrients (phosphate, NID and silicate) and metals/micronutrients (Fe, V, Mn, Co, Cu, Zn in particulate and dissolved fractions) between samplings (Nov/2015, Jan/2016. Feb/2016a, Feb/2016b and Apr/2016) and sectors of sampling (South, Central and North) in the continental shelf adjacent to the Doce River mouth. Bold F-values indicate significant p values.

Paramaters	SS(trace)	Pseudo-F	P	Prop.
pFe	2511.4	**4.0557**	**0.013**	2.57E-02
pV	3274.9	**5.3313**	**0.001**	3.35E-02
pMn	428.93	0.67788	0.604	4.38E-03
pCu	1618.2	**2.5889**	**0.050**	1.65E-02
pZn	4982.2	**8.2597**	**0.001**	5.09E-02
dFe	2170.1	**3.492**	**0.014**	2.22E-02
dV	622.53	0.98579	0.389	6.36E-03
dMn	542.91	0.85901	0.389	5.55E-03
dCu	1002.8	1.5942	0.161	1.02E-02
dZn	372.9	0.58899	0.620	3.81E-03
Phosphate	816.85	1.2961	0.251	8.35E-03
DIN	3162.6	**5.1424**	**0.006**	3.23E-02
DSi	1699	**2.7205**	**0.035**	1.74E-02
SPM	758.57	1.2029	0.283	7.75E-03
Temperature	862.17	1.3687	0.241	8.81E-03
Salinity	1806.7	**2.8962**	**0.040**	1.85E-02

Table 15. BEST correlations between phytoplankton community, physico-chemical parameters (salinity, temperature and SPM), macronutrients (phosphate, NID and silicate) and metals/micronutrients (Fe, V, Mn, Co, Cu, Zn in particulate and dissolved fractions) in the continental shelf adjacent to the Doce River mouth. P_w = weighted Spearman coefficients.

Number of parameters	P_w	Parameters
4	0.226	pV; pCu; pZn; Salinity
3	0.222	pCu; pZn; Salinity
3	0.220	pV; pZn; Salinity
5	0.219	pV; pCu; pZn; DSi; Salinity
4	0.218	pCu; pZn; DSi; Salinity

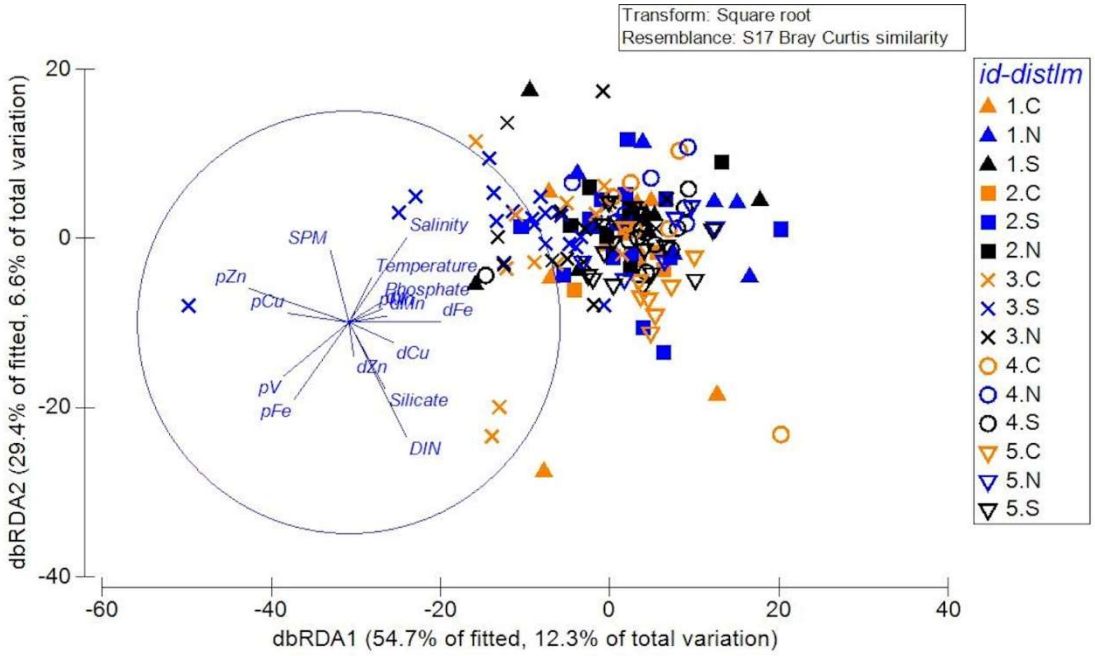

Figure 19. DistLM distance-based redundancy analysis (dbRDA) plot based on physico-chemical parameters (salinity, temperature and SPM), macronutrients (phosphate, NID and silicate), particulate metals (pFe, pV, pMn, pCo, pCu, pZn) and dissolved metals (dFe, dV, dMn, dCo, dCu, dZn) that best explained the phytoplankton community in the continental shelf adjacent to the Doce River mouth.

Considering the phytoplankton taxa that showed changes with sampling period, diatoms and pZn were weakly correlated (Pearson, r = 0.23, p = 0.006; Table 17) and inversely correlated with dFe (Pearson, r = -0.21, p = 0.011; Table 17), while Cryptophyceae showed a positive correlation with all of the metals in particulate fraction included by multivariate analyses: pFe (Pearson, r = 0.42, p = 0.004; Table 17), pV (Pearson, r = 0.28, p = 0.0008; Table 17), pCu (Pearson, r = 0.20, p = 0.019; Table 17) and pZn (Pearson, r = 0.18, p = 0.039; Table 17) and also with silicate (Pearson, r = -0.27, p = 0.0014; Table 17).

Similarly, the group phytoflagellates also presented positive correlation with those particulate metals: pFe (Pearson, r = 0.40, p = 0.01; Table 17), pV (Pearson, r = 0.23, p = 0.007; Table 17), pCu (Pearson, r = 0.36, p = 0.00001; Table 17) and pZn (Pearson, r = 0.18, p = 0.039; Table 17). The most frequent group Cyanophyceae was correlated positively with pFe (Pearson, r = 0.49, p = 0.00001; Table 17), pCu (Pearson, r = 0.18, p = 0.030; Table 17), pZn (Pearson, r = 0.28, p = 0.001; Table 17) and silicate (Pearson, r = 0.50, p = 0.000003; Table 17).

Table 16. Pearson correlation analyses of particulate metals (pFe, pV, pCu, pZn), dFe, DIN, silicate and salinity with phytoplankton groups densities (diatoms, Cyanophyceae, Chlorophyceae, Cryptophyceae and phytoflagellates). *r* Pearson's correlation coefficient and p-value (between brackets) are showed. Significant correlations ($p < 0.05$) are indicated as bold letters. Geochemical and physico-chemical parameters used in this analyse were selected from the DistLM results. Haptophyta densities were not included due to the very low frequency during the samplings.

	Diatoms	Cyanophyceae	Chlorophyceae	Cryptophyceae	Phytoflagellates
pFe	0.06 (0.50)	**0.49** **(0.00001)**	0.03 (0.73)	**0.42** **(0.004)**	**0.40** **(0.01)**
pV	0.14 (0.10)	0.33 (0.78)	0.03 (0.72)	**0.28** **(0.0008)**	**0.23** **(0.007)**
pCu	0.14 (0.11)	**0.18** **(0.030)**	0.04 (0.65)	**0.20** **(0.019)**	**0.36** **(0.00001)**
pZn	**0.23** **(0.006)**	**0.28** **(0.001)**	-0.03 (0.75)	**0.22** **(0.010)**	**0.18** **(0.039)**
dFe	**-0.21** **(0.011)**	0.02 (0.84)	-0.02 (0.78)	-0.11 (0.20)	0.16 (0.06)
DIN	-0.08 (0.32)	0.07 (0.42)	0.06 (0.46)	-0.08 (0.34)	-0.07 (0.40)
DSi	-0.09 (0.30)	**0.50** **(0.000003)**	-0.03 (0.77)	**0.27** **(0.0014)**	0.14 (0.11)
Salinity	-0.06 (0.47)	0.00 (0.96)	0.00 (0.96)	-0.07 (0.38)	0.01 (0.90)

The control sample selected to represent the enrichment background for particulate metals was predomitanly composed by Cyanophyceae (49%) and Chlorophyceae (44%) with minor occurrence of diatoms and Cryptophyceae. The higher enrichment with pFe and pCu (19 and 11-fold higher than the background, respectively) had not changed the main composition in terms of

the predominant groups, but allowed the growth of Cryptophyceae organisms. Interestingly, the frequency of the main taxa was nearly the same when an equal level of Fe enrichemnt was observed in Jan/2016, Feb/2016b and Apr/2016 (3pFe; Cyanopheceae 66%; Chlorophyceae 29 – 31%; Figure 19), indicating that this metal is the main factor controlling Cyanophyceae and Chlorophyceae growth. Changes in the phytoplankton composition by the growth of diatoms and Cryptophyceae in Fev/2016a occurred in conditions of high enrichment of pFe (7pFe), pV (5pV) and pZn (8pZn), while pCu enrichement decreased compared to Nov/2015 (Figure 19).

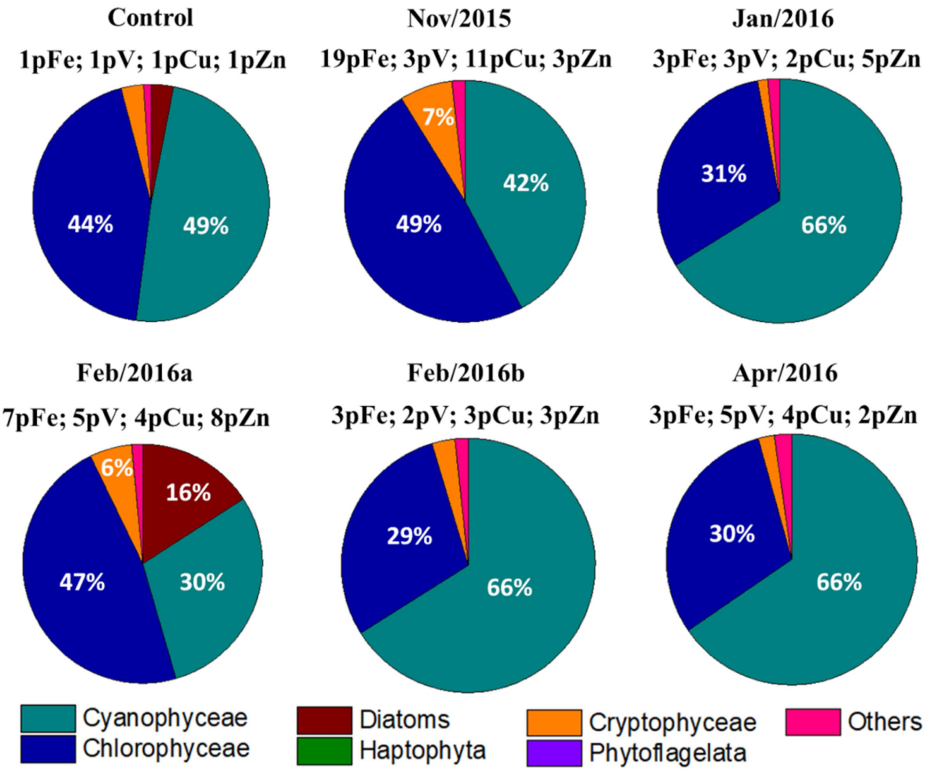

Figure 20. Median of relative abundance (%) of each phytoplankton group at the continental shelf adjacent to the Doce River mouth following the levels of particulate metals enrichment in the water column. Control sample was FRD-6 Surface (Apr/2016) and the background pMe concentrations were: 1pFe = 4.0 µM; 1pV = 0.01 µM; 1pCu = 0.01 µM; 1pZn = 0.02 µM.

21 DISCUSSION

21.1 Metals distribution and bioavailability

This study reveals that the phytoplankton community in the continental shelf adjacent to the Doce River mouth has been controlled by particulate metals (mainly pV, pCu, pZn and pFe secondarily) after the mining tailings reached the coastal area. Changes in particulate metal concentrations were remarkable in the acute phase of the disaster (Nov/2015, for pFe and pCu) and after a flooding event by the end of Jan/2016 (Fev/2016a, mainly for pV and pZn) indicating the remobilization of the material accumulated along the river bank and/or resuspension through wave action along the continental shelf (see OLIVEIRA; ALBINO; VENANCIO, 2015).

The tailings from the Fundão dam spillage are important source of SPM and metals to the downstream area after the disaster (GOMES *et al*., 2017; HATJE *et al*., 2017). Indeed, the higher concentrations of pMe in Nov/2015 are related to the higher SPM levels registered in the same sampling. From the fluvial and estuarine input, the preference of metals occurring as particulate form (high K_d), especially for Fe, is explained by the precipitation of dissolved fraction from the water column due to the neutralization of metal-organic matter complex by cations in the estuary. This process even favours the flocculation of colloidal organic matter and then the removal rates of associated dissolved metal during the estuarine transport (BOYLE; EDMOND; SHOLKOVITZ, 1977; SHOLKOVITZ; BOYLE; PRICE, 1978). The decrease of metal in dissolved phase is also related to the presence of stable mineralogical lattice (KUMA; NISHIOKA; MATSUNAGA, 1996), such as the crystalline oxides which are widespread in the Fundão dam tailings (QUEIROZ *et al*., 2018). These particles can resist the estuarine removal and reach the coastal area as particulate matter (TREFRY, 1977). Furthermore, increase of SPM loads results on removal of dissolved metals from the water column by *scavenging* due to its high propensity to adsorb on particles surface (BRULAND; LOHAN, 2003). This process can be more representative than the precipitation from the estuarine trapping (HATJE *et al*., 2003). Therefore, the stability of the material in the Fundão tailings mostly composed by crystalline oxide (goethite) has contributed to the high inputs of metals in particulate form to the coastal area.

Apart from the continental/fluvial delivery of the tailings after the disaster, sedimentary inputs are also important sources of particulate metals to the water column in the study area as this material remain as fluid mud in the continental shelf and it is easily remobilized after resuspension events (BASTOS *et al*., 2017). These processes are intensified as by the increase of Doce River discharge (observed in Feb/2016a survey) as well as by the incidence of *swell* waves with higher energy from south associated to the cold fronts passage (QUARESMA *et al*., 2015). In general, metal concentrations in sediment presented similar temporal distribution compared to particulate metals, with higher concentrations occurring in Nov/2015 and Feb/2016a (Supplemental Table S10). This finding supports the hypothesis of sedimentary inputs to the water column.

Regarding of the chemical metal speciation and bioavailability, our results showed a possibly uptake of metals by phytoplankton as particulate forms. Study focusing on Fe size-fractionated and its relation with organic compounds (specifically humic substances - HS) in the same study area has suggested that dissolved (< 0.45 µm; < 0.22 µm) and soluble (< 0.02 µm) Fe fractions are present as colloidal nanoparticulate Fe(III) oxy-hydroxides and/or as iron complexes with amine compounds. Both might be preventing iron precipitation from the water column and allowing the high stability of this metal in seawater after the Fundão dam disaster (LONGHINI *et al*., submitted). *In situ* experiments evidence an increase of phytoplankton production as a result of SPM and particulate Fe addition (SUGIE *et al*., 2013). As our results for the different size fractions are resulting from the cut-off filtration procedure it is likely that the bulk of particulate fraction is composed by small colloidal sized particles (BENOIT; ROZAN, 1999; HURST; BRULAND, 2007).

Trace metals acquisition by the biology was formerly believed to be restricted to free ions or the kinetically labile inorganic metal complexes (SUNDA, 1989) and then colloidal and particulate metal *pool*s were not considered directly accessible to phytoplankton. However, ongoing studies have shown that the bioavailability and algal uptake strategies are greatly variable among phytoplankton groups and trace metals can be acquired either from chemical reduction of chelated organic-metal complexes (MALDONADO *et al*.,

2005; ROSE *et al*., 2005; SHAKED; KUSTKA; MOREL, 2005; HASSLER; SCHOEMANN, 2009; HASSLER *et al*., 2015; LIS *et al*., 2015) or directly assimilated as particulate forms (RUBIN; BERMAN-FRANK; SHAKED, 2011; SUGIE et al., 2013). For cyanobacteria, chemical reductive mechanism is widely used to acquire Fe as free ion as well as in forms of stable siderophore complex (LIS *et al*., 2015). These authors suggested that reductive uptake strategy can be used by phytoplankton to access Fe from a wide type of substrates, including colloidal and particulate forms (LIS *et al*., 2015).

Evidences of metal assimilation (specifically Fe) of particulate fraction by the marine cyanobacteria dinitrogen-fixer *Trichodesmium* sp. (RUBIN; BERMAN-FRANK; SHAKED, 2011; POLYVIOU *et al*., 2018; BASU *et al.,* 2019) and diatoms (GOLDBERG, 1952; SUNDA, 2001) should improve these taxa density through an opportunistic and tolerant strategy during mining tailing disasters, as seen for other biological taxa (GOMES *et al*., 2017). For example, *Trichodesmium* sp. assimilate the particulate material by trapping mineral dust of Fe oxy-hydroxide into the colony and subsequent assimilation by active shuttling (RUBIN; BERMAN-FRANK; SHAKED, 2011) whereas diatoms adsorb Fe oxy-hydroxide to the cell surface and then assimilate free iron after a bio-reductive dissolution step by membrane proteins (SUNDA, 2001). Colony formation and colonial morphologies as occur for *Trichodesmium* sp. would be an adaptive strategy to mineral iron acquisition in environments where particles provide a significant source of iron and other elements (RUBIN; BERMAN-FRANK; SHAKED, 2011) similarly what has been observed in the coastal area after the Fundão dam disaster. Indeed, our study demonstrates a predominance of Cyanophyaceae taxa and a positive correlation between this group and pFe indicating a direct effect of pFe inputs and cyanobacteria proliferation. In this context, the phytoplankton community before the Fundão dam disaster was mostly composed by Coccolitophyceae (PETROBRAS, 2005) against the high frequency of Cyanophyceae consistently registered in our study post dam failure. Therefore, the community structure in the continental shelf adjacent to the Doce River mouth seems to be changed after the tailings impact and these changes are probably related to the high and continuing inputs of pFe from the tailings. Qualitative analyses of phytoplankton provide further evidence of this

process as it has been registered the predominance of colonial *Trichodesmium* sp. in the study area after the Fundão dam tailings reached the coast (Supplemental Fig. S2).

The relation among particulate metals and phytoplankton community can also be explained by the metal phase exchange from dissolved to particulate form after cellular incorporation of these micronutrients. Partitioning exchange and increase of metals K_d are described to occur as a consequence of phytoplankton *bloom* and efficiency of biological recycling in a timescale of days (ELLWOOD *et al.*, 2014). In our study, this process was mainly observed from Jan/2016 to Feb/2016a which matched with the increase in micro-phytoplankton and diatoms growth. In addition, there was observed a negative correlation between diatoms densities and dFe concentrations indicating the following stage of metal enrichment and decrease of dFe as a response of the phytoplankton *bloom* (de BAAR *et al*., 1995; COALE *et al*., 1996; LANCELOT *et al*., 2000).

21.2 Factors controlling phytoplankton composition after the Fundão dam disaster

In our study area, Fe levels remained high during the samplings indicating continuous enrichment of this metal on water column. Experimental studies using Fe fertilization in marine ecosystems have shown significant changes on ecological structure and phytoplankton composition related to increases of dFe concentrations (BIZSEL; ÖZTÜRK; METIN, 1997; QUÉGUINER, 2013; YOON *et al*., 2016). In general, the growth of cells larger than 10 µm is favoured (TAKEDA; OBATA, 1995) while diatoms (MARTIN; GORDON; FITZWATER, 1991; PRICE; ANDERSEN; MOREL, 1991; COALE *et al*., 1996; FITZWATER *et al*., 1996; BIZSEL; ÖZTÜRK; METIN, 1997; TWINING *et al*., 2004) and flagellates (BIZSEL; ÖZTÜRK; METIN, 1997; TWINING *et al*., 2004) become the main algae groups under Fe-enrichment conditions. However, our results showed a predominance of nano-phytoplankton as Cyanophyceae and Chlorophyceae whereas diatoms and phytoflagellates were present in low densities (except by Feb/2016a for diatoms) indicating a different behaviour of phytoplankton community in response to Fe enrichment. Cyanobacteria are a widespread algae group in coastal waters and some species are able to

produce siderophores chelates as a strategy to assimilate Fe in limiting conditions (BARBEAU *et al*., 2003; GLEDHILL *et al*., 2004; HOPKINSON; MOREL, 2009; MAWJI *et al*., 2008). However, experiments on the coastal cyanobacteria *Synechococcus* sp. showed that siderophores are also released at iron levels in excess and could be a competitive advantage to Fe assimilation compared to other groups (TRICK; WILHELM, 1995). Thus, it is likely that the Fe forms present in the system after the tailings deposition (mainly in form of particulate and colloidal fraction as previously discussed) can be acting as a selective factor to favour the cyanobacteria predominance in the study area due to their versatile strategies to Fe uptake.

The community structure only changed after variations of pZn, pCu and pV, which allowed diatoms and Cryptophyceae growth in Feb/2016a, suggesting that these metals other than Fe might play a role in controlling phytoplankton assemblage (HASSLER *et al*., 2012) in the middle-term stages of the impact. These algae groups increased under specific conditions of high Doce River discharge, metals enrichment (7pFe, 5pV, 4pCu, 8pZn) and high DSi concentrations indicating a complex interaction among continental input of tailings, micronutrients (mainly V, Cu and Zn) and macronutrients (DSi) controlling phytoplankton composition in the study area after the disaster.

Despite of the DSi-limited condition described in Feb/2016a according to the DIN: DSi Redfield ratio, this limitation can be related to nutrients consumption by phytoplankton, since the algae response does not occur immediately after the nutrient inputs. In laboratory experiments, the maximum growth rate in *Skeletonema costatum* and *Prorocentrum donghaiense* diatoms occurred after five and six days, respectively, as a result of DIN and DSi enrichment (ZHOU *et al*., 2017), confirming the time lag between the nutrient input and algae growth. Moreover, the affinity for silic acid by diatoms was shown to be increased under Fe-enriched conditions and thus diatom *bloom* was able to persist even in DSi-limited conditions (MOSSERI *et al*., 2008).

Regarding to micronutrients, pZn might play a main and positive influence on diatoms (see Pearson Correlation results on Table 17) which is in agreement with the high Zn requirements to sustain growth of this algae group (SUNDA; HUNTSMAN, 2000), especially for coastal species (SUNDA; HUNTSMAN,

1992). Metabolic systems in diatoms are highly controlled by cellular Zn concentrations in association with other metals, such as Co, Cd and Cu (e.g. SUNDA; HUNTSMAN, 1995, 2000; SAITO; GOEPFERT, 2008; MASMOUDI *et al*., 2013). In this context, Zn and Cu act as essential as well as toxic agents and they control important mechanisms at cellular level, such as silicon uptake (RUETER; MOREL, 1981; ELLWOOD; HUNTER, 2000), enzymatic activities, the final metabolism and consequently the cellular growth and diatoms densities (MASMOUDI *et al*., 2013). The silicic acid uptake in this algae group is driven by a Zn-activated enzymatic system which is directly determined by the Zn concentration and inversely related to the Cu levels (RUETER; MOREL, 1981). As a result, the enzyme activity reaches the maximum response at intermediate range of free ions concentration (SUNDA, 1989) and high levels of Cu become toxic for inactivating the Zn molecular site and suppressing the enzymatic mechanism (RUETER; MOREL, 1981).

Therefore, at cellular and physiological levels, diatoms growth in Feb/2016a could be explained by higher DSi concentrations from continental inputs associated to adequate conditions in terms of Zn and Cu concentrations sustaining diatoms requirements for silica shell formation (COOMBS; VOLCANI, 1968). On the contrary, lower densities (or absence) of diatoms in other samplings but Feb/2016a probably occurred due to unfavourable conditions such as DSi limitation, imbalance of Cu: Zn ratio resulting on DSi uptake deficiency by Zn-activated enzyme and/or Cu toxicity. The growth of various marine diatoms species was showed to be inhibited when they were exposed to Cu enrichment at 0.15 µM while more sensitive species exhibited significant decrease on growth rate even at concentrations as low as 0.01 µM of Cu (TADROS; MBUTHIA; SMITH, 1990). In the acute phase of the disaster (Nov/2015) the concentrations of pCu reached up to 0.65 µM indicating toxic levels to diatoms community and growth inhibition is a likely consequence. Cryptophyceae were influenced by a wide group of micronutrients and macronutrients (pFe, pV, pCu, pV and silicate; see Pearson Correlation results on Table 17) suggesting that this group of algae and geochemical factors are been delivered to the coastal area from the same source, mainly continental input from the Doce River. Phytoplankton qualitative analyses support this

hypothesis as Cryptophyceae presented high contribution of continental species (BASTOS *et al*., 2017).

Aside from the physico-chemical and geochemical parameters evaluated by this study, it is worthy to mention that there are other factors controlling the phytoplankton community not considered here, such as grazing, temperature and luminosity limitation. All of these aspects act changing the algal growth and productivity from biomolecular, cellular to community level and then the phytoplankton structure and composition will be a result of these interactions (HASSLER *et al*., 2012).

21.3 Perspectives and predicted impacts

Fe-enrichement conditions have been discussed to favour specific groups of phytoplankton, including toxic microalgae (LAMPITT *et al*., 2008). The Dinophyceae *Scrippsiella trochoidea* is an example of harmful algae growing as a response of combined effects between high Fe concentrations and high luminosity (ZHUO-PING *et al*., 2009). Furthermore, in situ observations and experimental analyses have shown that Fe-fertilization lead to the growth increase of toxic diatom *Pseudo-nitzschia* spp. and also their production of neurotoxin domoic acid (DA) (SILVER *et al*., 2010), mainly as synergistic effect um other trace metals, such as Cu (WELLS *et al*., 2005; TRICK *et al*., 2010). Cyanotoxin production by *Trichodesmium* sp. is another harzard consequence of harmful algae bloom in coastal waters (NARAYANA *et al*., 2014; DETONI *et al*., 2016). Toxic cyanobacterial blooms of *Trichodesmium* sp. are recognized to be lethal to zooplankton community, including shrimp larvae mortality (NARAYANA *et al*., 2014; DETONI *et al*., 2016) and also for inhibiting the growth of other phytoplankton and causing damage in human cells (NARAYANA *et al*., 2014).

Monitoring program has been developed monthly in the area affected by the Fundão dam tailings since the disaster and the results have shown that the material remains present in the continental shelf and have affected the suspended particles and metal distribution in the water after resuspension events (BASTOS *et al*., 2017). Thus, it is worth to consider the interrelations between phytoplankton and the metals pointed by our study during the following

stages of monitoring in the impacted area. These further studies should make special attention to the possibility of harmful diatoms and the cyanobacteria *Trichodesmium* sp. proliferation, as we have shown that these groups are growing as a response of specific enrichment conditions after tailings remobilization.

22 CONCLUSION

Our study shows that the phytoplankton community has been controlled by metals/micronutrients in particulate form (mainly pZn, pCu, pV and pFe with lesser contribution) and these changes were related to the load of tailings in the acute stage of the disaster and also by the remobilization of this material under high Doce River discharge conditions. The interrelations between particulate metals and phytoplankton in the continental shelf adjacent to the Doce River mouth can be explained by two cycles: 1) Cyanobacteria growing over up other algae groups in all samplings as a result of pFe continuous input; 2) diatoms growth allowed by favourable conditions related to the silic acid uptake metabolism (e.g. higher DSi concentrations, Fe-enriched conditions and optimum ratio between Zn and Cu). The bioavailability of metals (mainly Fe) as particulate and possibly colloidal forms seems to be a key factor sustaining the predominance of cyanobacteria due to their capacity to assimilate metals from a wide range of substrates as by siderophores releasing as well as by particulate uptake. Therefore, the impacts related to the Fundão dam tailings in the coastal area adjacent to the Doce River mouth vary from changes on nutritional source due to the presence of different fractions of metals/micronutrients to ecological shifts on phytoplankton community. In this sense, the assessment presented here may assist monitoring and restoration efforts of this ecosystem, as well as, highlights the harmful potential of toxic algal *blooms* to the ecosystems and human health. The production of neurotoxin should be further investigated in the area.

23 REFERENCES

ALBINO, J.; CONTTI NETO, N.; OLIVEIRA, T.C.A. The Beaches of Espírito Santo. In: Short, A.D.; Klein, A.H.F. (Org.). **Brazilian Beach Systems**. Springer. 2016, 624 p.

ALVARES, C.A.; STAPE, J.L.; SENTELHAS, P.C.; GONÇALVES, J.L.M.; SPAROVEK, G. Köppen's climate classification map for Brazil. **Meteorologische Zeitschrift**, v. 22, n. 6, p. 711–728, 2014.

ANDERSON, M.J.; GORLEY, R.N;, CLARKE, K.R. **PERMANOVA. PRIMER: guide to software and statistical methods**. Plymouth: PRIMER-E Ltd., 2008, 214 p.

AMERICAN PUBLIC HEALTH ASSOCIATION (APHA). **Standard method for examination of water and wastewater**. Washington, DC, New York: American Public Health Association, 22nd ed., 2012, 1496 p.

BARBEAU, K.; RUE, E.L.; TRICK, C.G.; BRULAND; K.W.; BUTLER, A. Photochemical reactivity of siderophores produced by marine heterotrophic bacteria and cyanobacteria based on characteristic Fe(III) binding groups. **Limnology and Oceanography**, v. 48, n. 3, p. 1069–1078, 2003.

BASTOS, A.C.; OLIVERIA, K.S.S.; FERNANDES, L.F.; PEREIRA, J.B.; DEMONER, L.E.; NETO, R.R.; COSTA, E.S.; SÁ, F.; SILVA, C.A.; LERHBACK, B.D.; DIAS JR., C.; QUARESMA, V.S.; ORLANDO, M.T.D.; TURBAY, C.V.G.; LOPES, B.A.; LEITE, M.D.; GHISOLFI, R.D.; LEMOS, A.T.; PIVA, T.R.M.; LÁZARO, G.C.S.; CONCEIÇÃO, J.R.; LEMOS, K.N.; ZEN, C.M.; BONECKER, A.C.T.; CASTRO, M.S.; QUINTAS, M.C.; CAVAGGIONI, L.; OLIVEIRA, E.M.C. **Monitoramento da Influência da Pluma do Rio Doce após o rompimento da Barragem de Rejeitos em Mariana/MG – Novembro de 2015**: Processamento, Interpretação e Consolidação de Dados. Vitória: Universidade Federal do Espírito Santo, 2017, 254p. Disponível em: http://www.icmbio.gov.br/portal/images/stories/Rio_Doce/relatorio_consolidado_ufes_rio_doce.pdf [acesso em 07 Agosto de 2017]

BASU, S.; GLEDHILL, M.; DE BEER, D.; MATONDKAR, S.G.P.; SHAKED, Y. Colonies of marine cyanobacteria *Trichodesmium* interact with associated bacteria to acquire iron from dust. **Communications Biology,** v. 2, p. 1–8, 2019.

BEHRENFELD, M.J.; BOSS, E.; SIEGEL, D.A.; SHEA, D.M. Carbon-based ocean productivity and phytoplankton physiology from space. **Global Biogeochemical Cycles**, v. 19, p. 1–14, 2005.

BENOIT, G.; ROZAN, T.F. The influence of size distribution on the particle concentration effect and trace metal partitioning in rivers. **Geochimica et Cosmochimica Acta**, v. 63, p. 113–127, 1999.

BIZSEL, N.; ÖZTÜRK, M.; METIN, G. The role of iron on the phytoplankton growth in heavily polluted Izmir Bay, Aegean Sea. **Transactions on Ecology and the Environmen**t, v. 14, p. 659 – 669, 1997.

BOYLE, E.A.; EDMOND, J.M.; SHOLKOVITZ, E.R. The mechanism of iron removal in estuaries. **Geochimica et Cosmochimica Acta**, v. 41, p. 1313–1324, 1977.

BRULAND, K.W.; LOHAN, M.C. Controls of trace metals in seawater, p. 23-47. In: Turekian, K.K.; Holland, H.D. (Orgs.). **Treatise on Geochemistry**. 1st ed. Elsevier, Pergamon, v. 6. 2003, 9144 p.

CARMO, F. F. do; KAMINO, L. H. Y.; TOBIAS JUNIOR, R.; CAMPOSA, I.C. de; CARMO, F.F. do; SILVINO, G.; CASTRO, K.J.S.X. de; MAURO, M.L.; RODRIGUES, N.U.A.; MIRANDA, M.P.S.; PINTO, C.E.F. Fundão tailings dam failures: the environment tragedy of the largest technological disaster of Brazilian mining in global context. **Perspectives in Ecology and Conservation**, v. 15, p. 145–151, 2017.

CLARKE, K.R.; GORLEY, R.N. **PRIMER v6: User Manual/Tutorial**, 6 ed, Plymouth, 2006.

COALE, K.H.; JOHNSON, K.S.; FITZWATER, S.E.; GORDON, R.M.; TANNER, S.; CHAVEZ, F.P.; FERIOLI, L.; SAKAMOTO, C.; ROGERS, P.; MILLERO, F.; STEINBERG, P.; NIGHTINGALE, P.; COOPER, D.; COCHLAN, W.P.; LANDRY, M.R.; CONSTANTINOU, J.; ROLLWAGEN, G.; TRASVINA, A.; KUDELA, R. A massive phytoplankton bloom induced by an ecosystem-scale iron fertilization experiment in the equatorial Pacific Ocean. **Nature**, v. 383, n. 6600, p. 495–501, 1996.

COOMBS, J.; VOLCANI, B.E. Studies on the biochemistry and fine structure of silica shell formation in diatoms. Silicon induced metabolic transients in *Navicula pelliculosa*. **Planta (Berl.)**, v. 80, p. 264-279, 1968.

de BAAR, H.J.W.; de JONG, J.T.M.; BAKKER, D.C.E.; LÖSCHER, B.M.; VETH, C.; BATHMANN, U.; SMETACEK, V. Importance of iron for plankton blooms and carbon dioxide drawdown in the Southern Ocean. **Nature**, v. 373, p. 412-415, 1995.

DERECZYNSKI, C.P.; LOPES, Í.D.R.; de CARVALHO, N.O.; da SILVA, M.G.A.J.; GROSSMANN, K.S.; MARTINS, R.P. Climatology of espírito santo and the northern campos basin, offshore southeast brazil. **Anuário do Instituto de Geociencias**, v. 42, p. 386–401, 2019.

DETONI, A.M.S.; COSTA, L.D.F.; PACHECO, L.A.; YUNES, J.S. Toxic *Trichodesmium* bloom occurrence in the southwestern South Atlantic Ocean. **Toxicon**, v. 110, p. 51-55, 2016.

ELLWOOD, M.J.; HUNTER, K.A. The incorporation of zinc and iron into the frustule of the marine diatom Thalassiosira pseudonana. **Limnology and**

Oceanography, v. 45, p. 1517–1524, 2000.

ELLWOOD, M.J.; NODDER, S.D.; KING, A.L.; HUTCHINS, D.A.; WILHELM, S.W.; BOYD, P.W. Pelagic iron cycling during the subtropical spring bloom, east of New Zealand. **Marine Chemistry**, v. 160, p. 18–33, 2014.

FITZWATER, S.E.; COALE, K.H.; GORDON, R.M.; JOHNSON, K.S.; ONDRUSEK, M.E. Iron deficiency and phytoplankton growth in the equatorial Pacific. **Deep Sea Research, Part II**, v. 43, n. 4-6, p. 995-1015, 1996.

FALKOWSKI, P.G.; BARBER, R.T.; SMETACEK, V.V. Biogeochemical Controls and Feedbacks on Ocean Primary Production. **Science**, v. 281, n. 5374, p. 200-206, 1998.

GLEDHILL, M.; MCCORMACK, P.; USSHER, S.; ACHTERBERG, E.P.; MANTOURA, R.F.C.; WORSFOLD, P.J. Production of siderophore type chelates by mixed bacterioplankton populations in nutrient enriched seawater incubations. **Marine Chemistry**, v. 88, p. 75–83, 2004.

GOLDBERG, E.D. Iron Assimilation by Marine Diatoms. **Biological Bulletin**, v. 102, n. 3, p. 243–248, 1952.

GOMES, L.E.O.; CORREA, L.B.; SÁ, F.; NETO, R.R.; BERNARDINO, A.F. The impacts of the Samarco mine tailing spill on the Rio Doce estuary, Eastern Brazil. **Marine Pollution Bulletin**, v. 120, p. 28–36, 2017.

HASSLER, C.S.; NORMAN, L.; NICHOLS, C.A.M.; CLEMENTSON, L.A.; ROBINSON, C.; SCHOEMANN, V.; WATSON, R.J.; DOBLIN, M.A. Iron associated with exopolymeric substances is highly bioavailable to oceanic phytoplankton. **Marine Chemistry**, v. 173, p. 136–147, 2015.

HASSLER, C.S.; SCHOEMANN, V. Bioavailability of organically bound Fe to model phytoplankton of the Southern Ocean. **Biogeosciences**, v. 6, p. 2281–2296, 2009.

HASSLER, C.S.; SINOIR, M.; CLEMENTSON, L.A.; BUTLER, E.C.V. Exploring the link between micronutrients and phytoplankton in the Southern Ocean during the 2007 austral summer. **Frontiers in Microbiology**, v. 3, p. 1–26, 2012.

HATJE, V.; PAYNE, T.E.; HILL, D.M.; McORIST, G.; BIRCH, G.F.; SZYMCZAK, R. Kinetics of trace element uptake and release by particles in estuarine waters: effects of pH, salinity, and particle loading. **Environment International**, v. 29, p. 619–629, 2003.

HATJE, V.; PEDREIRA, R.M.A.; de REZENDE, C.E.; SCHETTINI, C.A.F.; de SOUZA, G.C.; MARIN, D.C.; HACKSPACHER, P.C. The environmental impacts of one of the largest tailing dam failures worldwide. **Scientific Reports - Nature**, v. 7, p. 1–13, 2017.

HO, T.-Y.; QUIGG, A.; FINKEL, Z.V.; MILLIGAN, A.J.; WYMAN, K.; FALKOWSKI, P.G.; MOREL, F.M.M. The elemental composition of some marine phytoplankton. **Journal of Phycology**, v. 39, p. 1145–1159, 2003.

HO; T.-Y.; WEN, L.-S.; YOU, C.-F.; LEE, D.-C. The trace-metal composition of size-fractionated plankton in the South China Sea: Biotic versus abiotic sources. **Limnology and Oceanography**, v. 52, n. 5, p. 1776–1788, 2007.

HOPKINSON, B.M.; MOREL, F.M.M. The role of siderophores in iron acquisition by photosynthetic marine microorganisms. **BioMetals**, v. 22, p. 659–669, 2009.

HURST, M.P.; BRULAND, K.W. An investigation into the exchange of iron and zinc between soluble, colloidal, and particulate size-fractions in shelf waters using low-abundance isotopes as tracers in shipboard incubation experiments. **Marine Chemistry**, v. 103, p. 211–226, 2007.

JOHNSON, K.S.; GORDON, R.M.; COALE, K.H. What controls dissolved iron concentrations in the world ocean? Authors' closing comments. **Marine Chemistry**, v. 57, n. 3–4, p. 181–186, 1997.

KUMA, K.; NISHIOKA, J.; MATSUNAGA, K. Controls on iron(III) hydroxide solubility in seawater: The influence of pH and natural organic chelators. **Limnology and Oceanography**, v. 41, p. 396–407, 1996.

LAMPITT, R.S.; ACHTERBERG, E.P.; ANDERSON, T.R.; HUGHES, J.A.; IGLESIAS-RODRIGUEZ, M.D.; KELLY-GERREYN, B.A.; LUCAS, M.; POPOVA, E.E.; SANDERS, R.; SHEPHERD, J.G.; SMYTHE-WRIGHT, D.; YOOL, A. Ocean fertilization: A potential means of geoengineering? **Philosophical Transactions of the Royal Society A: Mathematical, Physical and Engineering Sciences**, v. 366, p. 3919–3945, 2008.

LANCELOT, C.; HANNON, E.; BECQUEVORT, S.; VETH, C.; de BAAR, H.J.W. Modeling phytoplankton blooms and carbon export production inthe Southern Ocean: Dominant controls by light and iron in the Atlanticsector in austral spring 1992. **Deep Sea Research Part I**, v. 47, p. 1621– 1662, 2000.

LIS, H.; SHAKED, Y.; KRANZLER, C.; KEREN, N.; MOREL, F.M.M. Iron bioavailability to phytoplankton: An empirical approach. **ISME Journal: Multidisciplinary Journal of Microbial Ecology**, v. 9, p. 1003–1013, 2015.

LONGHINI, C.M.; SÁ, F.; NETO, R.R. Review and synthesis: iron input, biogeochemistry, and ecological approaches in seawater. **Environmental Reviews**, v. 27, p. 125–137, 2019.

LORENZEN, C.J. Determination of chlorophyll and pheopigments: spectrophotometric equations. **Limnology and Oceanography**, v. 12, p. 343-346, 1967.

LUND, J. W. G.; KIPLING C.; LE CREN, E. D. The inverted microscope method of estimating algal numbers and the statistical basis of estimations by counting. **Hydrobiologia**, v. 11, p. 143-70, 1958.

MALDONADO, M. T.; STRZEPEK, R. F.; SANDER, S.; BOYD, P.W. Acquisition of iron bound to strong organic complexes, with different Fe binding groups and photochemical reactivities, by plankton communities in Fe-limited subantarctic waters. **Global Biogeochemical Cycles**, v. 19, n. 4, p. 1-13, 2005.

MARTIN, J.H.; GORDON, M.; FITZWATER, S.E. The case for iron. **Limnology and Oceanography**, v. 36, n. 8, p. 1793–1802, 1991.

MAGALHAES, M.S.; BRANDAO, P.R.G.; TAVARES, R.P. Types of goethite from Quadrilátero Ferrífero's iron ores and their implications in the sintering process. **Mineral Processing and Extractive Metallurgy Review**, v. 116, p. 54–64, 2007.

MASMOUDI, S.; NGUYEN-DEROCHE, N.; CARUSO, A.; AYADI, H.; MORANT-MANCEAU, A.; TREMBLIN, G.; BERTRAND, M.; SCHOEFS, B. Cadmium, Copper, Sodium and Zinc Effects on Diatoms: from Heaven to Hell - a Review. **Cryptogamie, Algologie**, v. 34, n. 2, p. 185–225, 2013.

MAWJI, E.; GLEDHILL, M.; MILTON, J.A.; TARRAN, G.A.; USSHER, S.; THOMPSON, A.; WOLFF, G.A.; WORSFOLD, P.J.; ACHTERBERG, E.P. Hydroxamate siderophores: Occurrence and importance in the Atlantic Ocean. **Environmental Science & Technology**, v. 42, p. 8675–8680, 2008.
McARDLE, B.H.; ANDERSON, M.J. Fitting multivariate models to community data: a comment on distance-based redundancy analysis. **Ecology**, v. 82, n. 1, p. 290-297, 2001.

MOREL, F.M.M.; PRICE, N.M. The biogeochemical cycles of trace metals in the oceans. **Science**, v. 300, n. 5621, p. 944–947, 2003.

MOREL, F.M.M.; HUDSON, R.J.M.; PRICE, N.M. Limitation of productivity by trace metals in the sea. **Limnology and Oceanography**, v. 36, p. 1742–1755, 1991.

MOREL, F.M.M.; COX, E.H.; KRAEPIEL, A.M.L.; LANE, T.W.; MILLIGAN, A.J.; SCHAPERDOTH, I.; REINFELDER, J.R.; TORTELL, P. D. Acquisition of inorganic carbon by the marine diatom *Thalassiosira weissflogii*. **Functional Plant Biology**, v. 29, p. 301–308, 2002.

MOREL, F.M.M.; MILLIGAN, A.J.; SAITO, M.A. Marine Bioinorganic Chemistry: The Role of Trace Metals in the Oceanic Cycles of Major Nutrients. In: Turekian, K.K.; Holland, H.D. (Orgs.). **Treatise on Geochemistry.** 1st ed. Elsevier, Pergamon, v. 6. 2003, 9144 p.

MOSSERI, J.; QUÉGUINER, B.; ARMAND, L.; CORNET-BARTHAUX, V. Impact of iron on silicon utilization by diatoms in the Southern Ocean: A case study of Si/N cycle decoupling in a naturally iron-enriched area. **Deep-Sea**

Research Part II: Topical Studies in Oceanography, v. 55, p. 801–819, 2008.

NARAYANA, S.; CHITRA, J.; TAPASE, S.R.; THAMKE, V.; KARTHICK, P.; RAMESH, C.; MURTHY, K.N.; RAMASAMY, M.; KODAM, K.M.; MOHANRAJU, R. Toxicity studies of *Trichodesmium erythraeum* (Ehrenberg, 1830) bloom extracts, from Phoenix Bay, Port Blair, Andamans. **Harmful Algae**, v. 40, p. 34-39, 2014.

NÓBREGA, N.E.F.; SILVA, J.G.F.; RAMOS, H.E.A.; PAGUNG, F.S. Balanço hídrico climatológico e classificação climática de Thornthwaite e Köppen para o município de Linhares – ES. In: **Anais do Congresso Nacional de Irrigação e Drenagem**. O equilíbrio do fluxo hídrico para uma agricultura irrigada sustentável. São Mateus: ABID, 2008. 6p.

O'KELLEY, J.C. Inorganic nutrients. In: StewarT, W.D.P. (Org.) **Algal physiology and biochemistry**. University of California Press. Berkeley and Los Angeles, 1974, 989 p.

OLSEN, C.R.; CUTSHALL, N.H.; LARSEN, I.L. Pollutant-particle associations and dynamics in coastal marine environments: A review. **Marine Chemistry**, v. 11, p. 501-533, 1982.

PETROBRAS. **Relatório Final do Projeto de Caracterização Ambiental Regional da Bacia do Espírito Santo e Parte Norte da Bacia de Campos (PCR-ES/AMBES)**, 2015.

NASSAR, C.A.G.; SALGADO, L.T.; YONESHIGUE-VALENTIN, Y.; AMADO FILHO, G.M. The effect of iron-ore particles on the metal content of the brown alga Padina gymnospora (Espírito Santo Bay, Brazil). **Environmental Pollution**, v. 123, p. 301–305, 2003.
OLIVEIRA, T.C.A.; ALBINO, J.; VENANCIO, I. Transporte longitudinal de sedimentos no litoral da planície deltaica do Rio Doce. **Quaternary and Environmental Geosciences**, v. 6, n. 1, p. 20-25, 2015.

POLYVIOU, D.; BAYLAY, A.J.; HITCHCOCK, A.; ROBIDART, J.; MOORE, C.M.; BIBBY, T.S. Desert dust as a source of iron to the globally important diazotroph *Trichodesmium*. **Frontiers in Microbiology**, v. 8, n. 1–12, 2018.
PRICE, N.M.; ANDERSEN, L.F.; MOREL, F.M. Iron and nitrogen nutrition of equatorial Pacific plankton. **Deep-Sea Research, Part A**, v. 38, n. 11, p. 1361-1378, 1991.

QUARESMA, V.S.; CATABRIGA, G.; BOURGUIGNON, S.N.; GODINHO, E.; BASTOS, A.C. Modern sedimentary processes along the Doce river adjacent continental shelf. **Brazilian Journal of Geology**, v. 45, n. 4, p. 635-644, 2015.

QUÉGUINER, B. Iron fertilization and the structure of planktonic communities in high nutrient regions of the Southern Ocean. **Deep-Sea Research Part II: Topical Studies in Oceanography**, v. 90, p. 43–54, 2013.

QUEIROZ, H.M.; NÓBREGA, G.N.; FERREIRA, T.O.; ALMEIDA, L.S.;

ROMERO, T.B.; SANTAELLA, S.T.; BERNARDINO, A.F.; OTERO, X.L. The Samarco mine tailing disaster: A possible time-bomb for heavy metals contamination? **Science of the Total Environment**, v. 637–638, p. 498–506 2018.

REDFIELD, A.C. **On the Proportions of Organic Derivatives in Sea Water and Their Relation to the Composition of Plankton**. James Johnstone Memorial Volume, University Press of Liverpool, 176-192, 1934.

ROSE, A.L.; SALMON, T.P.; LUKONDEH, T.; NEILAN, B.A.; WAITE, T.D. Use of superoxide as an electron shuttle for iron acquasition by the marine cyanobacterium Lyngbya majuscula. **Environmental Science & Technology**, v. 39, p. 3708–3715, 2005.

RUBIN, M.; BERMAN-FRANK, I.; SHAKED, Y. Dust-and mineral-iron utilization by the marine dinitrogen-fixer *Trichodesmium*. **Nature Geoscience**, v. 4, p. 529–534, 2011.

RUDORFF, N.; RUDORFF, C.M.; KAMPEL, M.; ORTIZ, G. Remote sensing monitoring of the impact of a major mining wastewater disaster on the turbidity of the Doce River plume off the eastern Brazilian coast. **ISPRS Journal of Photogrammetry and Remote Sensing**, v. 145, p. 349–361, 2018.

RUETER, J.G.; MOREL, F.M.M. The interaction between zinc deficiency and copper toxicity as it affects the silicic acid uptake mechanisms in Thalassiosira pseudonana. **Limnology and Oceanography**, v. 26, p. 67–73, 1981.

SAITO, M.A.; GOEPFERT, T.J.; RITT, J.T. Some thoughts on the concept of colimitation: Three definitions and the importance of bioavailability. **Limnology and Oceanography**, v. 53, p. 276–290, 2008.
SERVINO, R.N.; GOMES, L.E.O.; BERNARDINO, A.F. Extreme weather impacts on tropical mangrove forests in the Eastern Brazil Marine Ecoregion. **Science of the Total Environment**, v. 628-629, p. 233–240, 2018.

SHAKED, Y.; KUSTKA, A.B.; MOREL, F.M.M. A general kinetic model for iron acquisition by eukaryotic phytoplankton. **Limnology and Oceanography**, v. 50, p. 872–882, 2005.

SHANNON, C. E.; WEAVER, W. **The mathematical theory of communication**. Urbana: University of Illinois Press, 1949.

SHOLKOVITZ, E.R.; BOYLE, E.A.; PRICE, N.B. The removal of dissolved humic acids and iron during estuarine mixing. **Earth and Planetary Science Letters**, v. 40, p. 130–136, 1978.

SILVER, M.W.; BARGU, S.; COALE, S.L.; BENITEZ-NELSON, C.R.; GARCIA, A.C.; ROBERTS, K.J.; SEKULA-WOOD, E.; BRULAND, K.W.; COALE, K.H. Toxic diatoms and domoic acid in natural and iron enriched waters of the oceanic Pacific. **Proceedings of the National Academy of Sciences of the**

United States of America, v. 107, p. 20762–20767, 2010.

SUGIE, K.; NISHIOKA, J.; KUMA, K.; VOLKOV, Y.N.; NAKATSUKA, T. Availability of particulate Fe to phytoplankton in the Sea of Okhotsk. **Marine Chemistry**, v. 152, p. 20–31, 2013.

SUNDA, W.G. Bioavailability and bioaccumulation of iron in the sea. In: Turner, D.R.; Hunter. K.A. (Orgs). **The biogeochemistry of iron in seawater**. John Wiley & Sons, Chichester, England. v. 7, 2001, 410 p.

SUNDA, W.G. Trace metal interactions with marine phytoplankton. **Biological Oceanography**, v. 6, n. 5-6, p. 411–442, 1988.

SUNDA, W.G.; HUNTSMAN, S.A., Effect of Zn, Mn, and Fe on Cd accumulation in phytoplankton: Implications for oceanic Cd cycling. **Limnology and Oceanography**, **v.** 45, p. 1501–1516, 2000.

SUNDA, W.G.; HUNTSMAN, S.A. Cobalt and zinc interreplacement in marine phytoplankton: Biological and geochemical implications. **Limnology and Oceanography**, v. 40, p. 1404–1417, 1995.

SUNDA, W.G.; HUNTSMAN, S.A. Feedback interactions between zinc and phytoplankton in seawater. **Limnology and Oceanography**, v. 37, p. 25–40, 1992.

TADROS, M.G.; MBUTHIA, P.; SMITH, W. Differential response of marine diatoms to trace metals. **Bulletin of Environmental Contamination and Toxicology**, v. 44, p. 826–831, 1990.

TAKEDA, S.; OBATA, H. Response of equatorial Pacific phytoplankton to subnanomolar Fe enrichment. **Marine Chemistry**, v. 50, n. 1–4, p. 219–227, 1995.

TILMAN, D.; KILHAM, S.S.; KILHAM, P. Phytoplankton community ecology: The role of limiting nutrients. **Annual Review of Ecology, Evolution, and Systematics**, v. 13, p. 348-372, 1982.

TREFRY, J.H. **The transport of heavy metals by the Mississippi River and their fate in the Gulf of Mexico**. Ph.D. Thesis. A&M University, 1977, 238 p.

TRICK, C.G.; BILL, B.D.; COCHLAN, W.P.; WELLS, M.L.; TRAINER, V.L.; PICKELL, L.D. Iron enrichment stimulates toxic diatom production in high-nitrate, low-chlorophyll areas. **Proceedings of the National Academy of Sciences of the United States of America**, v. 107, p. 5887–5892, 2010.

TRICK, C.G.; WILHELM, S.W. Physiological changes in the coastal marine cyanobacterium *Synechococcus* sp. PCC 7002 exposed to low ferric ion levels. **Marine Chemistry**, v. 50, p. 207–217, 1995.

TWINING, B.S.; BAINES, S.B.; FISHER, N.S. Element stoichiometries of

individual plankton cells collected during the Southern Ocean Iron Experiment (SOFeX). **Limnology and Oceanograph**y, v. 49, p. 2115–2128, 2004.

TWINING, B.S.; BAINES, S.B.; FISHER, N. S.; LANDRY, M.R. Cellular iron contents of plankton during the Southern Ocean Iron Experiment (SOFeX). **Deep-Sea Research Part II: Topical Studies in Oceanography**, v. 51, p. 1827–1850, 2004.

U.S. EPA. **Method 6020A**: Inductively Coupled Plasma-Mass Spectrometry, Revision 1. Washington, DC, 1998.

U.S. EPA. **Method 3051A (SW-846)**: Microwave Assisted Acid Digestion of Sediments, Sludges, and Oils, Revision 1. Washington, DC, 2007.

UEHLINGER, V. **Étude statistique des méthodes de dénombrement planctoniqu**e, 1964. 103p.

UTERMÖHL, H. **Zur Vervollkommnung der quantitativen Phytoplankton Methodik**. International Association of Theoretical and Applied Limnology, Mitteilungen, v. 9, p. 1-38, 1958.

WANG, W-X. Interactions of trace metals and different marine food chains **Marine Ecology Progress Series**, v. 243, p. 295-309, 2002.

WELLS, M.L.; TRICK, C.G.; COCHLAN, W.P.; HUGHES, M.P.; TRAINER, V.L. Domoic acid: The synergy of iron, copper, and the toxicity of diatoms. **Limnology and Oceanography**, v. 50, n. 6, p. 1908–1917, 2005.

YOON, J.-E.; YOO, K.-C.; MACDONALD, A.M.; YOON, H.I.; PARK, K.-T.; YANG, E.-J.; KIM, H.-C.; LEE, J.I.; LEE, M.K.; JUNG, J.; PARK, J.; SONG, J.-M.; CHOI, T.-J.; KIM, K.; KIM, I.-N. Ocean Iron Fertilization Experiments: Past–Present–Future with Introduction to Korean Iron Fertilization Experiment in the Southern Ocean (KIFES) Project. **Biogeosciences Discussions**, 2016.

YUAN-HUI, L. Distribution patterns of the elements in the ocean: A synthesis. **Geochimica et Cosmochimica Acta**, v. 55, p. 3223–3240, 1991.

ZHOU, Y.; ZHANG, Y.; LI, F.; TAN, L.; WANG, J. Nutrients structure changes impact the competition and succession between diatom and dinoflagellate in the East China Sea. **Science of the Total Environment**, v. 574, p. 499–508, 2017.

ZHUO-PING, C.; WEI-WEI, H.; MIN, A.; SHUN-SHAN, D. Coupled effects of irradiance and iron on the growth of a harmful algal bloom-causing microalga Scrippsiella trochoidea. **Acta Ecologica Sinica**, v. 29, p. 297–301, 2009.

CAPÍTULO 4

CONCLUSÕES

CONCLUSÕES

O rompimento da barragem de Fundão configura-se como um dos maiores desastres ambientais a nível global e os impactos na região marinha variam desde modificações nos ciclos geoquímicos dos elementos à contaminação de organismos em diferentes níveis tróficos. A Figura 21 apresenta o fluxograma dos impactos imediatos na área costeira após esse desastre, os quais motivaram a elaboração das hipóteses do presente trabalho, bem como as respectivas conclusões.

Com base nos resultados encontrados, contínuos processos de contaminação/enriquecimento por metais (especialmente Fe) ocorrem na plataforma continental adjacente à foz do Rio Doce. Em condições naturais, espera-se que ocorra alta taxa de precipitação de Fe dissolvido da coluna d'água decorrente da remoção estuarina, floculação da matéria orgânica e adsorção/*scavaging* do material particulado. No entanto, observa-se que as concentrações de dFe (< 0,45 µm e < 0,22 µm) e até mesmo solúvel (< 0,02 µm) apresentam alta estabilidade na área, uma vez que os níveis se mantém significativamente altos quando comparados à outros sistemas impactados por atividade de mineração. De acordo com a **Hipótese 1**, a complexação orgânica do Fe dissolvido (dFe) com substâncias húmicas (HS) mantem a estabilidade e disponibilidade desse elemento na coluna d'água após o desastre de Fundão. Entretanto, o presente estudo mostra que essa estabilidade não é explicada por fatores naturais (complexação com substâncias húmicas) e os resultados apontam para uma influência direta do rejeito, seja na forma de Fe complexado com aminas, as quais são largamente utilizadas como floculante nas etapas de beneficiamento do minério, e/ou pela presença de nanopartículas coloidais de óxido-hidróxidos de Fe, previamente identificadas em amostras do rejeito na forma de goetita. Assim, as formas químicas desse elemento, disponibilizadas a partir do aporte e remobilização do rejeito, são fundamentalmente diferentes das formas esperadas para ambientes costeiros não impactados. Além disso, considerando a alta estabilidade desse material e as características oceanográficas da plataforma continental em questão, existe a possibilidade de transporte e consequente enriquecimento de áreas oceânicas com Fe provenientes desse rejeito.

Considerando a **Hipótese 2**, o aporte de metais para a área costeira decorrente do desastre de Fundão modificou a estrutura da comunidade fitoplanctônica, permitindo o favorecimento de grupos com potencial tóxico para o ecossistema. Essa hipótese foi confirmada a partir da análise das inter-relações de metais-traço/micronutrientes com a comunidade fitoplanctônica, a qual mostra os efeitos de pFe sobre o crescimento de cianobactérias, bem como pZn e pCu como principais controladores da densidade de diatomáceas. As formas químicas de Fe disponibilizadas no ambiente estão possivelmente atuando como fator seletivo para a dominância de Cyanophycea, com evidências de floração de *Thichodesmium* sp. Essa última possui a capacidade de incorporar Fe particulado e coloidal, os quais constituem as principais formas químicas desse elemento na área de estudo. Assim, a plasticidade das espécies que compõem esse grupo em relação ao metabolismo de assimilação de metais configura-se como uma vantagem competitiva em detrimento dos demais grupos algais. Embora estudos anteriores tenham constatado o florescimento de diatomáceas em resposta à fertilização com Fe, o crescimento desse grupo algal na área de estudo esteve restrito às condições de incremento nas concentrações de pZn, DSi, aumento da vazão do Rio Doce e níveis específicos de enriquecimento de metais (7pFe, 5pV, 4pCu, 8pZn). A interação desses fatores levou ao favorecimento da assimilação de silicato, sustentando a demanda por esse nutriente para a formação da carapaça silicosa das espécies que compõem esse grupo.

O presente trabalho mostra que a comunidade fitoplanctônica comporta-se de forma diferente da esperada para áreas enriquecidas com Fe, em função da influência de outros metais e nutrientes, bem como pela predominância de diferentes formas químicas dos elementos que estão sendo disponibilizadas no ambiente. Assim, é possível que a fonte nutricional para o fitoplâncton na área de estudo tenha sido modificada após o desastre o que se reflete na composição e estrutura ecológica dessa comunidade.

Uma vez que esse material sofreu diversas modificações ao longo do processamento físico e químico do minério, os efeitos da sua assimilação a nível fisiológico ainda são desconhecidos. Além disso, considerando o contínuo aporte e alta estabilidade de metais por remobilização e ressuspensão do

rejeito, bem como as evidências de floração de *Tricodesmium* sp. na área, cujo potencial tóxico é reconhecido na literatura, recomenda-se a continuidade da análise entre metais e sua relação com a proliferação de cianobactérias e diatomáceas tóxicas. O presente estudo alerta para a possível produção de cianotoxinas e neurotoxinas na área em resposta às mudanças nos processos biogeoquímicos de metais após o desastre ambiental de Fundão. Os impactos previstos variam desde alterações no funcionamento ecológico deste ecossistema costeiro a possíveis riscos à saúde humana decorrentes da contaminação por atividades de mineração.

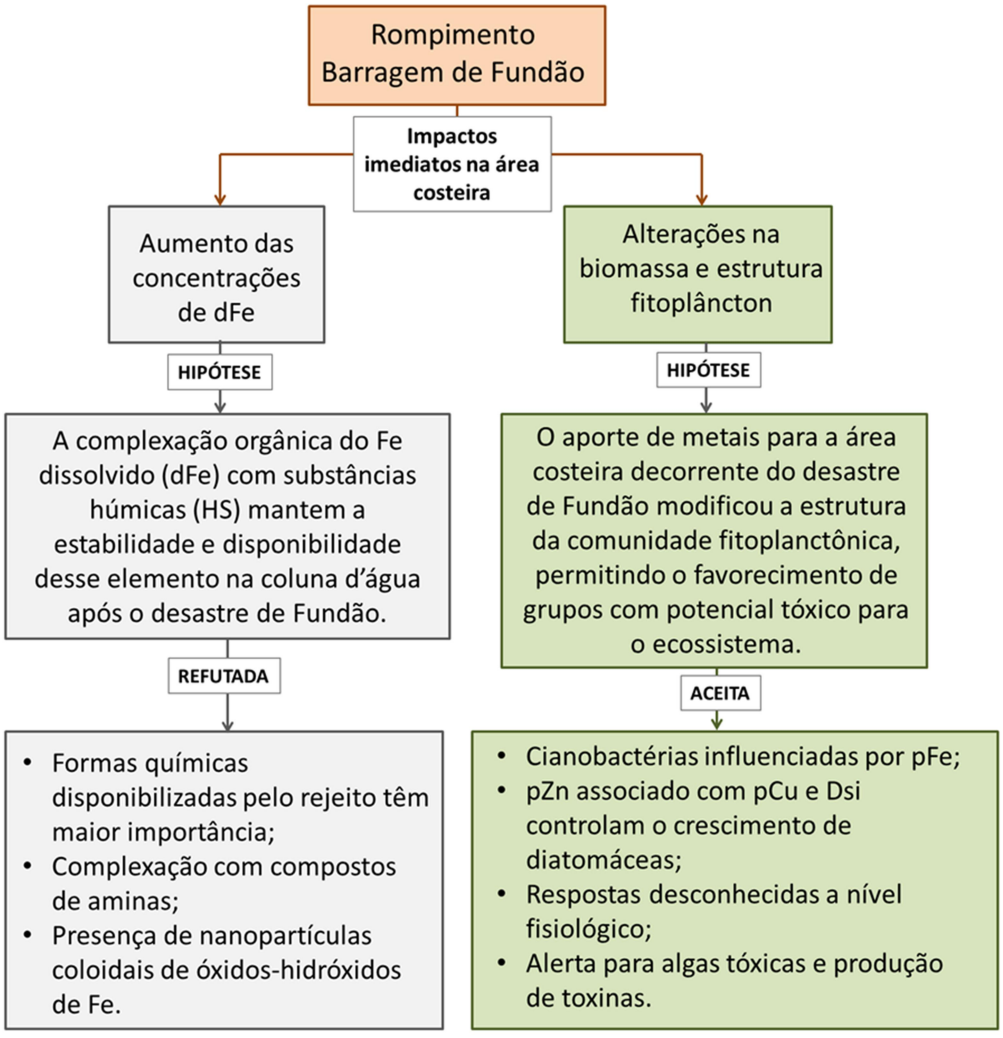

Figure 21. Impactos imediatos na área costeira após o desastre de Fundão, questões norteadoras baseadas nas hipóteses de pesquisa e respectivas conclusões do presente trabalho.

ANEXO I – SUPPLEMENTAL TABLE S1

Table S1. Sedimentary Fe concentrations in the continental shelf adjacent to the Doce River mouth in November 2015, February 2016 and August 2018.

Sample		Fe ($mg.g^{-1}$)
Nov/2015		
	N-20	38.7
	C-10	16.2
Feb/2016		
	N-25	21.2
	C-30	33.0
	S-20	18.3
Aug/2018		
	N-10	25.2
	N-20	27.6
	N-30	8.0
	C-10	3.5
	C-20	25.9
	C-30	17.5
	S-10	30.9
	S-20	26.6
	S-30	26.3

ANEXO II - SUPPLEMENTAL FIGURE S1

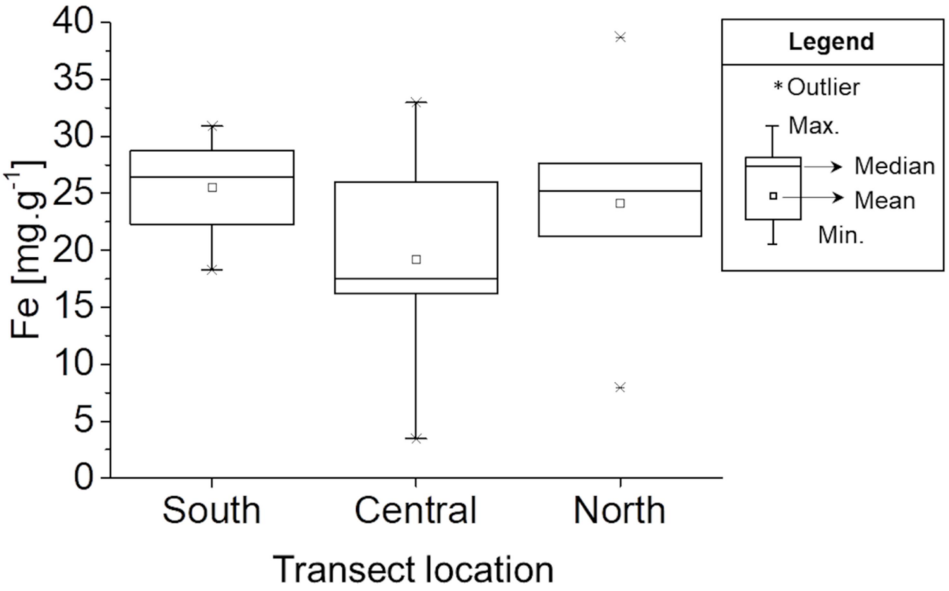

Fig. S1. Spatial distribution of sedimentary Fe concentrations over the course of the three samplings (Nov/2015, Feb/2016 and Aug/2018) in the continental shelf adjacent to the Doce River mouth.

ANEXO III – SUPPLEMENTAL TABLE S2

Table S2. Dissolved aluminium, copper and zinc concentrations (0.45 *μ*m). These high concentrations can indicate that these metals are occurring in colloidal form similarly what was found for dFe (0.45 *μ*m).

Sample	dAl (nM)		dCu (nM)		dZn (nM)	
	Surface	**Bottom**	**Surface**	**Bottom**	**Surface**	**Bottom**
Nov/15						
C-10	12,519	9,926	378	441	1,055	719
N-20	10,222	9,963	242	441	868	841
Feb/2016						
S-20	7,855	9,205	26	27	89	125
C-30	2,966	387	55	74	61	108
N-25	5,047	801	40	40	153	71
Aug/2018						
N-10	14,805	3,394	249	215	796	251
C-10	8,151	3,477	212	180	369	290
S-10	8,839	6,388	218	202	443	406
N-20	5,940	4,832	202	197	605	363
C-20	8,817	4,665	210	209	600	541
S-20	6,585	6,478	214	189	440	323
N-30	6,794	3,834	215	210	367	357
C-30	8,519	5,334	244	189	357	545
S-30	5,357	4,812	214	194	378	202
Min	2,966	387	26	27	61	71
Max	14,805	9,963	378	441	1055	841

ANEXO IV – SUPPLEMENTAL TABLE S3

Table S3 - Detection and Quantification Limit ($mg.L^{-1}$) for metals analyzed by ICP-MS and % of recovery from spiked samples.

Metals	Detection Limit ($mg.L^{-1}$)	Quantification Limit ($mg.L^{-1}$)	%Recovery (Spike)
V	0.0001	0.0002	97.1
Mn	0.0004	0.0013	85.2
Fe	0.0001	0.0004	107.2
Co	0.0001	0.0002	104.5
Cu	0.0001	0.0002	100.6
Zn	0.0001	0.0002	93.4

ANEXO V – SUPPLEMENTAL TABLE S4

Tabela S4 – Quantification limit (QL) and detection limit (DL) in µM for dissolved inorganic nutrientes.

	Phosphate	Nitrite	Nitrate	Ammoniacal nitrogen	Silicate
QL	0.0018	0.0015	0.006	0.006	0.009
DL	0.0006	0.0005	0.002	0.002	0.003

ANEXO VI – SUPPLEMENTAL TABLE S5

Table S5 - PERMANOVA post-hoc results showing significant differences of variables during the samplings.

Groups	t	p	Unique perms
Micro-phytoplankton			
2, 3	**3.749**	**0.001**	997
2, 4	0.851	0.429	999
2, 5	0.614	0.552	997
3, 4	**4.041**	**0.001**	997
3, 5	**3.397**	**0.002**	998
4, 5	1.231	0.239	996
Diversity			
2, 3	**3.940**	**0.001**	997
2, 4	0.683	0.485	999
2, 5	1.132	0.267	997
3, 4	**4.141**	**0.001**	998
3, 5	**4.712**	**0.001**	994
4, 5	0.298	0.757	995
Phytoplankton assemblage			
1, 2	**3.242**	**0.001**	998
1, 3	**2.615**	**0.001**	998
1, 4	**1.819**	**0.022**	999
1, 5	**2.551**	**0.002**	999
2, 3	**4.402**	**0.001**	998
2, 4	1.332	0.138	999
2, 5	0.841	0.530	999
3, 4	**3.473**	**0.001**	999
3, 5	**3.620**	**0.001**	999
4, 5	1.154	0.275	998
Diatomacea density			
1, 2	1.598	0.110	998
1, 3	**4.075**	**0.001**	996
1, 4	0.270	0.792	998
1, 5	0.109	0.906	996
2, 3	**5.002**	**0.001**	998
2, 4	0.998	0.370	999
2, 5	2.021	0.064	997
3, 4	**4.341**	**0.001**	998
3, 5	**4.493**	**0.001**	997
4, 5	0.225	0.824	999
Cryptophyceae density			
1, 2	**2.760**	**0.012**	995
1, 3	1.205	0.250	999
1, 4	1.421	0.156	995
1, 5	1.962	0.058	996
2, 3	**3.791**	**0.001**	999
2, 4	0.812	0.404	997
2, 5	0.612	0.559	999
3, 4	**2.634**	**0.012**	996
3, 5	**3.173**	**0.001**	996
4, 5	0.274	0.776	991
pFe			
1, 2	**3.709**	**0.002**	995
1, 3	**2.975**	**0.011**	999
1, 4	**3.425**	**0.002**	995
1, 5	**3.710**	**0.001**	995
2, 3	1.371	0.183	998
2, 4	0.298	0.823	997

Groups	t	p	Unique perms
2, 5	0.811	0.416	995
3, 4	1.132	0.295	998
3, 5	1.235	0.229	997
4, 5	0.010	0.994	998
pV			
1, 2	**2.327**	**0.017**	996
1, 3	0.498	0.632	996
1, 4	**2.581**	**0.012**	998
1, 5	1.359	0.209	997
2, 3	**2.491**	**0.010**	997
2, 4	0.472	0.650	997
2, 5	**2.046**	**0.039**	997
3, 4	**2.799**	**0.010**	999
3, 5	1.170	0.259	998
4, 5	**2.571**	**0.014**	997
pMn			
1, 2	**3.368**	**0.001**	993
1, 3	**5.490**	**0.001**	997
1, 4	**2.816**	**0.014**	994
1, 5	1.555	0.131	995
2, 3	1.167	0.238	998
2, 4	1.837	0.071	996
2, 5	**2.971**	**0.004**	995
3, 4	**4.752**	**0.001**	997
3, 5	**5.374**	**0.001**	999
4, 5	**2.002**	**0.048**	996
pCu			
1, 2	**4.504**	**0.001**	999
1, 3	**3.144**	**0.003**	998
1, 4	**2.842**	**0.008**	996
1, 5	**3.254**	**0.002**	997
2, 3	**3.146**	**0.003**	995
2, 4	**2.147**	**0.031**	999
2, 5	**2.285**	**0.028**	997
3, 4	0.709	0.504	996
3, 5	1.100	0.273	994
4, 5	0.276	0.814	997
pZn			
1, 2	0.566	0.615	996
1, 3	**2.296**	**0.033**	998
1, 4	0.261	0.804	999
1, 5	1.159	0.257	999
2, 3	**2.088**	**0.045**	998
2, 4	1.269	0.215	997
2, 5	**2.796**	**0.006**	996
3, 4	**2.823**	**0.010**	997
3, 5	**3.661**	**0.002**	997
4, 5	1.547	0.143	998
dFe			
1, 2	**2.540**	**0.025**	999
1, 3	**5.840**	**0.001**	996
1, 4	0.326	0.770	997
1, 5	**4.216**	**0.001**	997
2, 3	**2.274**	**0.026**	997
2, 4	**3.993**	**0.001**	997
2, 5	1.674	0.091	995
3, 4	**8.786**	**0.001**	997
3, 5	0.016	0.988	998
4, 5	**6.600**	**0.001**	996

Groups	t	p	Unique perms
dV			
1, 2	0.446	0.673	996
1, 3	**6.151**	**0.001**	999
1, 4	**5.764**	**0.001**	995
1, 5	1.124	0.273	997
2, 3	2.237	0.041	998
2, 4	1.748	0.100	996
2, 5	0.786	0.450	996
3, 4	2.011	0.047	998
3, 5	**6.267**	**0.001**	994
4, 5	**7.195**	**0.001**	999
dMn			
1, 2	1.323	0.228	996
1, 3	**2.653**	**0.007**	999
1, 4	**1.893**	**0.050**	997
1, 5	1.873	0.063	995
2, 3	**2.159**	**0.033**	998
2, 4	1.782	0.078	997
2, 5	1.565	0.112	999
3, 4	0.970	0.344	999
3, 5	0.100	0.940	998
4, 5	0.587	0.661	999
dCu			
1, 2	**3.9027**	**0.001**	994
1, 3	**10.052**	**0.001**	998
1, 4	**5.9336**	**0.001**	997
1, 5	**4.967**	**0.001**	997
2, 3	**7.3936**	**0.001**	997
2, 4	**3.1337**	**0.005**	998
2, 5	1.3298	0.198	999
3, 4	**7.6674**	**0.001**	997
3, 5	**7.1254**	**0.001**	997
4, 5	**2.1568**	**0.039**	999
dZn			
1, 2	**2.3846**	**0.013**	995
1, 3	**3.0041**	**0.003**	998
1, 4	**8.1506**	**0.001**	998
1, 5	**8.4118**	**0.001**	996
2, 3	**5.2814**	**0.001**	998
2, 4	**6.2248**	**0.001**	996
2, 5	**6.4037**	**0.001**	996
3, 4	**8.5152**	**0.001**	997
3, 5	**8.9144**	**0.001**	999
4, 5	0.30313	0.778	997
Phospate			
1, 2	**5.0639**	**0.001**	997
1, 3	0.83104	0.423	998
1, 4	**3.3722**	**0.004**	997
1, 5	**4.4274**	**0.001**	998
2, 3	**6.8138**	**0.001**	997
2, 4	**4.9995**	**0.001**	998
2, 5	**6.4273**	**0.001**	997
3, 4	**4.7333**	**0.001**	997
3, 5	**6.2233**	**0.001**	995
4, 5	0.19797	0.843	995
DIN			
1, 2	0.52863	0.621	994
1, 3	8.73E-02	0.942	998
1, 4	0.57669	0.645	998

Groups	t	p	Unique perms
1, 5	**9.9987**	**0.001**	997
2, 3	0.81407	0.429	996
2, 4	0.25064	0.816	999
2, 5	**7.3819**	**0.001**	996
3, 4	0.891	0.382	998
3, 5	**14.133**	**0.001**	997
4, 5	**4.680**	**0.001**	996
SPM			
1, 2	**3.290**	**0.002**	993
1, 3	**4.795**	**0.001**	996
1, 4	**4.029**	**0.001**	996
1, 5	**3.976**	**0.001**	996
2, 3	0.662	0.487	999
2, 4	**2.304**	**0.014**	998
2, 5	2.020	0.056	996
3, 4	1.372	0.183	996
3, 5	0.851	0.404	994
4, 5	1.091	0.299	993
KdZn			
1, 2	0.256	0.871	998
1, 3	2.008	0.055	996
1, 4	**2.112**	**0.035**	996
1, 5	**2.973**	**0.005**	992
2, 3	1.359	0.174	997
2, 4	**1.974**	**0.042**	997
2, 5	1.715	0.086	997
3, 4	1.985	0.053	997
3, 5	0.681	0.531	997
4, 5	1.257	0.225	996
KdCu			
1, 2	0.689	0.512	998
1, 3	**2.599**	**0.016**	997
1, 4	0.796	0.541	999
1, 5	**2.566**	**0.010**	993
2, 3	**2.680**	**0.011**	997
2, 4	0.909	0.442	998
2, 5	**2.758**	**0.008**	998
3, 4	**2.582**	**0.012**	999
3, 5	**2.474**	**0.013**	997
4, 5	0.945	0.373	998

ANEXO VII – SUPPLEMENTAL TABLE S6

Table S6 - Biological parameters recorded in the continental shelf adjacent to the Doce River mouth. Minimum, maximum, average and standard deviation of values in each sector (S- South, C- Central, S- South). ND = not determined; BDL = Below detection limit.

Sampling	Statistics	PARAMETERS AND SECTORS																																				
		Pigments (µg.L^{-1})									Phytoplankton assemblege density (x 10^3 orgs.L^{-1})																											Diversity		
		Chl-*a*			Phaeophytin			Total			Nano-phytoplankton			Micro-phytoplankton			Diatomaceae			Haptophyta			Cyanophyceae			Chlorophyceae			Cryptophyceae			Phytoflagelata			Others					
		S	C	N	S	C	N	S	C	N	S	C	N	S	C	N	S	C	N	S	C	N	S	C	N	S	C	N	S	C	N	S	C	N	S	C	N	S	C	N
Nov/2015 (n=14)	Min	ND	ND	ND	0	ND	0	212	127	266	209	ND	0	0	ND	0	0	0	0	0	0	0	47	38	51	81	35	77	0	0	0	0	0	0	0	0	0	2.9	ND	2.5
	Max	4.1	ND	5.3	1.9	ND	9.1	436	4824	521	390	ND	471	112	ND	50	72	48	54	0	5	0	223	4631	334	192	301	210	54	38	37	0	66	0	14	48	31	4.8	ND	4.4
	Average	1.4	ND	1.5	0.3	ND	2.8	297	696	354	280	ND	170	17	ND	7	7	6	8	0	0	0	101	531	142	129	117	137	20	17	12	0	5	0	5	9	8	3.9	ND	3.9
	± SD	1.3	ND	2.6	0.6	ND	4.3	83	1319	114	59	ND	191	39	ND	18	23	14	19	0	2	0	51	1299	97	42	85	63	16	11	15	0	19	0	5	13	10	0.7	ND	0.9
Jan/2016 (n=14)	Min	0	0.3	BDL	BDL	BDL	BDL	251	351	259	251	348	243	0	0	0	0	0	0	0	0	0	143	190	140	48	91	73	0	0	0	0	0	0	0	4	0	1.9	2.0	1.3
	Max	4.2	0.8	1.5	1.1	0.8	0.2	1452	1085	1325	1448	1066	1286	46	23	39	6	0	13	0	0	0	987	749	1166	319	228	164	52	7	27	0	0	0	44	48	8	3.7	3.1	2.8
	Average	0.8	0.6	0.6	0.4	0.5	0.1	486	626	615	476	622	605	9	8	10	1	0	3	0	0	0	301	437	472	137	123	112	12	0	9	0	0	0	9	16	3	2.8	2.6	2.1
	± SD	1.2	0.2	0.5	0.4	0.3	0.1	304	229	385	307	226	374	14	8	15	2	0	5	0	0	0	222	174	378	69	45	33	15	3	10	0	0	0	12	15	4	0.5	0.4	0.6
Feb/2016 a (n=27)	Min	BDL	BDL	BDL	BDL	BDL	BDL	274	112	189	23	112	93	0	0	0	0	0	0	0	0	0	12	44	31	3	12	56	0	0	0	0	0	0	0	0	0	1.0	0.9	2.4
	Max	4.0	4.5	3.7	5.1	0.9	1.7	2124	20549	18884	2085	20390	17494	780	158	1390	738	149	1322	616	27	0	1657	19371	1888	423	612	15674	149	204	63	0	0	0	36	44	20	4.7	4.4	4.6
	Average	1.2	0.9	0.7	0.4	0.2	0.3	664	2240	1444	480	2190	1289	184	49	156	176	44	140	45	2	0	229	1858	213	148	239	1051	34	53	15	0	0	0	10	7	7	3.3	3.1	3.8
	± SD	1.0	1.2	1.2	1.1	0.3	0.5	399	5732	4357	429	5745	4047	214	54	337	205	51	318	140	8	0	360	5523	424	88	197	3651	33	59	17	0	0	0	11	12	7	1.1	0.9	0.7
Feb/2016b (n=14)	Min	0	0	0	0	0	0	189	104	201	178	104	197	0	0	0	0	0	0	0	0	0	45	16	30	38	41	94	0	0	0	0	0	0	0	0	3	1.1	1.1	1.4
	Max	1.8	1.3	1.2	3.2	0.7	1.7	12319	788	587	12126	788	587	193	8	15	249	5	12	0	0	0	8833	646	470	2613	74	143	124	10	49	1	0	0	21	24	46	3.4	3.1	3.9
	Average	0.6	0.4	0.5	0.5	0.2	0.5	1190	449	335	1174	448	328	16	1	7	18	1	4	0	0	0	855	348	165	246	59	121	19	3	23	0	0	0	4	9	16	2.3	1.9	3.1
	± SD	0.7	0.5	0.5	0.8	0.2	0.6	2979	230	133	2932	229	136	47	3	6	62	2	5	0	0	0	2145	214	159	632	12	19	31	5	20	0	0	0	6	10	16	0.8	0.7	0.9
Apr/2016 (n=14)	Min	0.2	BDL	0.1	BDL	BDL	BDL	266	158	243	247	158	228	0	0	0	0	0	0	0	0	0	85	107	117	59	40	31	0	0	0	0	0	0	0	0	0	1.6	1.0	1.7
	Max	1.4	1.1	1.0	0.8	1.4	0.6	1942	1630	803	1680	1595	803	263	62	27	18	11	31	5	0	0	1379	1386	618	536	515	128	36	50	11	0	0	0	272	33	32	4.0	2.5	3.3
	Average	0.6	0.4	0.5	0.2	0.3	0.2	634	880	372	604	866	362	31	14	10	3	3	10	0	0	0	333	669	250	224	171	86	15	10	7	0	0	0	41	13	8	2.9	1.7	2.4
	± SD	0.4	0.3	0.3	0.2	0.5	0.2	429	469	220	368	462	227	69	22	11	6	5	14	1	0	0	319	438	189	141	160	35	13	18	4	0	0	0	75	13	12	0.8	0.5	0.6

ANEXO VIII – SUPPLEMENTAL TABLE S7

Table S7 - Concentrations of metals in particulate (> 0.45 µm) and dissolved fraction (< 0.45 µm) recorded in the continental shelf adjacent to the Doce River mouth. Minimum, maximum, average and standard deviation of values in each sector (S- South, C- Central, S- South).

Sampling	Statistics	METALS AND SECTORS																																				
		Particulate fraction (> 0.45 µm)																									Dissolved fraction (< 0.45 µm)												
		pFe (µM)			pV (µM)			pMn (µM)			pCo (µM)			pCu (µM)			pZn (µM)			dFe (µM)			dV (µM)			dMn (µM)			dCo (µM)			dCu (µM)			dZn (µM)		
		S	C	N	S	C	N	S	C	N	S	C	N	S	C	N	S	C	N	S	C	N	S	C	N	S	C	N	S	C	N	S	C	N	S	C	N	S	C	N
Nov/2015 (n=14)	Min	2.47	0.37	2.63	BDL	BDL	BDL	BDL	0.01	0.02	BDL	BDL	BDL	BDL	0.003	0.01	BDL	BDL	BDL	0.45	0.54	0.51	BDL	BDL	0.01	BDL	BDL	BDL	BDL	BDL	BDL	0.06	0.06	0.06	0.20	0.14	0.09
	Max	795.4	1536.5	823.7	0.70	0.33	0.14	32.0	1.2	35.5	BDL	BDL	BDL	0.28	0.65	0.14	0.48	0.82	0.13	2.34	4.04	1.34	0.26	0.14	0.25	1.03	0.33	1.14	0.01	BDL	0.01	0.86	0.77	0.56	1.50	1.54	0.68
	Average	159.0	381.3	205.0	0.14	0.08	0.07	14.7	0.3	14.1	BDL	BDL	BDL	0.15	0.14	0.07	0.13	0.15	0.07	1.18	1.38	1.02	0.15	0.07	0.08	0.16	0.15	0.20	0.01	BDL	0.01	0.30	0.35	0.20	0.55	0.84	0.28
	± SD	262.8	634.9	274.0	0.22	0.10	0.05	15.0	0.4	15.5	BDL	BDL	BDL	0.06	0.17	0.05	0.14	0.27	0.03	0.53	1.08	0.29	0.06	0.05	0.09	0.35	0.09	0.42	0.00	BDL	0.001	0.22	0.22	0.18	0.40	0.49	0.18
Jan/2016 (n=14)	Min	0.79	1.57	0.62	0.02	0.01	BDL	0.40	0.03	0.01	0.02	0.04	0.03	0.002	0.01	0.01	0.04	0.06	0.04	0.18	0.68	0.10	BDL	BDL	BDL	BDL	BDL	BDL	0.003	BDL	BDL	BDL	0.08	0.01	0.01	0.40	0.21
	Max	67.3	255.7	28.5	0.11	0.19	0.07	7.0	19.1	0.86	0.05	0.05	0.03	0.05	0.05	0.04	0.26	0.56	0.10	3.17	1.48	1.25	1.33	BDL	1.39	0.18	BDL	0.02	0.06	BDL	0.003	0.26	0.43	0.24	1.77	2.28	2.31
	Average	21.9	13.9	7.98	0.04	0.03	0.02	1.94	0.33	0.22	0.03	0.05	0.03	0.02	0.01	0.02	0.12	0.10	0.08	0.87	0.83	0.66	0.20	BDL	0.40	0.10	BDL	0.01	0.03	BDL	0.002	0.07	0.15	0.11	0.71	0.96	1.06
	± SD	23.7	86.4	10.49	0.03	0.06	0.03	1.95	6.62	0.32	0.01	0.004	0.003	0.02	0.01	0.01	0.06	0.17	0.03	0.81	0.29	0.46	0.40	BDL	0.66	0.06	BDL	0.01	0.02	BDL	0.002	0.08	0.14	0.10	0.60	0.57	0.89
Feb/2016 a (n=27)	Min	1.52	0.28	6.78	BDL	BDL	0.03	0.02	0.02	0.04	0.11	0.15	0.03	0.001	BDL	0.01	0.03	0.01	0.004	BDL	0.27	0.48	0.01	0.01	0.03	BDL	0.002	0.005	BDL	0.001	0.003	BDL	BDL	0.001	0.08	0.15	0.24
	Max	1602.4	1095.8	110.64	0.37	0.37	0.26	12.9	4.4	2.3	0.28	0.38	0.48	0.29	0.23	0.20	1.20	0.82	0.50	0.40	0.81	2.88	0.04	0.04	0.06	0.01	0.09	0.03	0.002	0.004	0.01	0.02	0.03	0.04	0.40	0.67	0.90
	Average	306.0	123.6	33.11	0.09	0.08	0.09	1.34	0.59	0.43	0.22	0.21	0.27	0.06	0.06	0.07	0.32	0.23	0.16	0.12	0.42	1.02	0.02	0.02	0.05	0.01	0.02	0.02	0.001	0.002	0.01	0.01	0.01	0.01	0.27	0.30	0.53
	± SD	486.2	308.3	26.52	0.11	0.11	0.06	2.77	1.25	0.58	0.04	0.06	0.13	0.07	0.07	0.05	0.28	0.29	0.13	0.11	0.17	0.70	0.01	0.01	0.01	0.002	0.03	0.01	0.001	0.001	0.003	0.01	0.01	0.01	0.10	0.17	0.22
Feb/2016 b (n=14)	Min	0.43	0.96	2.93	BDL	0.01	0.003	0.36	0.35	1.44	0.01	0.13	0.02	0.003	0.01	0.02	0.01	0.01	0.01	0.89	0.87	1.51	0.01	0.00	0.01	BDL	0.003	0.003	0.003	0.002	0.003	0.001	0.050	0.03	0.005	0.05	0.005
	Max	731.7	45.2	28.08	0.20	0.06	0.04	8.16	1.92	11.8	0.28	0.31	0.26	0.28	0.07	0.12	0.27	0.13	0.40	2.18	1.44	1.69	0.04	0.01	0.02	0.03	0.02	0.01	0.004	0.003	0.003	0.11	0.07	0.04	0.15	0.19	0.15
	Average	71.4	12.2	15.64	0.04	0.03	0.02	2.37	0.89	6.71	0.08	0.20	0.14	0.04	0.04	0.06	0.06	0.08	0.12	1.62	1.08	1.59	0.02	0.01	0.01	0.004	0.01	0.01	0.003	0.002	0.003	0.04	0.06	0.04	0.04	0.09	0.07
	± SD	179.2	16.9	8.64	0.05	0.02	0.01	2.26	0.57	3.56	0.08	0.06	0.10	0.06	0.03	0.03	0.06	0.06	0.14	0.34	0.25	0.07	0.01	0.00	0.01	0.01	0.005	0.003	BDL	BDL	BDL	0.03	0.01	0.004	0.05	0.05	0.06
Apr/2016 (n=14)	Min	0.98	3.33	3.53	0.004	0.004	0.01	0.46	1.72	1.75	0.12	0.12	0.11	0.01	0.01	0.001	0.003	0.002	0.01	0.08	0.06	0.08	0.04	0.04	0.05	0.01	0.01	0.01	0.003	0.004	0.007	0.04	0.002	0.002	0.01	0.05	0.02
	Max	59.8	127.8	184.11	0.10	0.18	0.14	30.6	13.5	9.52	0.15	0.38	0.15	0.13	0.13	0.19	0.07	0.17	0.32	2.45	0.64	1.43	0.11	0.07	0.09	0.06	0.04	0.04	0.013	0.008	0.010	0.25	0.02	0.24	0.21	0.21	0.07
	Average	18.6	26.2	55.26	0.05	0.07	0.05	8.23	6.11	4.19	0.13	0.18	0.14	0.04	0.05	0.06	0.03	0.06	0.10	0.61	0.29	0.65	0.07	0.05	0.07	0.02	0.02	0.02	0.007	0.005	0.009	0.11	0.01	0.13	0.07	0.11	0.05
	± SD	19.1	41.7	70.87	0.03	0.06	0.06	8.08	3.92	2.74	0.01	0.09	0.01	0.03	0.04	0.07	0.02	0.06	0.12	0.70	0.25	0.54	0.03	0.01	0.02	0.01	0.01	0.01	0.004	0.001	0.001	0.08	0.01	0.10	0.06	0.06	0.02

ANEXO IX – SUPPLEMENTAL TABLE S8

Table S8 – Metals patition coefficient (Kd) recorded in the continental shelf adjacent to the Doce River mouth. Minimum, maximum, average and standard deviation of values in each sector (S- South, C- Central, S- South).

Sampling	Statistics	Kd																	
		Fe			V			Mn			Co			Cu			Zn		
		S	C	N	S	C	N	S	C	N	S	C	N	S	C	N	S	C	N
Nov/2015 (n=14)	Min	1.1	2.18	2.96	0.11	0.02	0.02	8.89	0.14	0.28	_	_	_	0.17	0.14	0.01	0.16	0.00	0.00
	Max	636.3	1539.16	615.01	6.12	1.59	7.83	4047.88	16.23	2723.27	_	_	_	0.96	2.03	1.66	2.36	0.78	0.87
	Average	156.3	320.19	180.95	1.76	0.66	1.73	1500.41	3.68	959.70	_	_	_	0.58	0.68	0.81	0.52	0.13	0.34
	± SD	221.1	519.62	205.38	2.56	0.55	2.88	1749.33	6.31	1168.63	_	_	_	0.27	0.70	0.68	0.81	0.26	0.31
Jan/2016 (n=14)	Min	0.4	2.31	2.82	0.06	_	0.01	3.81	_	1.26	0.38	_	8.77	0.04	0.02	0.05	0.06	0.05	0.04
	Max	157.0	318.25	63.55	1.37	_	0.58	73.91	_	11.81	11.21	_	43.64	2.99	0.31	3.23	8.49	0.57	0.28
	Average	40.3	55.19	17.36	0.56	_	0.29	23.38	_	6.53	3.23	_	26.20	0.73	0.14	0.72	0.90	0.21	0.13
	± SD	47.1	116.32	23.83	0.39	_	0.28	21.81	_	7.46	4.72	_	24.66	0.80	0.10	1.26	2.21	0.19	0.09
Feb/2016 a (n=27)	Min	9.02	2.18	4.33	0.19	0.10	0.52	4.95	3.52	2.16	130.63	62.96	3.62	0.08	0.25	1.68	0.14	0.03	0.02
	Max	204442.0	1539.16	139.64	21.76	45.75	4.91	414.39	242.25	475.40	504.30	273.24	121.07	116.61	211.57	182.80	7.57	5.32	2.04
	Average	15661.8	359.15	43.32	4.79	5.55	1.87	139.05	39.43	63.55	293.37	126.30	66.28	20.59	24.27	43.54	1.38	0.98	0.37
	± SD	45249.5	510.95	35.50	6.45	12.77	1.07	122.04	66.58	119.88	116.41	73.17	41.69	31.35	65.89	57.11	1.64	1.52	0.46
Feb/2016 b (n=14)	Min	0.5	1.00	1.89	0.18	1.82	0.18	93.82	28.85	352.96	5.30	54.75	6.12	0.03	0.11	0.65	0.41	0.03	0.70
	Max	335.0	49.24	18.32	4.75	17.03	3.16	14537.45	265.37	2432.18	73.24	126.87	86.43	39.18	1.14	2.93	18.70	2.09	5.58
	Average	36.4	5.69	9.89	2.20	5.37	1.15	1788.86	112.41	1068.90	22.84	84.06	46.67	4.16	0.61	1.52	3.05	1.13	2.37
	± SD	82.0	18.66	5.63	1.35	5.81	1.09	3491.64	87.31	741.59	23.43	23.86	33.95	9.69	0.43	0.82	4.65	0.88	1.92
Apr/2016 (n=14)	Min	3.3	15.64	7.18	0.09	0.06	0.09	60.82	160.02	65.37	9.38	15.91	11.50	0.06	0.43	0.05	0.03	0.02	0.20
	Max	128.3	208.29	148.05	1.26	4.01	1.53	2676.07	1473.24	611.28	44.95	56.24	20.42	2.60	27.45	8.84	5.40	1.72	4.54
	Average	43.2	89.52	76.93	0.70	1.41	0.71	647.34	549.12	300.57	24.07	32.29	15.66	0.62	9.59	1.79	0.89	0.58	1.91
	± SD	35.8	67.65	52.58	0.43	1.40	0.68	688.88	453.34	203.84	11.43	11.43	3.05	0.67	10.07	3.47	1.35	0.54	1.77

ANEXO X – SUPPLEMENTAL TABLE S9

Table S9 - Concentrations of dissolved inorganic nutrients recorded in the continental shelf adjacent to the Doce River mouth. Minimum, maximum, average and standard deviation of values in each sector (S- South, C- Central, S- South).

Sampling	Statistics	DISSOLVED NUTRIENTS AND SECTORS								
		Phosphate (µM)			DIN (µM)			Silicate (µM)		
		S	C	N	S	C	N	S	C	N
Nov/2015 (n=14)	Min	0.07	0.02	0.02	1.34	2.25	1.85	1.24	0.99	1.87
	Max	0.10	0.28	0.17	10.3	28.0	14.3	4.58	65.6	41.7
	Average	0.09	0.14	0.11	3.40	7.45	5.33	2.39	7.77	7.63
	± SD	0.01	0.09	0.05	2.69	7.37	4.06	1.15	18.3	13.8
Jan/2016 (n=14)	Min	0.02	0.03	0.03	0.19	1.47	0.12	0.49	0.70	0.61
	Max	0.17	0.10	0.06	62.7	12.6	6.01	5.60	34.50	2.05
	Average	0.05	0.04	0.04	12.4	7.97	3.76	2.40	2.03	1.29
	± SD	0.05	0.03	0.01	19.1	3.57	2.76	1.81	11.50	0.47
Feb/2016a (n=27)	Min	0.01	0.06	0.06	0.34	2.91	0.34	0.01	0.13	0.01
	Max	0.38	0.20	0.18	41.2	21.5	24.22	65.71	54.78	6.09
	Average	0.14	0.12	0.10	9.08	8.56	5.68	13.07	7.93	1.12
	± SD	0.09	0.05	0.04	12.6	6.82	6.31	22.52	15.82	1.83
Feb/2016b (n=14)	Min	0.00	0.00	0.00	0.08	0.51	0.07	0.35	0.62	0.44
	Max	0.76	1.10	0.70	6.20	127.7	8.38	4.71	4.90	3.40
	Average	0.23	0.51	0.26	2.21	22.1	2.88	1.53	1.98	1.69
	± SD	0.20	0.43	0.25	1.77	51.7	2.93	1.12	1.57	1.12
Apr/2016 (n=14)	Min	0.11	0.13	0.16	7.65	28.3	20.6	1.92	1.92	1.99
	Max	0.43	1.15	0.98	45.0	66.4	45.7	10.1	3.99	3.13
	Average	0.18	0.38	0.45	16.7	51.2	30.4	3.25	2.80	2.60
	± SD	0.10	0.35	0.33	9.58	12.3	9.36	2.03	0.59	0.38

ANEXO XI – SUPPLEMENTAL TABLE S10

Table S10 - Sedimentary concentrations of metals in the continental shelf adjacent to the Doce River mouth. Minimum, maximum, average and standard deviation of values in each sector (S - South, C - Central, S - South).

Sampling	Statistics	METALS AND SECTORS																	
		Fe (mg.g^{-1})			V (mg.kg^{-1})			Mn (mg.kg^{-1})			Co (mg.kg^{-1})			Cu (mg.kg^{-1})			Zn (mg.kg^{-1})		
		S	C	N	S	C	N	S	C	N	S	C	N	S	C	N	S	C	N
Nov/2015 (n=14)	Min	36.0	9.3	0.0	19.8	5.9	7.7	544.5	62.5	419.5	5.3	1.1	1.6	6.7	0.5	0.5	21.9	2.3	1.2
	Max	41.4	33.2	38.7	32.8	18.8	26.8	1268.9	889.5	813.8	6.8	6.6	6.2	10.5	7.9	7.1	25.4	26.9	23.0
	Average	39.6	19.8	25.0	23.6	14.0	13.3	890.6	280.2	689.5	5.4	2.9	5.1	7.1	2.6	5.3	22.7	10.1	18.8
	± SD	2.1	8.6	16.9	5.6	6.1	8.9	263.9	254.7	148.8	0.6	1.7	2.1	1.3	2.5	3.2	1.1	7.6	10.7
Jan/2016 (n=14)	Min	2.0	18.1	8.9	6.5	3.3	22.8	403.3	540.0	235.0	1.0	1.1	2.9	1.3	2.6	4.6	4.2	6.2	9.5
	Max	22.4	73.9	21.2	67.9	18.2	26.6	1827.1	1158.4	1222.3	6.1	1.6	6.0	13.5	4.0	14.9	24.3	8.7	16.6
	Average	12.1	33.2	12.3	28.9	11.3	25.6	1078.9	805.9	789.4	3.5	1.3	3.0	5.4	3.3	6.2	8.5	6.9	10.4
	± SD	8.7	26.1	6.4	21.2	7.3	2.0	481.8	255.7	494.9	1.7	0.2	1.8	3.9	0.6	5.6	7.0	1.1	3.9
Feb/2016a (n=27)	Min	29.4	19.1	4.2	26.1	15.3	52.2	263.4	208.9	198.2	0.5	0.4	0.7	1.2	0.6	2.5	9.3	5.7	7.9
	Max	72.4	91.7	58.8	50.0	34.3	68.2	566.6	571.3	1374.2	3.0	2.8	4.5	6.7	8.0	7.1	26.4	25.0	17.3
	Average	57.7	43.5	51.2	40.1	23.4	58.9	386.1	303.7	843.6	1.9	2.5	3.5	4.3	4.4	3.7	21.4	22.9	11.9
	± SD	12.7	28.6	15.7	7.6	8.4	4.6	106.6	147.8	343.7	0.8	1.2	1.2	2.3	3.1	1.6	7.0	8.8	3.5
Feb/2016b (n=14)	Min	1.7	11.3	17.8	11.1	13.5	21.3	245.7	93.9	418.2	0.4	1.5	1.4	1.5	1.0	1.4	1.4	4.5	7.7
	Max	41.2	45.4	22.4	48.1	20.0	29.6	1477.6	470.7	654.4	4.3	2.3	4.1	12.4	6.6	8.2	21.3	15.5	23.1
	Average	12.5	33.0	21.2	27.1	15.6	25.1	649.0	275.3	559.7	1.5	1.6	2.6	7.2	1.2	5.9	6.3	5.5	22.2
	± SD	13.3	17.3	2.4	12.0	3.3	4.2	464.8	188.4	118.9	1.4	0.4	1.4	3.4	3.2	3.5	6.5	6.1	8.7
Apr/2016 (n=14)	Min	1.9	17.7	18.0	8.5	12.7	19.2	473.5	940.8	1376.6	1.1	0.8	1.8	2.5	2.7	8.6	1.0	3.1	8.8
	Max	27.2	118.8	18.2	31.2	25.6	24.4	1998.2	1690.7	1773.8	2.8	1.6	2.2	11.1	8.3	9.5	17.0	7.4	16.5
	Average	7.1	45.9	18.2	25.3	18.0	20.8	1183.3	1218.3	1414.9	2.2	1.1	2.1	5.2	6.4	8.9	6.7	6.1	10.3
	± SD	9.7	44.2	0.1	7.7	5.3	2.7	474.0	312.6	219.1	0.7	0.3	0.2	3.3	2.5	0.5	5.4	2.0	4.1

ANEXO XII – SUPPLEMENTAL FIGURE S2

Fig. S2. Phytoplankton *bloom* in the continental shelf adjacent to the Doce River mouth. The reddish color indicates the presence of phycoerythrin pigment which is commom to *Trichodesmium* sp. colony.